DOKUZ EYLÜL UNIVERSITY
GRADUATE SCHOOL OF NATURAL AND APPLIED SCIENCES

COAL QUALITY OF THE MIOCENE MUĞLA-HÜSAMLAR LIGNITE

by
Zeynep BÜÇKÜN

June, 2013
İZMİR

COAL QUALITY OF
THE MUĞLA-HÜSAMLAR LIGNITE

The Thesis Submitted to the
Graduate School of Natural and Applied Sciences of Dokuz Eylül University
In Partial Fulfillment of the Requirements for the Degree of Master of Science
in Geological Engineering, Economic Geology Program

by
Zeynep BÜÇKÜN

June, 2013
İZMİR

M.Sc THESIS EXAMINATION RESULT FORM

We have read the thesis entitled "**COAL QUALITY OF THE MIOCENE MUĞLA-HÜSAMLAR LIGNITE**" completed by **ZEYNEP BÜÇKÜN** under supervision of **PROF. DR. HÜLYA İNANER** and **PROF. DR. KIMON CHRISTANIS** and we certify that in our opinion it is fully adequate, in scope and in quality, as a thesis for the degree of Master of Science.

Prof. Dr. Hülya İNANER

Supervisor

Prof. Dr. Kimon CHRISTANIS

Supervisor

Prof. Dr. Mümtaz GOLAK

(Jury Member)

Prof. Dr. Halil ÖZSE

(Jury Member)

Prof. Dr. Ali İhsan KARAYİĞİT

(Jury Member)

Prof.Dr. Ayşe OKUR
Director
Graduate School of Natural and Applied Sciences

ACKNOWLEDGEMENTS

Firstly, I wish to thank my supervisors, Prof. Dr. Hülya İNANER, Dokuz Eylül University, İzmir, and Prof. Dr. Kimon CHRISTANIS, University of Patras, Rio-Patras, for their guidance and continuous encouragement throughout the work, especially with regard to field work, laboratory examinations and constructive discussions during the preparation of this thesis.

Special thanks go to George SIAVALAS and Rıza Görkem OSKAY for their kind assistance, collaboration and vital discussions throughout the studies at the Department of Geology, University of Patras. I would like to express my thanks to Mr. Dimitrios VACHLIOTIS, Laboratory of Instrumental Analysis, School of Natural Sciences, University of Patras, for carrying out the ultimate analyses, and to Dr. Paraskevi LAMPROPOULOU, Department of Geology, University of Patras, for XRD analyses. I would also like to express my thanks to all faculty people and staff of the University of Patras for their kind assistance during my 3-month long stay in Greece.

I am very thankful to Mr. Faruk ERİN and Mr. N. Engin KARAOSMANOĞLU for their supports during my studies in TKİ-YLİ (General Directorate of Turkish Coal), Muğla. I am also grateful to geological engineer Mr. Muzaffer MARÇALI for his assistance during the field work. I would like to thank the mining engineer Mr. Mehmet Ali DEMİRÖREN and chemical engineer Mr. Uğur YILDIZ, both from the laboratory of YLİ, for carrying out the proximate analysis. I am also grateful to all chemists and my friend Altınay GENÇER who helped me while working there.

I am in dept thankful to Assis. Prof. İsmail İŞİNTEK, Assis. Prof. Erhan AKAY and my friend specialist chemist Hilal KILINÇ for their supports during my studies.

Special thanks also go to my parents, Nurdan and Suat ARIK, who have always supported me through many years of my schooling and all my life.

I am very grateful to my husband, Mehmet BÜÇKÜN, who have patiently listened, waited, helped and supported me through this study and loved kindly despide of my stress.

The last and foremost, I wish to thank my little son, Kaan BÜÇKÜN, who had all my feelings inside me and made me happy infinitely.

Zeynep BÜÇKÜN

COAL QUALITY OF THE MIOCENE MUĞLA-HÜSAMLAR LIGNITE

ABSTRACT

The Hüsamlar coal deposit is located in the Muğla Basin, SW Turkey. It is exploited for power generation. The seam displays a banded structure consisting of matrix coal and inorganic intercalations. Coal and inorganic sediment samples were collected from one site in the Hüsamlar Open Pit applying channel sampling. Macroscopically, the lignite belongs to the light- to medium- gelified matrix lithotype. Inorganics mostly include claystone, mudstone, siltstone and limestone.

On average, total moisture is 20.50 wt. percent and ash yield 20.73 wt. percent (on dry basis), volatile matter and fixed carbon contents 60.71 wt. percent and 39.29 wt. percent (on dry, ash-free basis), respectively. The elemental composition of lignite proved to be as follows (all values in wt. percent, on dry, ash-free basis): carbon 61.1, hydrogen 7.7, nitrogen 1.9, sulphur 7.1 and oxygen 22.2. The gross calorific value is around 19.6 MJ/kg (on moist, ash-free basis). Considering the gross calorific values the Hüsamlar coal belongs to the low rank coal B to A.

Seventeen lignite samples were examined under the coal-petrography microscope under white incident light and blue-light excitation. Macerals of huminite group are the most abundant, inertinite is rare, whereas liptinite content strongly varies. On the basis of maceral composition the Hüsamlar peat was accumulating in a limnotelmatic environment, in a fen (topogenous mire), under anoxic, mesotrophic conditions. The maceral content indicates that the peat-forming vegetation consisted of both arboreal plants and herbs. The random reflectance of huminite is about 0.25 percent pointing to, coal rank between peat and lignite.

The lignite proved to contain calcite, aragonite, quartz, pyrite, feldspar and clay minerals. Density separation technique was applied on eleven lignite samples. But the procedure failed and the lack of time did not allow further experiments.

Keywords: Lignite, coal petrology, depositional environment, Hüsamlar, Muğla.

MİYOSEN YAŞLI MUĞLA–HÜSAMLAR LİNYİTLERİNİN ÖZELLİKLERİ

ÖZ

Bu çalışmada Muğla Kömür Sahası (GB Türkiye) bulunan Hüsamlar Kömür Sahası'ndan üretilen kömürlerin bileşenleri ve petrografik özelliklerinin belirlenmesi ve bu özelliklerin kömürün yoğunluğa bağlı olarak zenginleştirilmesi üzerindeki etkilerinin araştırılması amaçlanmıştır. Hüsamlar Kömür Sahası içinde işletilen kömür damarı matriks kömür ve inorganik ara kesmelerden oluşan bantlı bir yapı gösterir. Çalışmada kullanılan kömür ve inorganik tortul örnekleri Hüsamlar açık işletmesinde kanal örneklemesi yöntemi uygulanarak toplanmıştır. Örnekler makroskopik olarak linyit, az-orta jelleşmiş matriks litotipine sahiptir. İnorganik bileşenleri kiltaşı, çamurtaşı, silttaşı ve kireçtaşı oluşturur.

Ortalama toplam nem yüzde 20,50; kül miktarı yüzde 20,73 (kuru bazda); uçucu madde içeriği yüzde 60,71; karbon içeriği yüzde 39,29 (kuru, külsüz bazda) ölçülmüştür. Linyitin elementer içeriği (bütün değerler ağırlıkça yüzde, kuru, külsüz bazda) karbon yüzde 61,1; hidrojen yüzde 7,7; nitrojen yüzde 1,9; kükürt yüzde 7,1 ve oksijen yüzde 22,2 şeklindedir. Üst kalorifik değer göz önüne alındığında Hüsamlar kömürü B-A düşük dereceli kömür aralığına aittir.

On yedi linyit örneği kömür petrografisi mikroskobunda, beyaz ve mavi ışık uygulanarak incelenmiştir. Hüminit grubu maseralleri yaygın, inertinit seyrek olarak bulunurken liptinit içeriği oldukça değişkenlik göstermektedir. Maseral içeriği baz alındığında Hüsamlar turbası limnotelmatik ortamda, fende, anoksik, mezotrofik koşullarda birikmiştir. Rastgele hüminit yansıtması ortamala 0,25 olup turba ve linyit arası kömürleşme derecesine denk gelir.

Hüsamlar kömür örnekleri kalsit, aragonit, kuvars, pirit, feldspat ve kil mineralleri içermektedir. Yoğunluk ayırma tekniği onbir örnekte denenmiş, başarısızlıkla sonuçlanmıştır. Deneyler için geçirilen sürenin yetersizliği nedeniyle deneylerin tekrarı tamamlanamamış ve ileriki çalışmalara bırakılmıştır.

Anahtar Sözcükler: Linyit, kömür petrolojisi, oluşum ortamı, Hüsamlar, Muğla.

CONTENTS

Page

THESIS EXAMINATION RESULT FORM ii
ACKNOWLEDGEMENTS iii
ABSTRACT v
ÖZ vii
LIST OF FIGURES xii
LIST OF TABLES xiv

CHAPTER ONE – INTRODUCTION 1

1.1 Coal Deposits and Utilization in Turkey 1
1.2 Study Area 3
1.3 Previous Studies 5
1.4 Aim of the Study 8

CHAPTER TWO – GEOLOGICAL SETTING 10

2.1 The Muğla Basin 10
2.2 The Hüsamlar Area 12
2.2.1 Pre-Neogene Rocks 12
2.2.2 Neogene Sediments 15
2.2.2.1 Marine Sediments 15
2.2.2.2 Bottom Series (Ks 15
2.2.2.3 Coal Seam 15
2.2.2.4 Marl-Limestone Series (Mk 15
2.2.2.5 Talus, Landslides, Alluvium 17
2.3 Evolution of Milas Basin 18

CHAPTER THREE – MATERIALS AND METHODS 20

CHAPTER FOUR – RESULTS 23

4.1. Lithological Features 23
4.2 Laboratory Examination of Coal 30
4.2.1 Proximate Analysis 30
4.2.2 Ultimate Analysis 32
4.2.3 Coal Petrography 33
4.2.3.1 Macerals of Hüsamlar Lignite Deposit 34
4.2.3.1.1 Macerals of Huminite/Vitrinite Group 34
4.2.3.1.2 Macerals of Liptinite Group 35
4.2.3.1.3 Macerals of Inertinite Group 36
4.2.3.2 Maceral Composition 36
4.2.3.3 Huminite Reflectance 38
4.2.4 Mineralogical Determinations 38
4.2.4.1 The Bulk Coal Sample 39
4.2.4.2 The 350ºC Residue 41
4.2.4.3 The 750ºC Ash 44
4.2.5 Density Separation 46
4.2.5.1 Ultimate Analysis on Light Fraction 46
4.2.5.2 Mineralogical Determinations on Heavy Fraction 47
4.3 Inorganic Sediments 49
4.3.1 XRD Analyse of Dirt Bands 49

CHAPTER FIVE – DISCUSSION 51

CHAPTER SIX – CONCLUSION 63

REFERENCES 65

APPENDICES 78

APPENDIX I – Pictures from sampling at Hüsamlar Open Pit..... 79
APPENDIX II - Photomicrographs of the Hüsamlar lignite 85
APPENDIX III – X-Ray Diffractograms 97

LIST OF FIGURES

Page

Figure 1.1 Important coal deposits of Turkey (after İnaner and Nakoman, 2004; MTA, 2010; modified by Oskay et al., 2013..... 2
Figure 1.2 (a) The lignite deposits of Muğla Basin (after İnaner et al., 2008, modified). (b) Location map of the Hüsamlar Sector..... 4
Figure 2.1 Plate Tectonics in Turkey (from USGS, 1999..... 11
Figure 2.2. Tectonic map of the Aegean region (Okay, 2001 11
Figure 2.3. Location of the Miocene Mugla Basin, Turkey (after Querol et al., 1999, modified 13
Figure 2.4. The generalized coloumnar section of the Muğla Basin (Sun and Karaca, 2000..... 14
Figure 2.5.Geological Map of Hüsamlar Area (Yiğitel et al., 1981 16
Figure 2.6. Lithostratigraphic column of the Hüsamlar area (after Sun and Karaca,2000, modified..... 17
Figure 3.1 Flow chart of the methodology applied in the study Hüsamlar lignite samples..... 22
Figure 4.1 The sampled coal seam at Hüsamlar Open Pit 23
Figure 4.2. The studied lithostratigraphic column sampled at Hüsamlar Mine 24
Figure 5.1 Rank determinations of the Hüsamlar lignite samples according to the German and North American classifications (after Taylor et al., 1998..... 52
Figure 5.2 Rank determination of the Hüsamlar lignite samples according to the of ECE-UN (1998) classification..... 53
Figure 5.3 Plot of the Hüsamlar lignite samples on the van Krevelen diagram (maturity fields after Killops and Killops, 1993..... 54
Figure 5.4 Classification of mires and their peat (Diessel, 1992; partly after Grosse-Brauckmann, 1980; Martini and Glooschenko, 1984; and Moore, 1987) 54
Figure 5.5 Fresh-water peat formation by terrestrialisation. Not to scale. (Spackman et al., 1966, 1969; Diessel, 1992..... 55

Figure 5.6 ABC ternary plot of the Hüsamlar lignite samples (after Mukhopadhyay, 1989..... 56
Figure 5.7 The TPI/GI coal-facies diagramme after Diessel (1992..... 58
Figure 5.8 The GWI/VI coal-facies diagramme after Calder et al. (1991 58
Figure 5.9 Schematic reconstruction of the peat accumulation environment in the Hüsamlar Basin, during the deposition of lignite seam 60

LIST OF TABLES

Page

Table 1.1 The projects supplying Yatağan, Yeniköy and Kemerköy Thermal Power Plants(GELI, 2011 3
Table 4.1 Proximate analysis results of Hüsamlar coal 31
Table 4.2 Ultimate analysis results of Hüsamlar coal..... 33
Table 4.3 Subdivision of the maceral group huminite (Sýkorová et al., 2005)..... 35
Table 4.4 Macerals of the liptinite group (ICCP, 1963..... 35
Table 4.5 Macerals of the inertinite group (ICCP, 2001..... 36
Table 4.6 Maceral composition (vol.% on dry, mineral matter-free basis) and mineral matter (vol.% on whole sample) of Hüsamlar lignite samples..... 37
Table 4.7 Huminite random reflectance (%) of Hüsamlar lignite 38
Table 4.8 Rietveld-based quantification XRD results of Hüsamlar bulk coal samples, in wt. % of the crystalline phases 40
Table 4.9 Rietveld-based quantification XRD results of Hüsamlar 350° Residues, in wt. % of the crystalline phases 42
Table 4.10 Rietveld-based quantification XRD results of Hüsamlar 750°C ash samples, in wt. % of the crystalline phases 45
Table 4.11 Ultimate analysis results of heavy (organic matter-rich) fraction of Hüsamlar coal samples..... 47
Table 4.12 Rietveld-based quantification results of the light fraction of Hüsamlar coal samples, in wt.% of the crystalline phases..... 48
Table 4.13 Qualitative mineral composition of the inorganic intercalations of Hüsamlar lignite seam..... 50
Table 5.1 TPI, GI, GWI and VI indices calculated on the basis of the results of maceral analysis..... 56
Table 5.2 The results of density separation on the coal sample 62

CHAPTER ONE
INTRODUCTION

1.1 Coal Deposits and Utilization in Turkey

The important coal deposits in Turkey were mainly formed into two different geologic periods of time, namely Carboniferous and Tertiary. The Carboniferous coal deposits are located with in a 200-km wide belt in the western Black Sea Region (Fig. 1.1) with 1.3 Gt reserves (Şengüler, 2010). Tertiary deposits, with about 11.5 Gt reserves, are distributed to about 2% in Eocene and 6% Oligocene in NW Turkey, 41% Miocene in western Turkey and 51% Pliocene in eastern Turkey. Only the Oligocene lignite deposits were formed in paralic environments, whereas the rest were deposited in limnic environments (İnaner & Nakoman, 1997; Besbelli, 2009; Şengüler, 2010; Oskay et al., 2013). If the Jurassic coal deposits can be neglected due to its small reserves, the most common deposits are of Tertiary age.

Due to the accessibility and the availability of coal, the majority of the world's county densely used coal for electricity production in present. Most of the known lignite deposits in Turkey display low calorific value, high moisture, ash, volatile matter content and sulphur content. Almost 75% of the total reserves show calorific values <2500 kcal/kg, about 17% are between 2500 and 3000 kcal/kg. Nearly 85% of the annual coal production is consumed in thermal power plants (Besbelli, 2009; Şengüler, 2010).

1.2 Study Area

The coal-bearing Muğla Basin is located close to the eastern coast of the Aegean Sea, in southwestern Anatolia, Turkey. On the basis of the geomorphological features the Muğla Basin can be distinguished into two elongated sub-basins, namely these of Yatağan and Milas (Fig. 1.2a). The long axes of both sub-basins have a NW-SE orientation. Yatağan Basin at the east, is 12 km long and 11 km wide; it occupies an area of about 132 km^2 lying at altitudes between 200 m and 1500 m above sea

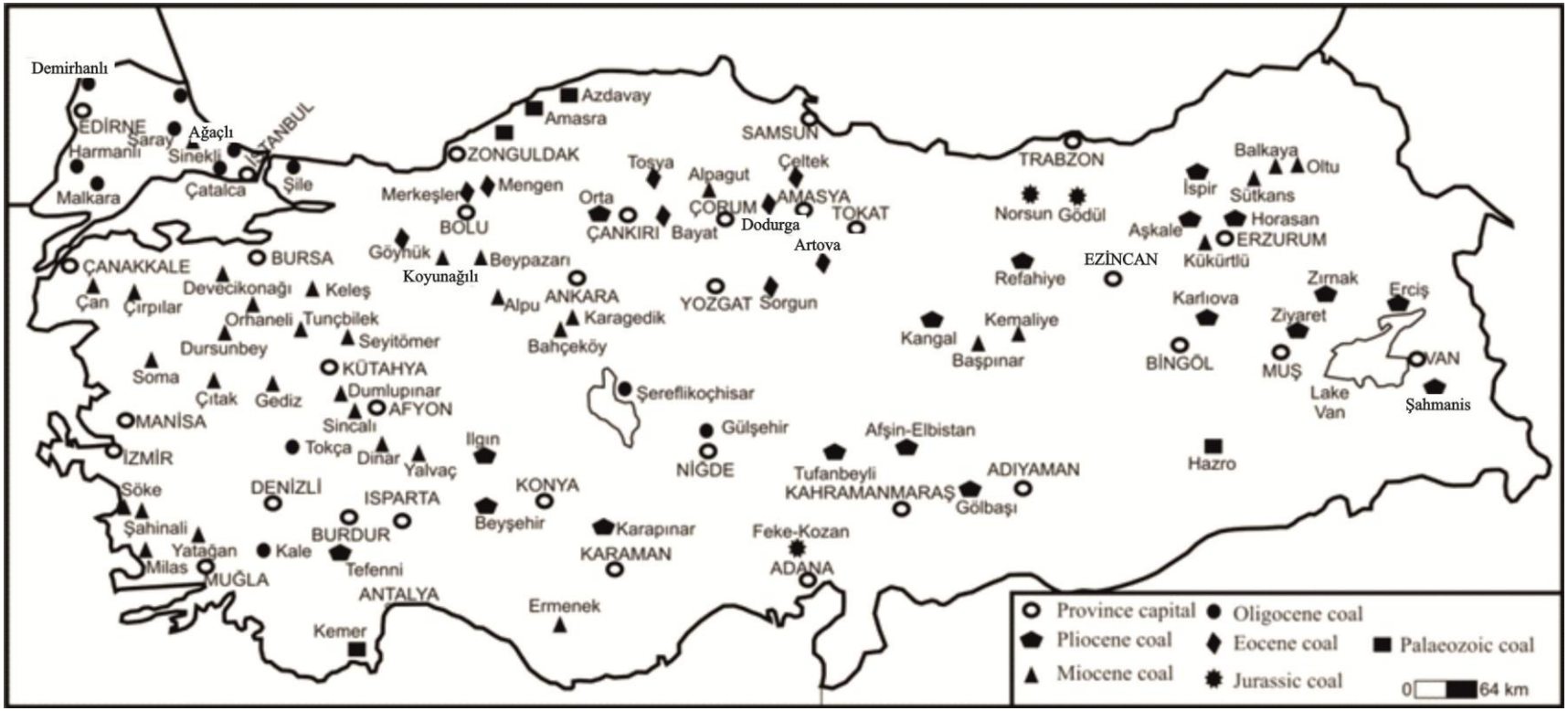

Figure 1.1 Important coal deposits of Turkey (after İnaner and Nakoman, 2004; MTA, 2010; modified by Oskay et al, 2013)

level. Milas Basin at the west, has a lenght of 19 km and a windth of 14 km; it extends over a 266 km^2 large area at an altitudes between 50 m and 1000 m. The Yatağan sub-basin extents at the east of Muğla Basin and hosts the lignite deposits of Turgut, Eskihisar, Bağyaka, Tınaz and Bayır, whereas the Milas sub-basin occupies the western part of the Basin and includes the lignite deposits of Ekizköy, Sekköy, Çakıralan, Karacahisar, Hüsamlar and Alatepe. Open-cast mines operate at Eskihisar, Bağyaka, Tınaz, Sekköy, Ekizköy, Hüsamlar and Çakıralan coal fields, whereas in Alatepe field both open-cast and underground mining methods are applied.

Most of the lignite production supplies three thermal power plants, namely these of Yatağan, Yeniköy and Kemerköy with 630, 420 and 630 MW installed capacity, respectively (Querol et al., 1999; İnaner et al., 2008). The projects to supply these thermal power plants are given in Table 1.1.

Table 1.1 The projects supplying Yatağan, Yeniköy and Kemerköy Thermal Power Plants (GELI, 2011)

Project Name	Capacity (Mt/yr)	Thermal Power Plant		Coal Consumption (Mt/yr)
		Name	Installed Capacity (MW)	
Yatağan	3.50	Yatağan I-II	420	3.120
Tınaz-Bağyaka	1.85	Yatağan III	210	1.725
Yeniköy	4.10	Yeniköy	210	3.750
Hüsamlar	5.70	Kemerköy	630	5.000
TOTAL	15.15		1680	13.595

The present study deals with Hüsamlar coal deposit which administratively belongs to the province of Muğla and the distinct of Milas. Muğla-Milas Hüsamlar open pit (Appendix I, Fig. 1) is located on the N19-C3 sheet of the 1/25.000 scale topographic map.

Hüsamlar coal deposit is bordered by Hayıtalan Hill (+360 m a.s.l.) in the north, Deliktaş Hill (+314 m) and Kuzupınar Hill (+300 m) and Okçular Hill (+280 m) in the east and (+260 m) south, whereas Değirmen River at the west of the coal deposit is flowing from south to North (Fig. 1.2b).

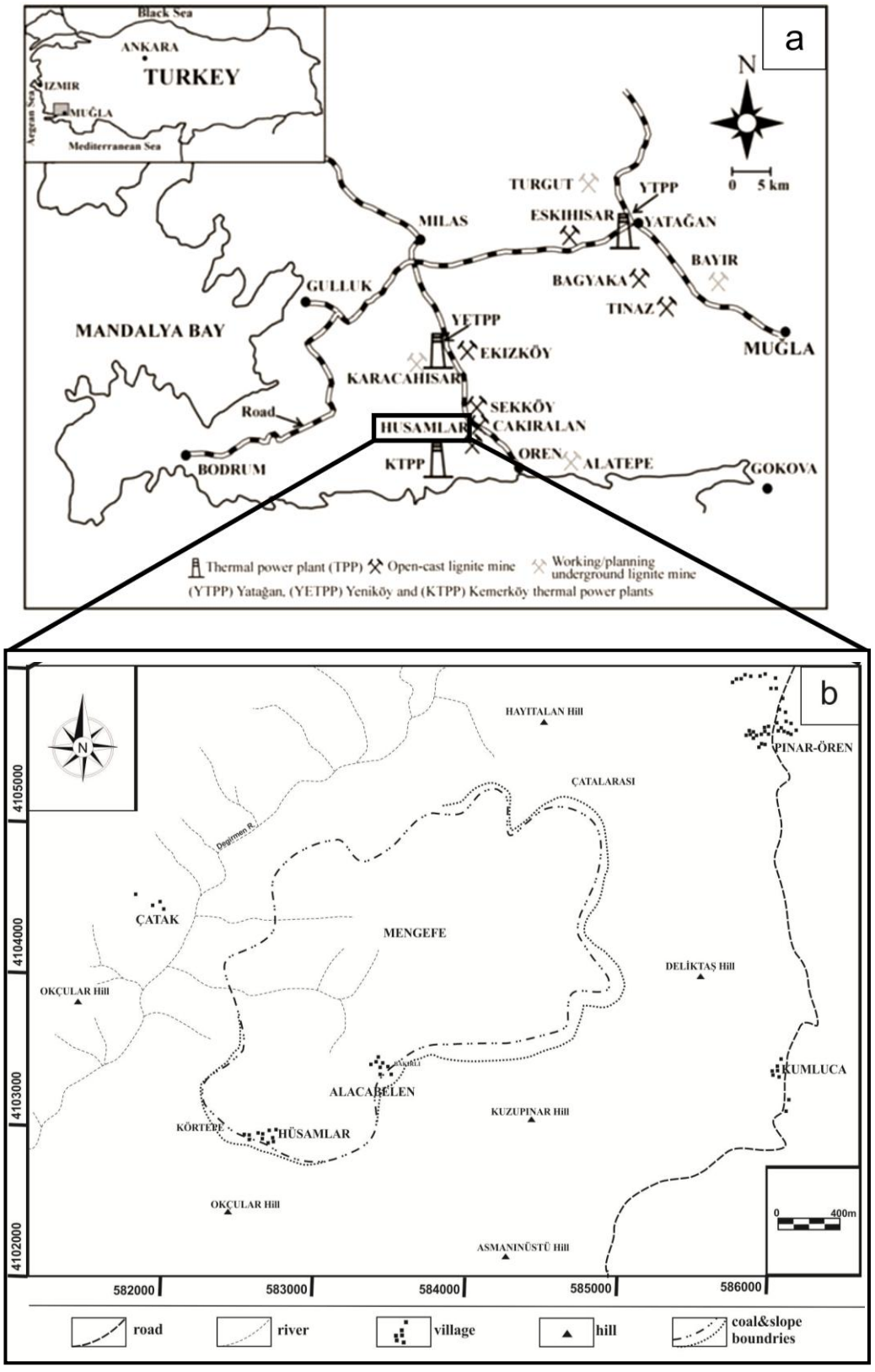

Figure 1.2 (a) The lignite deposits of Muğla Basin (after İnaner et al., 2008, modified). (b) Location map of the Hüsamlar Sector.

The lignite deposit has a general NE-SW orientation and hosts 50.992.000 t reserves. The production from Hüsamlar Mine (4.700.000 t/year) along with this from Belentepe (Çakıralan) Mine (1.000.000 t/yr) supplies the Kemerköy power plant (GELI, 2011).

Within the coal deposit an antique site called Mengefe (Appendix I, Fig. 2) is discovered and currently excavated under the supervision of the Museum Directorate of Milas.

In the entire area, a Mediterranean climate dominates. The summers are hot and arid, in the fall months the rainy season begins. This situation is very dominant especially during the summer months when most of the springs dry out.

The largest part of the area is forested. Olive trees are very common in this region. In limited areas outside the forested area, various food crops and tobacco are cultivated. Ranching is not widely developed with in this area.

1.3 Previous Studies

Previous studies in the broad area dealt with the general geologic and geotectonic setting of western Anatolia, but also with the economic coal geology in the surroundings of the study area.

There are various proposals about the stratigraphy, age and the factors which controlled the tectonic graben formation in western Anatolia.

Seyitoğlu & Scott (1991) studied Late Cenozoic crustal extension and basin formation in western Turkey. They propose that the E-W oriented grabens began forming throughout Late Oligocene-Early Miocene and are continuously evolving since that time.

Sengör & Yılmaz (1981), Paton (1992), Yılmaz et al. (2000), Koçyiğit et al. (1999), Bozkurt (2000) and Sarıca (2000) have the opinion that the E-W grabens are young tectonic features, and began forming in Late Miocene.

Şengör & Yılmaz (1981), Yılmaz et al. (2000) studied the geological and tectonic evolution of southwestern Anatolia as well. They agree that that the E–W grabens are relatively young tectonic features, which began forming in Late Miocene.

Gürer & Yılmaz (2002) accepted Ören Basin as a N–S trending basin possibly developed in an E–W extension and N–S compression stress field.

Many studies focusing on the Tertiary sedimentary sequence in western Anatolia have also been carried out.

Nebert (1957) studied the biostratigraphy of the marine sediments around the Ören-Alakilise and Pınar regions.

Becker-Platen (1970) contributed to the lithostratigraphy from Oligocene to Lower Quaternary sediments in southwestern Anatolia (*i.e.* Denizli, Muğla-Yatağan and Milas).

Atalay (1980) studied the Neogene terrestrial sediments in Muğla, Yatağan and the surrounding areas. He distinguished Eskihisar and Yatağan formations in Yatağan Basin.

Hakyemez et al. (1989) studied the geological and stratigraphic features of the Cenozoic sediments between Muğla and Denizli.

Kaya et al. (2001) studied mammalian fauna of early Middle Miocene in the Milas-Kultak region.

An important part of the previous studies deals with economic coal geology.

First searches for coal in Southwestern Anatolia began in 1956 by K. Nebert followed by L. Benda, J.D. Becker-Platen and A. Bering within the framework of *"The Programme of Turkish-German Technical Cooperation"*. As the area was promising, the above researchers have completed both the 1/25.000 and 1/10.000 geological maps and have calculated the reserves based on borehole data.

In 1965 the company OTTO-GOLD in collaboration with Bundesanstalt für Geowissenschaften und Rohstoffe, both from Germany, conducted a comprehensive geological study on the units outcropping in Hüsamlar Sector and the properties, quality and reserves of coal seam.

Nakoman (1978) carried out palynological and economic studies in the broad Muğla region.

In the 1980s the General Directorate of Turkish Coal (TKİ) began producing lignite from Eskihisar, Bağyaka, Tınaz, Sekköy and Ekizköy (İkizköy) open pits.

Yiğitel et al. (1981) prepared a report for TKİ including the 1/10.000 scaled geological map, as well as data about lithological features of the units and structural geology of the basin and the calculation of the reserves based on data from boreholes.

Aksoy & Demirok (1981) carried out a feasibility study including data about reserves and quality of coal, all based on borehole data.

Gelincik (1986) studied the geological and structural features of Hüsamlar Sector in detail also providing reserves calculation.

Ünal et al. (1987) implemented a project to examine if the capacity of both Hüsamlar and Çakıralan (Belentepe) open pits with an annual production totalling 3.3 Mt could supply with fuel a thermal power plant, whereas in another project Ünal

et al. (1988, 1990) studied the possibility to supply a thermal power plant with lignite from Hüsamlar open pit only (production 2 Mt/yr).

Querol et al. (1999) performed a study about coal geology and quality in Muğla region.

Sun & Karaca (2000) and Sun et al. (2001) prepared a report for the Mineral Research of Exploration Institute (MTA) dealing with the features of the lithological units and the structural geology of the basin on the basis of new borehole data, also comprising conclusions about the economics and the coal properties.

Arslan (2004, 2010) studied and reported about the technological features of Hüsamlar lignite in the frame of a project funded by TKİ.

Kayseri-Özer (2010) studied in her Ph.D. thesis palynology, palaeobotany, vertebrate and marine faunas and palaeoclimatology of the Oligo-Miocene Ören Basin.

1.4 Aim of the Study

Most of the previous works published about the Muğla coal deal with mainly the reserve estimation and the quality determination, including also some petrographic and palynological data obtained from randomly picked out samples from various stratigraphic levels.

The objectives of the present study focusing on the Hüsamlar lignite only are to determine:

- the geological features of the lignite seam including the inorganic sediments intercalating,

- the lignite quality,

- the petrographic composition,

- the mineralogical and geochemical composition.

The aim of the current work is:

- to reconstruct the palaeoenvironmental conditions and the factors controlling coal formation at Hüsamlar, and

- to contribute to a successful coal washing applying density separation techniques.

CHAPTER TWO
GEOLOGICAL SETTING

2.1 The Muğla Basin

The term neotectonic is explained as "the type of entire tectonism which occured in an area from the time when the last tectonic regime occured and changed into recent times." by Şengör (1980) in his paper "The principles of Neotectonics of Turkey". The events, which may have occured before the last tectonic regime may contain deformation stages. The collision of the Anatolian and Arabian (Eurasia-Arabia) plates in Turkey took place in Middle Miocene (Şengör, 1979; Şengör et al., 1985) and this event determined the last deformation stage in the tectonics of Turkey.

The stage which developed after this collision and is going on into recent times is called neotectonic stage. In this stage the northern and eastern Anatolia faults developed as seen in Figure 2.1. The Anatolian plate moved westwards with two strike-slip faults. The middle Anatolian plain area developed in the eastern part of the Anatolian plate, which also moved westwards. Thick Neogene sediments were deposited in this area where lacustrine-continental depositional environments were dominant. Further west, during the same time period, the Aegean graben system developed (Fig. 2.2). The west Anatolian lacustrine continental depositional basins formed approximately in a E-W graben system.

In the Gökova region, basins of various ages have been identified. The oldest basin, The Kale-Tavas molasse basin is ENE-WSW orientated (Şengör & Yılmaz, 1981). The youngest basin is the modern Gökova Graben. It is one of the major E-W-trending grabens of western Anatolia (Gürer and Yılmaz, 2002). The formation of the basin is explained using block diagrams in according to the study of Gürer and Yılmaz (2002).

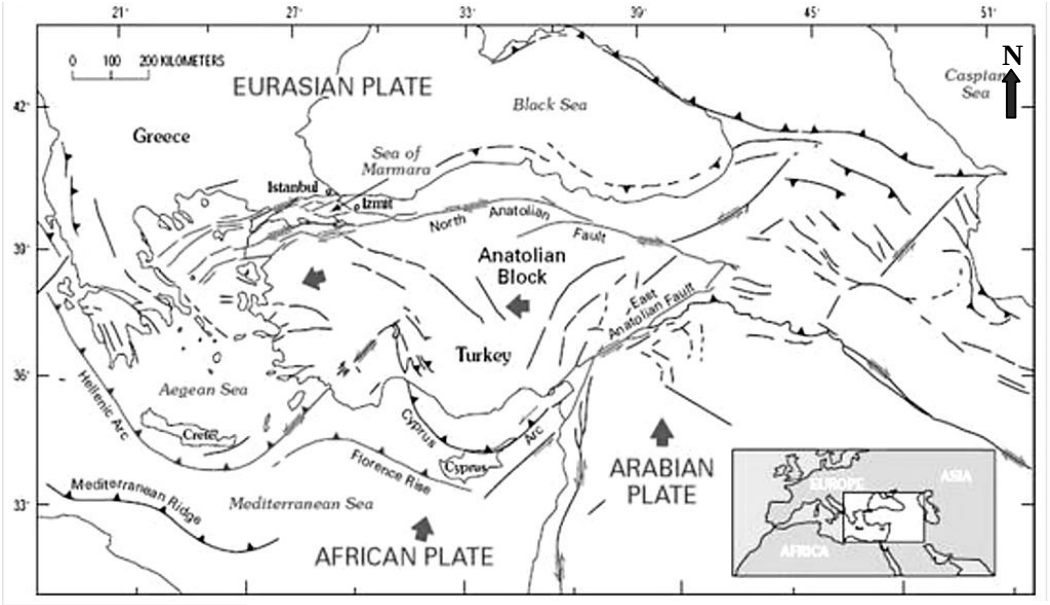

Figure 2.1 Plate Tectonics in Turkey (from USGS, 2000)

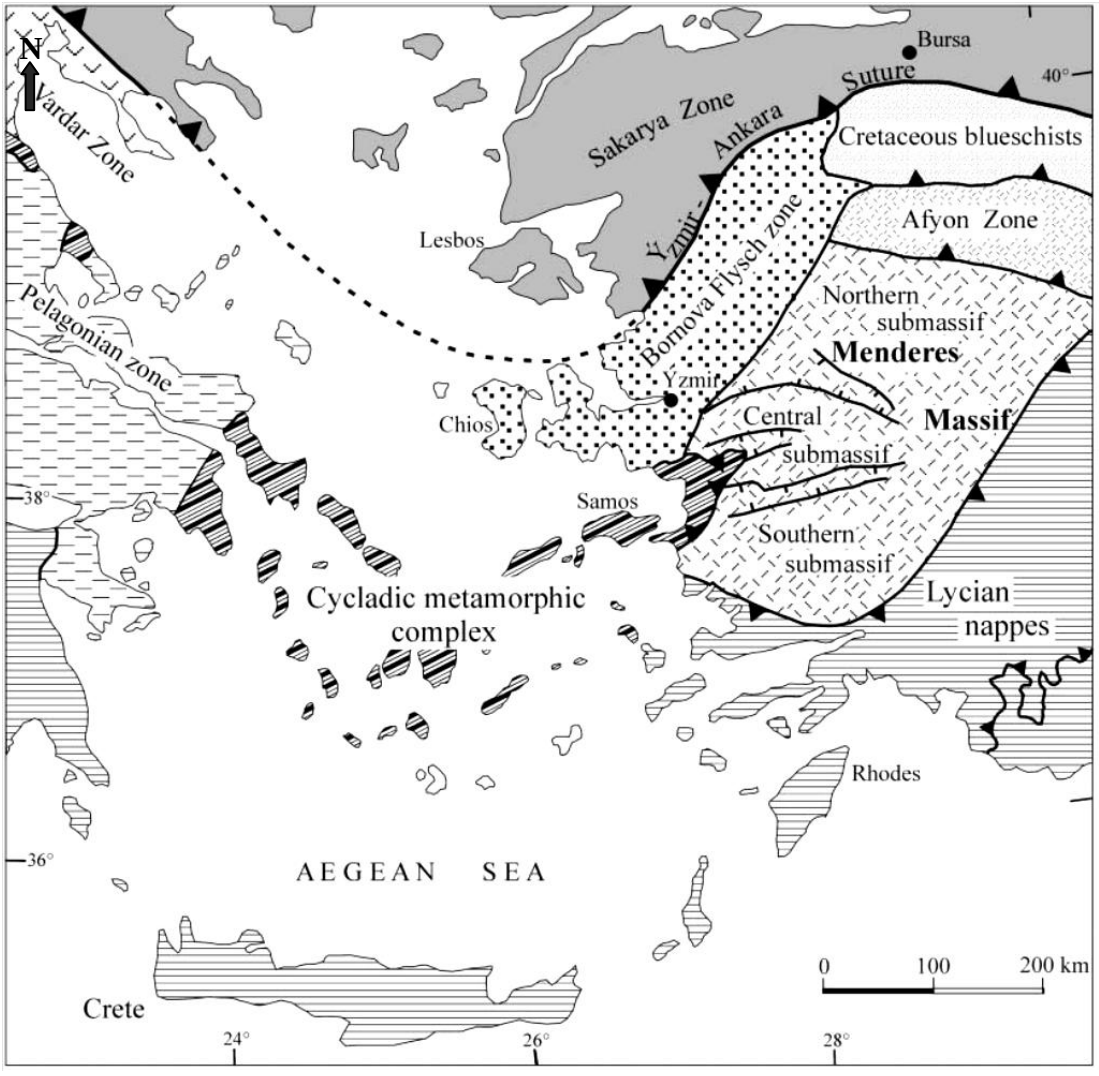

Figure 2.2 Tectonic map of the Aegean region (Okay, 2001).

The surface area of the Muğla Basin is about 350 km^2 large (Fig. 2.3). The basement consists of rocks of Menderes Massif and Lycian Nappes. The Lycian nappes, a complex nappe accumulation with both oceanic and continental affinities, in the south, and metamorphic lithologies, such as schist, gneis, amphibolite and marble belonging to the Menderes Massif, in the north. There are two younger series. The first, the marine Alatepe Unit is located in the south of the study area; it belongs to the Kale–Tavas foredeep and represents the southward moving Lycian nappes (Göktaş, 1982). The second overlies Alatepe Unit discordantly. It is located in the north. Previous authors (Gökmen, 1975; Yiğitel, 1979; Atalay, 1980; Göktaş, 1982) have proposed a generally accepted four-fold stratigraphy in the region for this second series. These are, from bottom to top, the Turgut Unit (mainly fluvial fines), Sekköy Unit (lacustrine marls), Yatağan Unit (alluvial coarse clastics) and Milet Unit (mainly freshwater limestone) (Fig. 2.4).

2.2 The Hüsamlar area

The western part of the Muğla Basin, the Ören area is located to the north of the Gökova Graben where there are large Neogene outcrops. This Neogene is commonly referred to as the Ören basin, which extends from the Gulf of Gökova in the south to Milas in the North. This basin hosts the Hüsamlar lignite deposit (Fig. 2.5).

The part of stratigraphic series of basin, which outcrops in Hüsamlar area is described below from bottom to top on the basis of the report of General Directorate of Turkish Coal (TKİ) compiled by Yiğitel et al (1981).

2.2.1 Pre-Neogene Rocks

In Hüsamlar region, the basement consists of Palaeozoic metamorphic shists and Mesozoic crystalline limestone.

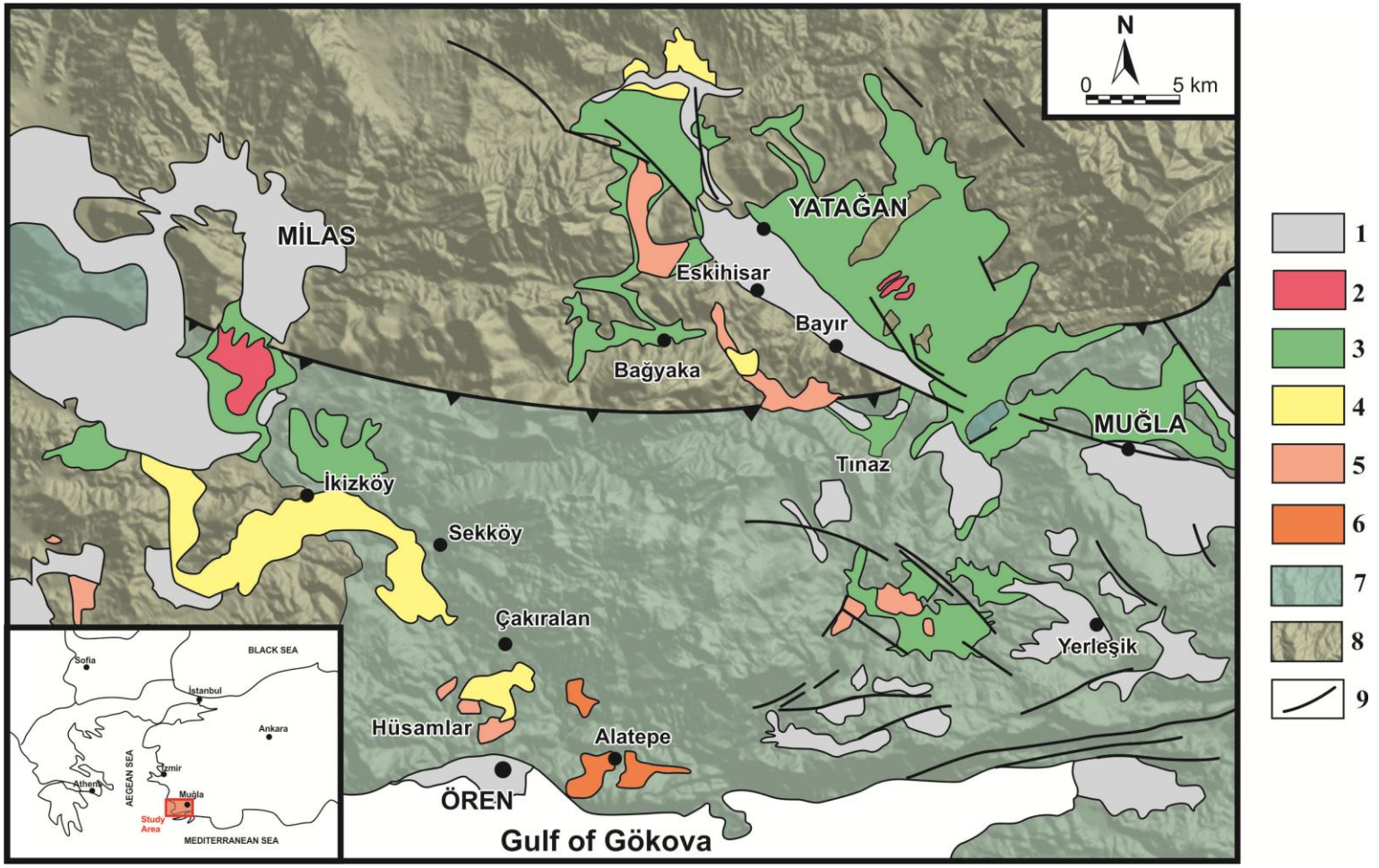

Figure 2.3 Location of the Miocene Mugla Basin, Turkey. (1. Quaternary deposits, 2. Milet Formation, 3. Yatağan Formation, 4. Sekköy Formation, 5. Turgut Formation, 6. Alatepe Formation, 7. Lycian nappes, 8. Menderes Massif rocks, 9. fault).(after Querol et al., 1999, modified).

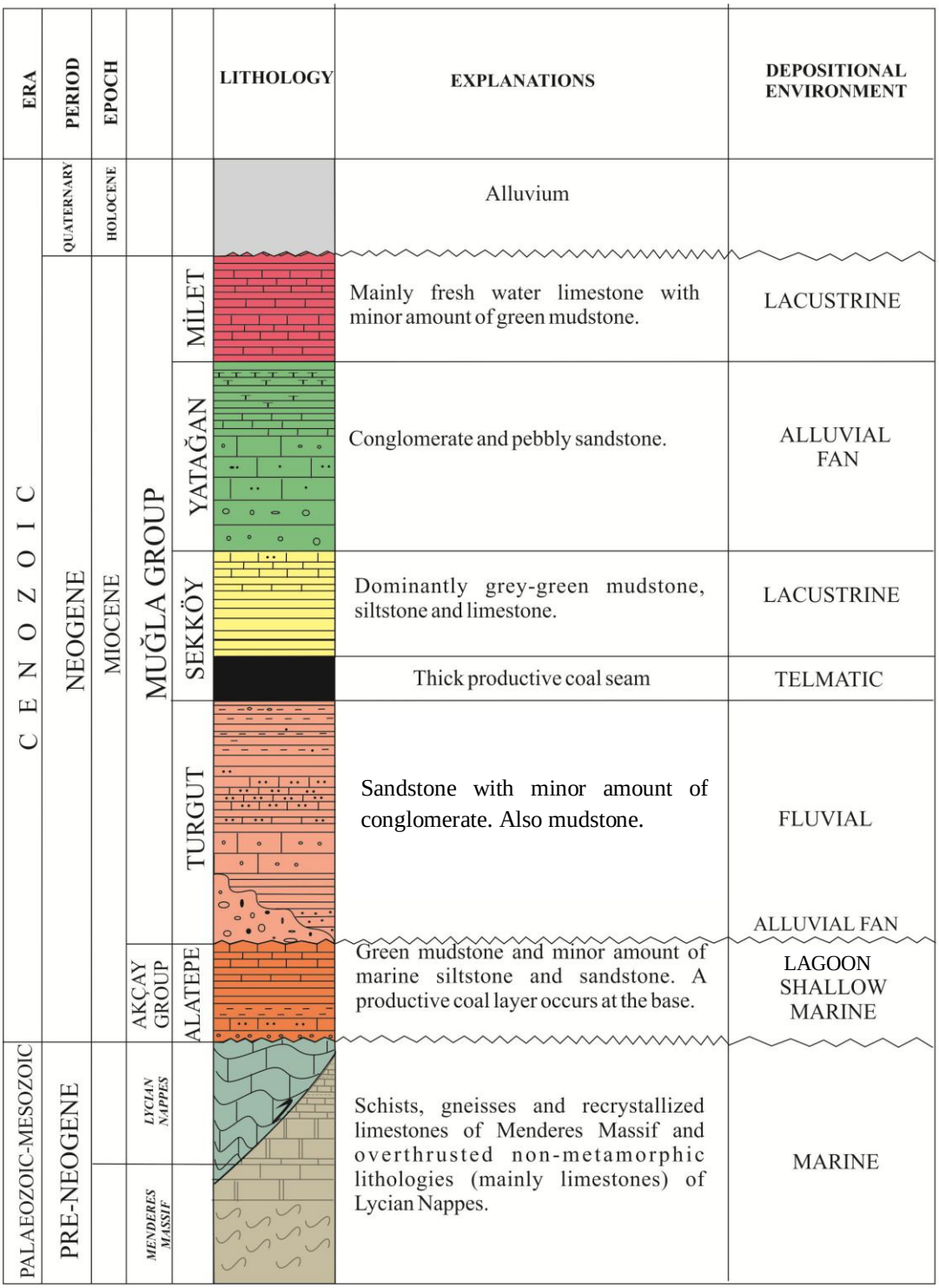

Figure 2.4 Lithostratigraphic column section of Muğla Basin (Sun & Karaca, 2000).

2.2.2 Neogene Sediments

2.2.2.1 Marine Sediments

The first sub-series (Ms) is composed of sand and silt. It also hosts conglomerates rarely. The second sub-series (M), a grey-white limestone, overlies the first one sometimes displaying a sandy lithology. This limestone extends in a huge area and contains zones with abundant shell fossils. These marine sediments corresponds to the Kerme Unit (see chapter two).

2.2.2.2 Bottom Series (Ks)

This series mainly includes claystone, siltstone, sandstone and pebblestone. This series extends in the west and south of Hüsamlar area. This Ks series equivalents to the Turgut Unit which is mentioned in regional setting (see chapter two).

2.2.2.3 Coal Seam

Coal overlies the Ks series and underlies the marl-limestone (Mk) one. The characteristics of Hüsamlar lignite seam differ from the other areas of Muğla Basin. It is much thicker (the thickest part is around 67 m) and consists of alternating benches of coal and inorganic (marl, clay, silt) intercalations.

2.2.2.4 Marl-Limestone Series (Mk)

In Hüsamlar area, beneath the coal seam, there is blue-grey marl that has thick and narrow layers. Below marl, there is a transition to limestone that has narrow layers and so many cracks.

Typical characteristic of this series is to be seen both vertical and horizontal transitions between limestone and marl. Molluscs occur frequently, whereas leaf remnants can be rarely recognized.

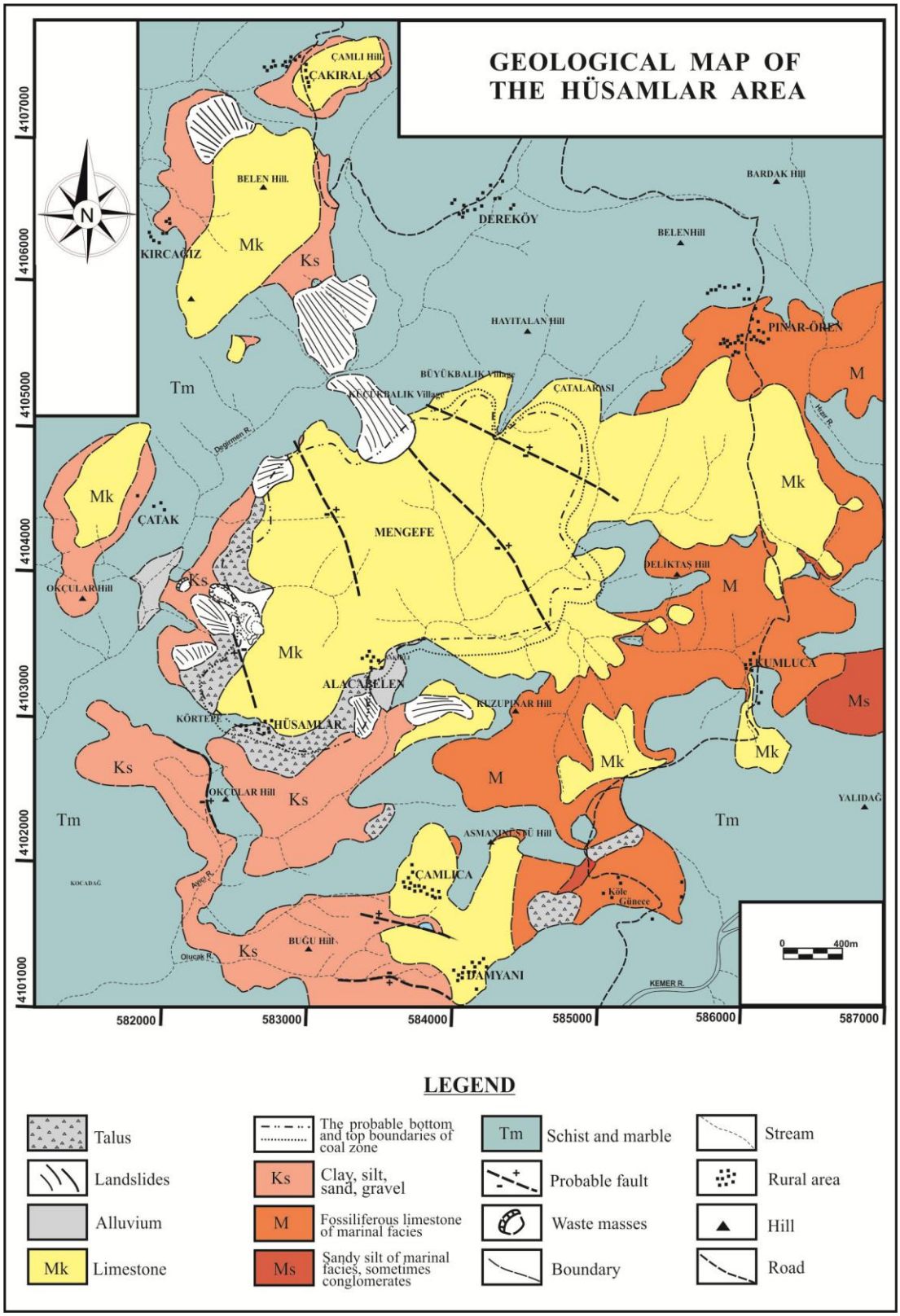

Figure 2.5 Geological Map of Hüsamlar area (Yiğitel et al., 1981).

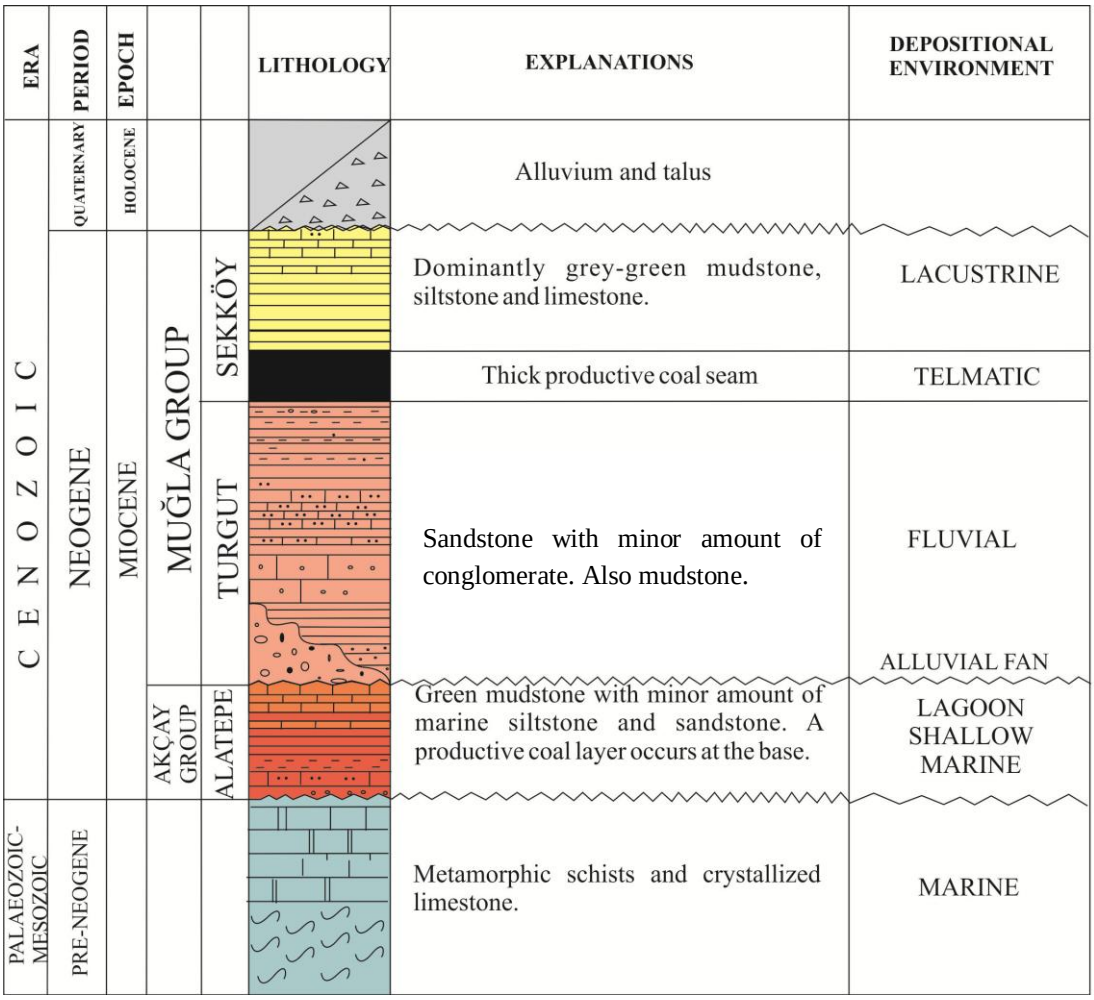

Figure 2.6 Lithostratigraphic column of the Hüsamlar area (after Sun & Karaca, 2000, modified).

In Hüsamlar area, close to the borders, the thickness of marl layers above coal seam decreases, while the thickness of limestone increases. Besides, in the deeper parts of the area the thickness of marl layers increases, whereas the thickness of limestone layers decreases.

2.2.2.5 Talus, Landslides, Alluvium

There are "old" landslides in the North of the Hüsamlar region. In the west and south of the region there are less significant landslides than the others. The western and the southwestern part of the area is covered by talus. Alluvium extends in a narrow area around Değirmendere River in the west (Fig. 2.5).

2.3 Evolution of Milas Basin

Milas subbasin is bordered by pre-Miocene NW-SE faults (Sun & Karaca, 2000). It is thought there was a braided river in the beginning of Middle Miocene (Early Serravallian) which extented in the middle of the basin and was probably flowing to the NW which transformed to meandering river. In the North of the basin alluvial fans formed which were oriented to south. Sometimes mires occurred in this river's flood plains or oxbow lakes. A wide mire formation has started to affect all precipitation basins since the second part of Serravallian. This environment would create the floor of Sekköy Formation, economical thick coal seam. This seam is a guide series of southwestern Anatolia due to being very wide.

The thick coal seam shows that the mire environment was stable for long time. Tectonic activity resulting in the separating into various coal fields such as these of Ekizköy, Sekköy, Çakıralan, Karacahisar, Hüsamlar and Alatepe.

The sharp contact between coal and marl in Sekköy Formation points to that sudden transformation of the telmatic to the lacustrine environment. The sudden increase at the lake level shows that the vertical tectonism activated suddenly at the beginning of Sarmatian which was stable during mire formation. The basin got deeper and transformed to lacustrine environment due to this vertical movement.

Marl was the first product of this basin. Limestone formation followed it. There are some sandstone-siltstone and coal layers between marl and limestone. This shows that the lake level lowered, the lake basin became narrow and shallow (with mire occurrences at some places) from time to time.

The volcanism which is contemporary to neotectonism, caused vast palaeogeographic and sedimentologic differences in Early Tortonian, caused to raise of heat in the region. So evaporation accelareted, lake dried, little water accumulated at some of the deepest parts. High volcanoclastic entry happened due to tuff accumulation and terrestrial movement into lake. Than started have transition period which is followed by alluvial fan and braided river systems.

I. stage of kalkalkaline volkanism, started at Early Tortonien and affected the whole southwestern Anatolia (Ercan et al., 1983), transformed the common humid climate during Middle Miocene to arid, semi-arid climate. The region was exposed to the erosions during upper Miocene, the dominant period of Yatağan alluvial fans.

During the end of the upper Miocene the climate turned to humid climate and the re-activated vertical tectonism created deep trenches and growing precipitations caused the formation of new lakes. Limestone is the main lithology of this lacustrine environment (Milet Formation).

Finally, Quaternary erosion formed the modern landscape.

CHAPTER THREE

MATERIALS AND METHODS

About 23 lignite and 26 dirt band samples were collected from Hüsamlar Open Pit, applying a channel sampling strategy (Thomas, 2002), *i.e.* digging 30 cm deep perpendicular to bedding from the roof to the floor of the entire coal seam, in order to get fresh representative sample. To sample full coal seam, the closest location was chosen which has the thickest coal seam data on the basis of borehole no:22 (TKİ, 1981). The sampling site has the following coordinates: 583.450/4.103.825 and 583.500/4.103.625 with small deviations, because of the terraces. The lithology of the profile was logged at site. The coal lithotypes were determined on the basis of the ICCP (1993) nomenclature. All samples were put in plastic bags and stored at +4°C to ensure as little loss of moisture and oxidation as possible.

Proximate analysis was conducted on all (23) the bulk coal samples. Moisture was determined according to ASTM D3302 (1989), ash yield and volatile matter content were determined according to ASTM D3174 (1989) and D3175 (1989), and gross calorific value according to ASTM D5865 (2004), in an IKAC5000 adiabatic bomb calorimeter. The proximate analyses were performed at the Laboratory of YLİ, Muğla, and the Laboratory of Energy Raw Materials, Department of Geology, The University of Patras.

Ultimate analysis was performed on all (23) the bulk coal samples, as well as on the light fraction of 12 coal samples (after applying density seperation; see below), using a Carlo Erba EAGER 200 C, H, N, S Automatic Analyzer calibrated against the AgroMAT CP-1 standard (certified reference material, SCP Science). The analysis was conducted at the Laboratory of Instrumental Analysis, School of Natural Sciences, University of Patras.

Polished blocks from 17 lignite samples were prepared according to ISO 7404-2 (2009) and examined using a LEICA DMRX coal petrography microscope.

Point counting for maceral analysis was conducted on the blocks in oil immersion under both white incident light and blue light excitation, 500x magnification (ISO 7404-3, 2009). The applied nomenclature followed the Stopes–Heerlen System as it is modified by ICCP (1971, 2001) and Sýkorová et al. (2005).

Huminite reflectance was measured on 4 blocks according to ISO 7404-5 (2009). The coal-petrography examination was performed at the Laboratory of Energy Raw Materials, Department of Geology, University of Patras.

Mineralogical analysis was performed (i) on all (23) the bulk coal samples, as well as on their residues after combustion at 350°C and 750°C ash; (ii) on the heavy fraction seperated applying density seperation (see further below) of 12 bulk coal samples; and (iii) on 26 inorganic sediment samples. The analysis was conducted at the Laboratory of Mineral & Rock Research, Department of Geology, University of Patras, using a Bruker D8 X-ray diffractometer equipped with LynxEye® detector. The scanning area covered the 2θ interval 4-70°, with a scanning angle step of 0,015° and a time step of 1 s. The mineral phases were qualified with the DIFFRAC^{plus} EVA® and quantified using a Rietveld-based quantification routine with the DIFFRAC^{plus} TOPAS® software.

About 11 bulk coal samples displaying high ash yields (up to 45.20 wt.%, db) were chosen for density separation. They were stirred in a $ZnCl_2$ solution of 1.8 g/cm^3 density, then centrifuged. The organic material (light fraction) floated and the inorganic one (heavy fraction) sank. Both the mineralogical composition of the heavy fraction and the chemical composition of the light fraction were determined *via* XRD and ultimate analysis, respectively.

The flow chart of the methodology applied to analyse the Hüsamlar lignite and inorganic samples is indicated in Figure 3.1.

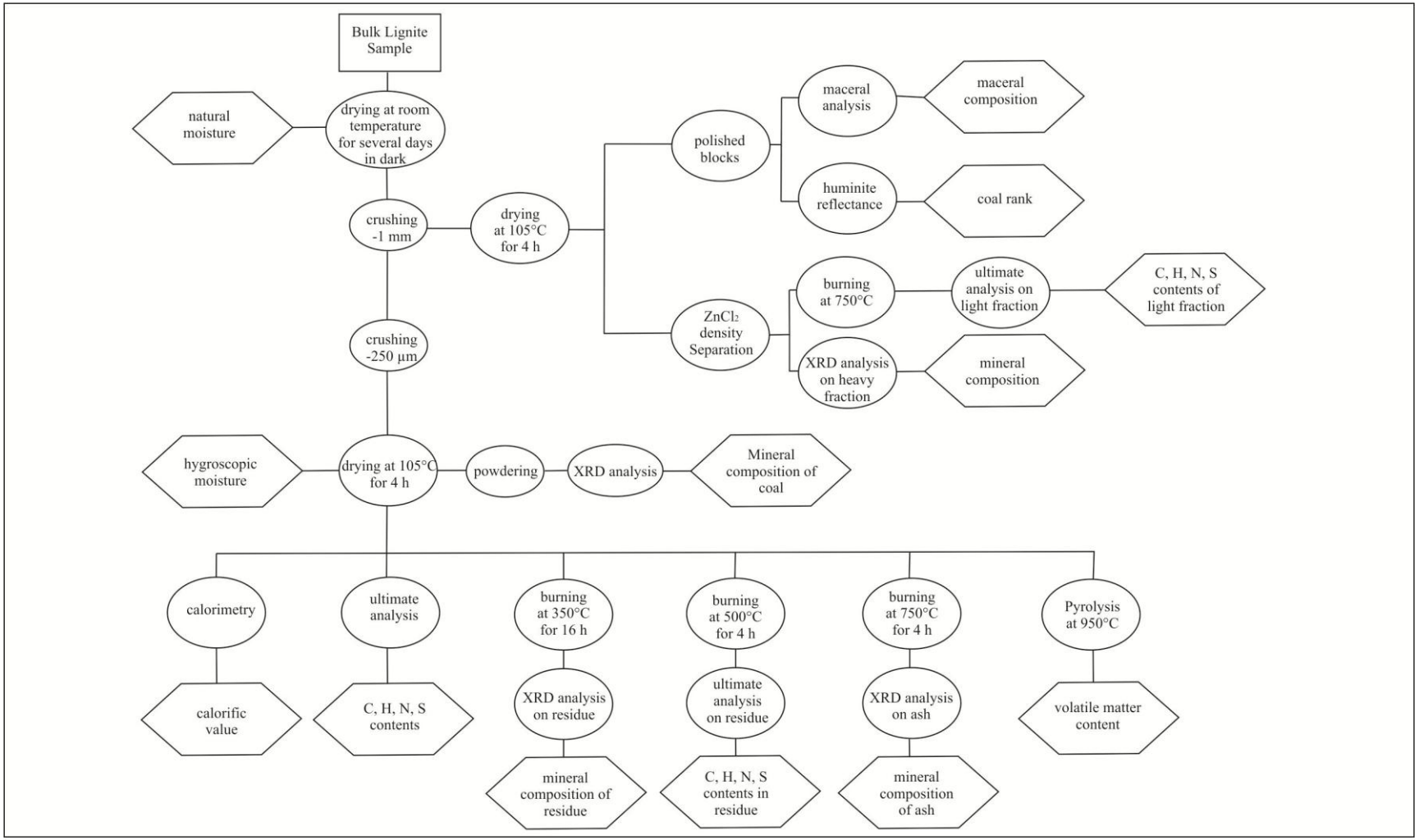

Figure 3.1 Flow chart of the methodology applied in the study Hüsamlar lignite samples (⬭ procedure, ⬡ result).

CHAPTER FOUR

RESULTS

4.1 Lithological Features

In the study area, there is one mineable coal seam consisting of alternating lignite benches (20 cm to 1.5 m thick) and inorganic intercalations (up to 3 m thick) (Fig. 4.1). The total thickness of the seam at the sampling site is about 60 m. On the basis of the existing mine terraces and the subsequent accessibility to certain parts of the coal seam profile the during sampling five sections (named A, B, C, D and E from top to bottom of the seam) were distinguished. The lithological details of the sampled profile are provided in Figure 4.2.

Figure 4.1 The sampled coal seam (red line) at Hüsamlar Open Pit.

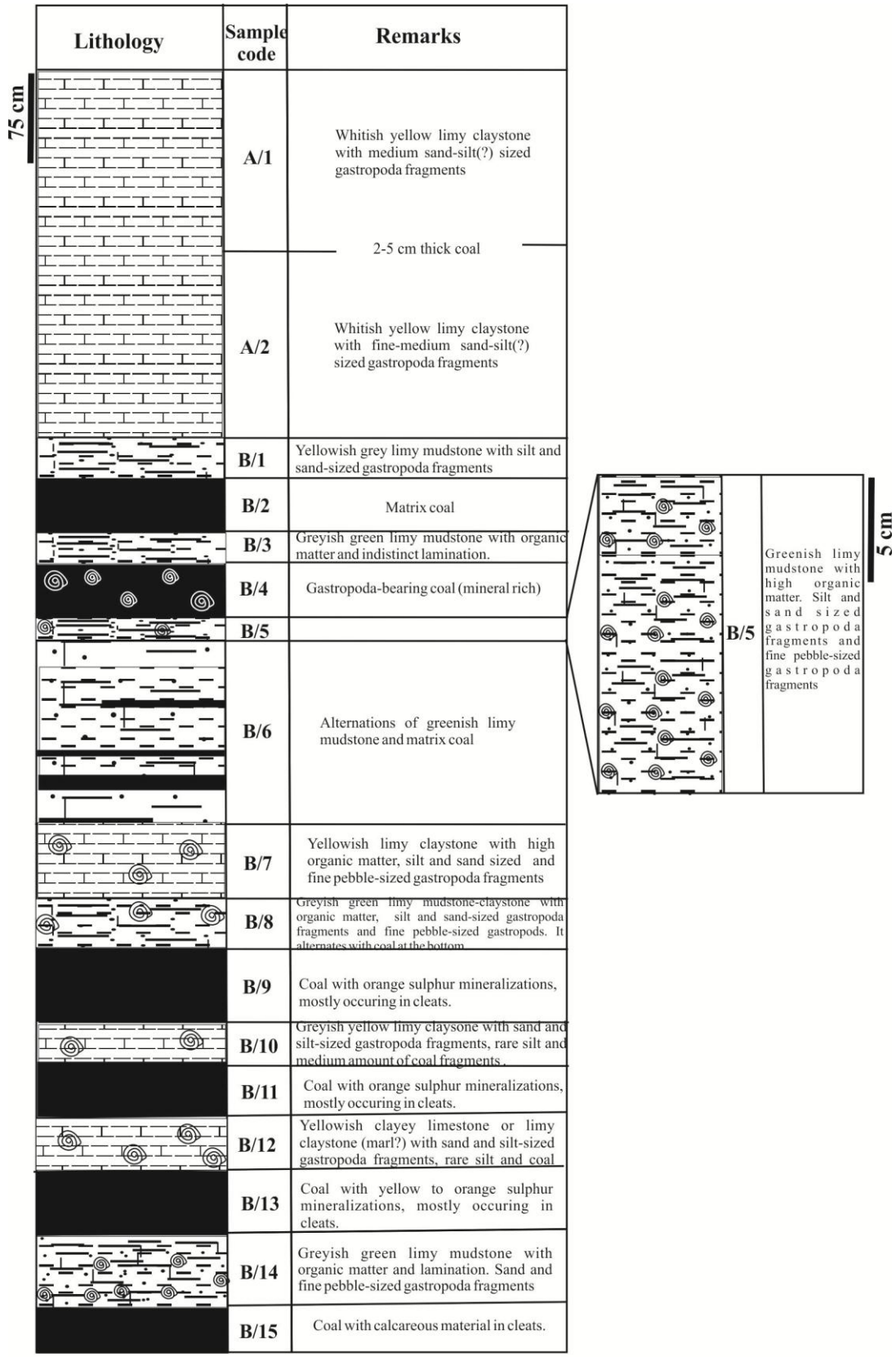

Figure 4.2 The studied lithostratigraphic column sampled at Hüsamlar Mine.

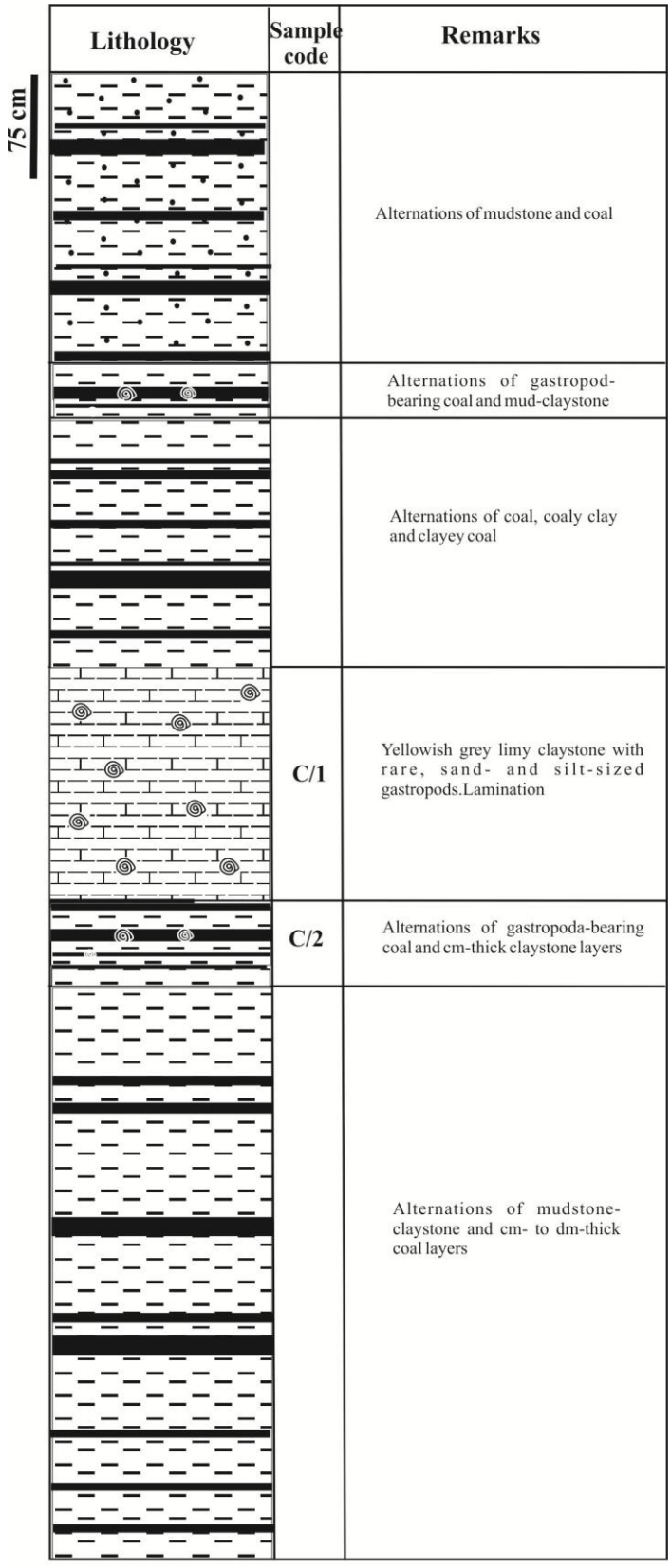

Figure 4.2 The studied lithostratigraphic column sampled at Hüsamlar Mine

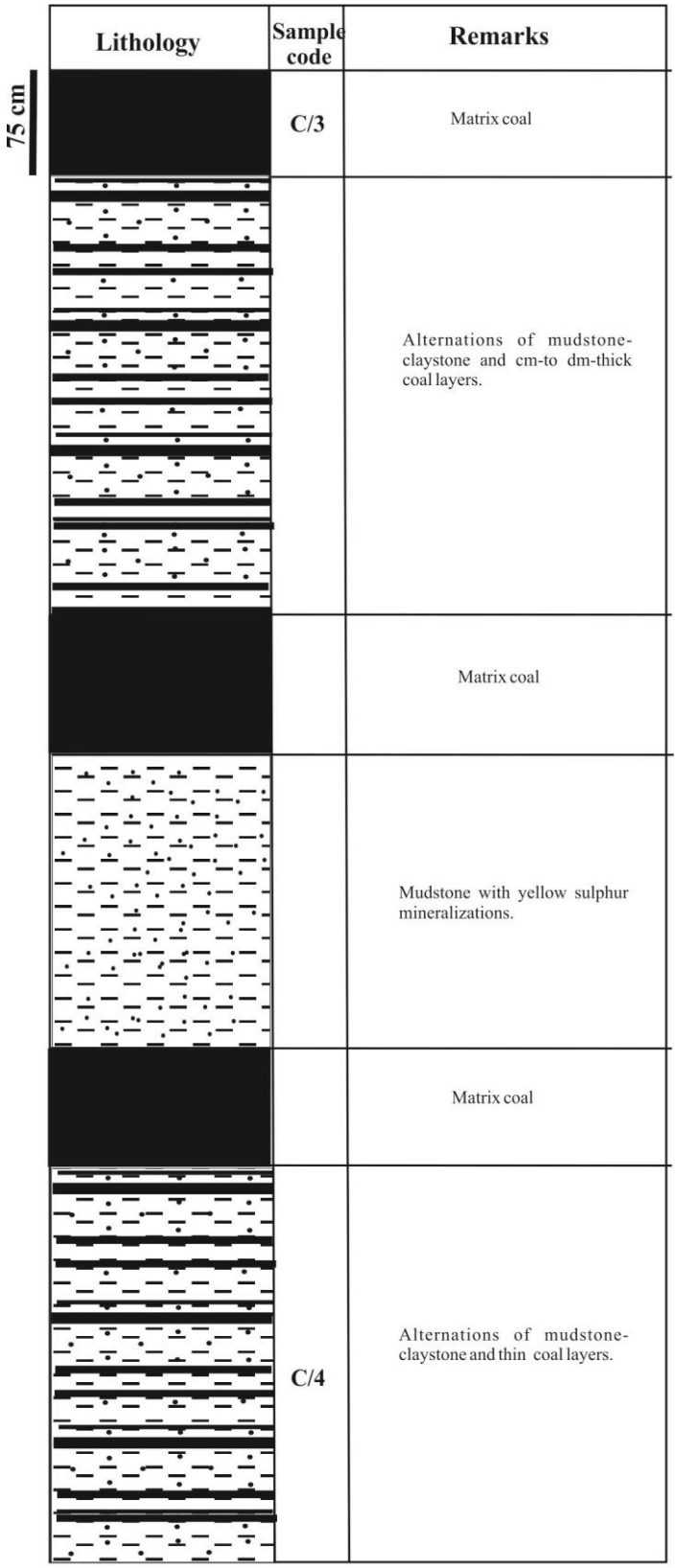

Figure 4.2 The studied lithostratigraphic column sampled at Hüsamlar Mine

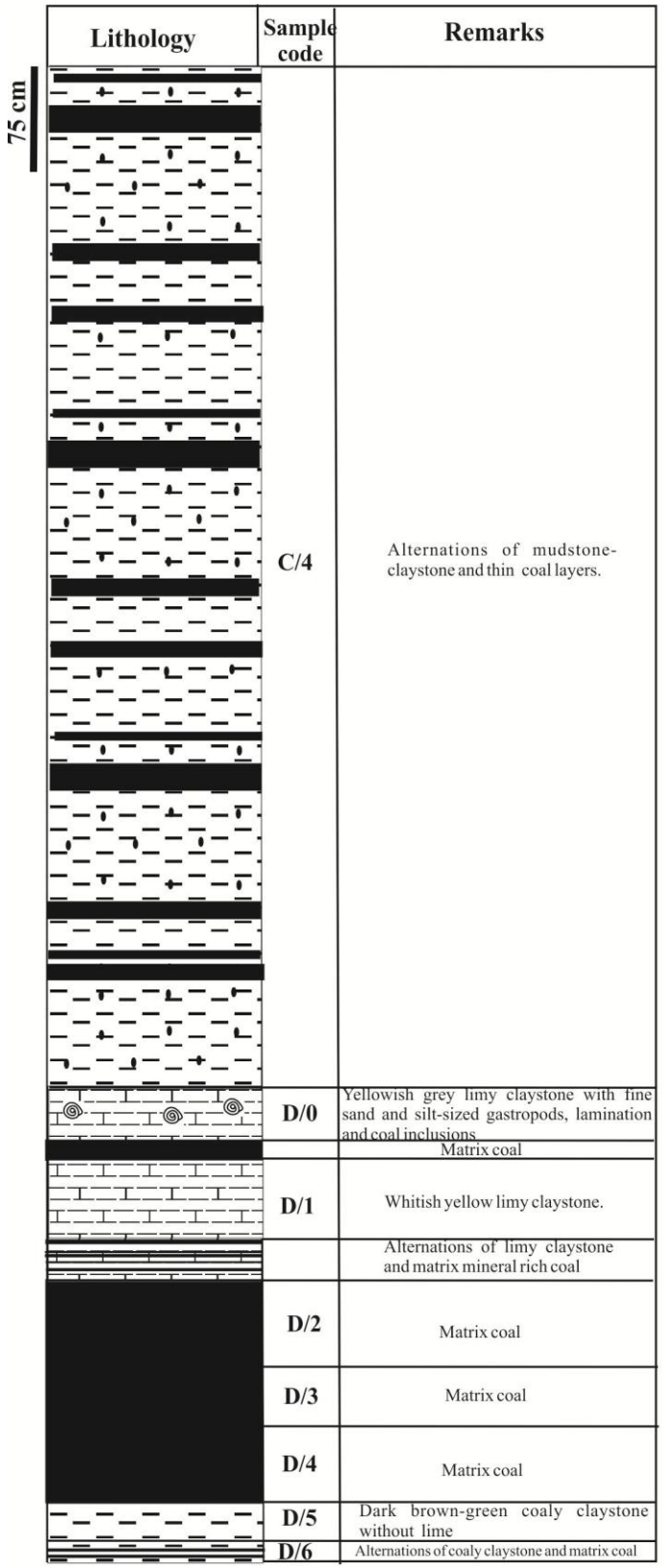

Figure 4.2 The studied lithostratigraphic column sampled at Hüsamlar Mine

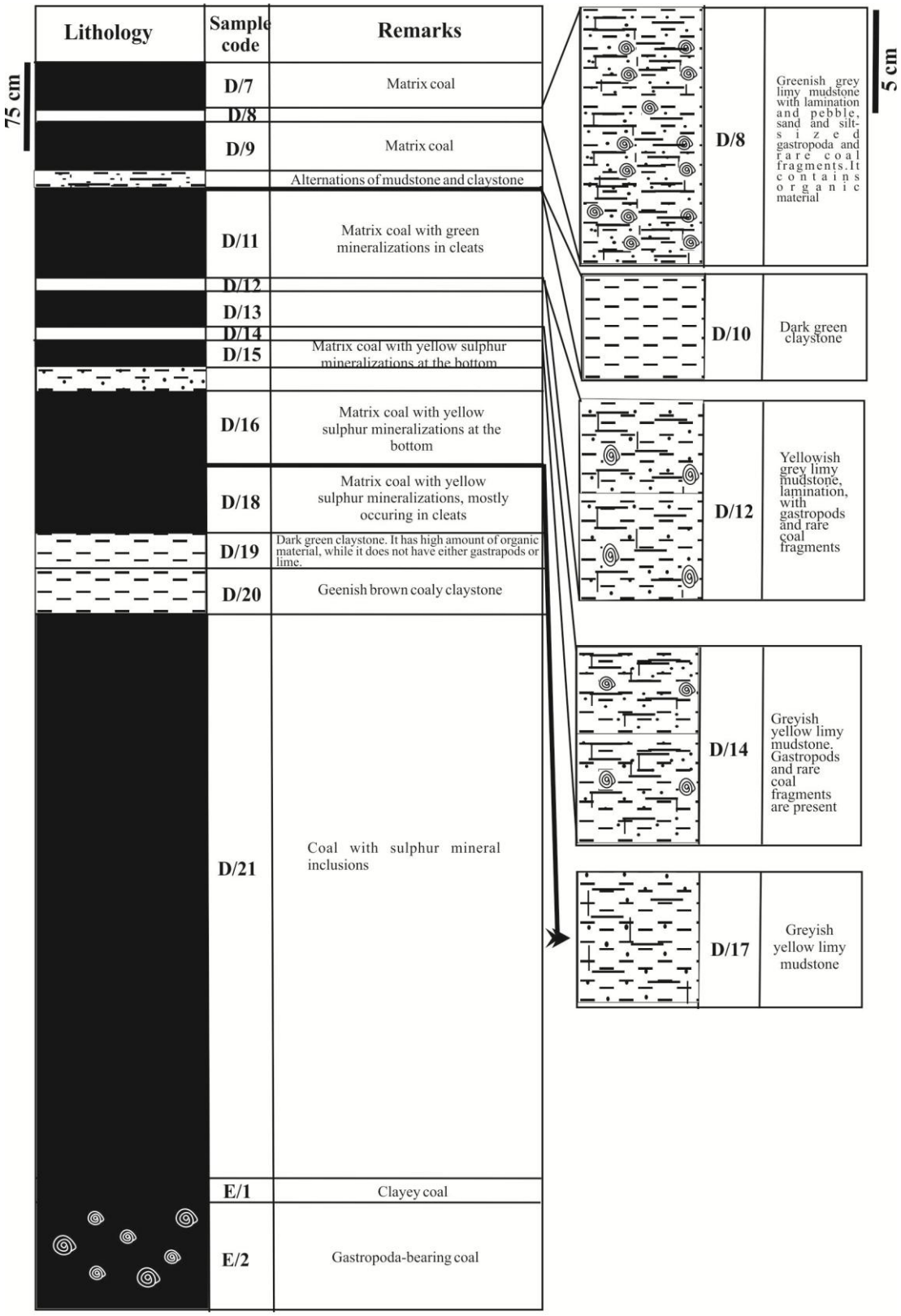

Figure 4.2 The studied lithostratigraphic column sampled at Hüsamlar Mine

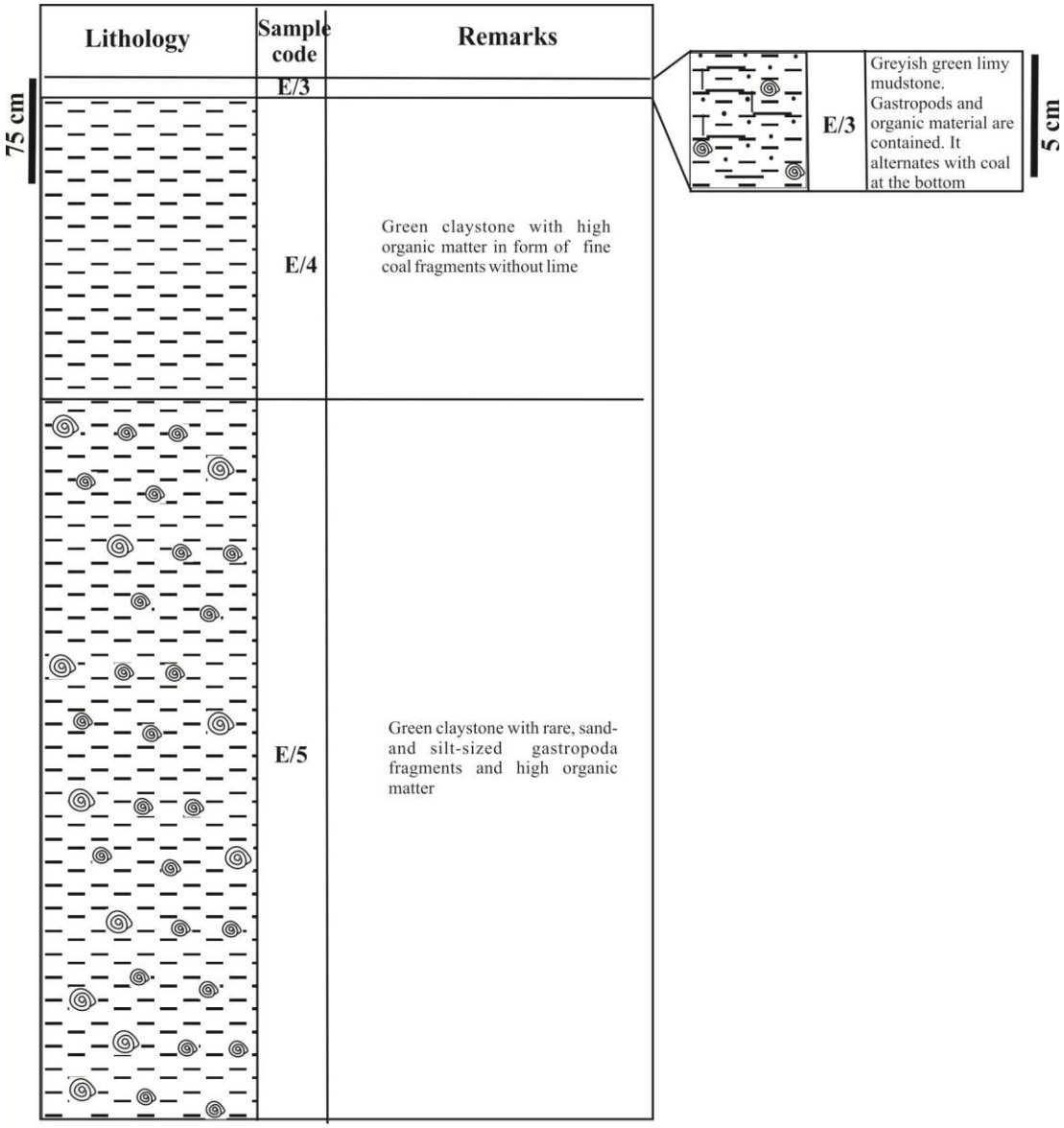

Figure 4.2 The studied lithostratigraphic column sampled at Hüsamlar Mine

The roof of the seam (section A) consists mostly of whitish yellow limy claystone (Appendix I, Figs. 3-4).

Section B consists of alternating benches of lignite and inorganic intercalations (Appendix I, Fig. 5). Gastropoda fragments ocur frequently (Appendix I, Fig. 6) and some lignite layers contain yellow to orange sulphur mineralizations, mostly occuring in cleats. About 15 samples were taken from this section (Fig. 4.2)

Section C consists of alternating benches of lignite and inorganic intercalations (Appendix I, Fig. 7). Some lignite layers contain yellow to orange sulphur mineralizations, mostly occuring in cleats. About four coal samples were taken from this section (Fig. 4.2).

Section D consists of alternating benches of lignite and inorganic intercalations (Appendix I, Fig. 8). Macroscopically, the lignite belongs to the light-to medium-gelified matrix lithotype. Some lignite layers contain yellow to orange sulphur mineralizations, mostly occuring in cleats. About 22 samples were obtained from this section (Fig. 4.2).

Section E is the lowest section of the seam and consists of alternating benches of lignite and inorganic intercalations (Appendix I, Fig. 9). About 5 samples were taken from this section (Fig. 4.2).

4.2 Laboratory Examination of Coal

4.2.1 Proximate Analysis

Proximate anaylsis of a coal sample comprises the determination of moisture, ash yield, volatile matter content, fixed carbon content and calorific value. The results of the proximate analysis are presented in Table 4.1.

The total moisture includes both surface and residual moisture; it does not include the crystalline water of the mineral matter and the water contained in the organic compounds. Moisture of the Hüsamlar lignite samples varies from 13.35 to 24.15 wt.%, with an average of 20.50 wt.%.

Ash is the residue remaining after the combustion of coal; it is composed primarily of oxides and sulfates. Ash is formed as the result of chemical changes that take place in the mineral matter during the ashing process. It shouldn't be confused with mineral matter, which is composed of the unaltered inorganic matter contained

in coal. Ash yield of Hüsamlar lignite samples varies from 10.47 to 45.20 wt.%, on dry basis, with an average of 20.73 wt.%.

Table 4.1 Proximate analysis results of Hüsamlar coal (db: dry basis, daf: dry, ash free basis, maf: moist, ash free basis).

Sample code	Moisture wt.%	Ash wt.%, db	Volatile Matter wt.%, daf	C_{fix} wt.%, daf	Calorific Value MJ/kg, maf
B/2	19.88	17.02	60.25	39.75	21.48
B/4	19.88	24.25	67.65	32.35	17.08
B/6	22.74	31.16	74.75	25.25	17.79
B/9	20.07	13.97	58.74	41.26	20.01
B/11	22.84	16.98	62.63	37.37	19.38
B/13	23.07	15.13	64.20	35.80	19.65
B/15	23.07	10.47	55.75	44.25	22.36
C/2	20.07	20.10	61.40	38.60	18.84
C/3	20.55	18.34	58.81	41.19	19.59
C/4	22.84	13.15	55.08	44.92	20.03
D/2	19.78	24.92	57.81	42.19	19.41
D/3	17.44	27.71	58.32	41.68	19.48
D/4	13.35	45.20	54.48	45.52	17.64
D/7	18.24	20.22	54.63	45.37	18.12
D/9	22.85	17.23	56.33	43.67	19.60
D/11	24.15	21.62	59.11	40.89	18.43
D/13	19.88	14.07	56.94	43.06	20.73
D/15	16.63	17.36	65.14	34.86	22.30
D/16	23.78	17.89	66.31	33.69	19.74
D/18	19.53	19.69	58.04	41.96	20.30
D/21	18.49	26.87	61.87	38.13	20.01
E/1	20.06	22.84	59.66	40.34	20.45
E/2	22.38	20.67	68.34	31.66	19.18

Fixed carbon is the solid combustible residue that remains after a coal particle is heated and the volatile matter is expelled. The fixed-carbon content of a coal is determined by subtracting the percentages of moisture, volatile matter, and ash from a sample. Fixed carbon content of Hüsamlar lignite samples varies from 25.25 wt.% to 54.52 wt.%, on dry-ash free basis (average 39.29 wt.%).

The gross calorific value (GCV) is defined as the quantity of heat released from coal combustion at constant volume. The gross calorific values of Hüsamlar lignite

samples are presented in Table 4.1; they varies from 17.08 to 22.36 MJ/kg, on moist, ash-free basis, with an average of 19.6 MJ/kg.

4.2.2 Ultimate Analysis

The ultimate analysis of coal comprises the determination of carbon, hidrogen, sulphur, nitrogen and oxygen (usually estimated by difference) contents of coal. The results of the ultimate analysis are presented in Table 4.2.

Carbon comprises both the organic carbon contained in the organic substances and the inorganic carbon present in the carbonate minerals. Carbon content of Hüsamlar lignite samples varies from 53.96 to 65.40 wt.%, on dry, ash-free basis, with an average of 61.14 wt.%.

Hydrogen is contained in the organic mater as well as in the water associated with the coal. Hydrogen content of Hüsamlar lignite samples varies from 6.08 to 10.00 wt.%, on dry-ash free basis, with an average of 7.67 wt.%.

Nitrogen occurs almost exclusively in the organic matter of coal. The original source of nitrogen is both plant and animal proteins. Nitrogen content of Hüsamlar lignite samples varies from 1.13 to 2.80 wt.%, on dry-ash free basis, with an average of 1.90 wt.%.

Sulphur occurs in three forms in coal: (1) as organic sulphur; (2) as inorganic sulphides that are, for the most part, primarily the iron sulphides pyrite and marcasite (FeS_2); and (3) as inorganic sulphates (e.g., Na_2SO_4, $CaSO_4$). Total sulphur content of Hüsamlar lignite samples varies from 2.26 to 10.34 wt.%, on dry, ash-free basis, with an average of 7.08 wt.%

Table 4.2 Ultimate analysis results of Hüsamlar coal (daf: dry, ash-free basis, *: calculated by subtraction: O = 100-C-H-N-S).

Sample	C	H	N	S	O*	H/C	O/C
	wt.%, daf					atomic ratio	
B/2	62.31	9.77	1.95	4.79	21.18	1.88	0.25
B/4	59.48	9.49	2.05	3.17	25.81	1.91	0.33
B/6	53.96	10.00	2.49	2.26	31.29	2.22	0.43
B/9	62.33	8.46	1.75	7.96	19.51	1.63	0.23
B/11	65.40	6.51	1.30	7.48	19.31	1.20	0.22
B/13	63.64	7.16	1.68	9.74	17.78	1.35	0.21
B/15	64.07	6.08	1.13	7.75	20.98	1.14	0.25
C/2	58.07	7.49	1.48	5.40	27.55	1.55	0.36
C/3	63.26	6.45	1.47	7.89	20.94	1.22	0.25
C/4	63.38	6.68	2.08	8.88	18.98	1.26	0.22
D/2	62.32	7.24	2.04	7.82	20.57	1.39	0.25
D/3	58.38	6.72	1.70	8.08	25.13	1.38	0.32
D/4	55.29	7.90	2.16	7.05	27.60	1.71	0.37
D/7	54.59	7.60	1.62	5.94	30.25	1.67	0.42
D/9	63.29	7.36	2.80	6.44	20.11	1.40	0.24
D/11	60.53	9.04	2.03	5.00	23.40	1.79	0.29
D/13	62.59	7.38	1.63	7.31	21.09	1.41	0.25
D/15	64.47	6.39	1.88	7.74	19.52	1.19	0.23
D/16	64.00	8.14	2.32	7.29	18.25	1.53	0.21
D/18	61.49	7.46	1.96	8.15	20.95	1.46	0.26
D/21	61.82	9.24	2.44	6.45	20.06	1.79	0.24
E/1	61.50	7.31	1.90	9.84	19.45	1.43	0.24
E/2	60.01	6.54	1.76	10.34	21.34	1.31	0.27

4.2.3 Coal Petrography

Coal Petrology deals with the study of coal in all its aspects, including organic and inorganic constituents, textures, structure, genesis and subsequent geological history, and properties. The key approach to Coal Petrology is Coal Petrography, i.e. the systematic description of coal in hand specimen and under the microscope.

4.2.3.1 Macerals of Hüsamlar Lignite Deposit

Coal is not a homogeneous substance but it consists of various constituents. In the same way as inorganic rocks are composed of minerals, coals consist of macerals. But there is a difference. Whereas a mineral is characterized by a fairly well-defined chemical composition, the uniformity of its substance, and the fact that most minerals are crystalline, a coal maceral varies widely in its chemical composition and physical properties and is amorphous (Stach, 1982).

The term "*maceral*" refers to the microscopically recognizable constituents of the coal. In order to distinguish the individual macerals it is necessary to choose parameters which can be determined under the microscope, such as reflectance, colour, shape and relief *sensu* polishing hardness. To exclude any ambiguity of the definitions of the various macerals, the International Committee for Coal and Organic Petrology (ICCP) has established standard nomenclature for the macerals according to their appearance under incident white light and blue-light excitation using oil immersion objectives and 250 to 500x total magnifition (ICCP, 1963).

4.2.3.1.1 Macerals of Huminite/Vitrinite Group. Huminite is the precursor of vitrinite. According to Sýkorová et al. (2005), the vitrinite and huminite systems have been correlated so that down to the level of sub-maceral groups, the two systems can be used in parallel. Huminite group macerals are defined only for lignite (soft brown coal). For subbituminous coal the vitrinite nomenclature is applied.

The huminite group is subdivided into three maceral subgroups including two macerals each; partly, maceral types, submacerals and maceral varieties can be further distinguished (Table 4.3).

Huminite is derived from parenchymatous and woody tissues and the cellular contents of roots, stems, barks and leaves composed of cellulose, lignin and tannin (Stach, 1982). Depending on the process of decomposition, the degree of humification and gelification and the rank, cell structures are preserved and visible to varying extents. The macerals of the huminite group are defined by the different

structures resulting from different sources and pathways of transformation within the mires (Sýkorová et al., 2005).

Macerals of humunite group are illustrated in Appendix II, Figure 1-2.

Table 4.3 Subdivision of the maceral group huminite (Sýkorová et al., 2005).

Maceral Group	Maceral Subgroup	Maceral	Maceral Type	Maceral Variety
HUMINITE	TELOHUMINITE	Textinite		A (dark)
				B (bright)
		Ulminite		A (dark)
				B (bright)
	DETROHUMINITE	Attrinite		
		Densinite		
	GELOHUMINITE	Corpohuminite	Phlobaphinite	
			Pseudophlobaphinite	
		Gelinite	Levigelinite	
			Porigelinite	

4.2.3.1.2 Macerals of Liptinite Group. Eight macerals are distinguished in the liptinite group (Table 4.4). These macerals consist of sporine, cutine, suberine, resins, waxes, fats and oils of vegetable origin.

Table 4.4 Macerals of the liptinite group (ICCP, 1963; Taylor et al., 1998)

Maceral Group	Maceral
LIPTINITE	Sporinite
	Cutinite
	Resinite (*incl*. fluorinite)
	Suberinite
	Alginite
	Liptodetrinite
	Chlorophyllinite
	Bituminite

All macerals of liptinite group (Appendix II, Figs. 3-4) are contained in the Hüsamlar samples at various contents.

4.2.3.1.3 Macerals of Inertinite Group. The inertinite group comprises macerals of diverse origin: (i) tissues (of fungi or higher plants) showing structural details; (ii) fine detrital fragments; (iii) gelified amorphous material of which the granular variety is generated preponderantly during coalification; and (iv) cell secretions altered by redox and biochemical processes during peatification (ICCP, 2001). Seven macerals are distinguished in the inertinite group (Table 4.5).

Table 4.5 Macerals of the inertinite group (ICCP, 2001)

Macerals with plant cell structures:	Fusinite
	Semifusinite
	Funginite
Macerals lacking plant cell structures:	Secretinite
	Macrinite
	Micrinite
Fragmented inertinite:	Inertodetrinite

Macerals of inertinite group (Appendix II, Fig. 5) display the lowest contents in Hüsamlar coal samples.

4.2.3.2 Maceral Composition

According to the results of point count analysis (Table 4.6) macerals of huminite group are the most abundant seen in Hüsamlar lignite samples. Textinite, ulminite and densinite are more common than attrinite, gelinite and corpohuminite. Huminite macerals vary from 69.8 to 94.0 %. Liptinite content strongly varies from 5.4 to 22.8 %. Inertinite macerals vary from 06 to 4.2 %. Semifusinite and inertodetrinite are seen commonly, while the others are rare.

Some oxidised particles are also contained in the Hüsamlar lignite (Appendix II, Fig. 6).

Table 4.6 Maceral composition (vol.% on dry, mineral matter-free basis) and mineral matter (vol.% on whole sample) of Hüsamlar lignite samples.

Samples / Maseral	B/2	B/4	B/6	B/9	B/13	C/2	C/4	D/3	D/4	D/7	D/9	D/11	D/13	D/16	D/18	D/21	E/2
HUMINITE	**77.7**	**69.8**	**75.9**	**77.8**	**85.9**	**86.5**	**92.0**	**94.0**	**86.6**	**92.9**	**76.7**	**83.3**	**91.1**	**85.7**	**86.8**	**88.0**	**91.7**
Textinite A	0.8		5.9	7.4	5.5	12.3	4.5	1.2	6.2	7.4	2.6	5.2		8.4	3.5	3.6	7.9
Textinite B		0.2	4.9	7.7	5.8	10.4	2.8	1.2	4.5	3.6	1.7	4.8		3.3	2.6		4.0
Texto-Ulminite A				3.1	9.2	4.9	5.4	4.2	6.4	10.6	7.8	5.6	6.4	6.2	7.5	4.5	5.5
Texto-Ulminite B				2.0	6.0	4.0	5.9	1.2	5.2	5.0	3.8	8.9		9.5	7.0	4.5	1.6
Eu-Ulminite A	8.8	8.2	9.6	4.5	4.6	5.8	8.3	13.9	5.2	12.5	14.2	10.4	11.5	9.1	9.3	9.4	11.9
Eu-Ulminite B	20.3	15.5	16.4	5.3	12.4	13.4	17.4	31.4	17.8	17.8	15.1	12.3	21.8	15.8	24.2	31.3	25.8
Attrinite	9.6	18.0	7.2	15.6	5.8	1.1		12.0	19.6	5.0	2.2	8.2	12.8	6.6	8.4	18.7	11.1
Densinite	31	15.8	21.9	18.7	19.1	26.8	37.4	22.9	15.7	22.8	22.4	19.3	30.8	18.4	19.4	13.3	10.4
Porigelinite	1.6	0.6	1.8	1.8	5.5	0.6	1.9	1.2	1.6	3.2	0.9	3.0	2.6	1.5		0.5	2.0
Levigelinite	3.6	1.4	3.7	4.3	7.6	4.7	7.0	1.8	2.1	2.5	4.7	2.6	3.9	4.0	3.1		2.4
Corpohuminite	2.0	10.1	4.5	7.4	4.4	2.5	1.4	3.0	2.3	2.5	1.3	3.0	1.3	2.9	1.8	2.2	9.1
INERTINITE	**4.0**	**2.0**	**1.4**	**2.9**	**2.3**	**4.2**	**2.4**	**0.6**	**3.8**	**1.1**	**7.3**	**3.0**	**1.2**	**3.7**	**3.5**	**1.3**	**2.8**
Pyrofusinite		0.2				0.2	0.2		0.5		1.3			0.4			
Degradofusinite		0.2	0.2	0.2	0.2	1.8			0.5								
Inertodetrinite	2.0	1.0	1.0	0.3		1.1	1.7		0.7		4.7			1.8	2.6		
Funginite				1.2	1.2				0.5	0.4		1.5				0.4	0.8
Semifusinite	2.0	0.6	0.2	1.2	0.9	1.1	0.5	0.6	1.6	0.7	1.3	1.5	1.2	1.5	0.9	0.9	2.0
LIPTINITE	**18.3**	**22.8**	**22.7**	**19.3**	**11.8**	**9.3**	**5.6**	**5.4**	**9.6**	**6.0**	**16.0**	**13.7**	**7.7**	**10.6**	**9.7**	**10.7**	**5.5**
Sporinite	4.4	2.1	2.2	1.2		0.5			0.3	0.7	0.9	1.1			0.9		0.4
Cutinite	7.2	5.4	3.3	1.2	1.2	1.6	0.2				1.3	1.5	1.3	2.2	2.2	0.9	
Resinite	0.4	1.4	0.8	1.2	0.9	2.0	0.7	3.0	2.1	1.1	1.7	2.6	1.3	1.1	3.1	3.2	1.2
Suberinite		5.8	3.1	2.4	2.8	1.4	0.9	0.6	1.7		0.9	2.2	1.3	1.1		0.4	2.0
Alginite	2.8	4.8	6.9	4.8	3.5	1.6	1.7		2.1	1.8	4.7	2.6	1.3	2.9	1.3	2.2	0.7
Liptodetrinite	3.5	8.7	6.5	3.9	3.4	2.2	2.1	1.8	3.1	2.1	6.5	3.7	2.5	3.3	2.2	4.0	1.2
Chlorophyllinite				4.6					0.3	0.3							
Total org. matter	**100.0**	**100.0**	**100.0**	**100.0**	**100.0**	**100.0**	**100.0**	**100.0**	**100.0**	**100.0**	**100.0**	**100.0**	**100.0**	**100.0**	**100.0**	**100.0**	**100.0**
Mineral Matter	6.6	20.4	31.4	2.8	5.5	3.2	2.8	6.3	4.7	7.0	4.5	8.2	2.5	6.8	5.8	5.9	3.5

4.2.3.3 Huminite Reflectance Measurement

Reflectance (in %) of a polished surface is the ratio of the intensity of the reflected light to this of the incident light (Stach, 1982).

Reflectance is strongly dependent on level of coalification, hence being a widely applied rank parameter. Reflectance may be measured on any of the coal macerals, although huminite/vitrinite macerals are always selected for rank studies. Their reflectance shows good correlation with other coal rank parameters (Stach, 1982). Additionally, the determination of vitrinite reflectance is a relatively rapid and precise technique, is applicable to coals of most ranks, and is independent of coal composition.

The random huminite reflectance was measured on four lignite blocks (Table 4.7).

Table 4.6 Huminite random reflectance (%) of Hüsamlar lignite

Sample	Reflectance			
	Minimum value	Maximum value	Mean value (%)	St. Deviation
B/2	0.242	0.331	0.274	0.024
B/13	0.182	0.357	0.231	0.031
D/4	0.237	0.359	0.276	0.027
E/2	0.176	0.371	0.231	0.046

4.2.4 Mineralogical Determinations

Coal is a complex mixture of organic and inorganic matter, containing fluid constituents and gaseous phases.

"Mineral matter" is defined by Gary et al. (1972) as "the inorganic material in coal". It is defined more significantly by Australian Standards (1995, 2000) as presenting "the sum of the minerals and inorganic matter in and associated with coal". Similar definations are provided by Harvey & Ruch (1986), and Finkelman (1994). All definitions meet three different types of inorganic components, namely:

- Dissolved salts and other inorganic substances in the coal's pore water;
- Inorganic elements incorporated within the inorganic compounds of the coal macerals; and
- Discrete inorganic particles (crystalline or non-crystalline) representing true mineral components.

The first two forms of mineral matter are described as non-mineral inorganics (Ward, 2002).

Quantitative anaylsis of minerals contributes to define coal quality. It may also be useful as an aid to stratigraphic correlation and to identify the mode of occurence and the mobility of particular trace elements. It is also a useful tool to evaluate the behaviour of particular coals in different utilization processes, such as the characteristics of fly ashes, slags and other combustion by-products (Ward, 2002).

X-ray diffraction patterns of bulk coal, 350°C residue and 750°C ash samples for the Hüsamlar lignite samples are given in Appendix III (Figs. 1-23).

4.2.4.1 The Bulk Coal Sample

The minerals found in 23 anaylsed bulk coal samples are listed in Table 4.8. The accuracy of the quantitative mineralogical analysis was checked using "Goodness of Fit (GOF)" rule, where the more the GOF value approaches one the better fit was achieved (Bish & Post, 1993). The GOF parameter ranges between 1.11 and 1.33 with an average of 1.24 showing that a good fit was achieved.

Silicates are the most common mineral in the samples with quartz being the most abundant with an average content of 32.9 wt.% of the crystalline mineral matter. It ranges between 9.0 and 57.9 wt.%. Mica is quantified in 8 samples with an average of 38.0 wt.%; it ranges between 2.1 and 65.1 wt.%. Orthoclase is quantified in three samples with an average of 10.3 wt.%, while albite is quantified only in one sample

Table 4.8 Rietveld-based quantification XRD results of Hüsamlar bulk coal samples, in wt. % of the crystalline phases (the numbers in parentheses in quantification errors. GOF: Goodness of fit, see text for details).

Mineral / Sample	*Carbonates*		*Sulphates*	*Silicates*					*Sulphide*	GOF
	Aragonite	**Calcite**	**Bassanite**	**Quartz**	**Orthoclase**	**Albite**	**Chlorite + Kaolinite**	**Mica**	**Pyrite**	
B/2	41.1 (2.4)	43.5 (2.1)		15.4 (2.1)						1.33
B/4	89.4 (0.6)	7.1 (0.4)							3.5 (0.5)	1.22
B/6	77.4 (0.5)	21.4 (0.5)							1.2 (0.2)	1.27
B/9				56.7 (6.1)					43.3 (6.1)	1.33
B/11			42.1 (1.8)	57.9 (1.8)						1.26
B/13										
B/15										
C/2		74.8 (0.9)		22.8 (0.8)					2.4 (0.3)	1.23
C/3				49.0 (1.6)	13.4 (1.0)			13.2 (2.3)	24.4 (1.1)	1.26
C/4										
D/2			6.6 (0.5)	38.8 (1.5)				40.3 (2.0)	14.2 (0.7)	1.26
D/3			10.3 (0.4)	27.7 (0.9)				45.6 (1.6)	16.4 (0.6)	1.19
D/4				25.6 (0.7)	2.1 (0.2)	3.9(0.5)	3.3(0.5)	65.1 (0.7)		1.26
D/7			27.4 (0.7)	30.3 (1.0)				13.9 (1.4)	28.5 (0.8)	1.11
D/9			11.2 (0.5)	53.0 (1.5)					35.8 (1.3)	1.26
D/11			14.4 (0.8)	9.0 (0.9)	15.3 (1.7)			41.2 (2.7)	20.1 (1.3)	1.21
D/13				28.0 (3.3)					72.0 (3.3)	1.32
D/15		44.1 (1.5)		13.6 (1.9)					42.3 (1.4)	1.26
D/16		7.9 (1.2)		41.0 (2.3)					51.1 (2.2)	1.28
D/18		3.7 (1.8)		39.0 (1.9)					57.3 (2.0)	1.24
D/21				23.0 (1.4)				41.1 (2.4)	35.9 (1.5)	1.20
E/1			6.8 (0.5)	15.2 (1.4)				43.6 (2.8)	34.4 (1.8)	1.22
E/2			43.8 (1.0)	46.6 (1.1)					9.6 (1.5)	1.16

with a value of 3.9 w.%. Clay minerals are quantified as chlorite and kaolinite only in one sample with a value of 3.3 wt.%.

Pyrite, as a sulphide mineral, is the second common mineral traced in 17 samples; it ranges between 1.2 and 72 wt.% with an average of 29.0 wt.%.

Carbonates are abundant especially in some samples. Calcite is the most abundant with an average of 28.9 wt.%; it ranges between 3.7 and 74.8 wt.% in 7 samples. Aragonite is quantified only in 3 samples with an average of 69.3 wt.%.

Bassanite, as a sulphate mineral, ranges between 6.6 and 43.8 wt.% in 8 samples with an average of 20.3 wt.%.

4.2.4.2 The 350°C Residue

Quantitative XRD analysis on coal and its 350°C residue shows that a number of mineral transformations accompanied by local exothermic reactions take place during low-temperature ashing (Vassilev et al., 1996).

The minerals found in 23 analysed 350°C residues are listed in Table 4.9. The GOF parameter ranges between 1.11 and 1.45 with an average of 1.27 showing that a good fit was achieved.

Silicates are the most common mineral group seen in all 350°C residue samples. Quartz is the most abundant with an average of 14.3 wt.%; it ranges between 2.1 and 39.4 wt.%. Mica ranges between 11.7 and 51.9 wt.% with an average of 27.2 wt.% in 11 samples. Orthoclase ranges between 8.4 and 35.2 wt.%. in 16 samples with an average of 20.2 wt.%. Albite ranges between 4.5 and 33.7 wt.% with an average of 16.7 wt.% in seven samples. Anorthite is quantified only in two samples with values of 25.3 and 14.8wt.%, respectively. Oligoclase, anatase and cordierite are quantified only in one sample with values of 29.9, 8.1 and 7.5 wt.%, respectively.

Table 4.9 Rietveld-based quantification XRD results of Hüsamlar 350°C residues, in wt.% of the crystalline phases (the numbers in parentheses indicate the quantification errors. GOF: Goodness of fit, see text for details).

Ar: Aragonite, Ca: Calcite, Si: Siderite, Ba: Bassanite, Anh: Anhydrite, Hae: Haematite, Q: Quartz, Orth: Orthoclase, Al: Albite, Olg: Oligoclase, Ana: Anatase, An: Anorthite, M: Mica, Crd: Cordierite, Ch: Chlorite, Kao: Kaolinite, Py: Pyrite.

Mineral / Sample	*Carbonates*			*Sulphates*		*Oxides*	*Silicates*									*Sulphides*	GOF
	Ar	**Ca**	**Si**	**Ba**	**Anh**	**Hae**	**Q**	**Orth**	**Al**	**Olg**	**Ana**	**An**	**M**	**Crd**	**Ch+ Kao**	**Py**	
B/2	14.2 (0.7)	16.3 (0.4)	4.3 (0.6)		16.0 (0.8)	1.6 (0.2)	4.7 (0.3)	8.4 (0.5)				25.3 (0.7)		7.5 (0.5)		1.7 (0.2)	1.38
B/4	51.6 (1.0)	9.9 (0.7)	4.0 (0.5)		23.9 (0.8)	2.7 (0.5)	7.9 (0.7)										1.36
B/6	57.5 (0.6)	22.3 (0.4)	2.2 (0.4)		15.9 (0.6)		2.1 (0.2)										1.25
B/9			3.9 (0.8)	8.2 (0.6)	58.9 (1.5)	5.4 (1.0)	15.5 (1.0)				8.1 (1.0)						1.45
B/11	3.6 (0.9)			8.4 (0.6)	42.3 (1.6)		9.0 (1.3)	19.0 (1.6)	17.7 (1.2)								1.28
B/13			10.1 (0.9)		71.0 (1.3)	1.1 (0.3)	17.8 (1.2)										1.38
B/15			3.7 (0.8)		57.7 (1.5)	1.3 (0.2)	10.9 (1.1)	11.6 (1.4)				14.8 (0.8)					1.41
C/2	5.7 (1.3)	37.4 (0.9)		5.9 (0.5)	16.4 (1.0)	1.2 (0.1)	11.6 (0.4)	16.7 (0.8)							3.8 (0.8)	1.3 (0.1)	1.34
C/3			7.0 (1.0)			7.7 (0.6)	33.4 (0.9)						51.9 (1.1)				1.37
C/4		7.3 (0.8)	4.2 (0.6)		34.4 (1.8)		14.1 (0.6)	22.4 (1.0)	17.6 (1.0)								1.42

Table 4. 9 (cont.)

D/2				17.5 (1.6)	4.5 (0.5)	26.9 (1.0)				44.8 (1.7)	6.3 (0.9)		1.29
D/3				15.9 (1.1)	4.7 (0.2)	21.5 (0.6)	10.3 (0.4)			38.8 (1.4)	7.8 (1.2)	1.0 (0.4)	1.22
D/4				7.6 (1.5)		39.4 (1.4)	13.6 (0.7)	4.5 (0.6)		24.5 (2.1)	9.4 (0.9)		1.33
D/7				28.4 (1.7)	6.5 (0.3)	16.2 (1.7)	17.0 (1.0)			31.9 (0.6)			1.11
D/9				21.9 (1.2)	7.0 (0.5)	13.2 (0.6)	18.8 (1.3)	17.6 (1.2)			21.5 (1.9)		1.21
D/11				29.3 (1.2)	6.0 (0.5)	4.8 (0.5)	17.4 (1.1)	12.5 (1.0)		30.0 (1.6)			1.16
D/13				21.9 (1.7)	9.9 (0.5)	16.8 (1.2)			29.9 (1.4)	21.5 (1.4)			1.17
D/15	23.6 (1.0)			20.1 (2.3)	11.4 (0.8)	9.8 (0.9)	35.1 (1.7)						1.22
D/16	10.7 (0.9)			20.8 (2.1)		18.2 (0.8)	15.1 (0.8)	33.7 (1.4)				1.5 (0.3)	1.28
D/18	6.1 (0.9)			21.6 (3.2)	10.0 (0.7)	11.7 (1.0)	21.8 (1.7)	13.3 (1.5)		15.5 (1.8)			1.16
D/21				16.4 (1.3)	7.4 (0.4)	12.5 (0.6)	31.7 (1.2)			11.7 (0.8)	20.3 (1.8)		1.18
E/1				16.3 (2.1)	10.8 (0.7)	6.1 (1.1)	35.2 (1.6)			35.6 (2.1)			1.14
E/2			6.5 (0.7)	23.7 (1.7)	4.0 (0.3)	4.6 (0.5)	28.4 (1.4)			32.8 (2.3)			1.15

Carbonates are quantified as aragonite, calcite and siderite. Calcite ranges between 6.1 and 37.4 wt.% with an average of 16.7 wt.% in eight samples. Aragonite ranges between 3.6 and 57.5 wt.% with an average of 26.5 wt.% in 5 samples. Siderite ranges between 2.2 and 10.1 wt.% with an average of 4.9 wt.% in 8 samples.

Anhydrite is the most common sulphate mineral with an average of 27.2 wt.%; it ranges between 7.6 and 71.0 wt.% in 22 samples. Bassanite ranges between 5.9 and 8.4 wt.% with an average of 7.3 wt.% in 4 samples only.

Haematite, as an oxide, is quantified in 18 samples with an average of 5.7 wt.%; it ranges between 1.1 and 11.4 wt.%.

4.2.4.3 The 750°C Ash

The main physicochemical processes taking place during high-temperature heating of coal can be summarized as: burning; volatilization of some compounds; decomposition; formation of new phases. transformation of some minerals and phases. Some mineral transformations taking place at 750°C, are the continuation of the transformation beginning at 350°C (Vassilev et al., 1996).

The minerals determined in 23 analysed 750°C ash samples are listed in Table 4.10. The GOF parameter ranges between 1.04 and 1.68 wt.% with an average of 1.23 showing that a good fit was achieved. Silicates are the most common mineral group. Quartz is the most abundant with an average of 10.8 wt.%; it ranges between 0.6 and 36.3 wt.%. Mica is quantified in 13 samples with an average of 12.5 wt.%; it ranges between 1.0 and 19.6 wt.%. Orthoclase is quantified in two samples with values of 1.4 and 12.6 wt.%. Albite, chlorite and kaolinite are quantified only in one sample with values of 7.0 and 7.9 wt.%, respectively.

Anhydrite, as a sulphate mineral, ranges between 15.4 and 94.0 wt.% with an average of 67.1 wt.%.

Table 4.10 Rietveld-based quantification XRD results of Hüsamlar 750°C ash samples, in wt. % of the crystalline phases (the numbers in parentheses indicate quantification errors. GOF: Goodness of fit, see text for details).

Mineral / Sample	*Sulphates*	*Oxides*		*Silicates*					GOF
	Anhydrite	**Haematite**	**Lime**	**Quartz**	**Orthoclase**	**Chlorite + Kaolinite**	**Albite**	**Mica**	
B/2	89.1 (0.3)	0.7 (0.1)	6.2 (0.1)	2.6 (0.1)	1.4 (0.2)				1.30
B/4	79.1 (0.4)	4.1 (0.3)	15.7 (0.2)	1.1 (0.1)					1.25
B/6	53.9 (0.9)	6.1 (0.4)	39.4 (0.8)	0.6 (0.1)					1.57
B/9	92.1 (0.3)	5.4 (0.2)		2.5 (0.2)					1.21
B/11	89.3 (0.3)	4.6 (0.2)		6.1 (0.2)					1.20
B/13	94.0 (0.3)	4.1 (0.2)		1.9 (0.2)					1.31
B/15	91.7 (0.3)	4.0 (0.2)		4.3 (0.2)					1.23
C/2	79.8 (0.4)	3.4 (0.3)	7.3 (0.2)	9.5 (0.2)					1.21
C/3	60.0 (0.8)	9.7 (0.3)		17.5 (0.4)				12.8 (0.8)	1.12
C/4	90.2 (0.3	2.8 (0.2)		7.0 (0.2)					1.24
D/2	41.4 (2.5)	11.2 (0.6)		27.8 (1.3)				19.6 (1.5)	1.19
D/3	36.5 (1.8)	14.1 (0.5)		28.2 (0.9)				21.2 (1.5)	1.14
D/4	15.4 (0.4)	1.8 (0.2)		36.3 (0.7)	12.6 (0.6)	7.9 (0.9)	7.0 (0.4)	18.9 (1.1)	1.37
D/7	34.4 (0.9)	27.8 (0.6)		22.0 (0.6)				15.8 (1.4)	1.04
D/9	69.1 (0.9)	10.2 (0.3)		10.0 (0.3)				10.7 (0.9)	1.21
D/11	65.3 (1.2)	12.4 (0.4)		7.3 (0.5)				15.0 (1.3)	1.18
D/13	72.8 (0.9)	14.3 (0.4)		5.2 (0.4)				7.7 (1.0)	1.13
D/15	82.3 (1.0)	12.1 (0.4)	1.0 (0.3)	3.6 (0.3)				1.0 (0.8)	1.15
D/16	79.0 (1.3)	11.4 (0.6)		6.8 (0.4)				2.8 (1.0)	1.16
D/18	67.0 (1.6)	19.2 (0.9)		9.8 (0.6)				4.0 (1.0)	1.11
D/21	44.0 (1.0)	19.1 (0.5)		21.6 (0.6)				15.3 (1.4)	1.21
E/1	52.1 (1.2)	20.4 (0.5)		9.4 (0.5)				18.1 (1.5)	1.12
E/2	65.3 (1.2)	26.6 (0.8)		8.1 (1.1)					1.68

Two types of oxides are quantified in 750°C ash samples. The first one, haematite, is the most abundant with an average of 10.7 wt.%; it ranges between 0.7 and 27.8 wt.%. The second one, lime is quantified in 5 samples, ranges between 1.0 and 39.4 wt.% with an average of 13.9 wt.%.

4.2.5 Density Separation

Density separation is a coal-cleaning process applied to remove mineral impurities from coal. It is based on the gravity seperation of coal from its associated gangue. The differences in density between pure coal particles and liberated mineral inclusions are sufficient to achieve almost complete separation fairly easily (Laskowski, 2001).

Since the density of coal (organic matter) is lower (<1.5 g/cm^3) than the density of mineral matter (inorganic matter, usually >2 g/cm^3), coal floats in a liquid of intermediate density whereas mineral matter sinks.

Arslan (2010) reported that density separation technique is not applicable on Hüsamlar lignite as a washing method. But in this study it is applied to get an idea about the separated parts of coal.

4.2.5.1 Ultimate Analysis on Light Fraction

Organic carbon content of the light fraction varies from 43.2 to 66.8 wt.%, on dry basis, with an average of 47.6 wt.%. Organic hydrogen content varies from 4.5 to 7.3 wt.%, on dry basis, with an average of 5.3 wt.%.Organic nitrogen content varies from 1.3 to 1.9 wt.%, on dry basis, with an average of 1.5 wt.%. Organic sulphur varies from 6.0 to 11.3 wt.%, on dry basis, with an average of 7.1 wt.%. The results of the ultimate anaylsis on light the fraction, are presented in Table 4.11.

Table 4.11 Ultimate analysis results of the light (organic matter-rich, float) fractions of Hüsamlar coal samples. All results in wt.%, on dry basis.

Sample	C_{lf}	H_{lf}	N_{lf}	S_{lf}
	wt.%, db			
B/2	49.9	5.7	1.5	6.0
B/4	46.8	5.3	1.5	6.6
B/6	45.9	5.7	1.9	6.9
D/2	43.3	4.7	1.3	6.0
D/3	44.9	4.7	1.3	6.3
D/4	43.2	4.5	1.4	6.1
D/7	43.9	4.6	1.2	7.2
D/11	47.4	5.2	1.4	6.9
D/21	43.6	4.8	1.5	6.7
E/1	66.8	7.3	1.9	11.3
E/2	47.9	5.3	1.3	7.8

4.2.5.2 Mineralogical Determinations on Heavy Fraction

The minerals determined in the heavy fraction of 8 coal samples are listed in Table 4.12. The GOF parameter ranges between 1.10 and 1.58 with an average of 1.31 showing that a good fit was achieved.

Silicates are the most common mineral group determined in all the sink fractions. Quartz is the most abundant phase ranging between 15.0 and 50.8 wt.% in 6 samples. Mica ranges between 10.0 and 45.8 wt.% in 5 samples, with an average of 32.1 wt.%. Orthoclase is quantified in two samples with values of 3.4 and 8.1 wt.%.

Hornblende is quantified only in one sample with value of 7.3 wt.%. Chlorite and kaolinite range between 7.2 and 37.4 wt.% in 6 samples with an average of 17.3 wt.%.

Carbonates are quantified as calcite and aragonite in three samples. Calcite values are 7.6, 9.0 and 10.8 wt.%, whereas aragonite contents are 5.1, 63.4 and 65.3 wt.%.

Table 4.12 Rietveld-based quantification XRD results of the heavy fraction of Hüsamlar coal samples, in wt.% of the crystalline phases (the numbers in parar indicate the quantification errors. GOF: Goodness of fit, see text for details).

Phs: phosphate. Ar: Aragonite, Ca: Calcite, Ba: Bassanite, Gy: Gypsum, Jr: Jarosite, Q: Quartz, Orth: Orthoclase, Al: Albite, M: Mica, Horn: Hornblende, Ch: Chlorite, Kao: Kaolinite, Mar: Marcasite, Py: Pyrite, Viv: Vivianite

Sample	***Carbonates***			***Silicates***						***Sulphides***		***Phs.***	**GOF**
	Ar	**Ca**	**Ba**	**Q**	**Orth**	**Al**	**M**	**Horn**	**Ch + Kao**	**Mar**	**Py**	**Viv**	
B/2	5.1 (1.1)	9.0 (0.6)		15.0 (0.8)	3.4 (0.7)	23.4 (1.5)			37.4 (2.0)		6.7 (2.6)		1.30
B/4	63.4 (1.5)	7.6 (0.4)	4.9 (0.4)					7.3 (0.7)	16.8 (1.3)				1.46
B/6	65.3 (1.0)	10.8 (0.3)							10.0 (1.1)		2.4 (0.3)	11.5 (0.6)	1.58
D/2				50.8 (1.4)		3.0 (0.5)	20.9 (2.0)			3.8 (0.7)	21.5 (0.7)		1.22
D/3				38.2 (0.9)			42.3 (1.3)		7.2 (0.7)		12.3 (0.3)		1.26
D/4				46.3 (0.8)	8.1 (0.5)	6.4 (0.4)	21.9 (0.9)		16.7 (0.8)		0.6 (0.1)		1.43
D/7				32.5 (1.2)			29.5 (2.0)		15.4 (1.9)		22.6 (0.8)		1.10
D/21				17.2 (0.7)			45.8 (1.8)				37.0 (1.2)		1.14

Pyrite (0.6 and 37.0 wt.% in 7 samples) and marcasite (3.8 and 15.8 wt.% in 2 samples), sulphide minerals, are also determined.

Vivianite, a phosphate mineral, is quantified only in one sample with a value of 11.5 wt.%.

X-ray diffraction patterns of heavy fraction (organic matter) of Hüsamlar coal samples are given in Appendix III (Figs. 24-34).

4.3 Inorganic Sediments

4.3.1 XRD Analyse of Dirt Bands

The Hüsamlar coal seam consists of alternations of coal and inorganic sediments which are excavated together. The mineral matter content of coals and surrounding country rock affects the washability of coal and consequently the ash yield of the clean coal. Mineral impurities affect the suitability of coal as a boiler fuel; the low ash fusion point causes deposition of ash and corrosion in the heating chamber and convection passes of the boiler (Thomas, 2002).

Carbonates constitute the most common mineral group determined in 25 inorganic sediment samples. These carbonates are mainly aragonite and calcite. Silicates are common in about half of the samples which are collected from the bottom layers (Sections D and E; see Fig. 4.2). These silicates are quartz, feldspar, pyrite, micas and clay minerals. Gypsum is present only in two samples (Table 4.13).

Table 4.13 Qualitative mineral composition of the inorganic intercalations of Hüsamlar lignite seam

Ar: Aragonite, Ca: Calcite, Gy: Gypsum, Haem: Haematite, Q: Quartz, Fel: Feldspar, Py: Pyrite, M: Mica, Ch: Chlorite, Kao: Kaolinite.

Mineral / **Sample**	***Carbonates***		***Sulphate***	***Oxide***	***Silicates***				
	Arg	Cal	Gy	Haem	Q	Fel	Py	M	Ch + Kao
A/1	+	+		?					
A/2	+	+		?					
B/1	+	+							
B/3	+	+					?		
B/5	+	+					+		
B/7	+	+					?		
B/8	+	+					?		
B/10		+							
B/12	+	+					?		
B/14	+	+					?		
C/1	+	+							
D/0	+	+					?		
D/1		+							
D/5						+		+	+
D/6			+		+			+	+
D/8	+	+					?		
D/10			+		+	?		+	+
D/12	+	+							
D/14	+	+							
D/17	+	+							
D/19					+	?		+	+
D/20					+		+	+	+
E/3	+	+			+		+		
E/4					+	?		+	+
E/5		+			+	?		+	+

CHAPTER FIVE
DISCUSSION

Considering the random reflectance of huminite (0.23-0.27%; see Table 4.7), Hüsamlar coal is classed between Torf and Weichbraunkohle according to the German, peat and lignite according to the American classification schemes (Fig. 5.1). Of course, huminite reflectance is not an appropriate parameter for rank determination in low rank coals. The volatile matter content (54.48-74.75%, on dry, ash-free basis; see Table 4.1) being a reliable rank parameter, is dependent upon the nature of precursor materials in low rank coals. This variability is significant even for samples from the same coal bed (Taylor et al., 1998). The C content (54-65.4%,on dry, ash-free basis; see Table 4.2) also points to a peat to lignite rank. The moisture (13.35-24.15%; see Table 4.1) cannot be considered reliable for rank determination, as the samples were picked up close to the surface and they may have lost some water, despite the fact of the channel sampling. For lignite the gross calorific value (17-22.4 MJ/kg or 4060-5350 kcal/kg on a dry, mineral matter-free basis) serves as a reliable rank parameter, particularly in low rank coals (Taylor et al., 1998). Considering the gross calorific values the Hüsamlar coal belongs to the Mattbraunkohle according to the German classification scheme, between lignite and subbituminous coal C according to the American one (Fig. 5.1). Of course, the very high S content (up to 10%, on dry, ash-free basis; see Table 4.2) occuring mostly in form of pyrite (Table 4.8), significantly affects the calorific value increasing the heat produced during combustion; thus, also the calorific value should be considered with precaution in this case.

According to ECE-UN (1998) the Hüsamlar coal is a medium- to low-grade, low rank coal B to A (Fig. 5.2).

From the C, H, O contents determined, the O/C and H/C atomic ratios were also calculated (Table 4.2). Although this method is not accurate regarding the organic C, H, N, S values, as well as those of oxygen being calculated and not directly determined, it can provide a general idea of the coalification degree of the samples.

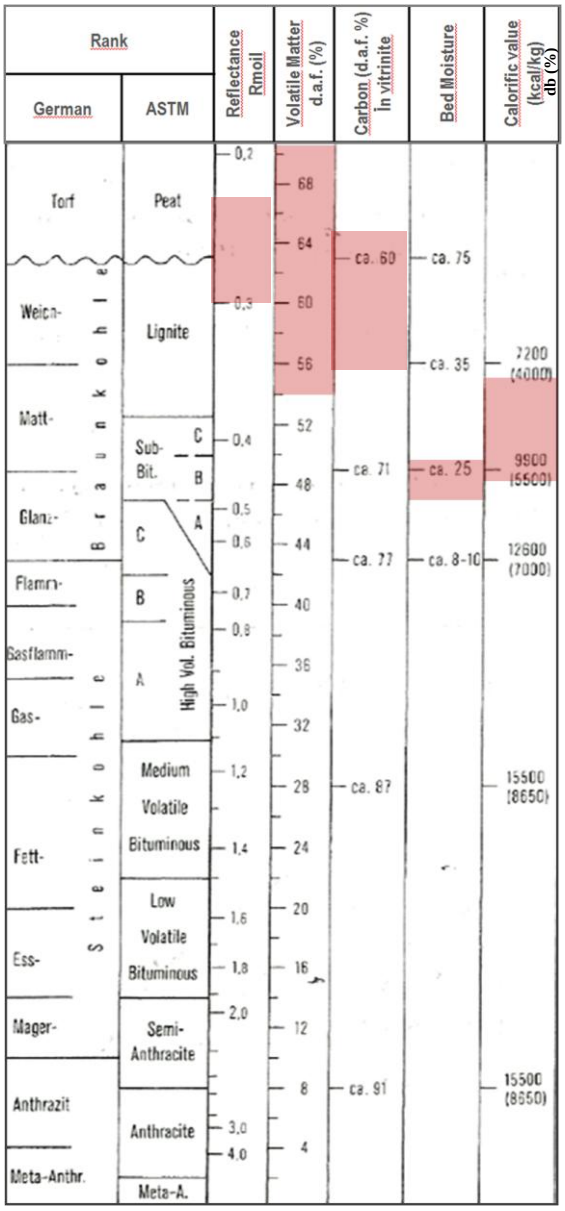

Figure 5.1 Rank determinations of the Hüsamlar lignite samples according to the German and North American classifications (after Taylor et al., 1998).

The Hüsamlar lignite samples are plotted mostly close to the sapropelic coals on the van Krevelen diagram (Fig. 5.3). Although this sounds remarkable, it can be explained considering the results of the coal-petrography examination (Table 4.6).

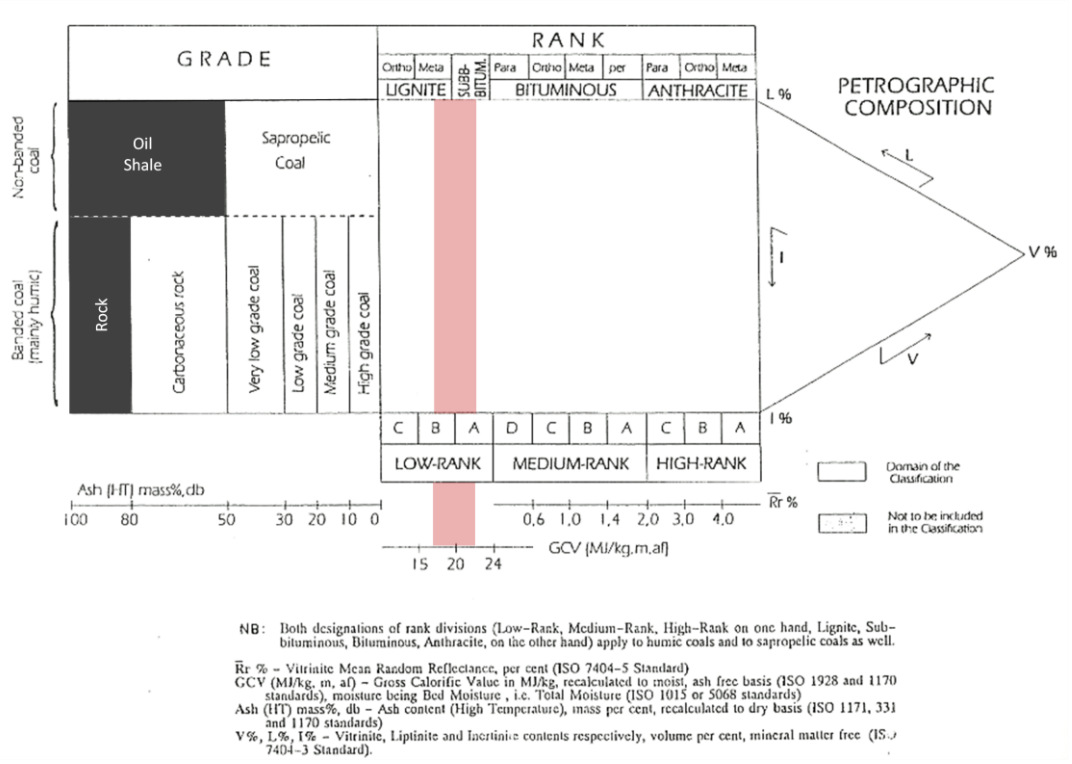

NB: Both designations of rank divisions (Low-Rank, Medium-Rank, High-Rank on one hand, Lignite, Sub-bituminous, Bituminous, Anthracite, on the other hand) apply to humic coals and to sapropelic coals as well.

$\bar{R}r$ % – Vitrinite Mean Random Reflectance, per cent (ISO 7404-5 Standard)
GCV (MJ/kg, m, af) – Gross Calorific Value in MJ/kg, recalculated to moist, ash free basis (ISO 1928 and 1170 standards), moisture being Bed Moisture , i.e. Total Moisture (ISO 1015 or 5068 standards)
Ash (HT) mass%, db – Ash content (High Temperature), mass per cent, recalculated to dry basis (ISO 1171, 331 and 1170 standards)
V%, L%, I% – Vitrinite, Liptinite and Inertinite contents respectively, volume per cent, mineral matter free (ISO 7404-3 Standard).

Figure 5.2 Rank determination of the Hüsamlar lignite samples according to the of ECE-UN (1998) classification.

Significant contents of huminite macerals are gouped under “type A” of telohuminite (textinite, ulminite); these macerals appear darker under white incident light and fluorescent under blue-light excitation in comparison to these of “type B” due to finely dispersed resin contained in the telohuminite; the latter results in high hydrogen content shifting to higher H/C values.

The term “coal facies” refers to the primary genetic types of coal, which are dependent on the environmental conditions under which peat was accumulating (Fig. 5.4). The facies of a coal expresses itself through the maceral and mineral contents of the coal, through certain of its chemical properties, which are largely independent of rank (Stach, 1982).

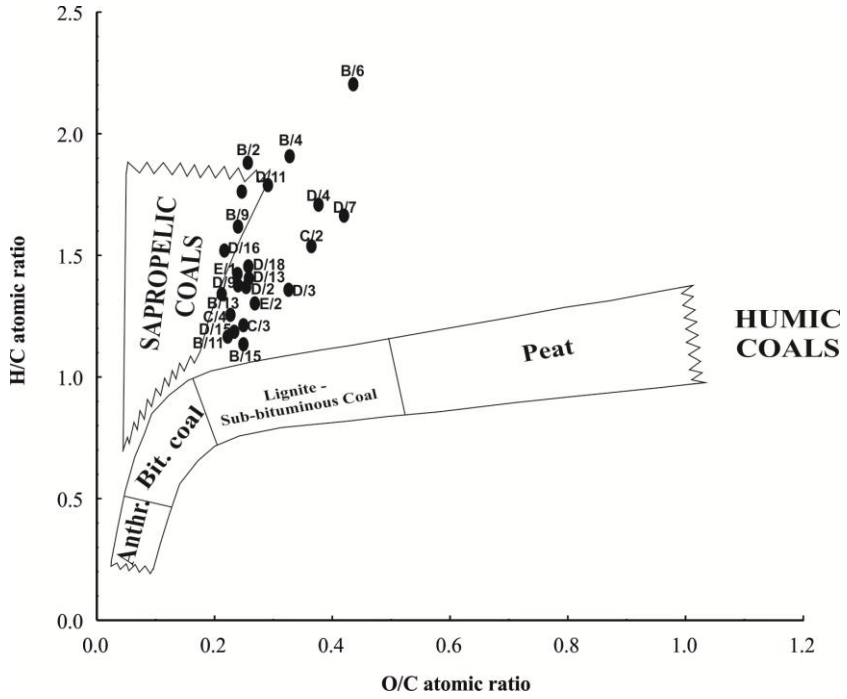

Figure 5.3 Plot of the Hüsamlar lignite samples on the van Krevelen diagram (maturity fields after Killops and Killops, 1993).

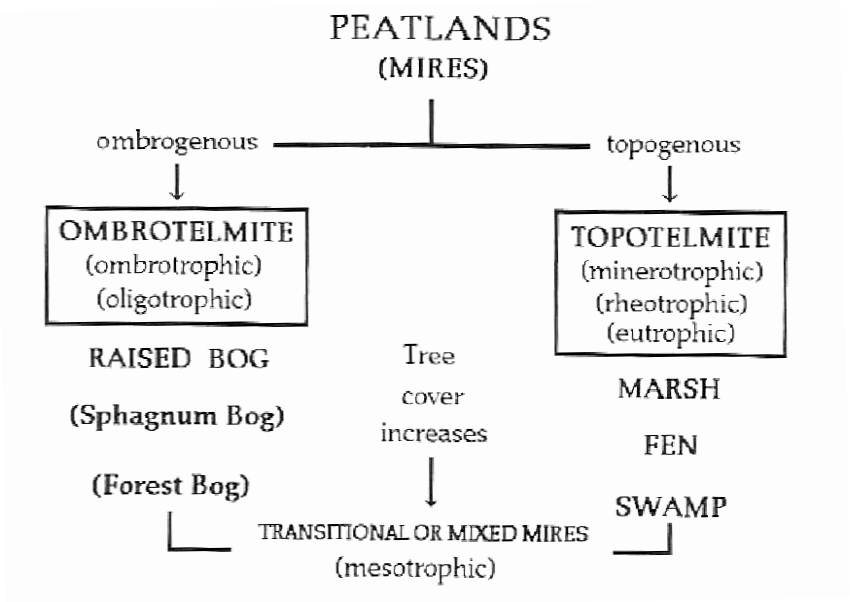

Figure 5.4 Classification of mires and their peat (from Diessel, 1992; partly after Grosse-Brauckmann, 1980; Martini & Glooschenko, 1984; Moore, 1987).

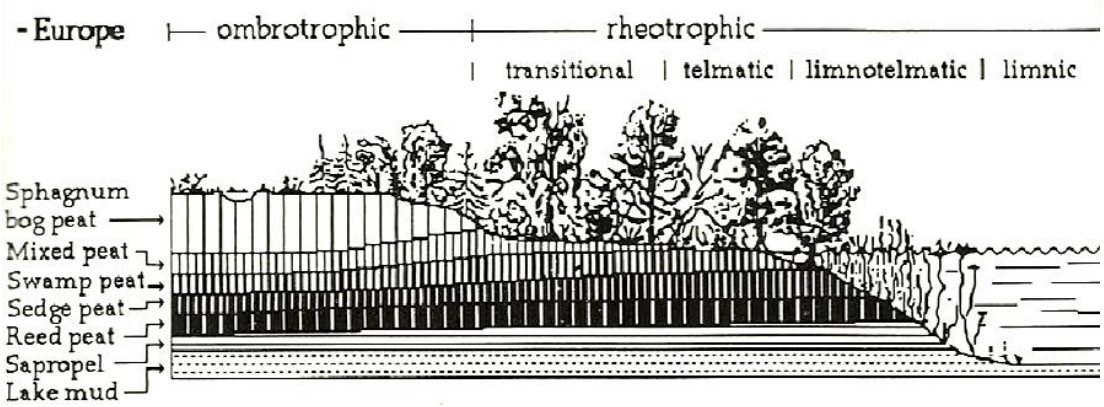

Figure 5.5 Fresh-water peat formation by terrestrialisation. Not to scale (Spackman et al., 1966, 1969; Diessel, 1992).

Coal depositional environment can be assessed through the presence or absence of certain macerals (Teichmüller, 1989) and hence, maceral indices were established and applied in order to describe some genetic features of coals (e.g. von der Brelie & Wolf, 1981; Diessel, 1986, 1992; Kalkreuth et al., 1991a, b; Lamberson et al., 1991; Hawke et al., 1999; Singh & Singh, 2000; Kalaitzidis et al., 2004). Of course, there are some limitations regarding the application of maceral ratios to define the depositional environment, as seen in recent studies (Crosdale, 1993; Wüst et al., 2001; Moore & Shearer, 2003). These studies mainly refer to ombrogenous peat, indicating that the petrographic features of the organic matter displayed no significant correlation with the tectonic setting or climate. In topogenous mires, the tectonic and the sedimentary regimes in the surrounding area strongly affect coal formation. So the exclusive use of coal petrography to interpret the depositional palaeoenvironment should be avoided (Kalaitzidis et al., 2004). The use of maceral ratios is only indicative and complementary to the sedimentological features and not a panacea for describing and reconstructing the palaeoenvironmental conditions in this study.

Mukhopadhyay (1989) proposed the relevant ternary diagram providing general information about the dominant vegetation type in the palaeomire and the oxic/anoxic conditions that pravailed during peat accumulation.

The maceral composition of each Hüsamlar coal sample is plotted on this ternary diagramme (Fig. 5.7). Almost all of the lignite samples are projected to the lowest part displaying relatively anoxic conditions suggesting rather high water table in the palaeomire.

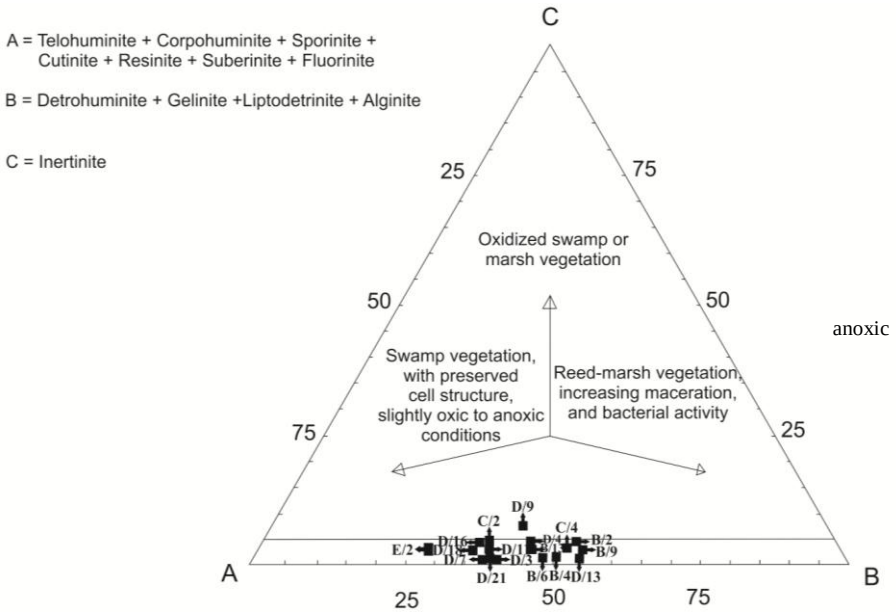

Figure 5.6 ABC ternary plot of the Hüsamlar lignite samples (after Mukhopadhyay, 1989).

The Tissue Preservation (TPI) and Gelification Indices (GI) proposed by Diessel (1992), as well as the Groundwater Influence (GWI) and Vegetation Indices (VI) proposed by Calder et al. (1991) have been also calculated in an attempt to reconstruct the depositional palaeoenvironment of the Hüsamlar lignite deposit.

In this study, the ratios as being modified by Kalaitzidis et al. (2001) are applied; modifications were applied in the TPI, GI, GWI and VI indices (Table 5.1).

Table 5.1 TPI, GI, GWI and VI indices calculated on the basis of the results of maceral analysis (Table 4.5)

Samples / Indices	B/2	B/4	B/6	B/9	B/13	C/2	C/4	D/3	D/4	D/7	D/9	D/11	D/13	D/16	D/18	D/21	E/2
TPI	0.7	0.9	1.2	0.9	1.3	1.6	1.0	1.5	1.2	1.8	1.4	1.5	0.8	1.7	1.7	1.7	2.5
GI	4.7	2.6	3.0	1.4	3.5	2.2	8.7	5.3	1.7	4.5	5.1	3.1	5.6	3.1	4.0	2.8	2.7
GWI	1.1	1.2	1.4	0.8	0.9	0.7	1.1	0.5	0.4	0.6	0.7	0.7	0.8	0.6	0.5	0.3	0.4
VI	0.9	0.8	1.1	0.8	1.6	1.8	1.1	1.6	1.3	1.9	1.3	1.7	0.9	1.8	1.8	1.5	2.7

The TPI, GI, GWI and VI indices are calculated as follows:

$$TPI = \frac{\text{telohuminite + corpohuminite + fusinite}}{\text{attrinite + densinite + gelinite + inertodetrinite}}$$

$$GI = \frac{\text{ulminite + gelohuminite + densinite}}{\text{textinite + attrinite + inertinite}}$$

$$GWI = \frac{\text{gelohuminite + densinite + mineral matter}}{\text{telohuminite + attrinite}}$$

$$VI = \frac{\text{telohuminite + fusinite + semifusinite + cutinite + sporinite + suberinite + resinite}}{\text{detrohuminite + inertodetrinite + other liptinite macerals}}$$

*Other liptinite macerals are alginite, liptodetrinite, chlorophyllinite, fluorinite, bituminite.

The Tissue Preservation Index (TPI) is a measure of the humification degree of the initial organic matter. TPI is an indicator of the degree of organic tissue preservation in the palaeomire, as well as a function of the contribution of arboreal vegetation to peat formation. The TPI values show that arboreal vegetation used to be more dominant than the herbaceous one in the Hüsamlar palaeomire. The Gelification Index (GI) reflects the homogenization (*sensu* gelification) of the organic matter. The calculated TPI and GI values (Table 5.1) are plotted on the diagram (Fig. 5.7).

The Ground Water Influence (GWI) is an indicator of the hydrogeological conditions, whereas the Vegetation Index (VI) is an indicator of the nature of the peat-forming vegetation. Calculated GWI and VI values (Table 5.1) are plotted on the GWI/VI diagramme (Fig. 5.8). Most of the samples are projected to the fen peat-forming environment, under mesotrophic conditions (Fig. 5.8).

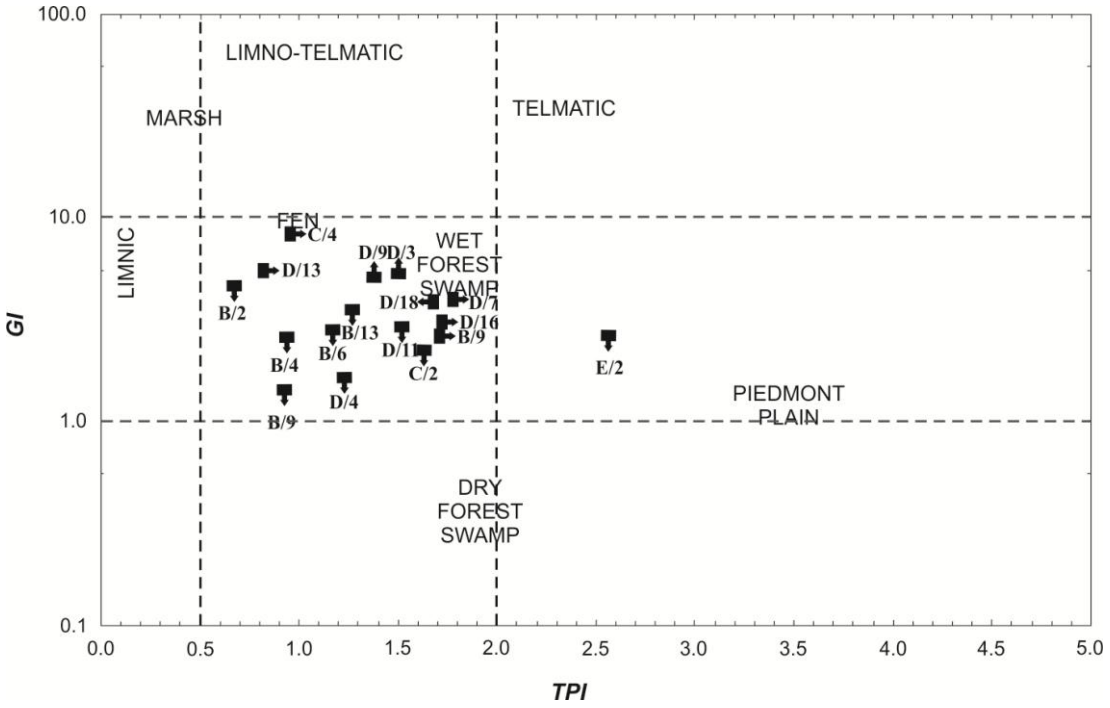

Figure 5.7 The TPI/GI coal-facies diagramme after Diessel (1992).

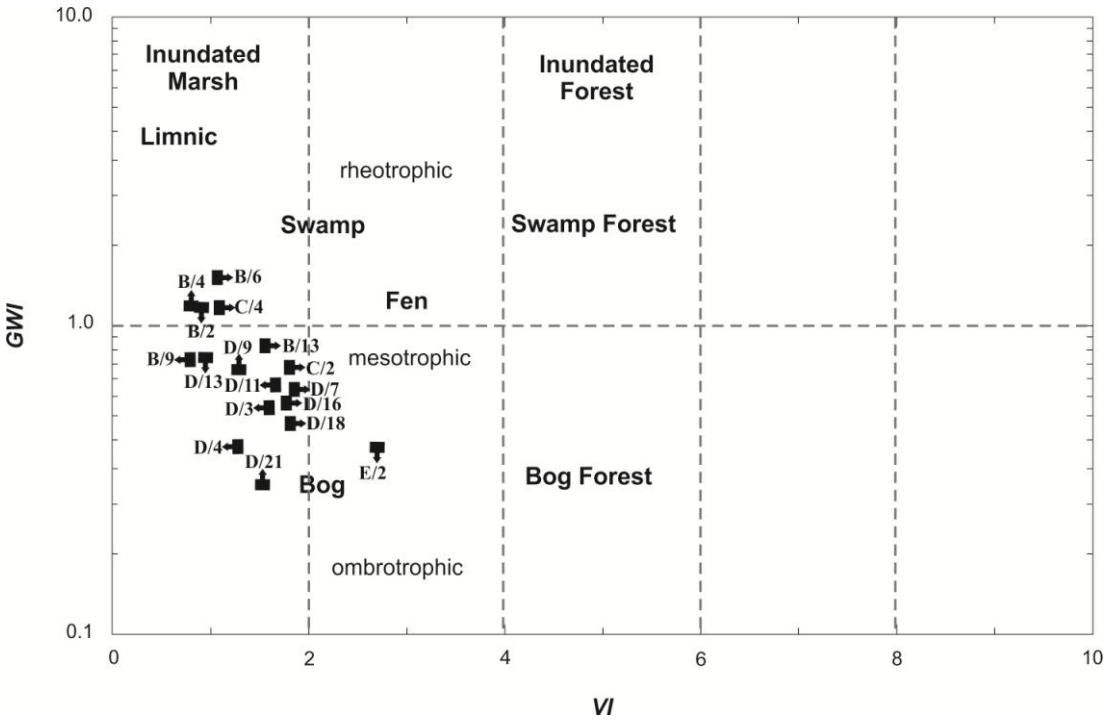

Figure 5.8 The GWI/VI coal-facies diagramme after Calder et al. (1991).

These diagrammes (Fig. 5.7 and 5.8) indicate that the Hüsamlar peat was accumulating in a limnotelmatic environment, in a fen (topogenous mire), under mesotrophic conditions (Fig. 5.9). The maceral composition indicates that the peat-forming vegetation consisted of both arboreal and herbaceous plants.

Kayseri-Özer (2010) performed palynological, palaeobotanical, vertebrate and marine fauna, and palaeoclimatological studies in the Oligo-Miocene Ören Basin. A late Early to-early Middle Miocene (Burdigalian-Langian) time is recorded for the basin formation based on the palynoflora, leaf fossils, mammalian fossils, strontium isotope results at Hüsamlar. According to her results beyond *Pinus, Quercus, Cingulum,* Oleaceae thriving in the mire surroundings, *Sparganium, Nymphaea* are the specific genera dominating in the mire. Palynoflora of the early Middle (Langhian) time (Polypodiaceae, *Pinus haploxylon*, Cupressaceae, *Engelhardtia, Ulmus, Carya, Quercus, Castanea,* Cyrillaceae, Osmundaceae, Taxodiaceae, Cycadaceae, *Picea, Pinus sylvestris* tip, Poaceae, *Pterocarya*, Myricaceae, *Salix*, Simaraubaceae, Oleaceae, Schizaeaceae, *Abies, Calamus* (Calamoid palmiye), Sphagnaceae, *Sequoia,* Juglandaceae, Umbelliferae, Fagaceae, Sapotaceae and *Avicennia)* are recorded in Milas-Kultak, Milas-Karaağaç and Milas-Hüsamlar regions. In this period, the climatic conditions in the lacustrine environment of Hüsamlar area must have been the following: mean annual temperature (MAT) 17.0-21.3°C, the mean annual coldest month (CMT) 6.2-13.3°C, the mean annual warmest month (WMT) 27.3-28.1°C, the mean annual precipitation (MAP) 1146-1322 mm). These subtropical humid conditions dominated in the area during the early Middle Miocene (Langhian), whereas during the late Middle Miocene (Serravallian) they changed from subtropical to temperate ones (Kayseri-Özer & Akgün, 2011).

The mineralogical features of coals strongly depend on the conditions that dominated during peat accumulation; thus, they contribute to the interpretation of coal facies (McCabe, 1984). The predominance of clastic silicate grains implies increased inorganic inlux from the surrounding metamorphic and sedimentary rocks by enhanced weathering and transportation activity of streams. Clay minerals are both detrital and authigenic in origin. Although carbonates usually are authigenic

minerals, they may be mainly due to gastropod remains in Hüsamlar lignite samples. Sulphides are characteristic authigenic minerals in coal. Both syngenetic and epigenetic pyrites are present in the samples. Syngenetic pyrite is abundant in the samples. It appears mainly in huminite as individual or clusters of framboids and euheral crystals (Plate 4.1-e,f). Pyrite is also found as infillings of cell cavity structures or as encrustation in the cell lumens of fusinite and semifusinite. Epigenetic pyrite occurs as massive and polycrystalline pyrite veinlets. The crystallization of pyrite is probably related to H changes in the micro-environment during and after peat accumulation (Vassilev & Vassileva, 1996). The bassanite may derive partly from dehydrated gypsum, being produced by reactions between calcite and suphuric acid with the latter being produced by oxidation of pyrite in the coal during storage (Rao & Gluskoter, 1973; Pearson & Kwong, 1979). Bassanite in such cases may possibly be formed by precipitation and dehydration of gypsum, following evaporation of the pore water during sample drying (Ward, 2002).

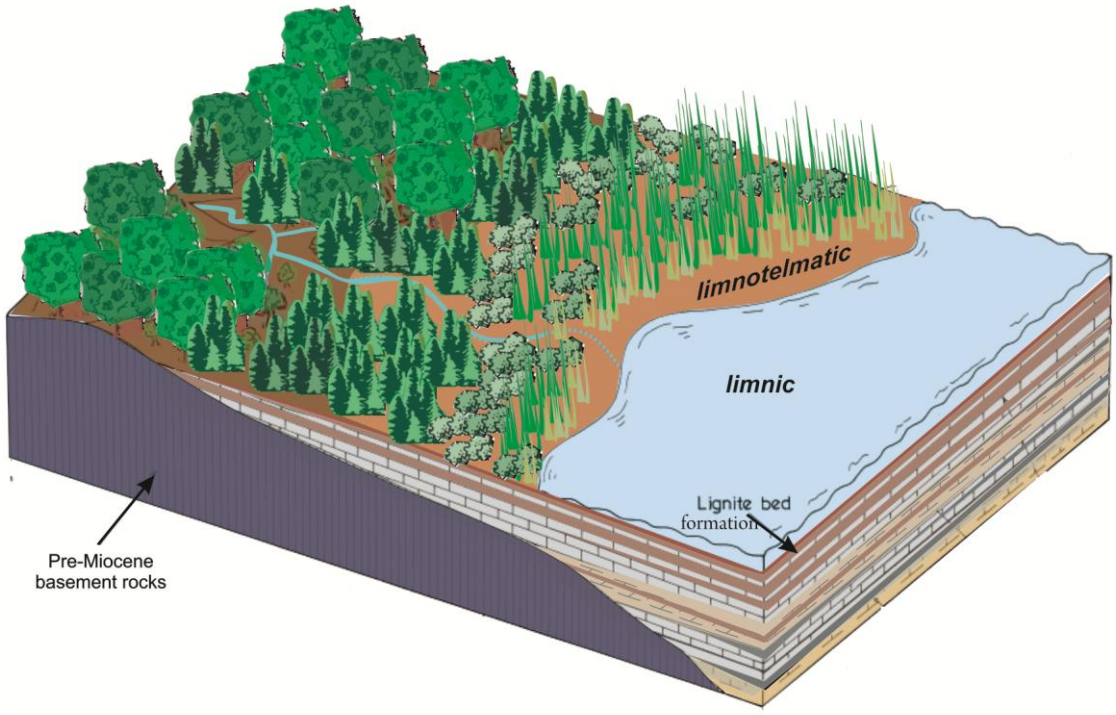

Figure 5.9 Schematic reconstruction of the peat accumulation environment in the Hüsamlar Basin, during the deposition of lignite seam.

The identified minerals can also be distinguished into a clastic (i.e. quartz, feldspars) and an authigenic fraction of both syngenetic (i.e. pyrite) and epigenetic origin (i.e. bassanite). The clastic minerals indicate an intense influx of clastic material during peat accumulation, which coincides with high ash yields (up to 45.20%, db). Besides, the high quartz content in the lignite indicates a relatively high stream energy during deposition. Additionaly, the presence of framboidal pyrite indicates pH values in the palaeomire water >4.5 (Renton & Bird, 1991).

Palaeoenvironmental comments and mineralogical determinations show that this limnotelmatic environment was not stable. Water table fluctuated due to the climatic and tectonic changes during peat accumulation. The palaeomire was being covered by lake water from time to time and inorganic sediment accumulation was taking place. This is the reason of the banded structure of Hüsamlar coal seam.

The presence of some oxidised particles in Hüsamlar bulk coal samples (Plate 4.6) may be caused by oxidation of pyrite and the bacterial activity in the outcrops and probably in the stockpiles iniciate self combustion of coal (Appendix, Fig. 10). This is not related to the depositional environment.

The main minerals in the 350°C residues are anhydrite and haematite. Anhydrite may form by reactions between Ca oxides and S oxides, whereas haematite derives from Fe compounds.

The main minerals contained in the lignite ash are anhydrite, haematite and lime. Aragonite and calcite minerals undergo significant alteration and transformation to lime during the combustion at 750°C.

Considering the mineral composition of the heavy fractions of Hüsamlar samples (Table 4.12), silicate and carbonate minerals were mainly separated from coal. Marcasite and pyrite (sulphide minerals) could be separated as well.

The butch experiments on density separation unfortunately failed. The separation results are presented in Table 5.2. It is obvious that in the light fraction went most of

the coal (92.45 %), the heavy fraction ranged between 2.01 to 31.12 %, despite the fact that the material lost during the procedure was small (in most cases <14%). Thus the procedure failed and the lack of time during the stay in Patras did not allow further experiments.

Table 5.2 The results of density separation on the coal samples

Sample Code	Bulk Coal Sample	Heavy Fraction		Light Fraction		Missing Amount	
	(g)	(g)	(%)	(g)	(%)	(g)	(%)
B/2	11.26	0.31	2.87	10.48	97.13	0.47	4.36
B/4	12.81	0.68	5.91	10.83	94.09	1.3	11.29
B/6	15.12	2.04	16.52	10.31	83.48	2.77	22.43
D/2	16.6	0.47	3.10	14.71	96.90	1.42	9.35
D/3	13.91	0.65	4.89	12.65	95.11	0.61	4.59
D/4	12.54	3.85	31.12	8.52	68.88	0.17	1.37
D/7	12.17	0.47	4.17	10.8	95.83	0.9	7.99
D/11	11.3	0.22	2.01	10.7	97.99	0.38	3.48
D/21	12.87	0.76	6.03	11.84	93.97	0.27	2.14
E/1	15.1	0.36	2.63	13.34	97.37	1.4	10.22
E/2	13.08	0.44	3.84	11.01	96.16	1.63	14.24

Hüsamlar coal seam displays many alternations of coal and inorganic sediments being co-exploited. The mineral content of these inorganic sediments and coal is very important to comment on their effects during combustion. Coal contains carbonates and sulphides (mainly pyrite). Pyrite is mainly attributed to the structure of coal. By burning it forms haematite up to 27.8 wt.% that exceed 7% the risk factor for slagging problems. Besides, lime (CaO) in the ash may be useful to bind S. But if lime in ash is between 5-40%, it may cause slagging problems (Arslan, 2010) as seen in Kemerköy Power Plant. Clay minerals constitute another risk factor for slagging problems. Moreover, the co-excavation of the coal and the inorganics deteriorates coal quality increasing this slagging trend.

CHAPTER SIX

CONCLUSION

The Hüsamlar lignite seam consists of alternating benches of several coal layers and inorganic intercalations. Macroscopically, the lignite belongs to the light- to medium-gelified matrix lithotype. Gastropods occur frequently; plant remnants can rarely be recognised. Some coal layers contain sulphur mineralizations, mostly occurring in cleats. Inorganic sediments intercalating with coal mostly consists of claystone, mudstone, siltstone and limestone. Gastropods occur frequently; lamination can occasionally be recognized. The banded structure of Hüsamlar coal seam indicates an unstable water table during the peat accumulation due to changing climatic or/and tectonic conditions.

The random reflectance of huminite, the volatile matter content, the C content and the moisture are not appropriate parameters for rank determination of Hüsamlar lignite. The calorific value should be considered with precaution while considering the gross calorific values the Hüsamlar coal as Mattbraunkohle (between lignite and subbituminous coal C), because the effect of high S content (up to 10%, on dry, ash-free basis; occuring mostly in form of pyrite) is to increase the heat produced during combustion.

On the basis of maceral composition the Hüsamlar peat was accumulating in a limnotelmatic environment, in a fen (topogenous mire), under mesotrophic hydrological and anoxic conditions. The maceral content shows that the peat-forming vegetation consisted of both arboreal and herbaceous plants.

The minerals contained in the coal can also be distinguished into a clastic fraction (i.e. quartz, feldspars) that indicates an intense influx of clastic material during peat accumulation and, authigenic fraction of both epigenetic (i.e. bassanite) and syngenetic (i.e. pyrite) origin which are affected by the pH values of the palaeomire water. The presence of framboidal pyrite indicates pH values in the palaeomire higher than 4.5, in acidic conditions.

Self-combustion of coal in the outcrops and probably in the stockpiles occurs frecquently; the phenomenon is accelerated due to pyrite oxidation and the bacterial activity.

Certain minerals (anhydrite, haematite and lime) forming during combustion along with the contained clay minerals may cause slagging problems in the boilers of Kemerköy Thermal Power Plant.

The variable results of density separation show that the procedure failed and the lack of time did not allow further experiments.

REFERENCES

Aksoy, D. & Demirok, Y. (1981). Hüsamlar (Muğla-Milas) sahası linyit kömürü Fizibilite araştırması. *Rezerv, II, Mineral Research and Exploration Institute of Turkey (MTA) report*, (Unpublished), Ankara.

American Society for Testing and Materials (ASTM) D3174. (1989). Standard method of ash in the analysis sample of coal and coke from coal. *1989 Annual Book of ASTM Standards, Part 26. Gaseous Fuels: Coal and Coke*. ASTM, Philadelphia, PA, pp. 291-294.

American Society for Testing and Materials (ASTM) D3175. (1989). Standard method of volatile matter in the analysis sample of coal and coke from coal. *1989 Annual Book of ASTM Standards, Part 26. Gaseous Fuels: Coal and Coke*. ASTM, Philadelphia, PA, pp.392-395.

American Society for Testing and Materials (ASTM) D3302. (1989). Standard method of total moisture in coal. *1989 Annual Book of ASTM Standards, Part 26, Gaseous Fuels: Coal and Coke*. ASTM, Philadelphia, PA, pp.326–332.

American Society for Testing and Materials (ASTM) D5865. (2004). Standard test method for gross calorific value of coal and coke. *2004 Annual Book of ASTM Standards.*

Arslan, V. (2004). TKİ GELİ Yeniköy İşletmesi Hüsamlar ocağı kömürlerinde $CaCO_3$ içeriğinin yıkama yoluyla azaltılabilirliğinin etüdü. *Report of General Directorate of Turkish Coal (TKİ)*.

Arslan, V. (2010). TKİ GELİ Yeniköy linyit işletmesi Hüsamlar-Belentepe kömürlerinin curuf oluşturma potansiyelini etkileyen $CaCO_3$ içeriği açısından incelenmesi projesi. *Report of General Directorate of Turkish Coal (TKİ)*.

Atalay, Z. (1980). Muğla Yatağan ve Yakını Dolayı Karasal Neojen'inin Stratigrafik Araştırılması. *Türkiye Jeoloji Kurultayı Bülteni. 23, 1,* 93–99.

Becker-Platen, J.D. & Bering. A. (1966). Yatağan (Muğla) sahasının linyit etüdü. *Mineral Research and Exploration Institute of Turkey (MTA), 5995.* (Unpublished), Ankara.

Becker–Platen, J.D. (1970). Lithostratigraphische Untersuchungen im Känozoikum Südwest–Anatoliens (Türkei). *Beihhefte zum Geologischen Jahrbuch, 97,* 244.

Benda, L. (1968). *Wichtige biostratigraphische Einzelergebnisse: Sporomorphen*. In: Gold, O., Abschlußbericht Türkei, 1, Untersuchung auf Braunkohle, 2, Geologie, S. 457–466, Köln.

Benda, L. (1971a). Grundzüge einer pollenanalytischen Gliederung des türkischen Jungtertiärs (Känozoikum und Braunkohle der Türkei). 4. *Beihhefte zum Geologischen Jahrbuch, 113,* 1–46.

Benda, L. (1971b). Principles of the palynologic subdivision of the Turkish Neogene (Kanozoikum und Braunkohlen der Türkei–3.) *Newsletter Stratigraphy, 1*, 23–26.

Benda, L., Meunlenkamp, J.E., Schmidt, R.R., Steffens, P., & Zachariasse, J.W. (1977). Biostratigraphic correlations in the Eastern Mediterranean Neogene. 2. Correlation between sporomorph Associations and marine microfossils from the Upper Oligocene–Lower Miocene of Turkey. *Newsletter Stratigraphy, 6(1), 1–22,* Berlin–Stuttgart.

Benda, L. & Meunlenkamp, J.E. (1990). Biostratigraphic correlations in the Eastern Mediterranean Neogene 9. Sporomorph associations and event stratigraphy of the Eastern Mediterranean. *Newsletter Stratigraphy, 2*3, 1–10.

Besbelli, B. (2009). Coal potential of Turkey and the importance of coal in electricity supply. *62nd Geological kurultai of Turkey, Abstracts.*

Bish, D.L. & Post, J.E. (1993). Quantitative mineralogical analysis using the Rietveld full-pattern fitting method. *American Mineralogist. 78.* 932-940.

Bozkurt, E. (2000). Timing of Extension on the Büyük Menderes Graben, Western Turkey and its tectonic implications. *In*: Bozkurt, E., Winchester, J.A. & Piper, J.D.A. (eds) Tectonics and Magmatism in Turkey and the Surrounding Area. *Geological Society, London, Special Publications 173*, 385−403.

Calder, J., Gibling, M. & Mukhopadhyay, P. (1991). Peat formation in a Westphalian B piedmont setting, Cumberland Basin, Nova Scotia. *Bulletin de la Societe Geologique de France, 162/2*. 283– 298.

Crosdale, P.J. (1993). Coal maceral ratios as indicators of environment of deposition: do they work for ombrogenous mires? An example from the Miocene of New Zealand. *Organic Geochemistry, 20*(6), 797–809.

Diessel, C.F.K. (1986). *On the correlation between coal facies and depositional environments*. Advances in the Sydney Basin. Proc. 20th Symposium. Department of Geology, University of Newcastle, May 15–18. 19–22.

Diessel, C.F.K. (1992). *Coal-Bearing depositional systems*. Springer Verlag, Berlin.

Economic Commission for Europe-United Nations (ECE-UN). (1998). International classification of in-seam coals. *Energy 19*. 41.

Ercan , T., Günay, E. & Savasçın, M.Y. (1983-a). Simav ve çevresindeki Senozoyik yaşlı volkanizmanın bölgesel yorumlanması. *MTA Dergisi. 97\98*. 86-101.

Finkelman, R.B. (1994). Abundance, source and mode of occurance of the inorganic constituents in coal. O. Kural, (Ed.), *Coal (115-125).* İstanbul: İstanbul Technical University.

Gary, M., McAfee, R. & Wolf, C.L. (Eds.). (1972). *Glossary of geology*. American Geological Institute, Washington, DC, 805 pp.

Güney Ege Linyit İşletmesi (GELI). (2011). TKİ Kurumu Genel Müdürlüğü, Güney Ege Linyit İşletmesi Müessesesi Müdürlüğü. *Brifing Raporu*.

Gelincik, Y. (1986). Muğla–Milas kömürlü Neojeni Hüsamlar (Çakıralan) Sektörü Jeolojik Raporu, Kö:47.

Gökmen, V. (1975). Muğla-Yatağan-Eskihisar Kömür yatağı Fizibilite Araştırması. *Mineral Research and Exploration Institute of Turkey (MTA),* Jeoloji: I, (Unpublished), Ankara.

Göktas, F. (1982). Mugla Bölgesi civarı Senezoik yaslı sedimanter kayaçların sedimantolojik ve paleocografik incelenmesi. MTA Rapor no. 519, 84p.

Grosse-Brauckmann, G. (1980). Stoffliches. K. Göttlich (Ed.), *Moor- und Torfkunde. Schweizerbart (Nägele und Obermiller)*(130-173). Stuttgart.

Gürer, Ö.F. & Yılmaz, F. (2002). Geology of the Ören and surrounding regions, SW Turkey. *Turkish Journal of Earth Science, 11*, 2–18.

Hakyemez, H.Y. (1989). Kale–Kurbalık (GB Denizli) bölgesindeki Senozoyik yaşlı çökel kayaların jeolojisi ve stratigrafisi. *Bulletin Mineral Research Exploration Institute, 109*, 9–21.

Harvey, R.D. & Ruch, R.R. (1986). Mineral matter in Illinois and other US coals. K.S. Vorres, (Ed.). *Mineral Matter in Coal Ash and Coal* (American Chemical Society Symposium Series 301) (10-40).

Hawke, M.I., Martini, I.P. & Stasiuk, L.D. (1999). A comparison of temperate and boreal peats from Ontario, Canada: a possible modern analogue for Permian coals. *International Journal of Coal Geology, 41,* 213– 238.

İnaner, H. (1994). *Güneybatı Anadolu linyit havzalarının değerlendirilmesi*. Dokuz Eylül Üniversitesi, Fen Bilimleri Enstitüsü, Ph.D thesis, (unpublished).

İnaner, H., Nakoman, E. & Karayiğit, A.I. (2008). Coal resource estimation in the Bayir Field, Yatağan-Muğla, SW Turkey. *Energy Sources, Part A, 30,* 1000-1015.

İnaner, H. & Nakoman, E. (1997). Turkish lignite deposits. *European Coal Geology and Technology, Geological Society Special Publication No. 125.* 77-99.

International Committee for Coal Petrology (ICCP). (1963). *International handbook of coal petrography* (2nd ed). Centre National de la Recherche Scientifique, Paris, France.

International Committee for Coal Petrology (ICCP). (1971). *International handbook of coal petrography* (2nd ed). Centre National de la Recherche Scientifique, Paris, France. 1st supplement to.

International Committee for Coal Petrology (ICCP). (1993). *International Handbook of Coal Petrography* (3rd supplement to the 2nd ed). Centre National de la Recherche Scientifique, Paris.

International Committee for Coal Petrology (ICCP). (2001). The new inertinite classification (ICCP System 1994). *Fuel 80.* 459-471.

International Standard Organization (ISO) 7404-2. (2009). *Methods for the petrographic analysis of coals — Part 2: Methods of Preparing Coal Samples.* International Organization for Standardization, Geneva, Switzerland. 12 pp.

International Standard Organization (ISO) 7404-3. (2009). *Methods for the Petrographic Analysis of Coals—Part 3: Method of Determining Maceral Group Composition.* International Organization for Standardization, Geneva, Switzerland. 7 pp.

International Standard Organization (ISO) 7404-5. (2009). Methods for the Petrographic Analysis of Coal—Part 5: Methods of Determining Microscopically the Reflectance of Vitrinite. *International Organization for Standardization, Geneva, Switzerland.* 14 pp.

Kalaitzidis, S., Papazisimou, S. & Christanis, K. (2001). Forming conditions of the Grekas lignite, Northern Peloponnese. *Bulletin of Geological Society of Greece XXXIV/3*. 1195– 1204.

Kalaitzidis, S., Bouzinos, A., Papazisimou, S. & Christanis, K. (2004). A short-term establishment of forest fen habitat during Pliocene lignite formation in the Ptolemais Basin, NW Macedonia, Greece. *International Journal of Coal Geology, 57,* 243-263.

Kalkreuth, W., Kotis, T., Papanicolaou, C. & Kokkinakis, P. (1991a). The geology and coal petrology of a Miocene lignite profile at Meliadi Mine, Katerini, Greece. *International Journal of Coal Geology*, 17, 51– 67.

Kalkreuth, W., Marchioni, D., Calder, J. & Lamberson, M. (1991b). The relationship between coal petrography and depositional environments from selected coal basins in Canada. *International Journal of Coal Geology*. 19, 21– 76.

Kaya, T., Tuna, V. & Geraads, D. (2001). A new Late Orleanian/early astaraccian Mammalian Fauna from Kultak (Milas–Muğla), Southwestern Turkey. *Geobios 34* (6), 673–680.

Kayseri-Özer, M.S. (2010). *Oligo-Miocene palynology, palaeobotany, vertebrate, marine, faunas, palaeoclimatology and palaeovegetation of the Ören Basin (North of the, Gökova Gulf),* Western Anatolia. Dokuz Eylül University, Graduate School of Natural and Applied Sciences. Ph.D thesis, (unpublished).

Kayseri-Özer, M.S. & Akgün. F. (2011). Ören Havzası'nın Orta Miyosen sürecindeki paleoiklimsel ve paleovejetasyonel özellikleri. *64. Jeoloji Kurultayı*. Ankara. p.138-139.

Killops, S.D. & Killops, V.J. (1993). *An Introduction to organic geochemistry.* Singapore: Longman Scientific & Technical.

Koçyiğit, A., Yusufoğlu, H. & Bozkurt, E. (1999). Evidence from the Gediz Graben for episodic two-stage extension in western Turkey. *Journal of the Geological Society, London 156,* 605–616.

Lamberson, M.N., Bustin, R.M. & Kalkreuth, W. (1991). Lithotype (maceral) composition and variation as correlated with paleowetland environments, Gates Formation, northeastern British Columbia, Canada. *International Journal of Coal Geology*, 18. 87–124.

Laskovski, J.S. (2001). *Coal Flotation and Fine Coal Utilization. In D.W. Fuerstenau*, (Ed.), Developments in Mineral Processing (volume 14). The Netherlands: Elsevier.

Maden Tetkik ve Arama Genel Müdürlüğü (MTA). (2010). Inventory of Turkish lignites. Ankara: MTA Publication (in Turkish).

Martini, I.P. & Glooschenco, W. (1984). Cold climate environments of peat formation in Canada. Advances in the study of the Sydney Basin. 18 Newcastle Symposium. 18-28.

McCabe, P. (1984). Depositional environments of coal and coalbearing strata. R.A. Rahmani & R.M. Flores (Eds.), *Sedimentology of Coal and Coal-Bearing Sequences*. *Specical Publicatio, International Association of Sedimentologists.* (vol. 7) *(*13– 42). Blackwell, Oxford.

Moore, P.D. (1987). Ecological and hydrological aspects of peat formation. A.C. Scott (Ed.), *Coal and coal-bearing strata, recent advances* (32) (7-15). Geol. Soc. Am. Spec. Publ.

Moore, T.A. & Shearer, J.C. (2003). Peat/coal type and depositional environment—are they related? *Int. J. Coal Geol.*, *56*, 233–252.

Mukhopadhyay, P. (1989). Organic petrography and organic geochemistry of Tertiary coals from Texas in relation to depositional environment and hydrocarbon generation. Report of Investigations. Bureau of Economic Geol., Texas. 118 pp.

Nakoman, E. (1978). *Güneybatı Anadolu'daki Tınaz, Bağyaka, Bayır, Eskihisar, Sekköy ve Hüsamlar kömür sahalarının incelemeleri.* Doçentlik Tezi, *(Unpublished)*, İzmir.

Nebert, K. (1956). Denizli-Acıgöl merkezinin jeolojisi, 1/100.000 ölçekli Denizli 105/1, 105/2 ve Isparta 106/1 paftalarının sahası içinde yapılan jeolojik haritaları hakkında rapor. *Mineral Research and Exploration Institute of Turkey (MTA),(2509).*

Nebert, K. (1957). *Die Braunkohlenvorkommen von Oeren*. Mineral Research and Exploration Institute of Turkey (MTA) Report 3011 (unpublished).

Nebert, K. (1961). Kale-Tavas bölgesine ait yeni müşahedeler. *Bulletin Mineral Research Exploration Institution, 57,* 57-64.

Nebert, K. (1978). Linyit içeren Soma Neojen bölgesi, Batı Anadolu. *Journal of Mineral Research and Exploration Institute of Turkey (MTA), 90,* 20-70.

Okay, A.I. (2001). Stratigraphic and metamorphic inversions in the central Menderes Massif: a new structural model. *International Journal of Earth Sciences (Geologische Rundschau), 89,* 709-727.

Oskay, R.G., Inaner, H., Karayiğit, A.I. & Christanis, K. (2013). Coal deposits of Turkey: Properties and importance on energy demand. *Bulletin of the Geological Society of Greece, vol. XLVII 2013 Proceedings of the 13th International Congress,* Chania-Crete (submitted).

OTTO-GOLD (1965). *Linyit Etüdü (Jeoloji).* Cilt II, M.T.A. yayını, Ankara.

Paton, S. (1992). Active normal faulting, drainage patterns and sedimentation in southwestern Turkey. *Journal of the Geological Society, London 149,* 1031-1044.

Pearson, D.E., & Kwong, J. (1979). Mineral matter as a measure of oxidation of coking coal. *Fuel, 58.* 63-65.

Querol, X., Alastuey, A., Plana, F., Lopez-Soler, A., Tuncali, E., Toprak, S., et al. (1999). Coal geology and coal quality of the Miocene Mugla Basin, southwestern Anatolia, Turkey. *International Journal of Coal Geology, 41,* 311-332.

Rao, C.P. & Gluskoter, H.J. (1973). Occurrence and distribution of minerals in Illinois coals. *Illionis State Geological Survey, Circular, 476,* 56.

Renton, J. & Bird, S. (1991). Association of coal macerals, sulphur, sulphur species and the iron disulphide minerals in three columns of the Pittsburg coal. *International Journal of Coal Geology, 17,* 21-50.

Sarıca, N. (2000). The Plio-Pleistocene age of Büyük Menderes and Gediz grabens and their tectonic significance on N-S extensional tectonics in West Anatolia: mammalian evidence from the continental deposists. *Geological Journal, 35*, 1-24.

Seyitoğlu, G. & Scott, B (1991). Late Cenozoic crustal extenension and basin Formation in west Turkey. *Geological Magazine, 128,* 155–166.

Siavalas, G., Linou, M., Chatziapostolou, A., Kalaitzidis, S., Papaefthymiou, H. & Christanis, K. (2009). Palaeoenvironment of Seam I in the Marathousa Lignite Mine, Megalopolis Basin (Southern Greece). *International Journal of Coal Geology, 78,* 233-248.

Singh, M.P. & Singh, A.K. (2000). Petrographic characteristics and depositional conditions of Eocene coals of platform basins, Meghalaya, India. *International Journal of Coal Geology, 42,* 315–356.

Spackman, W., Dolson, C.P. & Riegel, W. (1966). Phytogenic organic sediments and sedimentary environments in the Everglades-Mangrove complex. *Palaeontographia B: 117,* 135-152.

Spackman, W., Riegel, W. & Dolson, C.P. (1969). Geological and biological interactions in the swamp-marsh complex of southern Florida. In: E.C. Dapples, & M.E. Hopkins (Eds.). Environments of coal deposition. *Geological Society of America Special Paper, 114,* 143-192.

Stach, E., Mackowsky, M., Teichmüller, M., Taylor, G., Chandra, D. & Teichmüller, R. (1982). *Stach's textbook of coal geology*. Berlin: Gebrüder Borntraeger.

Standards Australia. (1995). Coal and Coke – glossary of terms. *Australian Standard 2418*.

Standards Australia. (2000). Higher rank coal – mineral matter and water of constitution. *Australian Standard 1038, Part 22.*

Sun, S., Gelincik, Y. & Ünal, D. (1987). Muğla–Milas–Sekköy–Karaağaç Linyit sektörü 1986 yılı çalışma raporu, *Mineral Research and Exploration Institute of Turkey (MTA) report*.

Sun, S. & Karaca, K. (2000). Muğla-Milas Hüsamlar ve Ekizköy linyit sahaları jeoloji, jeofizik ve rezerv raporu. *Mineral Research and Exploration Institute of Turkey (MTA) report*.

Sun, H.E., Sun, R.S. & Karaca, K. (2001). Muğla–Milas–Ekizköy–Hüsamlar Sektörlerinin Jeoloji ve Fizibilite ve Jeofizik Raporu. *Mineral Research and Exploration Institute of Turkey (MTA) report*.

Sýkorová, I., Pickel, W., Christanis, K., Wolf, M., Taylor, G.H. & Flores, D. (2005). Classification of Huminite – ICCP System 1994. *International Journal of Coal Geology, 62*, 85-106.

Şengör, A.M.C. (1979). The Nortyh Anatolian transform fault: Its age, offset and tectonic significance. *Journal of the Geological Society, London, 136*, 269-282.

Şengör, A.M.C. (1980). Türkiye'nin neotektoniğinin esasları: *Champer of Geological Engineers of Turkey.* Conference Serie. 2, 40p.

Şengör, A.M.C. & Yılmaz, Y. (1981). Tethyan evolution of Turkey: a plate tectonic approach. *Tectonophysics, 75*, 181–241.

Şengör, A.M.C., Görür, N. & Şaroğlu, F. (1985) Strike-slip faulting and related basin formation in zones of tectonic escape; Turkey as a case study. *Society of Economic Paleontologists and Minerologists, Special Publication. 37,* 227-264.

Şengüler, İ. (2010). Lignite explorations in Turkey: New projects and new reserves. *27th Annual International Pittsburgh coal conference, oral presentation.* İstanbul.

Taylor, G.H., Teichmüller, M., Davis, A., Diessel, C.F.K., Littke, R. & Robert, P. (1998). *Organic petrology*. Berlin-Stuttgart: Gebrüder Borntraeger.

Teichmüller, M. (1989). The genesis of coal the viewpoint of coal petrology. In: P. Lyons & B. Alpern (Eds.). Peat and Coal: Origin, Facies and Depositional Model. *International Journal of Coal Geology, 12.* 1-87.

Thomas, L. (2002). *Coal geology.* West Sussex: John Wiley & Sons Ltd.

U.S. Geological Survey (USGS). (2000). Implications for Earthquake Risk Reduction in the United States from the Kocaeli, Turkey, Earthquake of August 17, 1999, *USGS Circular 1193* available at the WEB site http://pubs.usgs.gov/circ/2000/c1193/index.html.

Ünal, D. (1987). Muğla-Milas Sekköy-Ekizköy (Karacaağaç Bölümü) Linyit Sektörü 1987 Yılı Çalışma Raporu. *M.T.A. Rap.* (Yayınlanmamış), İzmir.

Ünal, D. (1988 a). Muğla–Milas–Ören–Alatepe kömür sahası jeolojisi. *Mineral Research and Exploration Institute of Turkey (MTA) report.*

Ünal, D. (1988 b). Muğla–Milas–Sekköy Linyit sahası jeolojisi. *Mineral Research and Exploration Institute of Turkey (MTA) report.*

Ünal, D. (1990). Muğla–Milas–Sekköy–İkizköy linyit sektörü jeolojisi. *Mineral Research and Exploration Institute of Turkey (MTA) report*.

Vassilev, S.V. & Vassileva, C.G. (1996). Occurance, abundance and origin of minerals in coals and coal ashes. *Fuel Processing Technology, 48,* 85-106.

von der Brelie, G. & Wolf, M. (1981). Zur Petrographic and Palynologie heller und dunkler Schichten im rheinischen Hauptbraun-kohlenflöz. *Fortschritte in der Geologie Rheinland und Westfal, 29,* 95-163.

Ward, C.R. (2002). Analysis and significance of mineral matter in coal seams. *International Journal of Coal Geology, 50.* 135-168.

Wüst, R.A.J., Hawke, M.I. & Bustin, R.M. (2001). Comparing maceral ratios from tropical peatlands with assumptions from coal studies: do classic coal petrographic interpretation methods have to be discarded? *Int. J. Coal Geol., 48,* 115–132.

Yılmaz, Y., Genç, Ş. C., Gürer, F., Bozcu, M., Yılmaz, K., Karacık, Z., et al. (2000). When did the western Anatolian Grabens begin to develop? E. Bozkurt, J. A. Winchester, & J.A.D. Piper, (Eds.) *Tectonics and Magmatism in Turkey and the Surrounding Area (*vol. 173) (131-162). *Geological Society, Special Publications, London.*

Yiğitel, İ. (1981). Muğla-Milas Kömürlü Neojeni Hüsamlar Sektörü jeoloji raporu. *Report of General Directorate of Turkish Coal (TKİ), (Unpublished), 15,3,82.*

APPENDICES

APPENDIX I

Pictures from sampling

at Hüsamlar Open Pit

Figure 1. Muğla-Milas Hüsamlar open pit

Figure 2. The Mengefe antique site

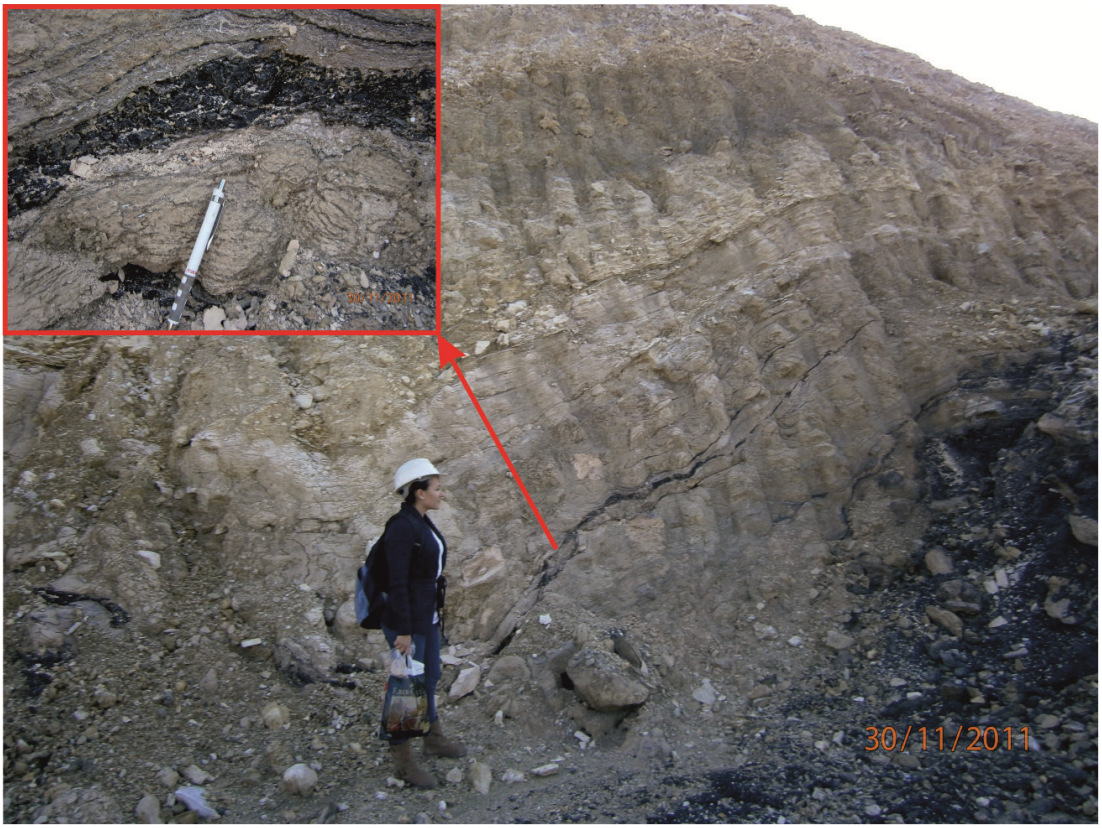

Figure 3. The roof of the coal seam

Figure 4. Section A at Hüsamlar Mine

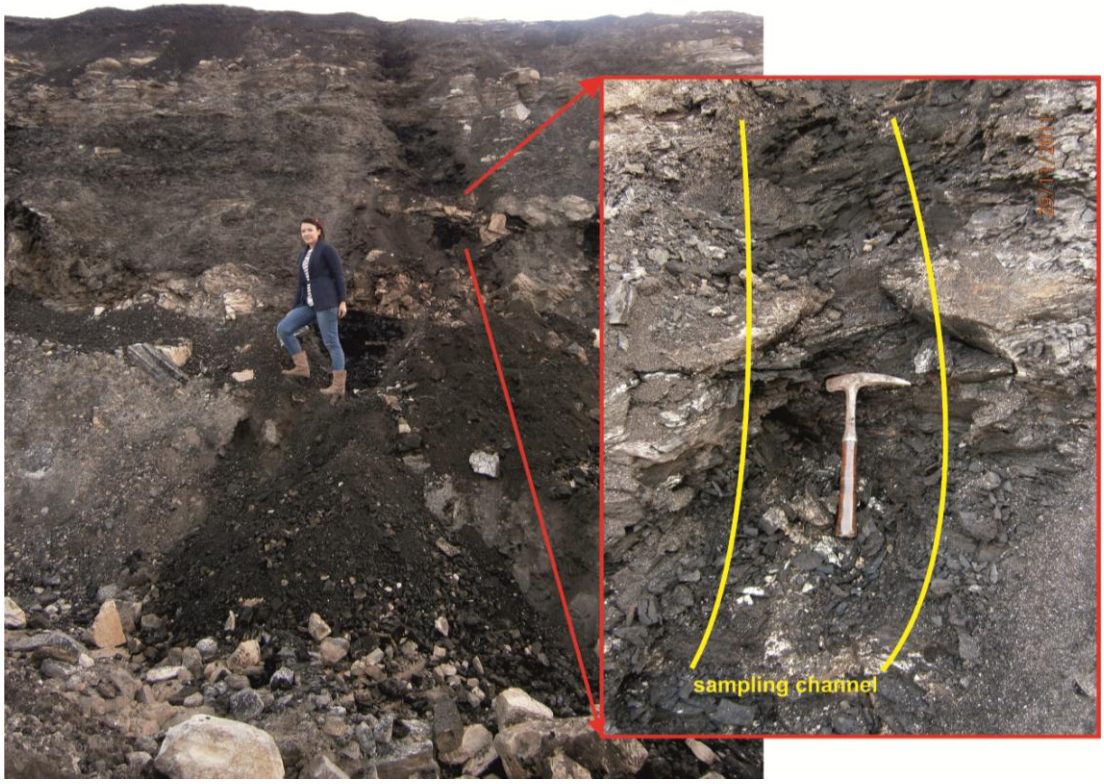

Figure 5. Section B at Hüsamlar Mine

Figure 6. Gastropoda fragments in coal

Figure 7. Section C at Hüsamlar Mine

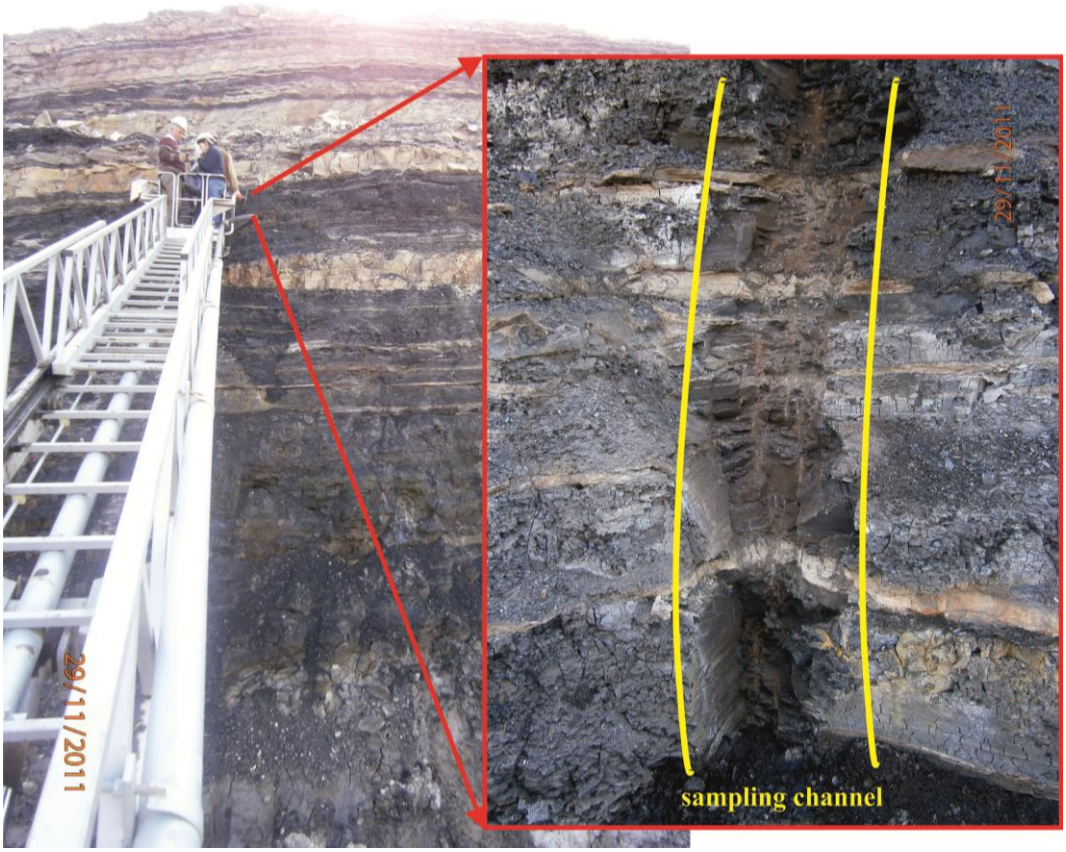

Figure 8. Section D at Hüsamlar Mine

Figure 9. Section E at Hüsamlar Mine

Figure 10. Self combustion at Hüsamlar Mine

APPENDIX II

Photomicrographs of the Hüsamlar lignite

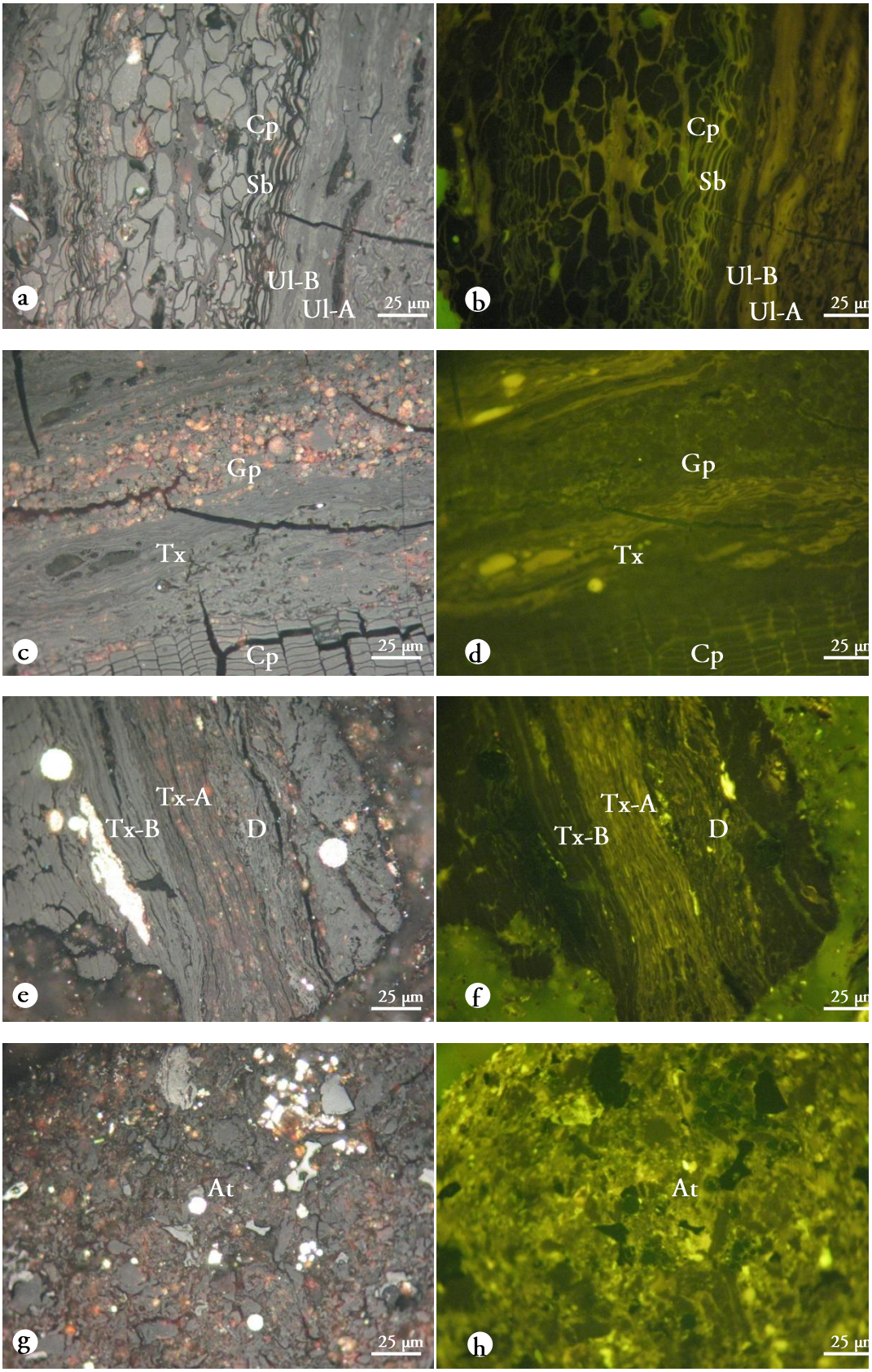

Figure 1. Huminite Macerals

Figure 1. Huminite macerals contained in the Hüsamlar lignite. All photomicrographs are taken under incident white light (a, c, e, g) and blue-light excitation (b, d, f, h), oil immersion, 500x total magnification.

a. Corpohuminite (Cp), ulminite A (Ul-A), ulminite B (Ul-B) (sample D/3).

b. Corpohuminite (Cp), ulminite A (Ul-A), ulminite B (Ul-B). Suberinite (Sb) with typical "lacy" habit. (sample D/3).

c. Porigelinite (Gp), corpohuminite (Cp), textinite (Tx) (sample C/3).

d. Porigelinite (Gp), corpohuminite (Cp), textinite (Tx) (sample C/3).

e. Textinite A (Tx-A), textinite B (Tx-B) (sample D/4).

f. Textinite B (Tx-B), textinite A (Tx-A) (sample D/4).

g. Attrinite (At) (sample D/16).

h. Attrinite (At) (sample D/16).

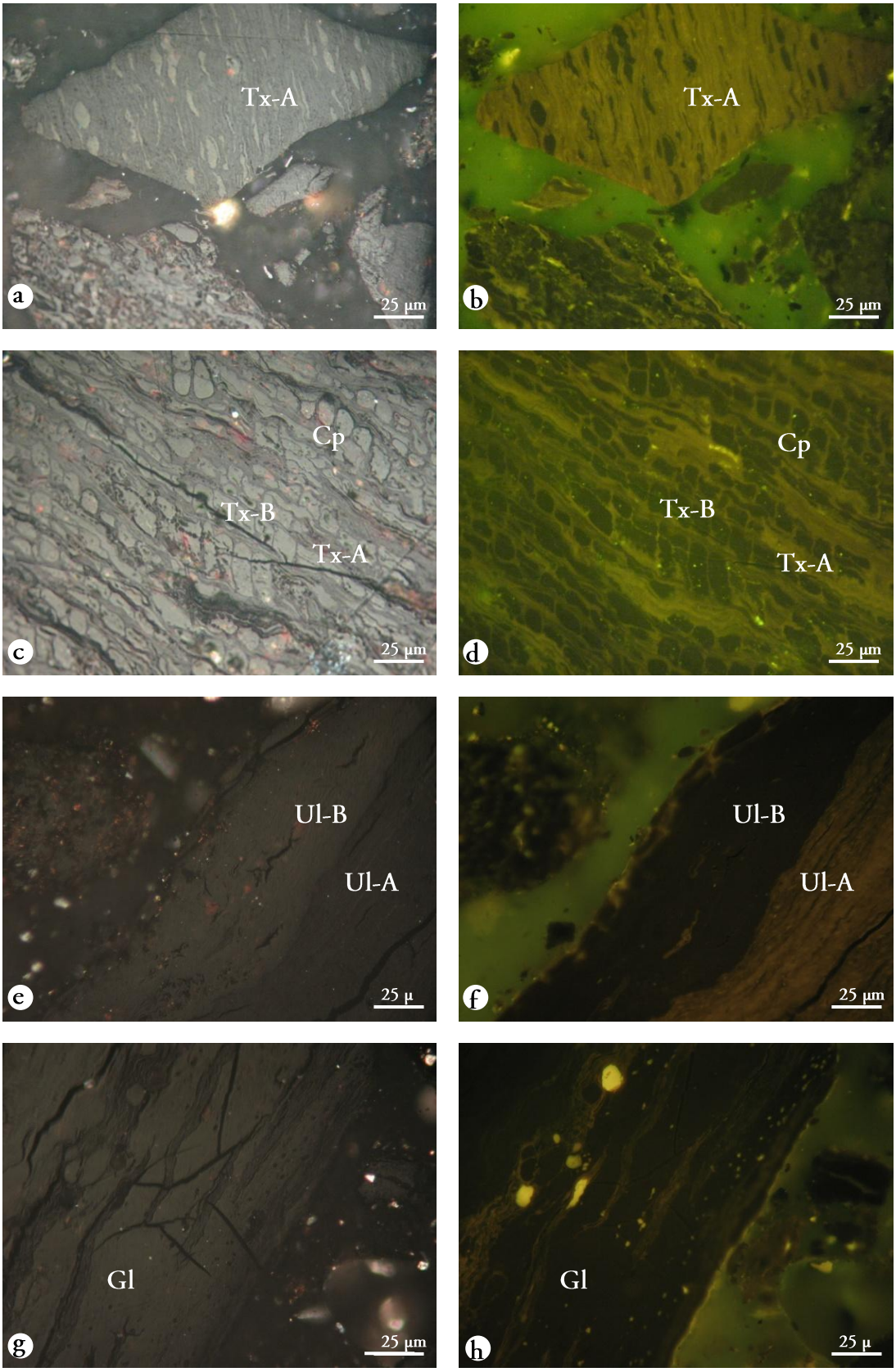

Figure 2. Huminite Macerals

Figure 2. Huminite macerals contained in the Hüsamlar lignite. All photomicrographs are taken under incident white light (a, c, e, g) and blue-light excitation (b, d, f, h), oil immersion, 500x total magnification.

a. Textinite A (Tx-A) impregnated with finely dispersed resinite (R) (sample C/2).

b. Textinite A (Tx-A) fluorecent (sample C/2).

c. Textinite A (Tx-A), textinite B (Tx-B), corpohuminite (Cp) (sample C/2).

d. Textinite A (Tx-A), textinite B (Tx-B), corpohuminite (Cp) (sample C/2).

e. Ulminite A (Ul-A), ulminite B (Ul-B) (sample B/4).

f. Ulminite A (Ul-A), ulminite B (Ul-B) (sample B/4).

g. Levigelinite (Gl) (sample B/2).

h. Levigelinite (Gl) (sample B/2).

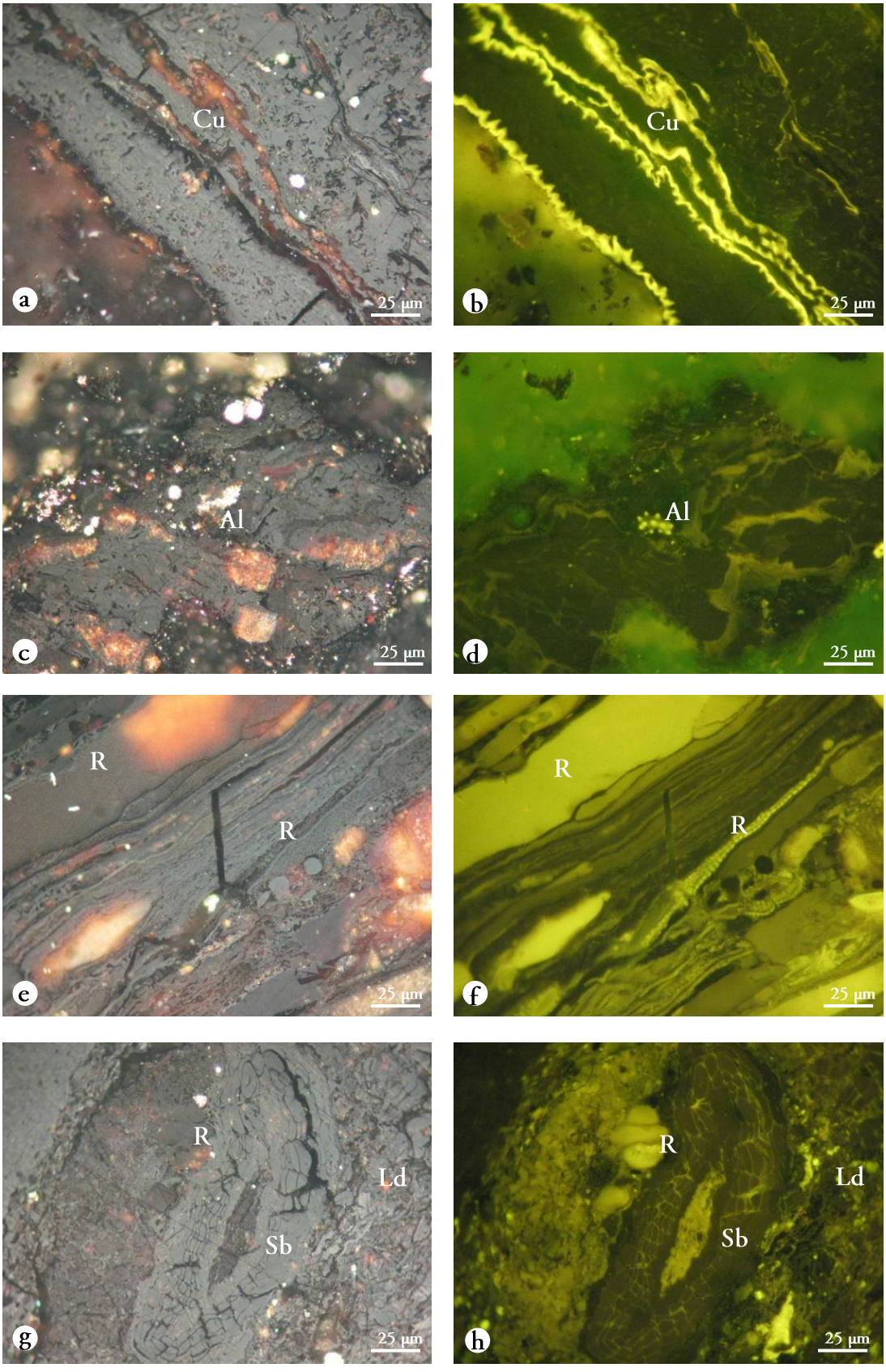

Figure 3. Liptinite Macerals

Figure 3. Liptinite macerals contained in the Hüsamlar lignite. All photomicrographs are taken under incident white light (a, c, e, g) and blue-light excitation (b, d, f, h), oil immersion, 500x total magnification.

a. Cutinite (Cu) (sample B/9).

b. Cutinite (Cu) (sample B/9).

c. Alginite (A) (sample B/9).

d. Alginite (A) (sample B/9).

e. Huminite (H) impregnated with resinite (R) and resin droplets are seen as resinite (R) (sample B/9).

f. Resinite (R) (sample B/9).

g. Suberinite (Sb) with typical "lacy" habit. Huminite (H) impregnated with resinite (R). Liptodetrinite (Lp), fragments and fine degradation remains of liptinite macerals (sample B/6).

h. Suberinite (Sb), resinite (R), liptodetrinite (Ld) (sample B/6).

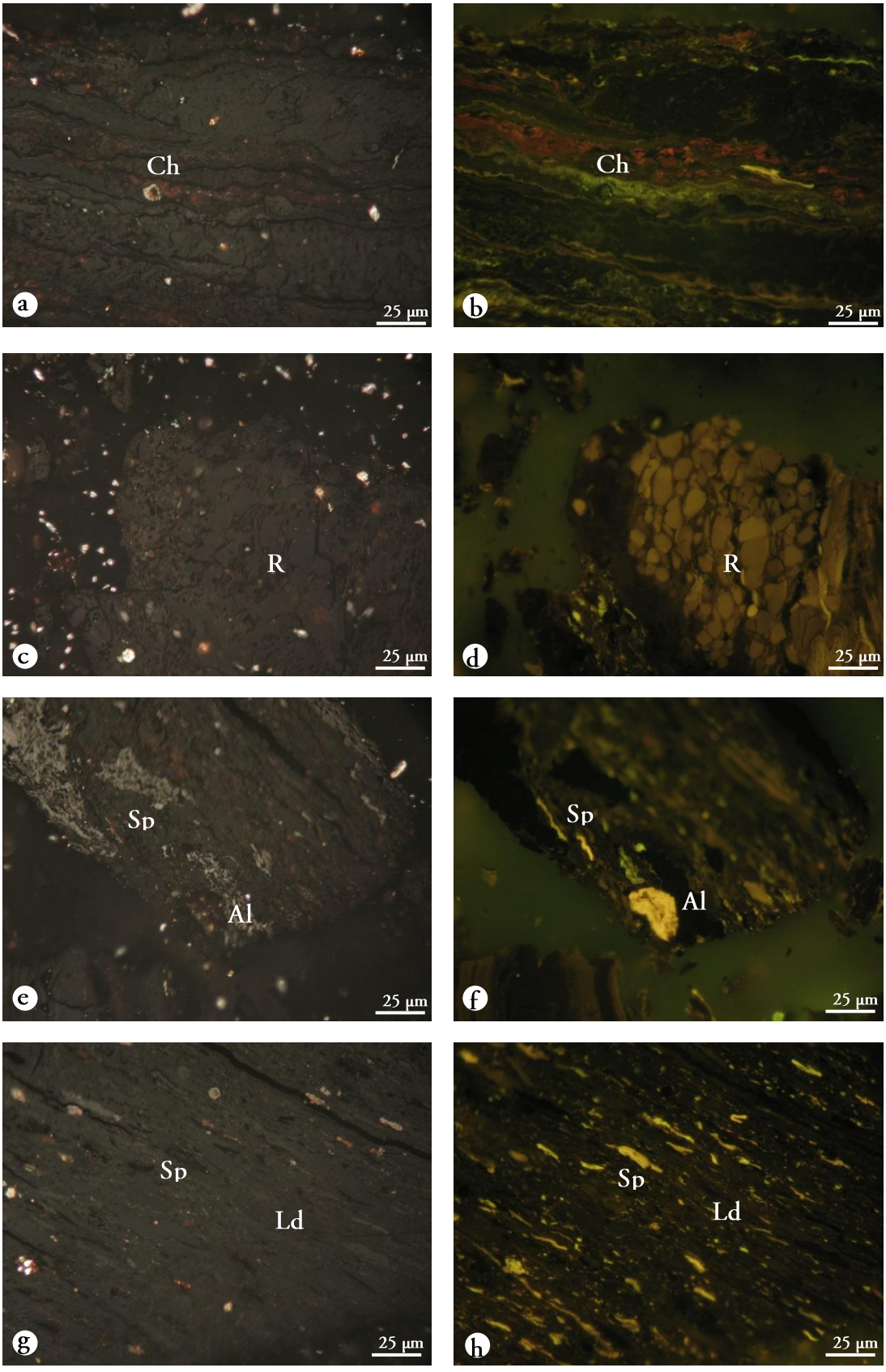

Figure 4. Liptinite Macerals

Figure 4. Liptinite macerals contained in the Hüsamlar lignite. All photomicrographs are taken under incident white light (a, c, e, g) and blue-light excitation (b, d, f, h), oil immersion, 500x total magnification.

a. Chlorophyllinite (Ch) (sample B/).

b. Chlorophyllinite (Ch) shows redish fluoresence (sample B/9).

c. Resinite (R) (sample B/9).

d. Resinite (R) (sample B/9).

e. Alginite (Al) (sample B/9).

f. Alginite (Al) (sample B/9).

g. Sporinite (Sp), liptodetrinite (Ld) embedded in densinite (sample B/6).

h. Sporinite (Sp), liptodetrine (Ld) (sample B/6).

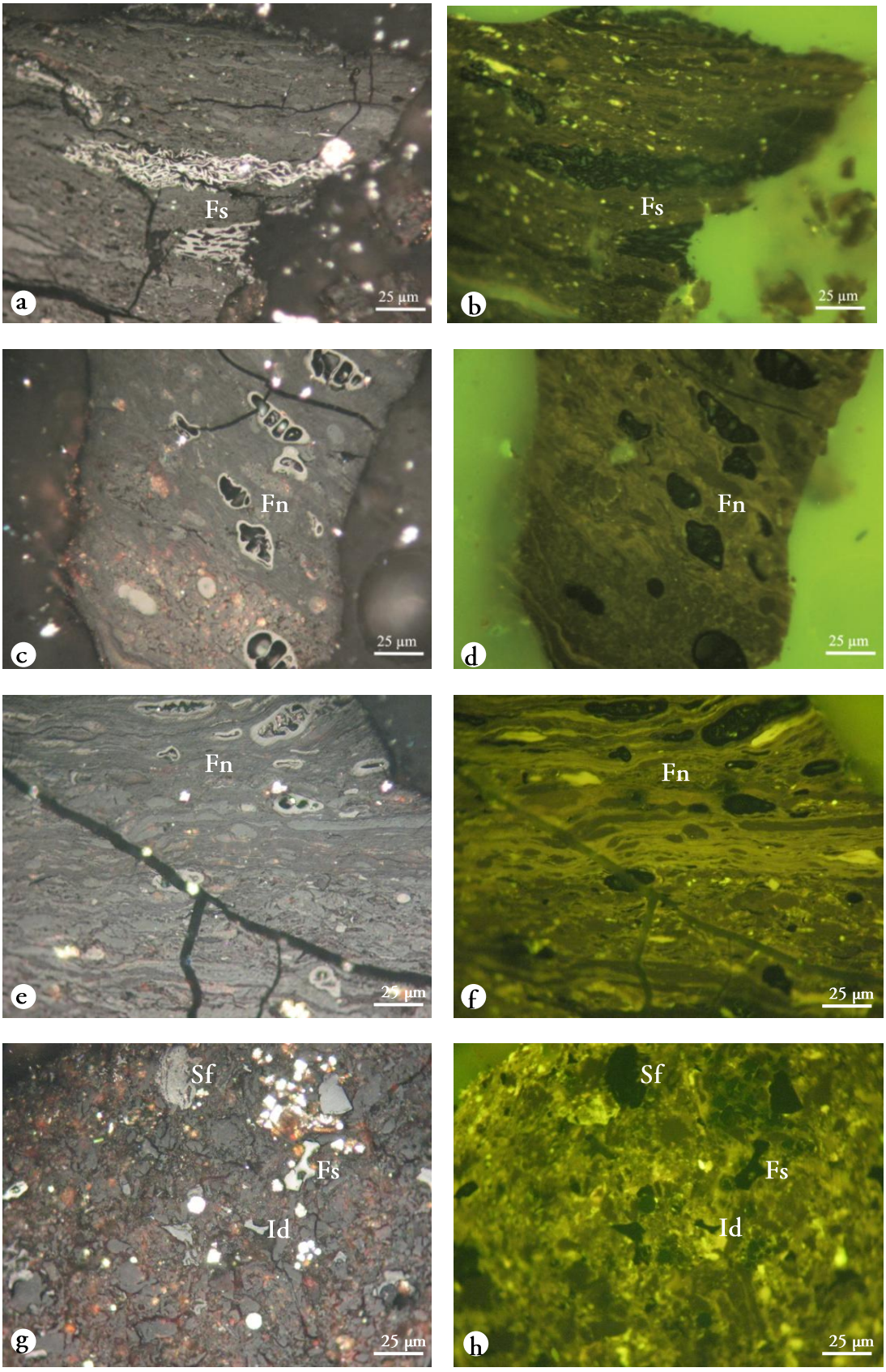

Figure 5. Inertinite Macerals

Figure 5. Inertinite macerals contained in the Hüsamlar lignite. All photomicrographs are taken under incident white light (a, c, e, g) and blue-light excitation (b, d, f, h), oil immersion, 500x total magnification.

a. Fusinite (Fs) (sample C/4).

b. Fusinite (Fs) (sample C/4).

c. e. Funginite (Fn) consists of roundish unicellular to multicellular oval forms (sample B/13).

d. f. Funginite (Fn) (sample B/13).

g. Semifusinite (Sf), fusinite (Fs), inertodetrinite (Id) (sample D/16).

h. Semifusinite (Sf), fusinite (Fs), inertodetrinite (Id) (sample B/13).

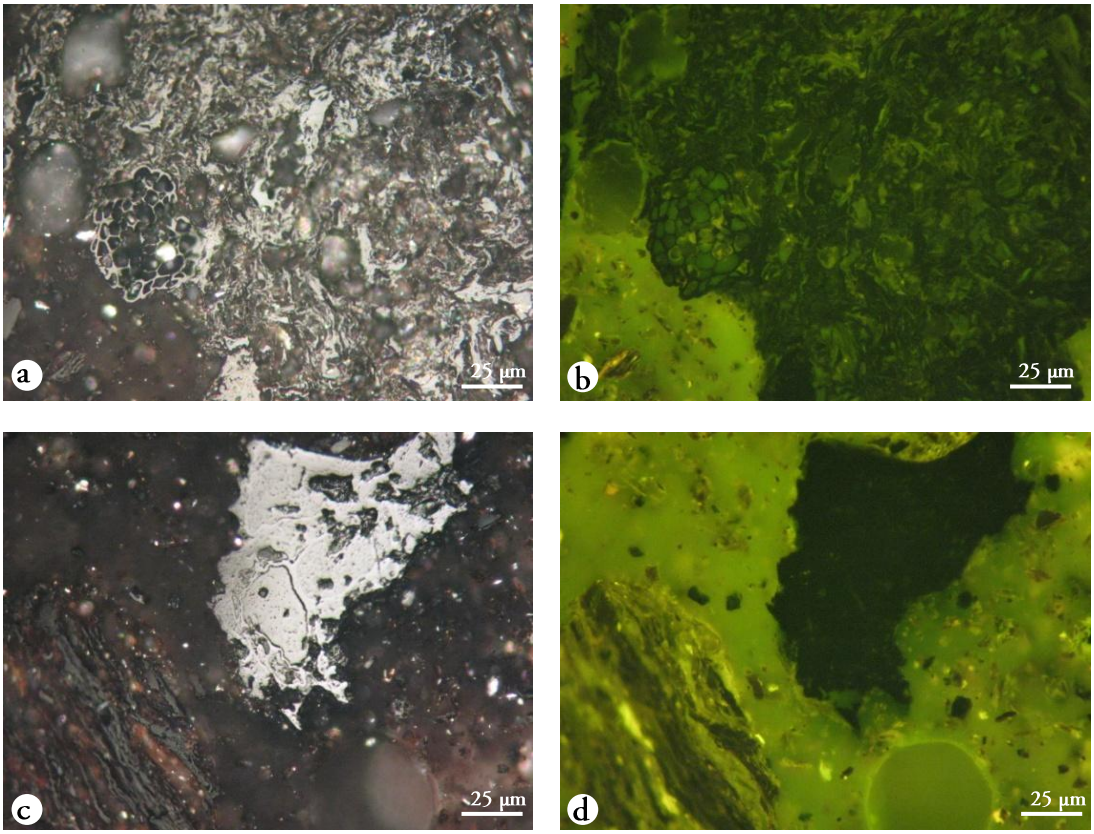

Figure 6. Oxidised Particles. Photomicrographs are taken under incident white light (a, c) and blue-light excitation (b, d), oil immersion, 500x total magnification.

APPENDIX III

X-Ray Diffractograms

Explanations

Al: Albite

An: Anorthite

Ana: Anatase

Anh: Anhydrite

Arg: Aragonite

Ba: Bassanite

Ca: Calcite

Ch: Chlorite

Fel: Feldispar

Gy: Gypsum

Hem: Haematite

Horn: Hornblende

Jr: Jarosite

Kao: Kaolinite

Li: Lime

M: Mica

Mar: Marcasite

Olg: Oligoclase

Orth: Orthoclase

Py: Pyrite

Q: Quartz

Si: Siderite

Viv: Vivianite

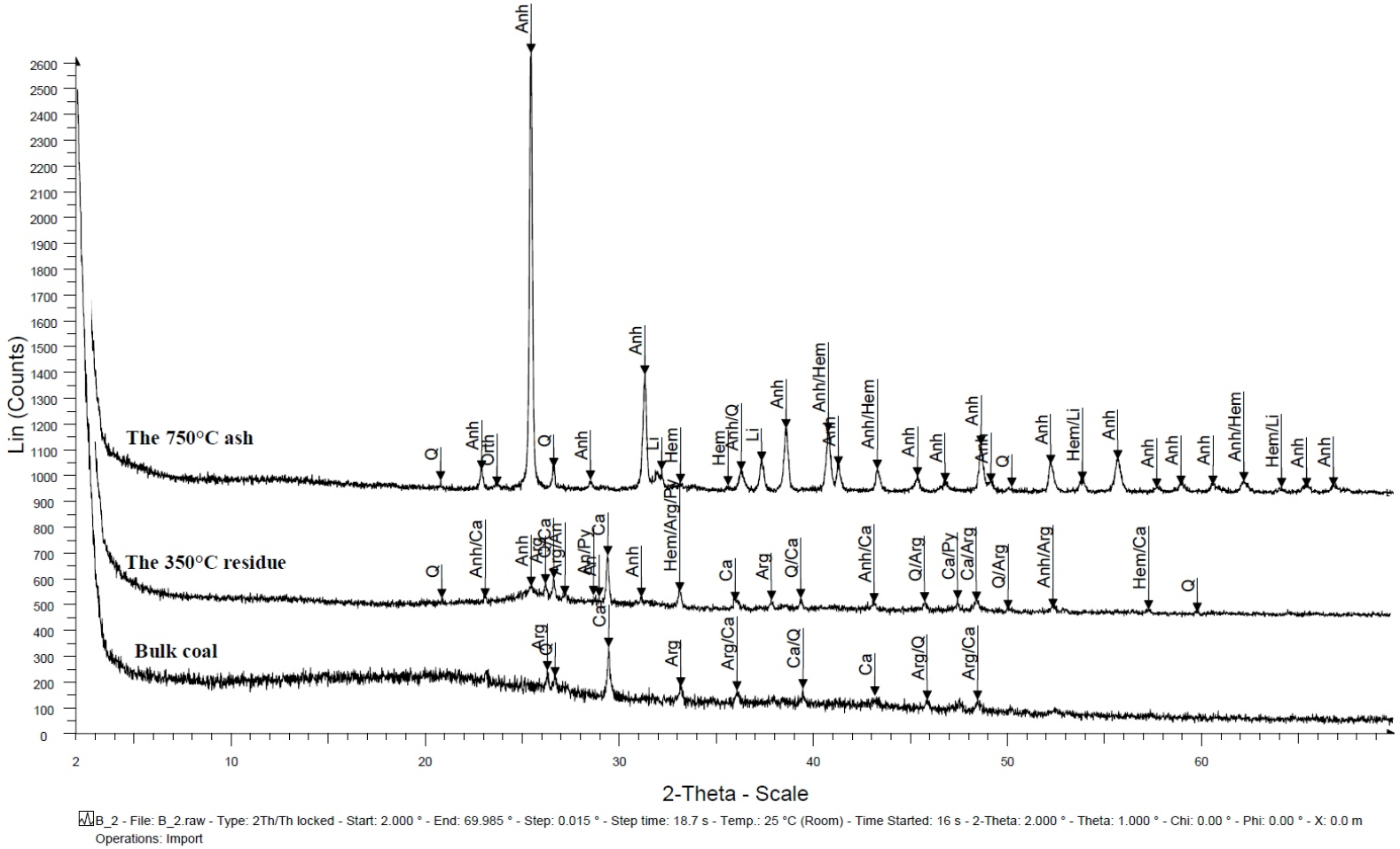

Figure 1. X-ray diffractograms of bulk coal, 350°C residue and 750°C ash samples for B/2

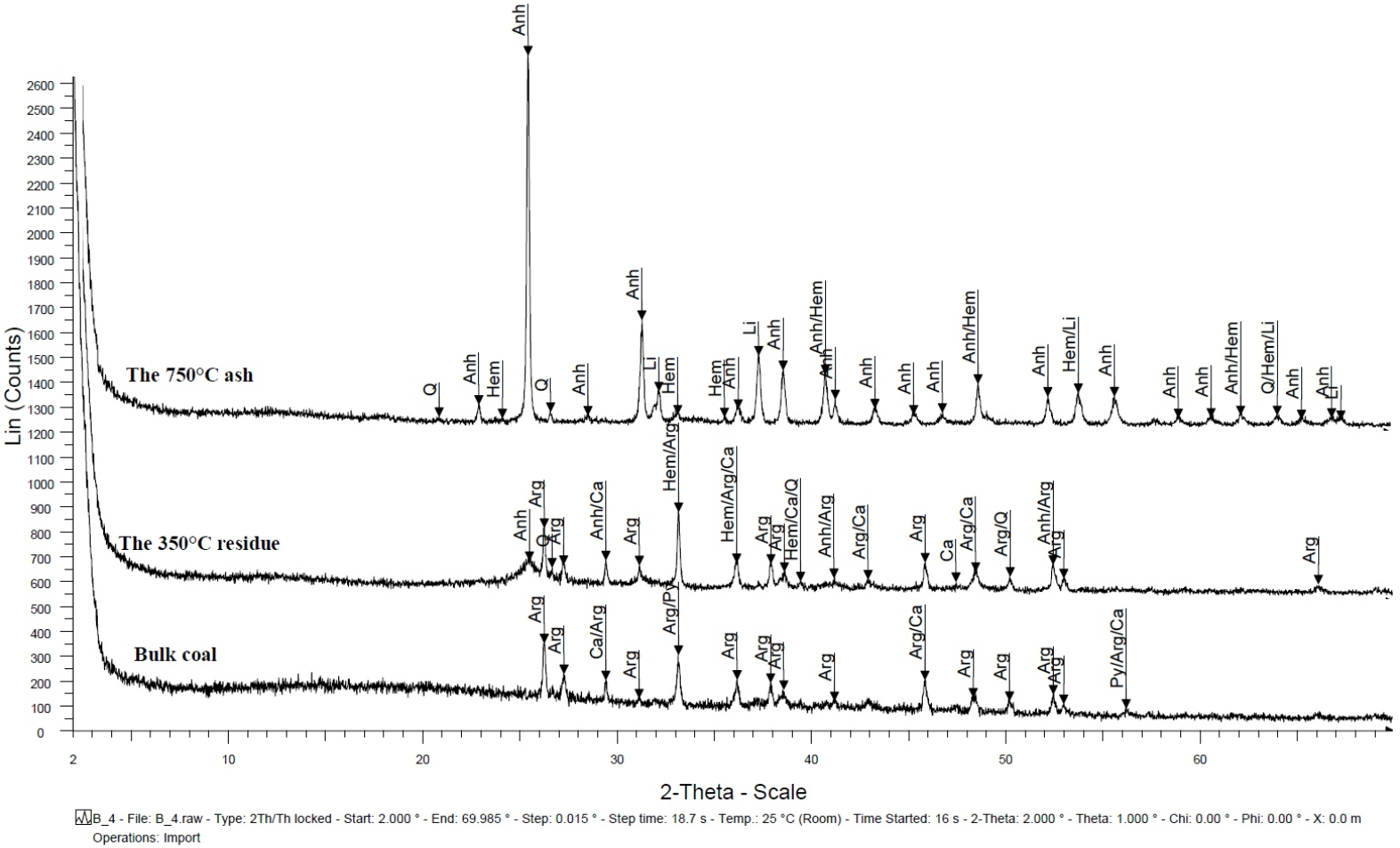

Figure 2. X-ray diffractograms of bulk coal, 350°C residue and 750°C ash samples for B/4

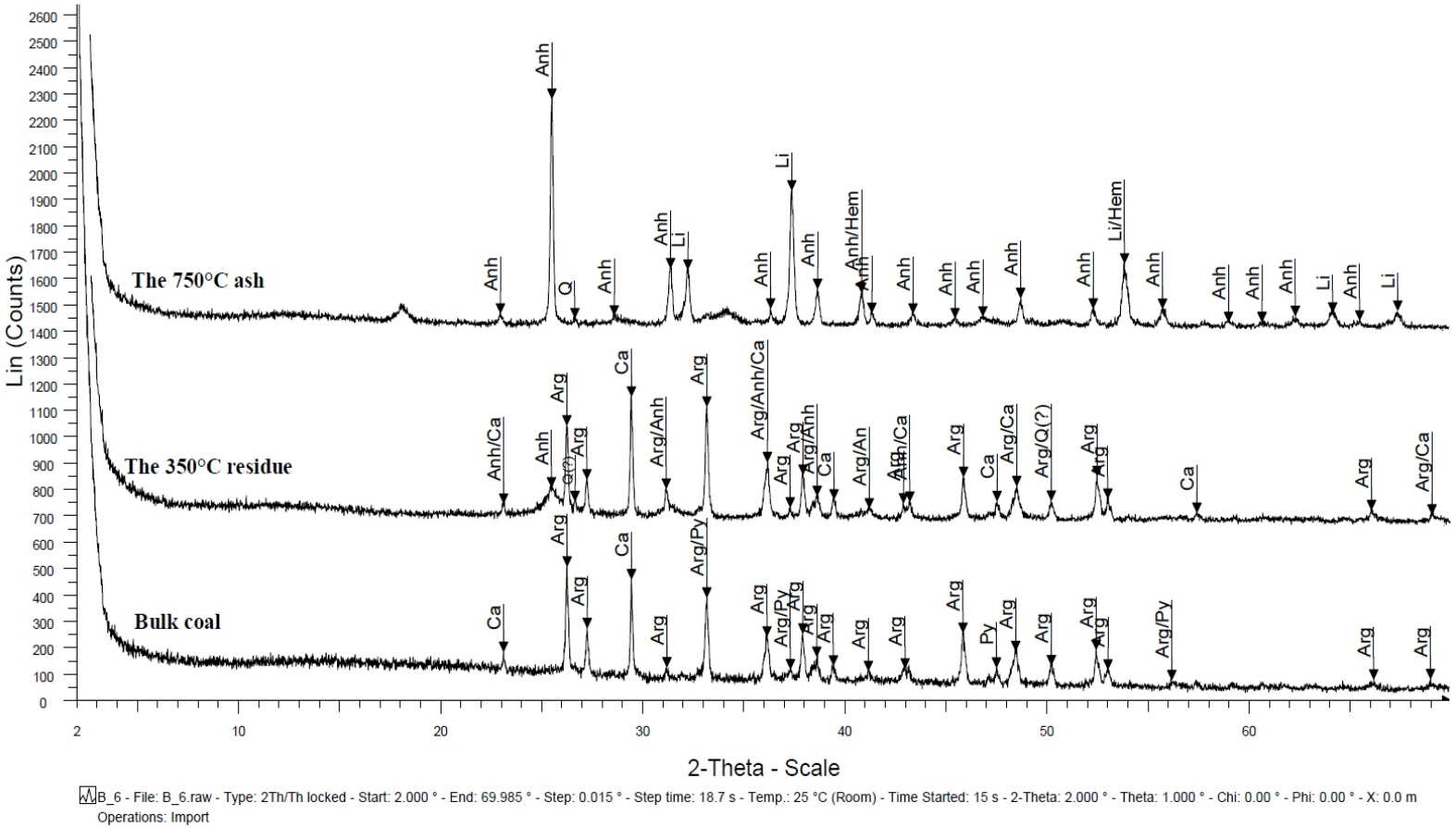

Figure 3. X-ray diffractograms of bulk coal, 350°C residue and 750°C ash samples for B/6

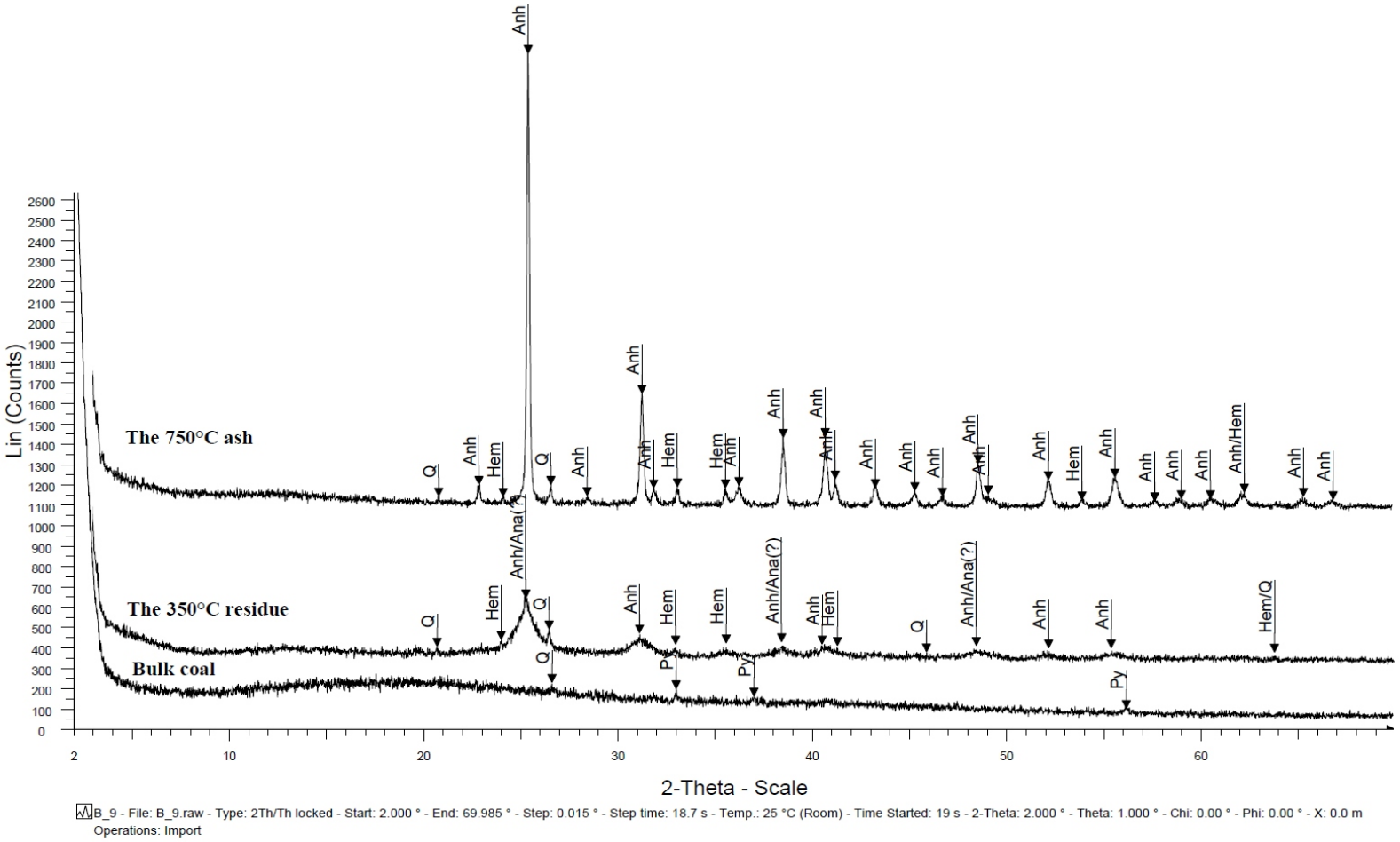

Figure 4. X-ray diffractograms of bulk coal, 350°C residue and 750°C ash samples for B/9

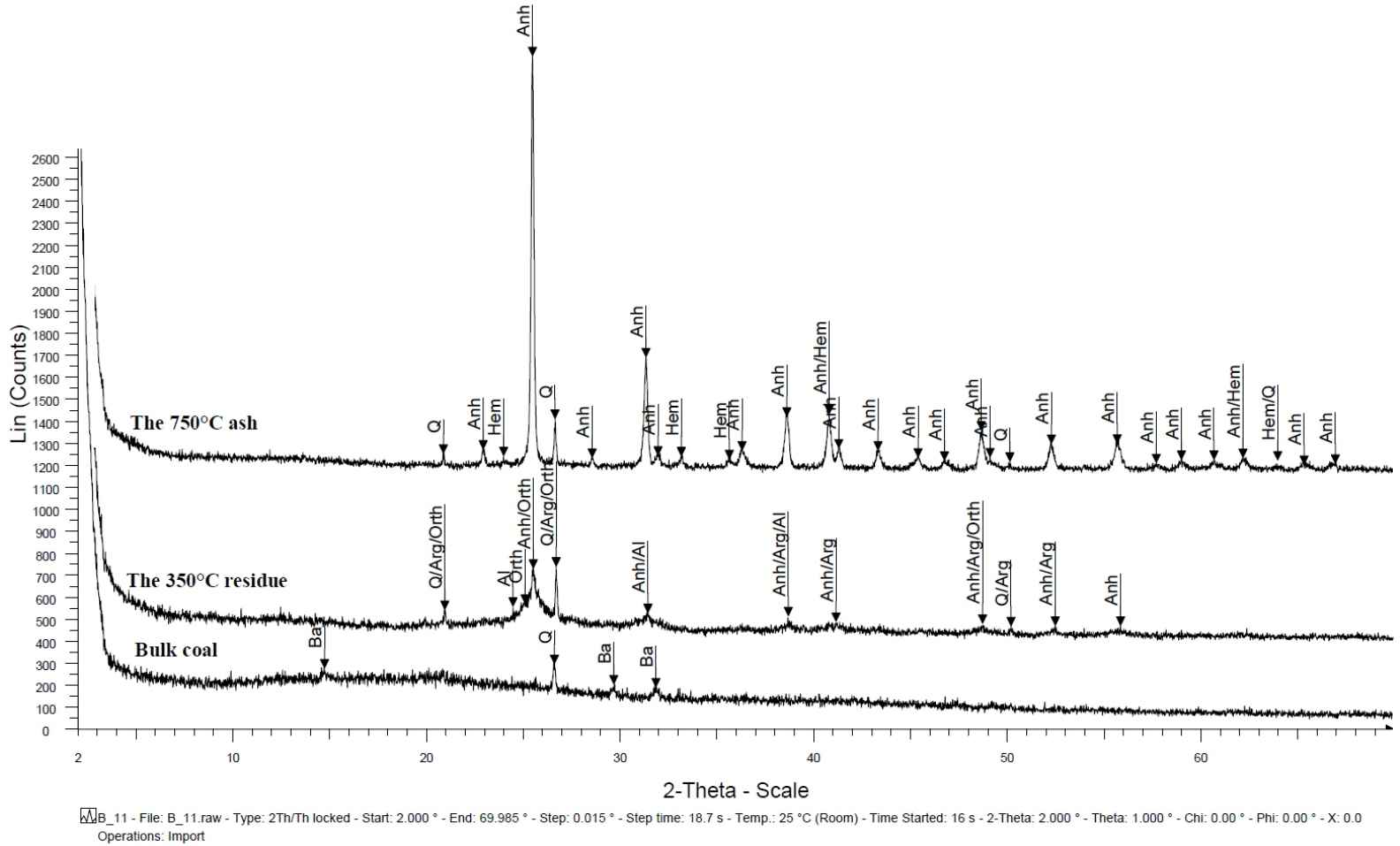

Figure 5. X-ray diffractograms of bulk coal, 350°C residue and 750°C ash samples for B/11

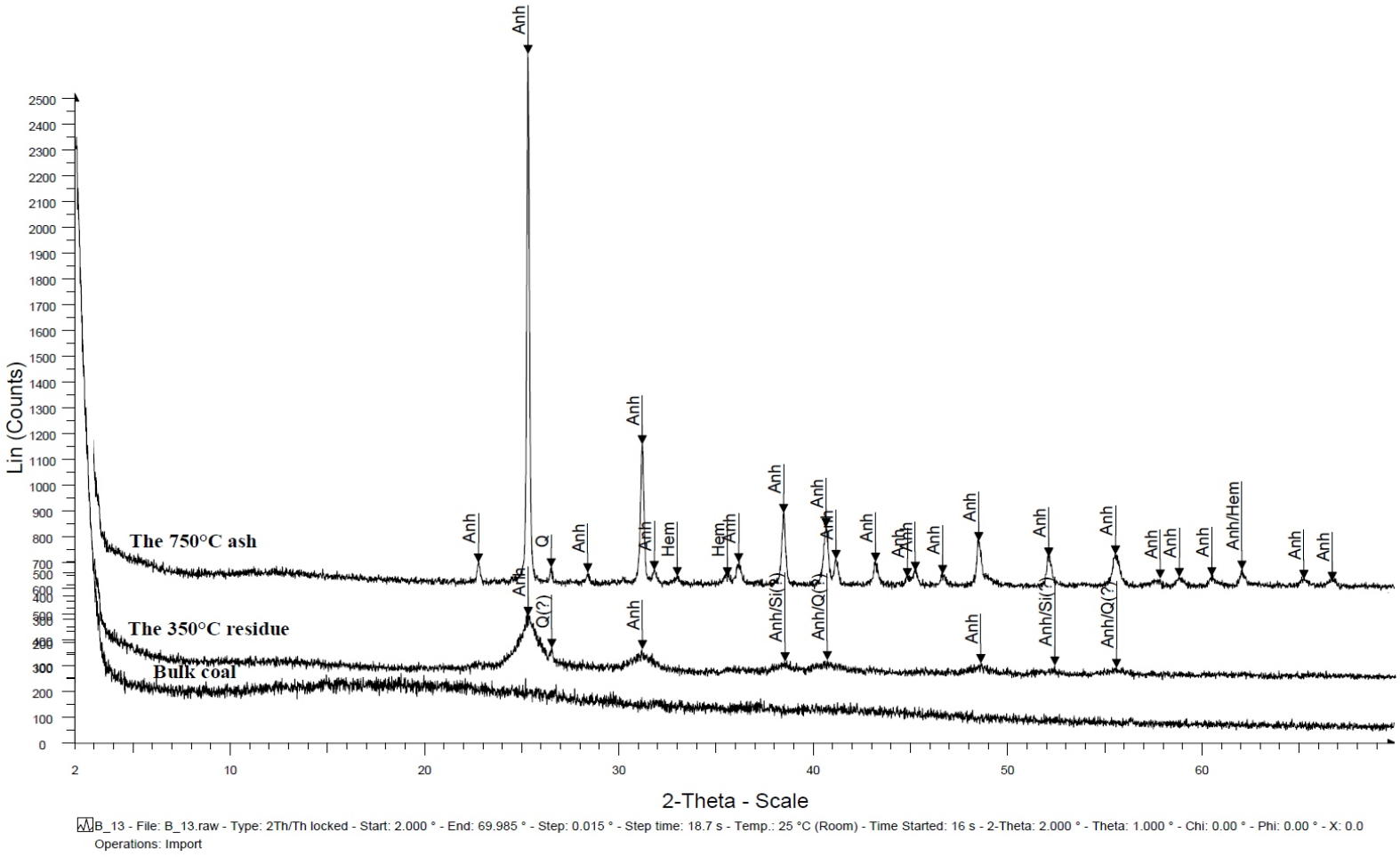

Figure 6. X-ray diffractograms of bulk coal, 350°C residue and 750°C ash samples for B/13

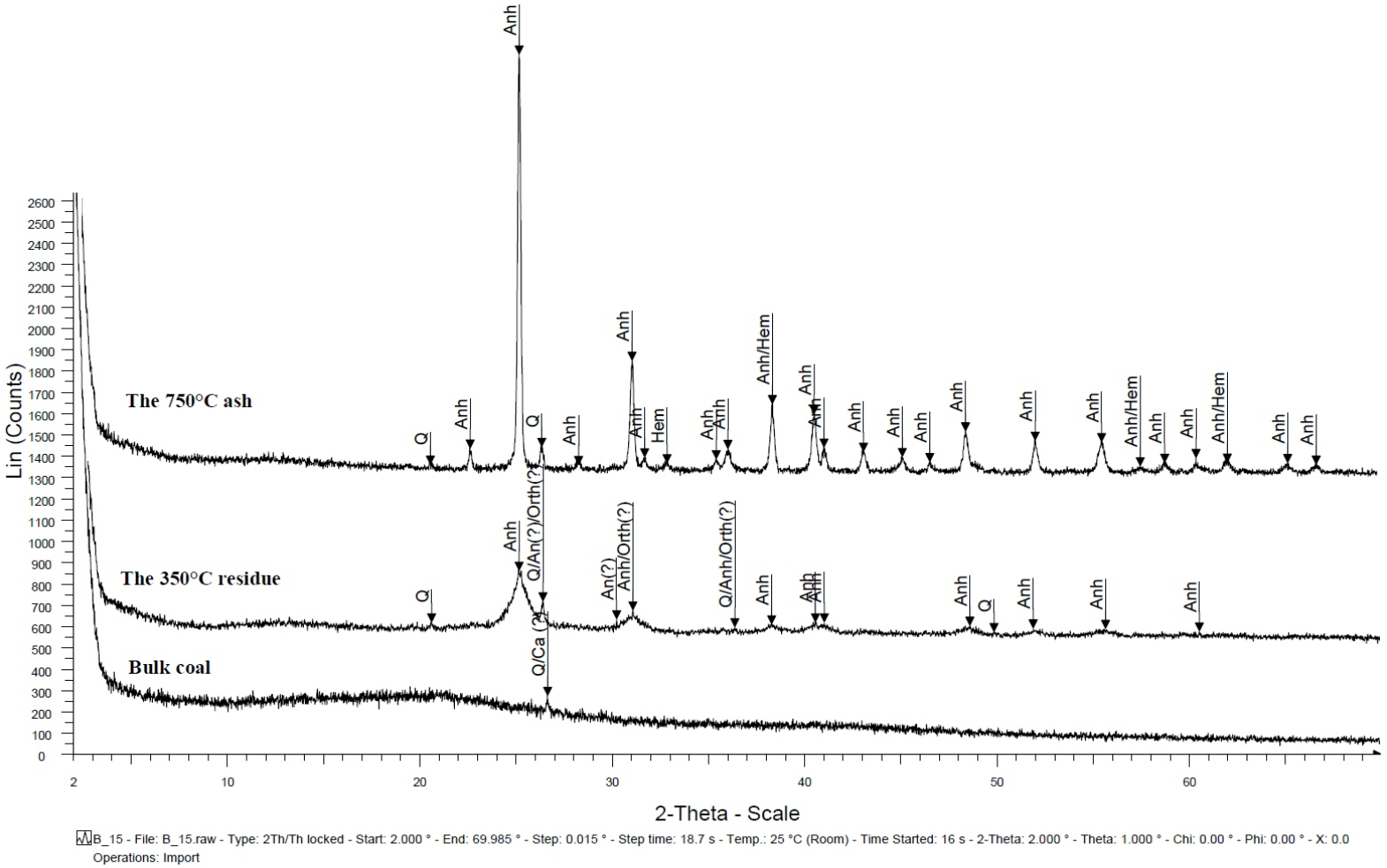

Figure 7. X-ray diffractograms of bulk coal, 350°C residue and 750°C ash samples for B/15

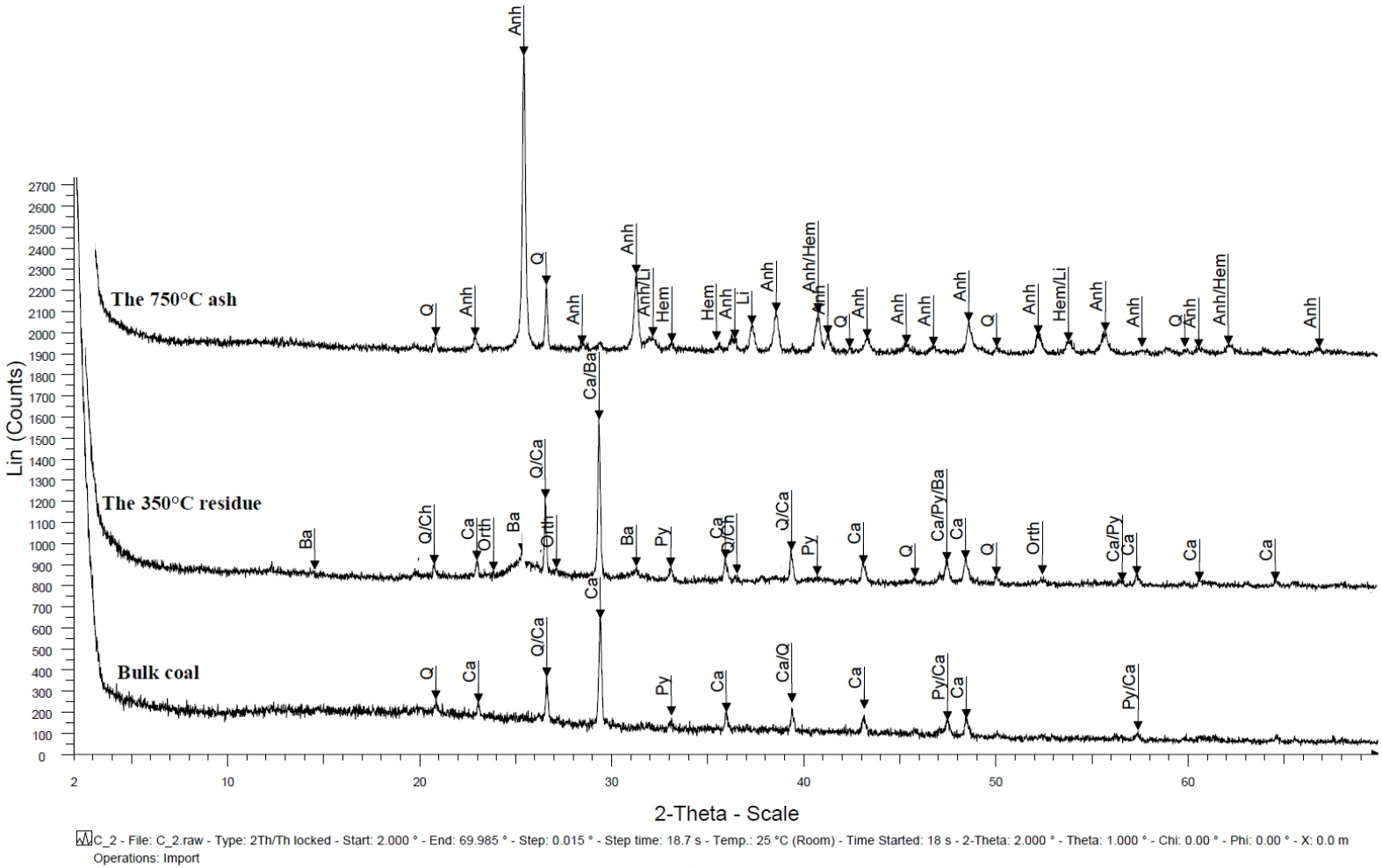

Figure 8. X-ray diffractograms of bulk coal, 350°C residue and 750°C ash samples for C/2

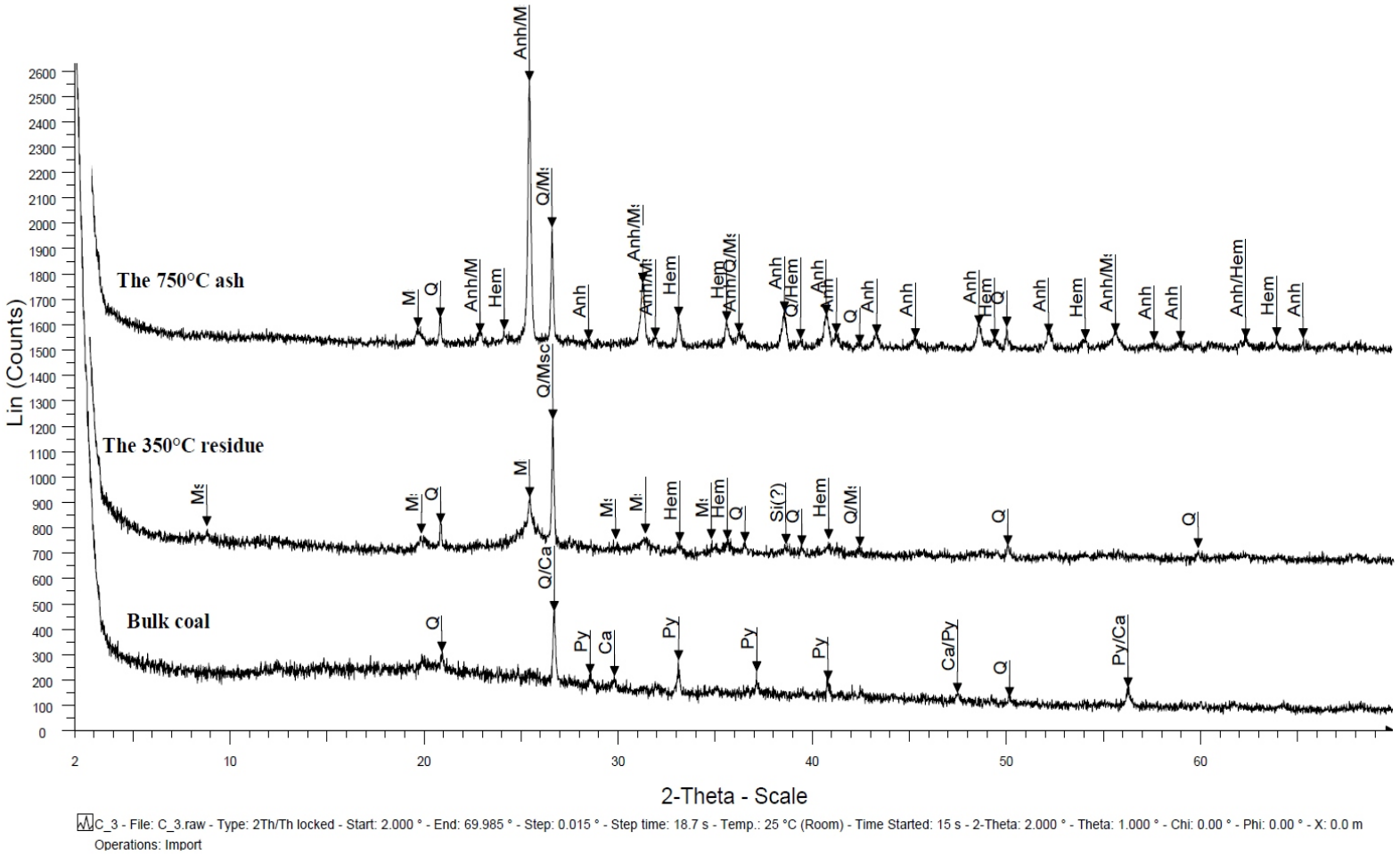

Figure 9. X-ray diffractograms of bulk coal, 350°C residue and 750°C ash samples for C/3

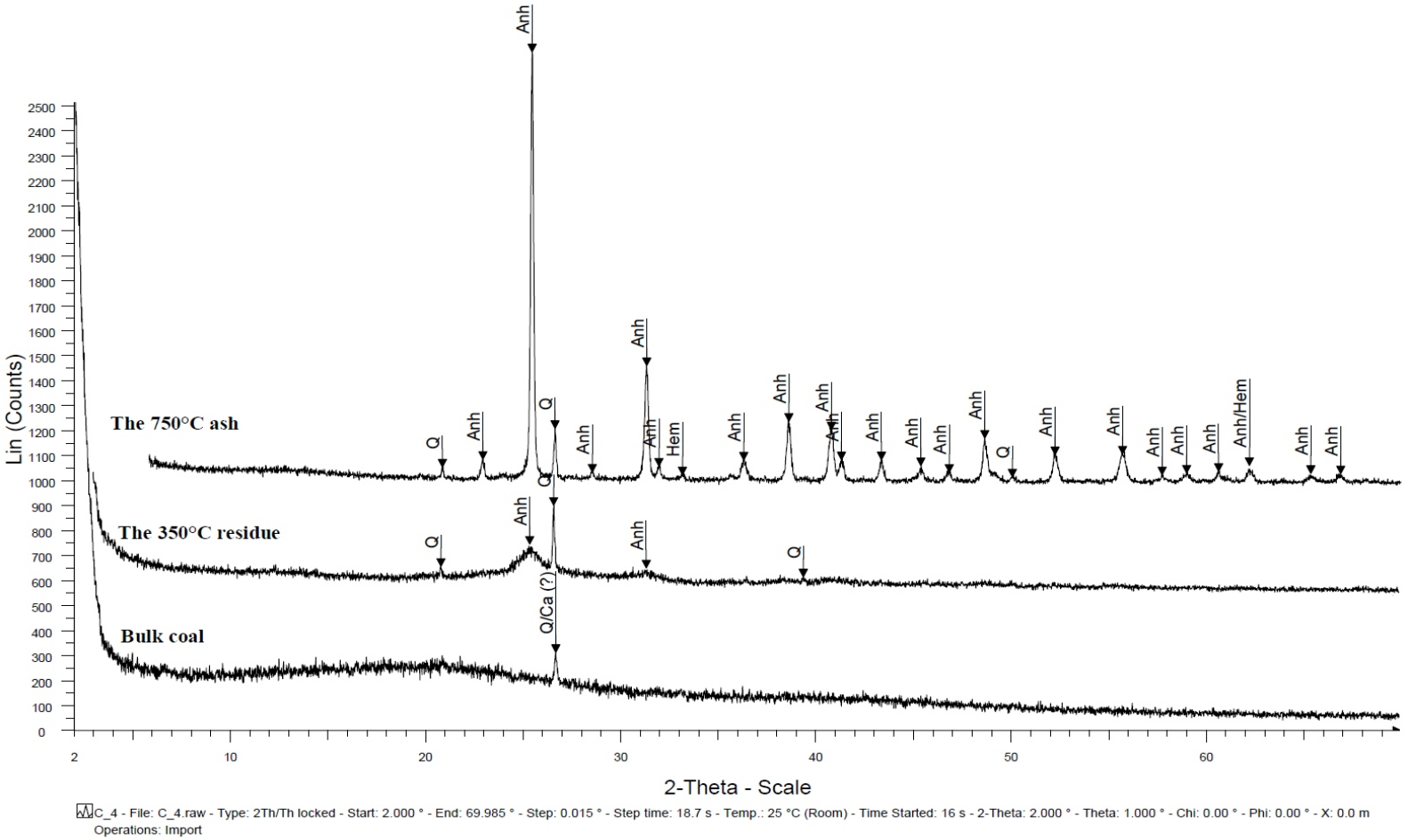

Figure 10. X-ray diffractograms of bulk coal, 350°C residue and 750°C ash samples for C/4

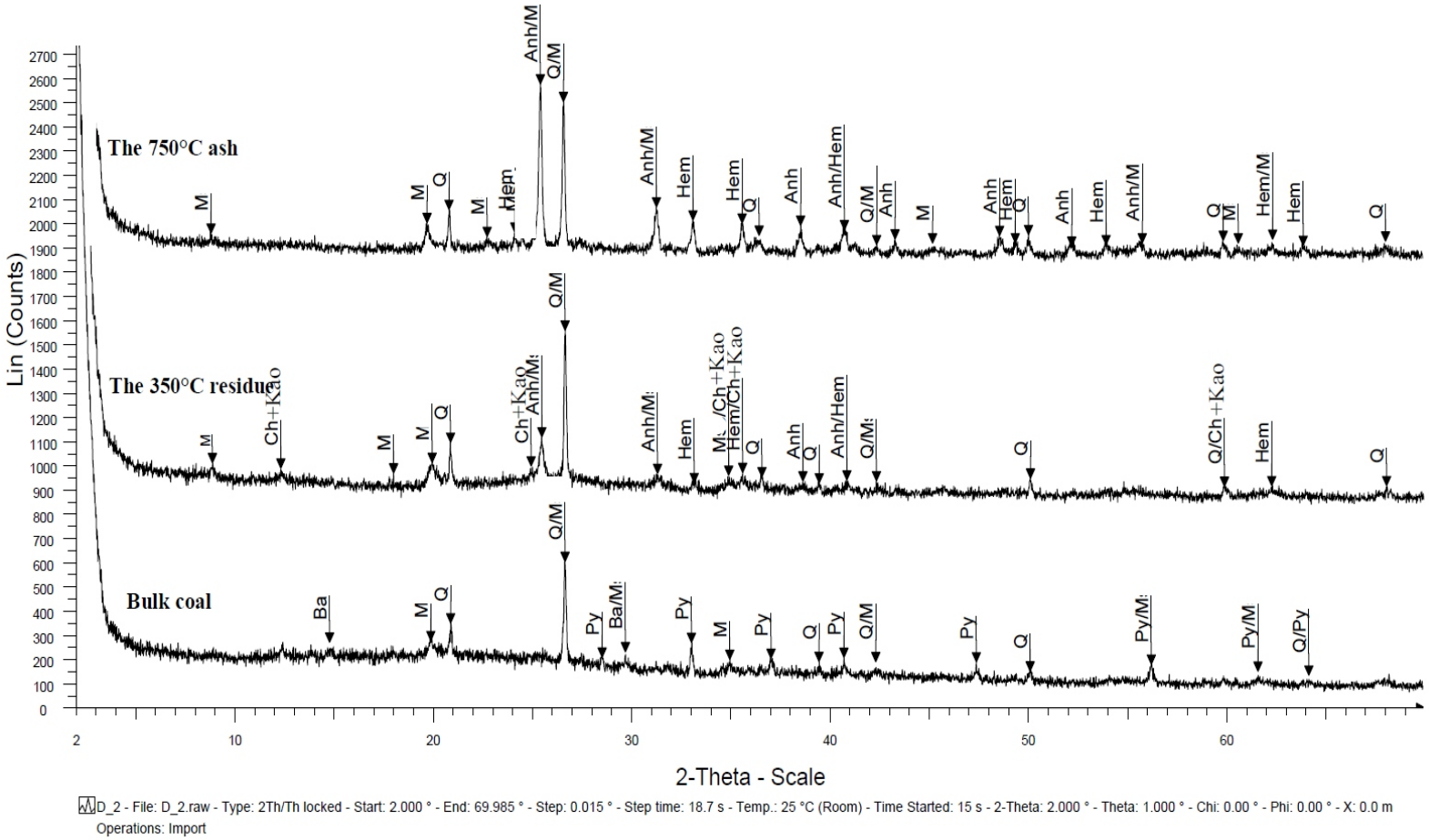

Figure 11. X-ray diffractograms of bulk coal, 350°C residue and 750°C ash samples for D/2

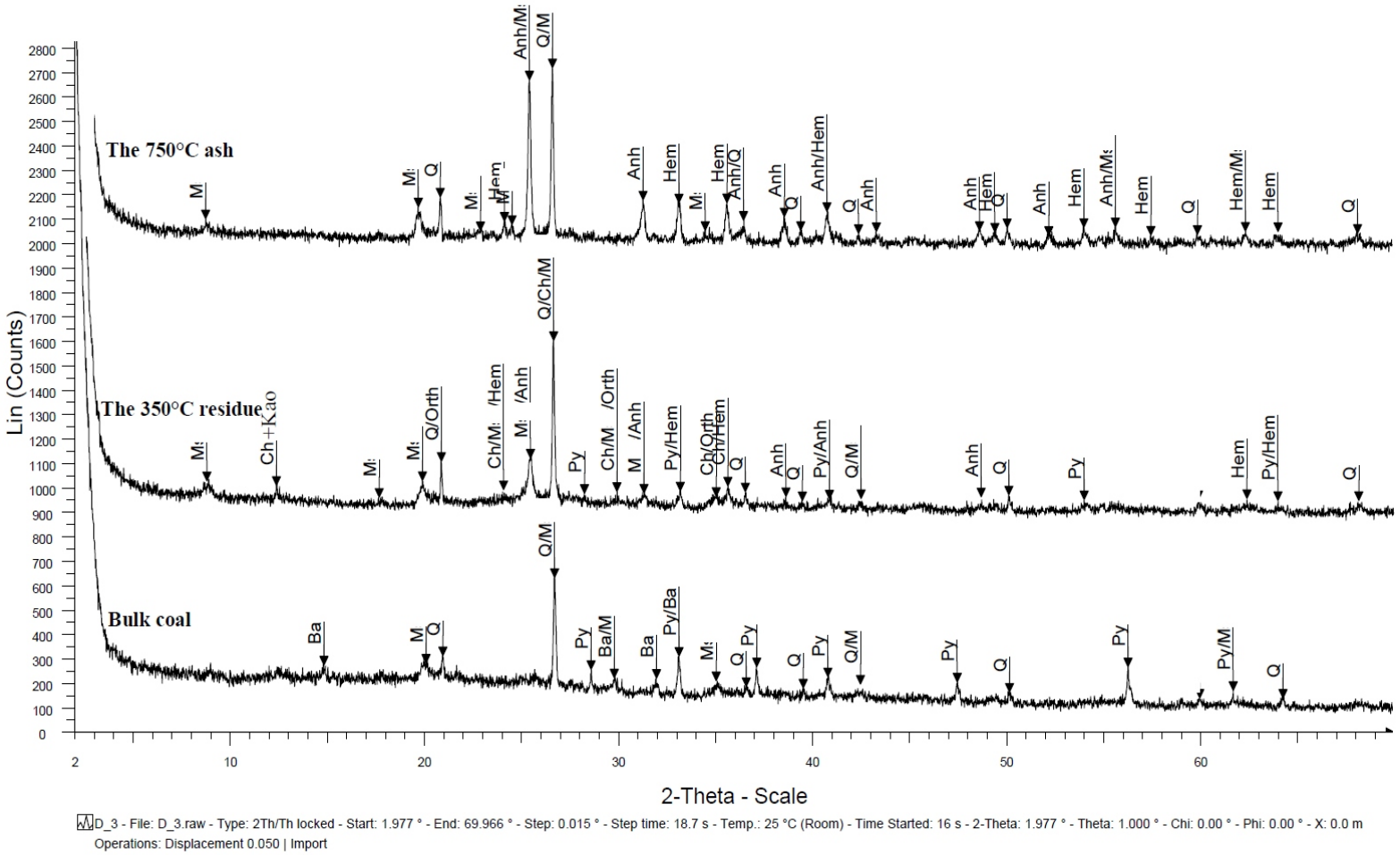

Figure 12. X-ray diffractograms of bulk coal, 350°C residue and 750°C ash samples for D/3

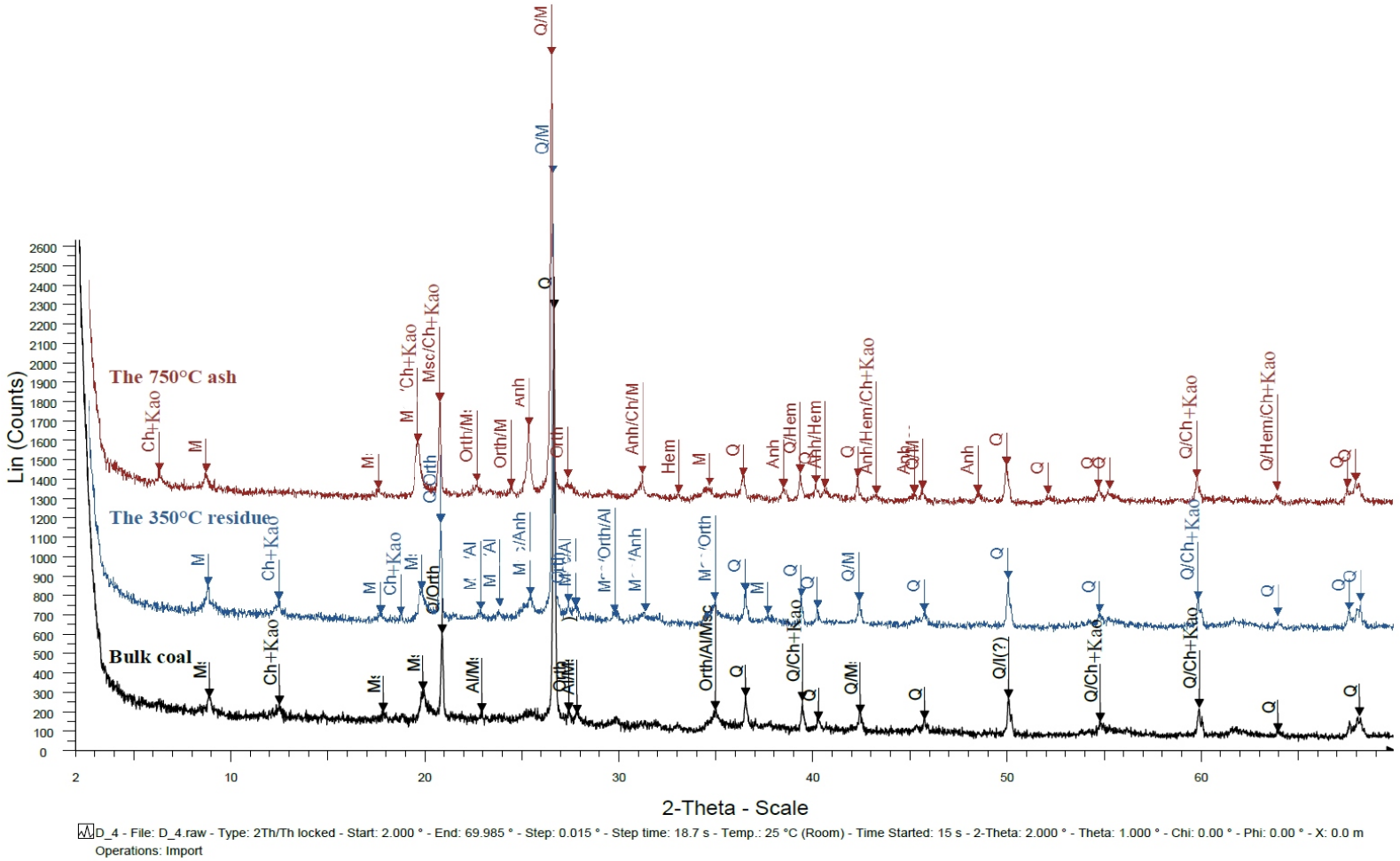

Figure 13. X-ray diffractograms of bulk coal, 350°C residue and 750°C ash samples for D/4

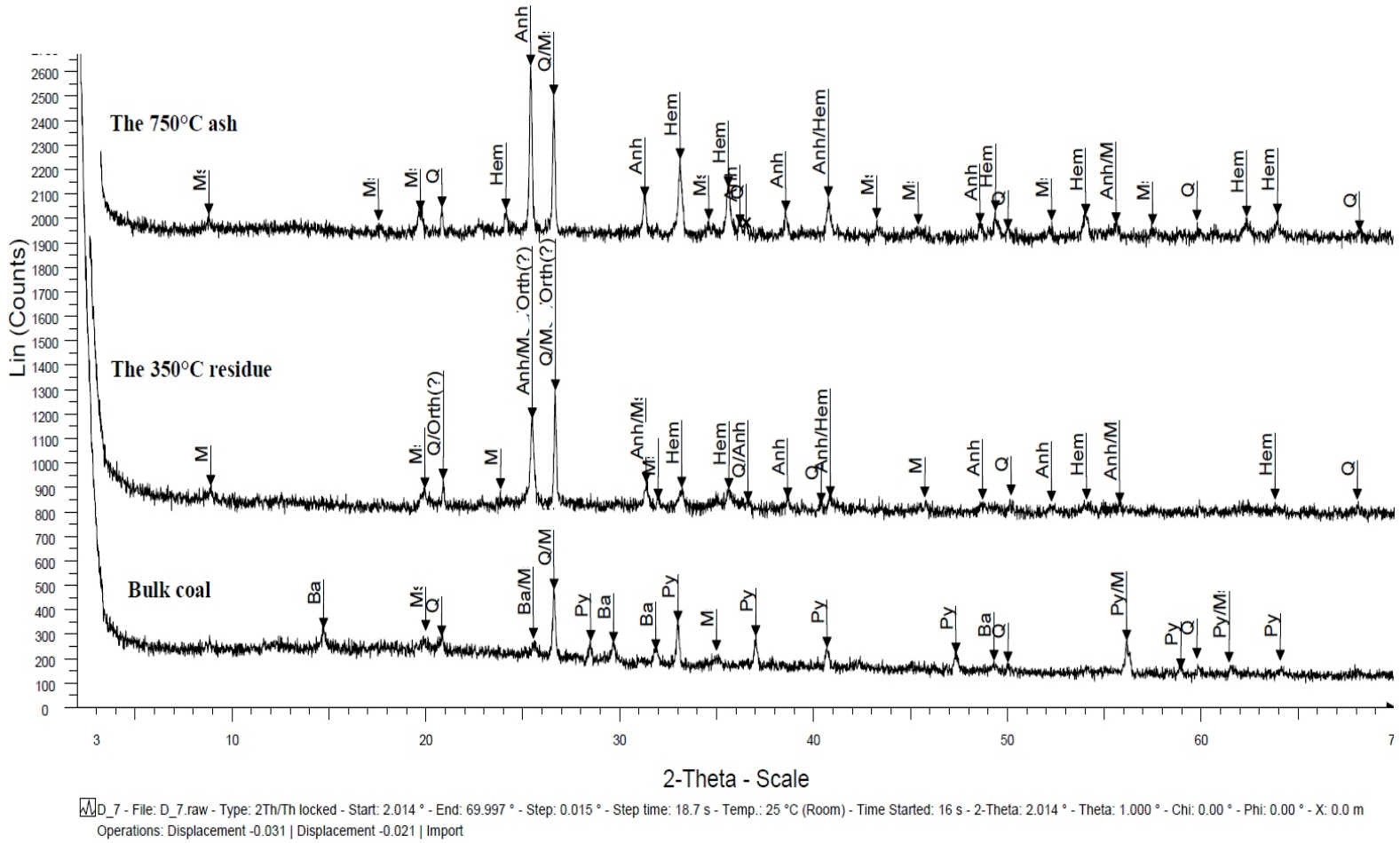

Figure 14. X-ray diffractograms of bulk coal, 350°C residue and 750°C ash samples for D/7

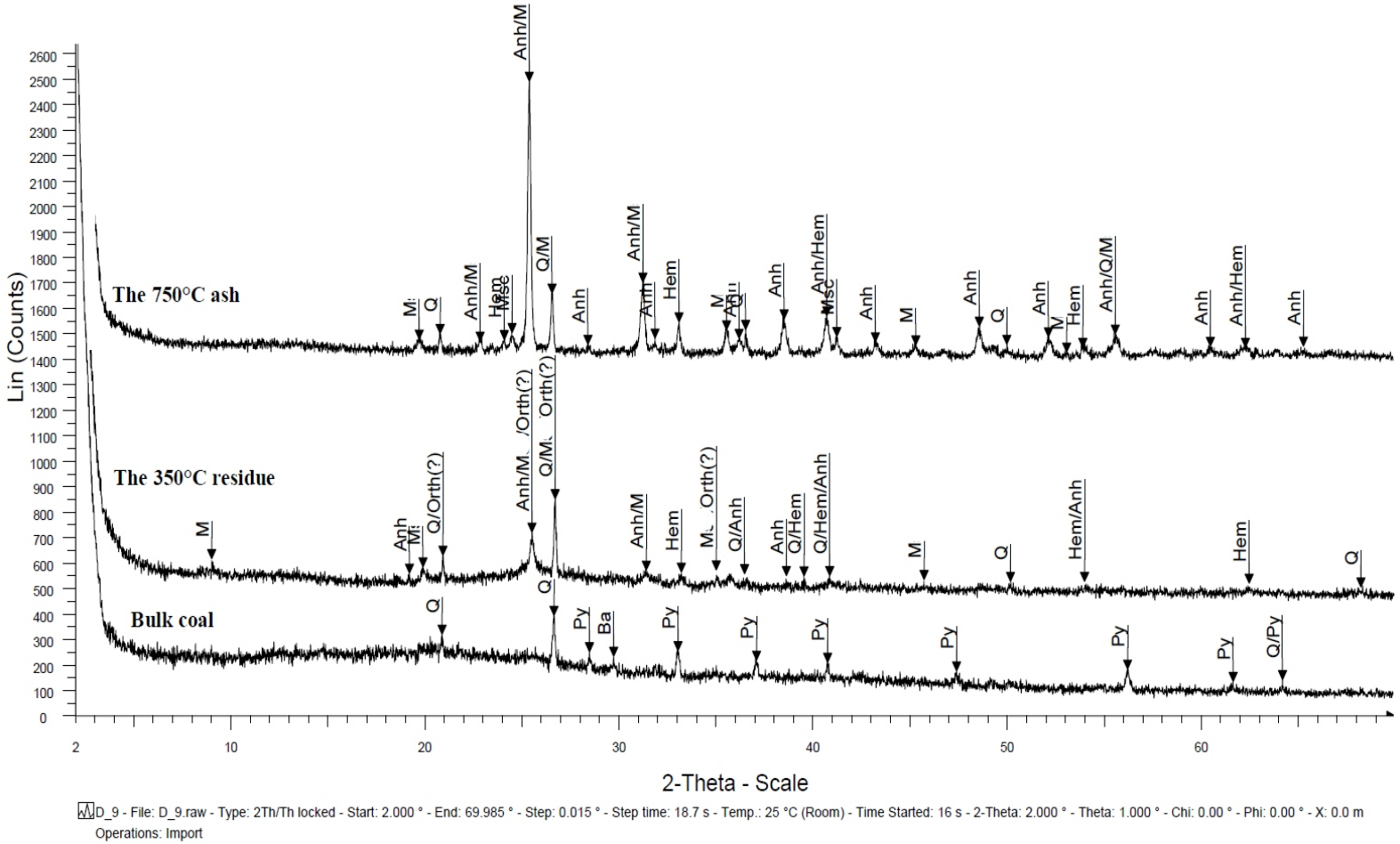

Figure 15. X-ray diffractograms of bulk coal, 350°C residue and 750°C ash samples for D/9

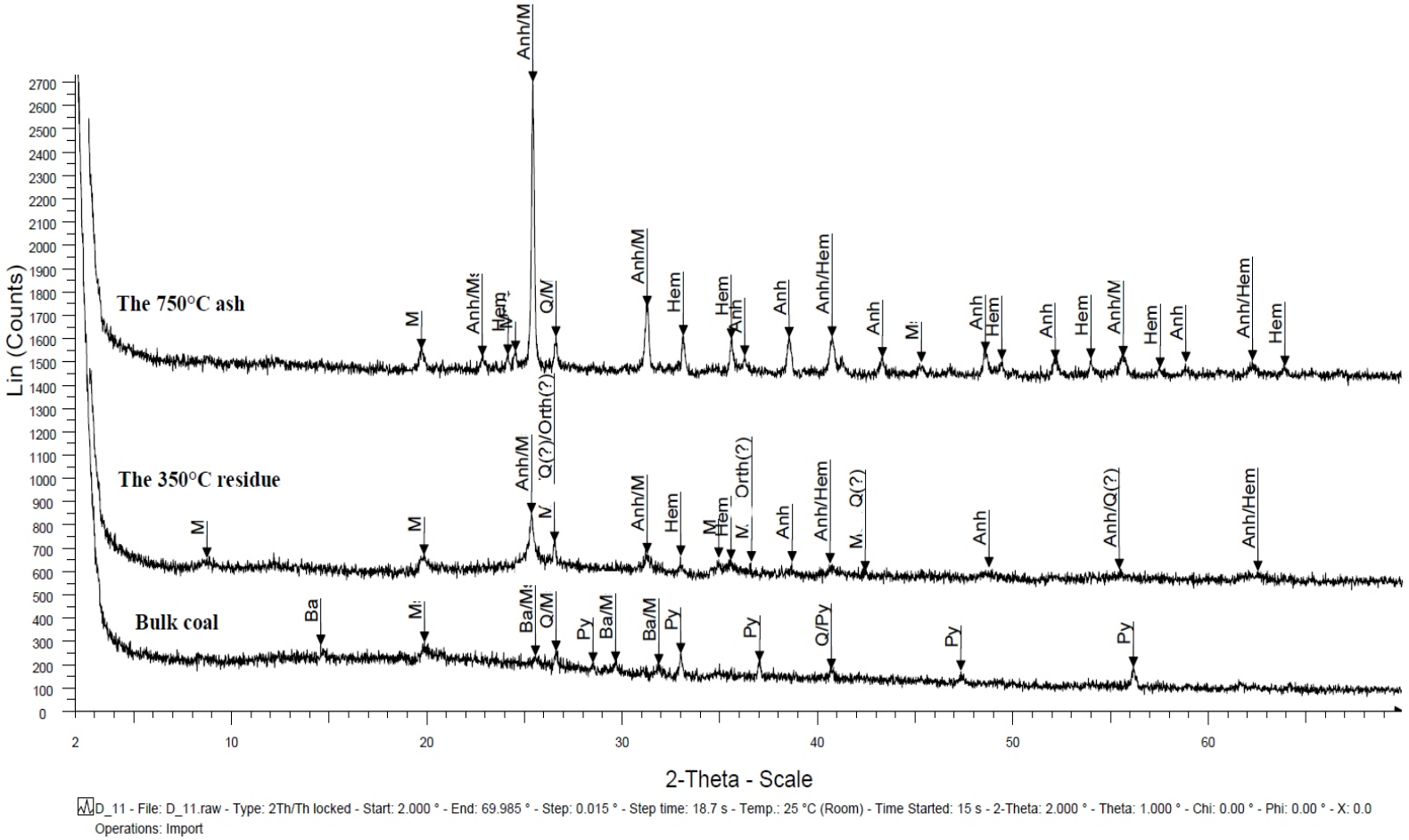

Figure 16. X-ray diffractograms of bulk coal, 350°C residue and 750°C ash samples for D/11

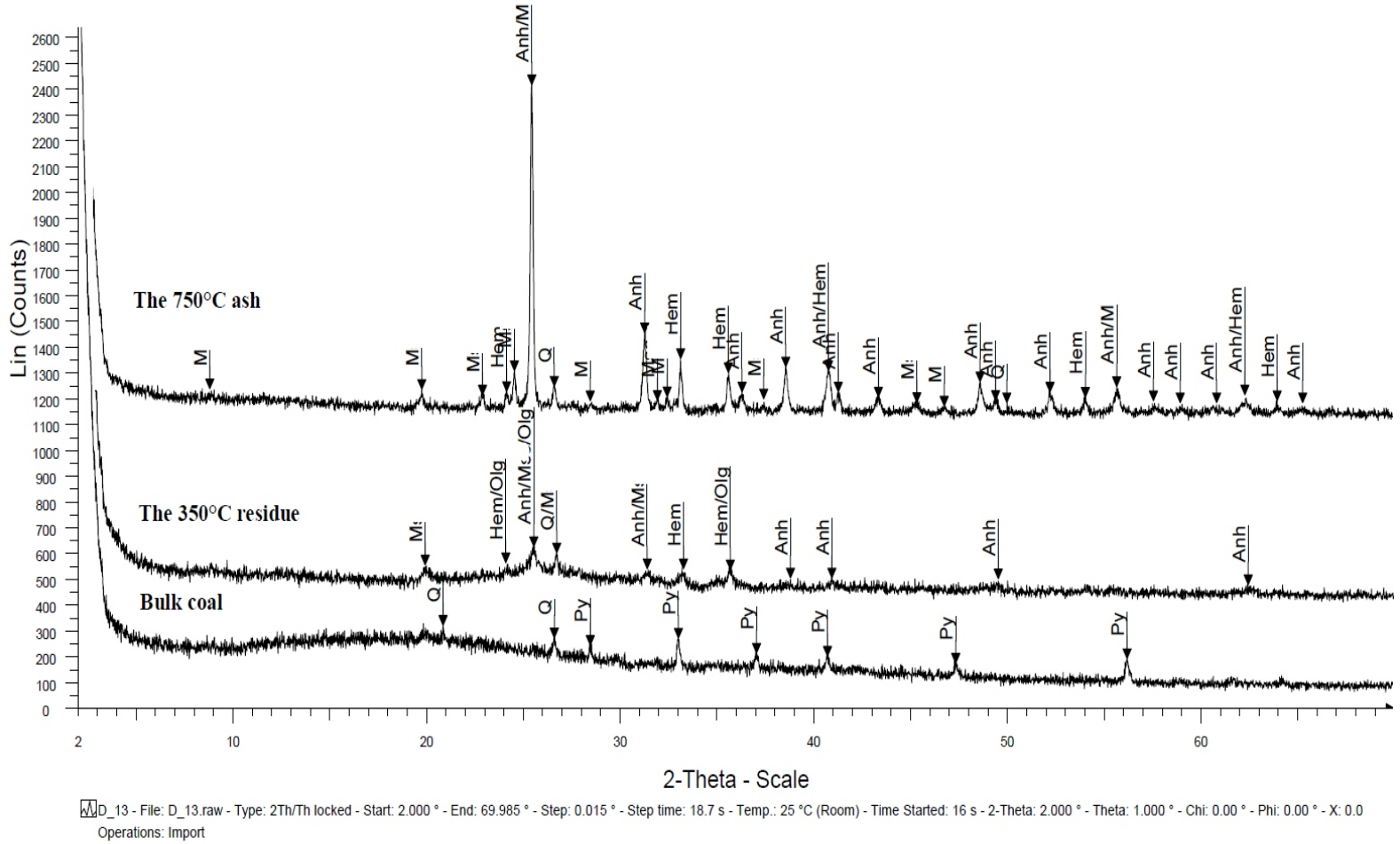

Figure 17. X-ray diffractograms of bulk coal, 350°C residue and 750°C ash samples for D/13

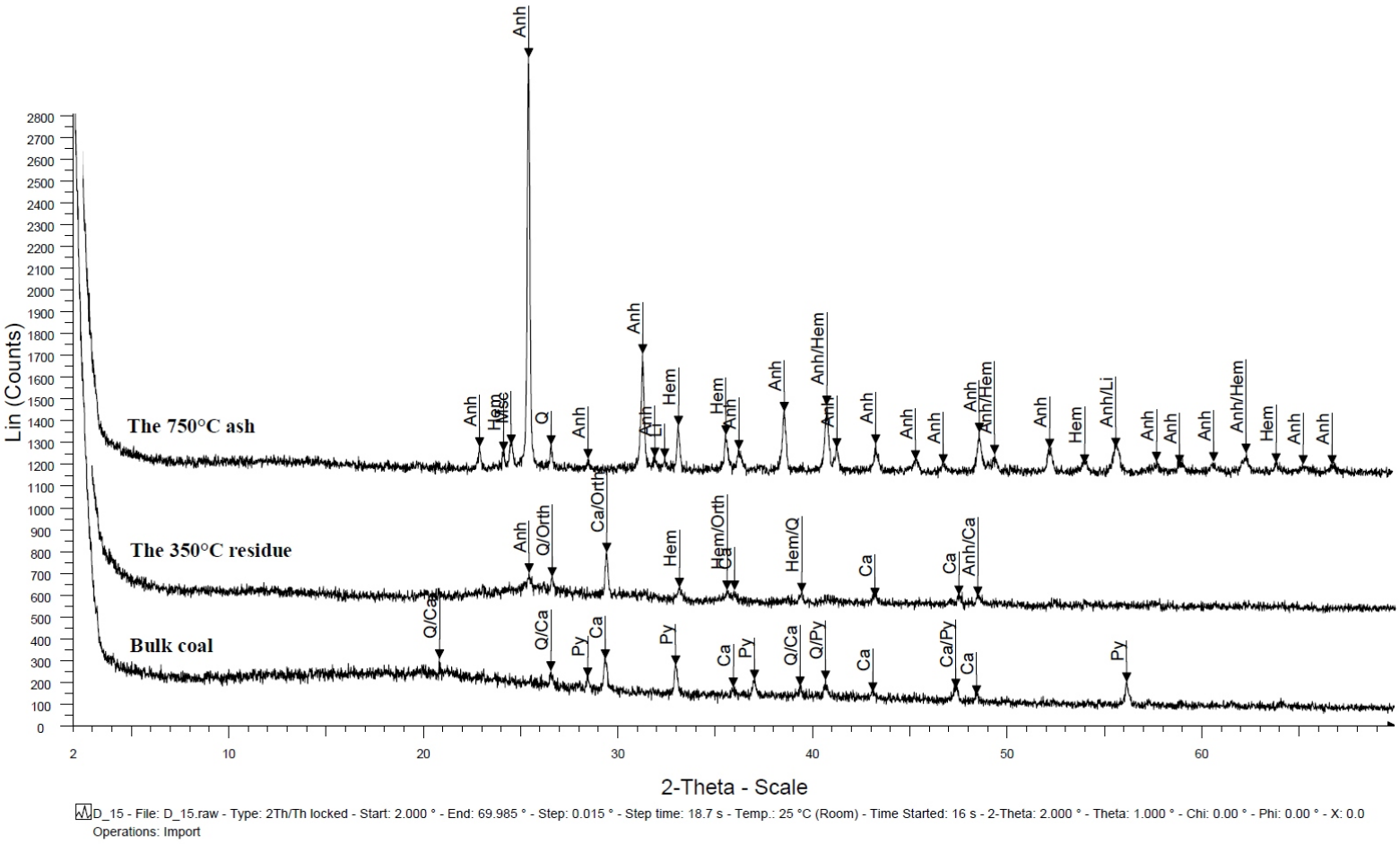

Figure 18. X-ray diffractograms of bulk coal, 350°C residue and 750°C ash samples for D/15

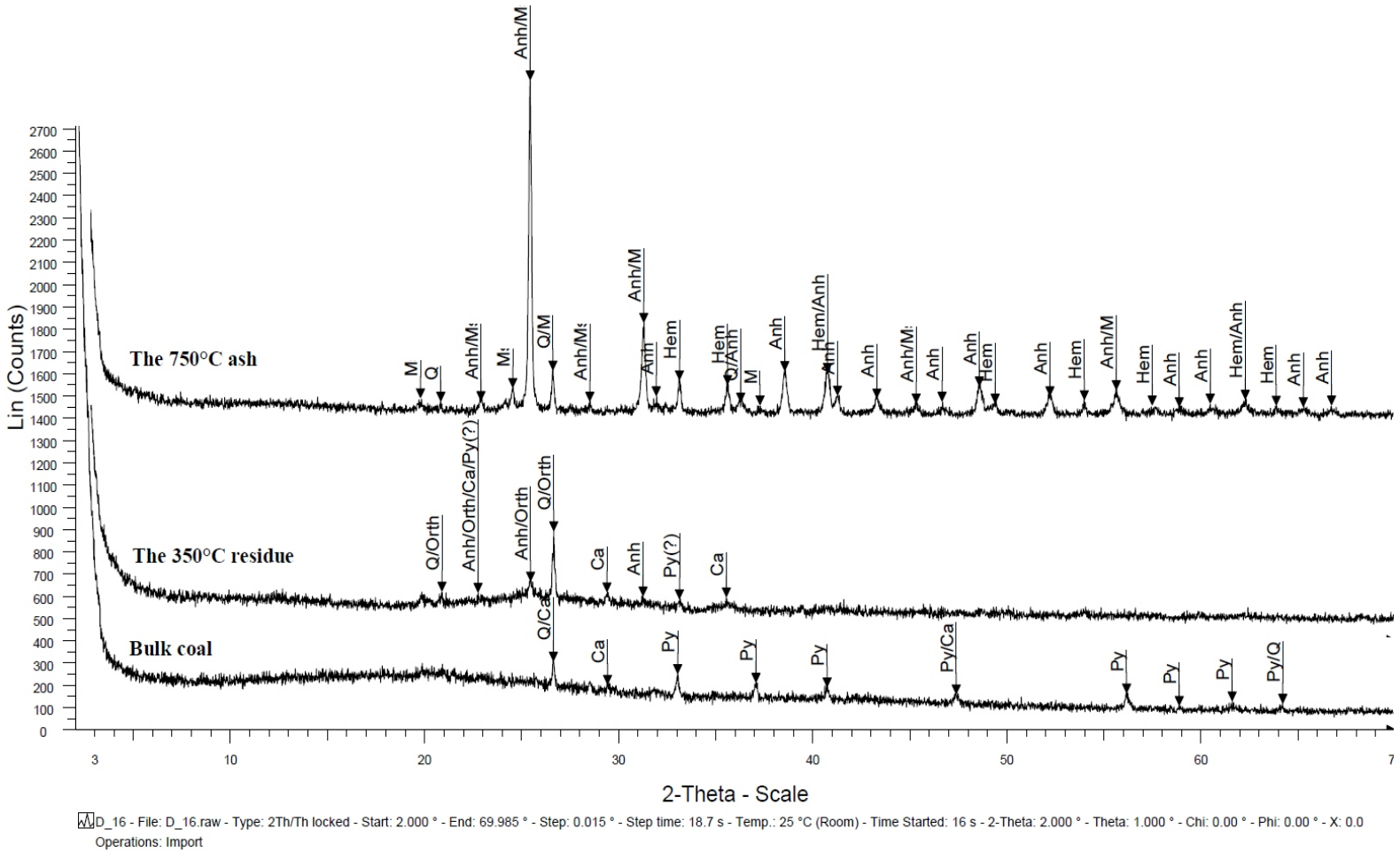

Figure 19. X-ray diffractograms of bulk coal, 350°C residue and 750°C ash samples for D/16

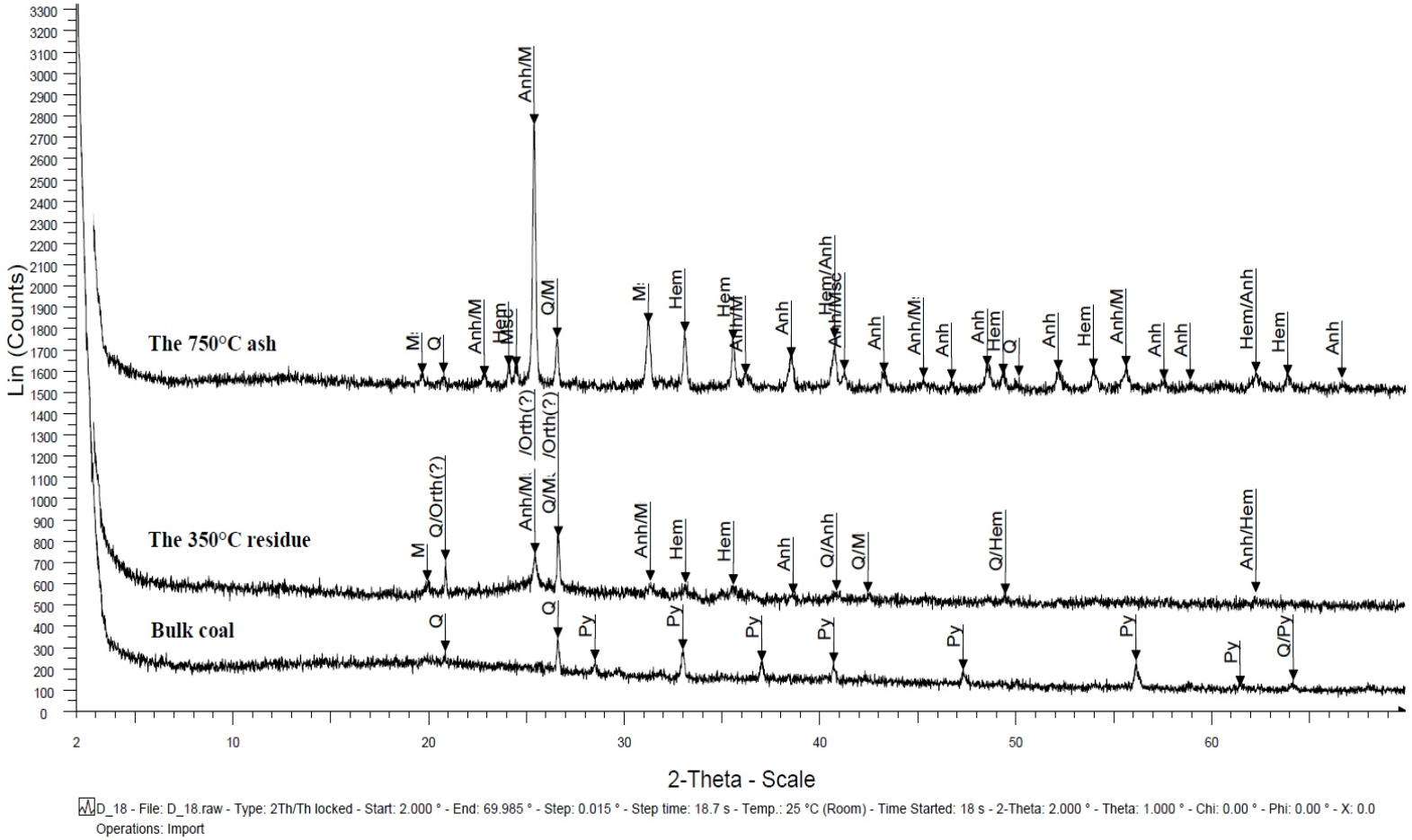

Figure 20. X-ray diffractograms of bulk coal, 350°C residue and 750°C ash samples for D/18

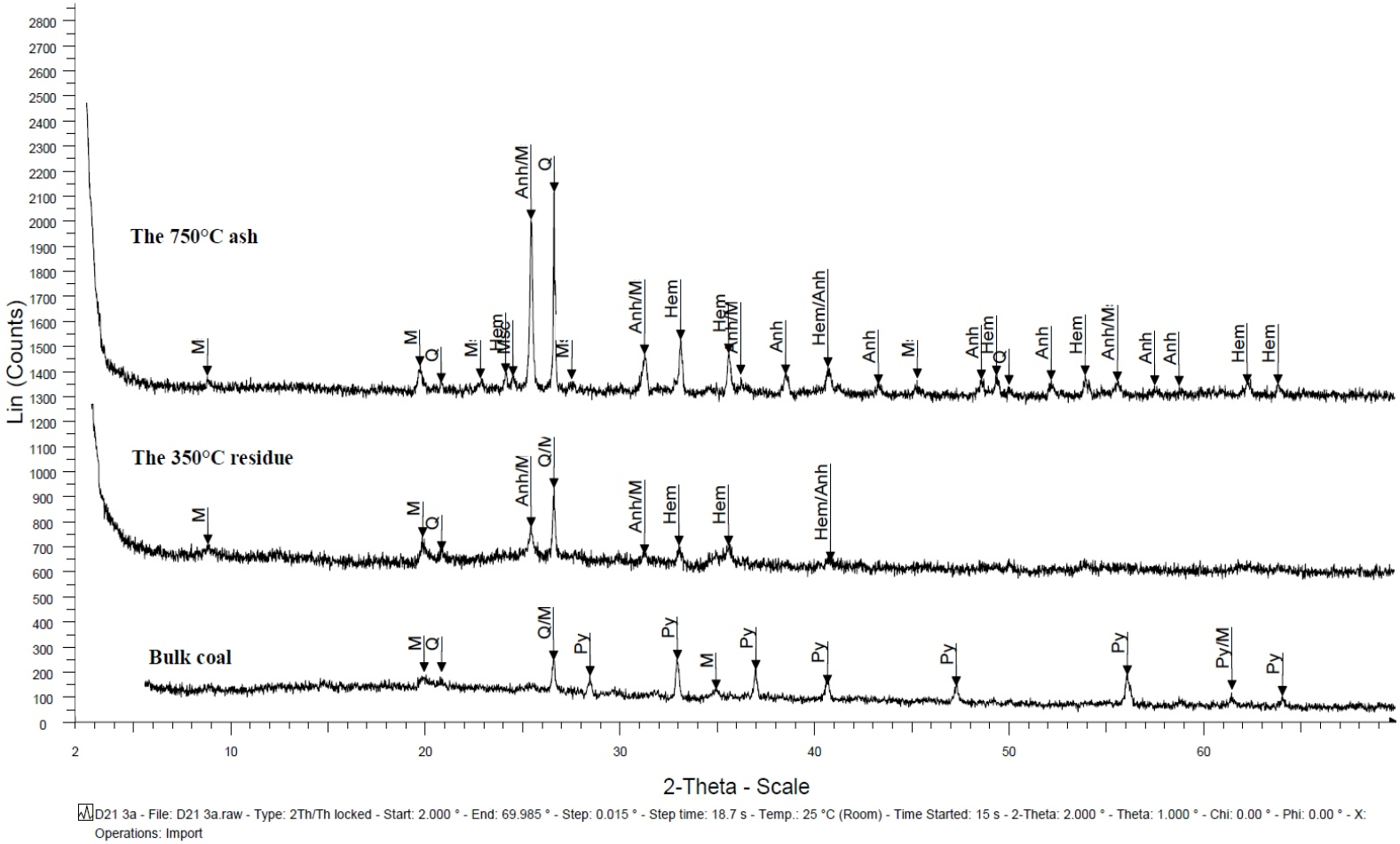

Figure 21. X-ray diffractograms of bulk coal, 350°C residue and 750°C ash samples for D/21

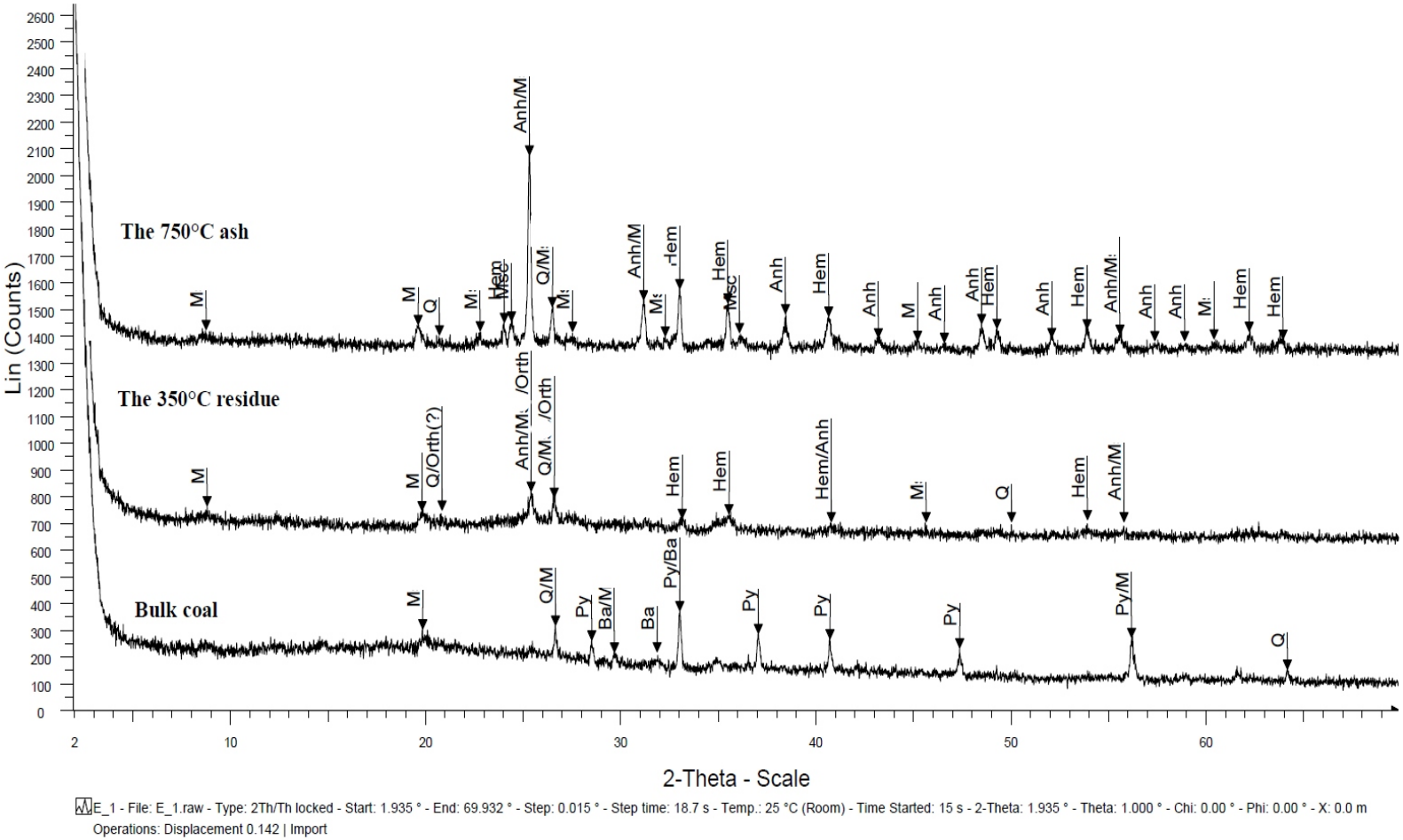

Figure 22. X-ray diffractograms of bulk coal, 350°C residue and 750°C ash samples for E/1

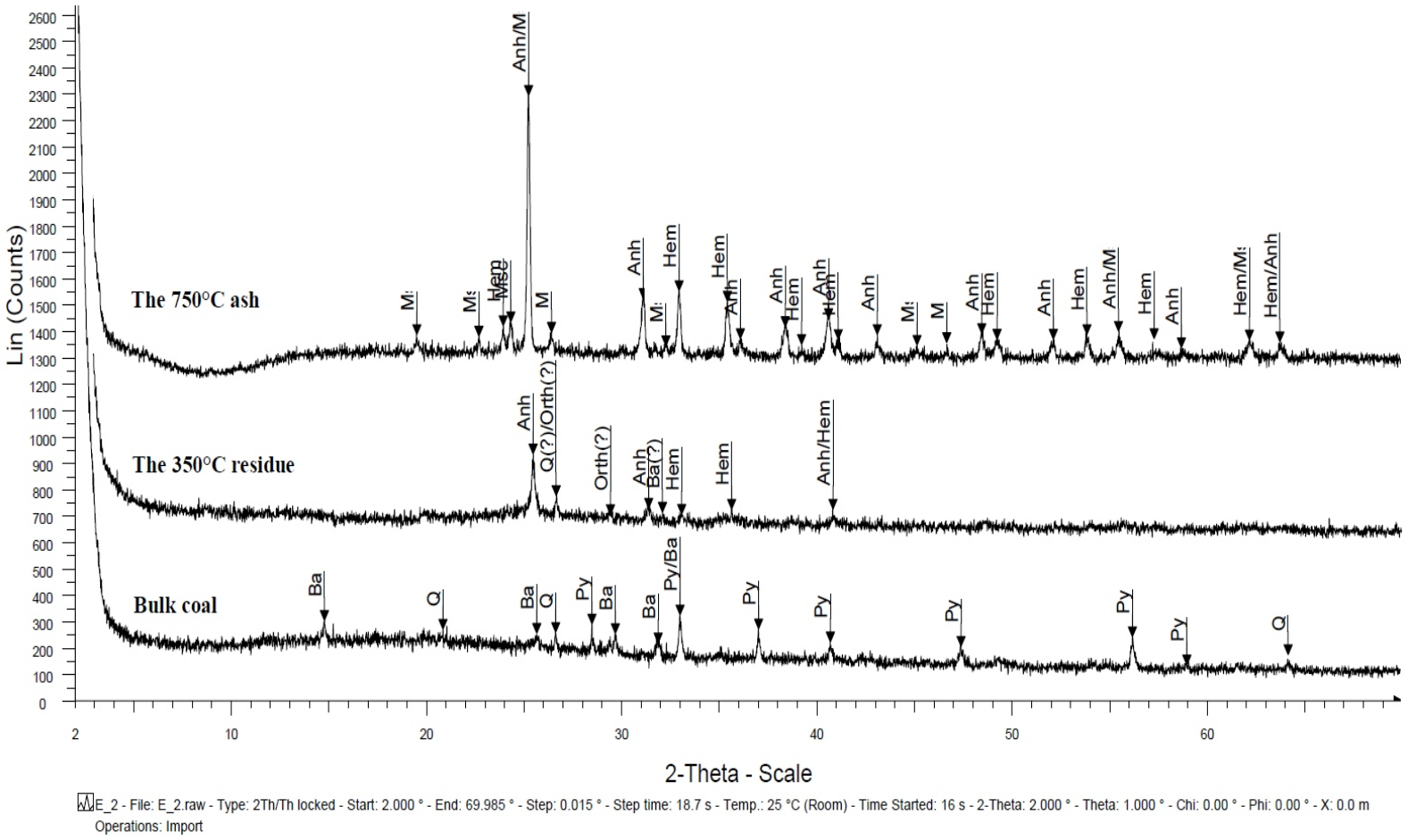

Figure 23. X-ray diffractograms of bulk coal, 350°C residue and 750°C ash samples for E/2

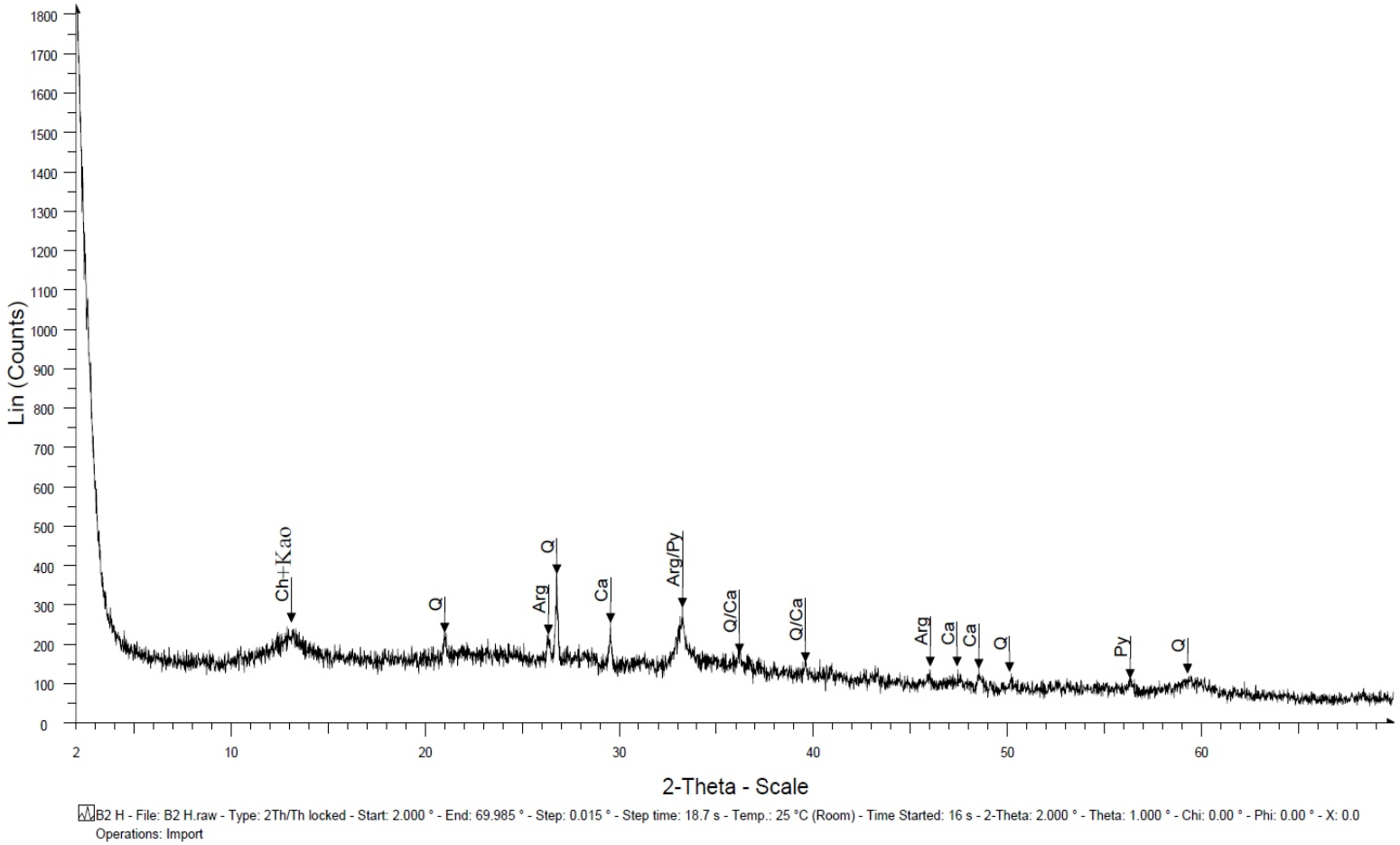

Figure 24. X-ray diffractogram of heavy fraction (inorganic matter) of sample B/2

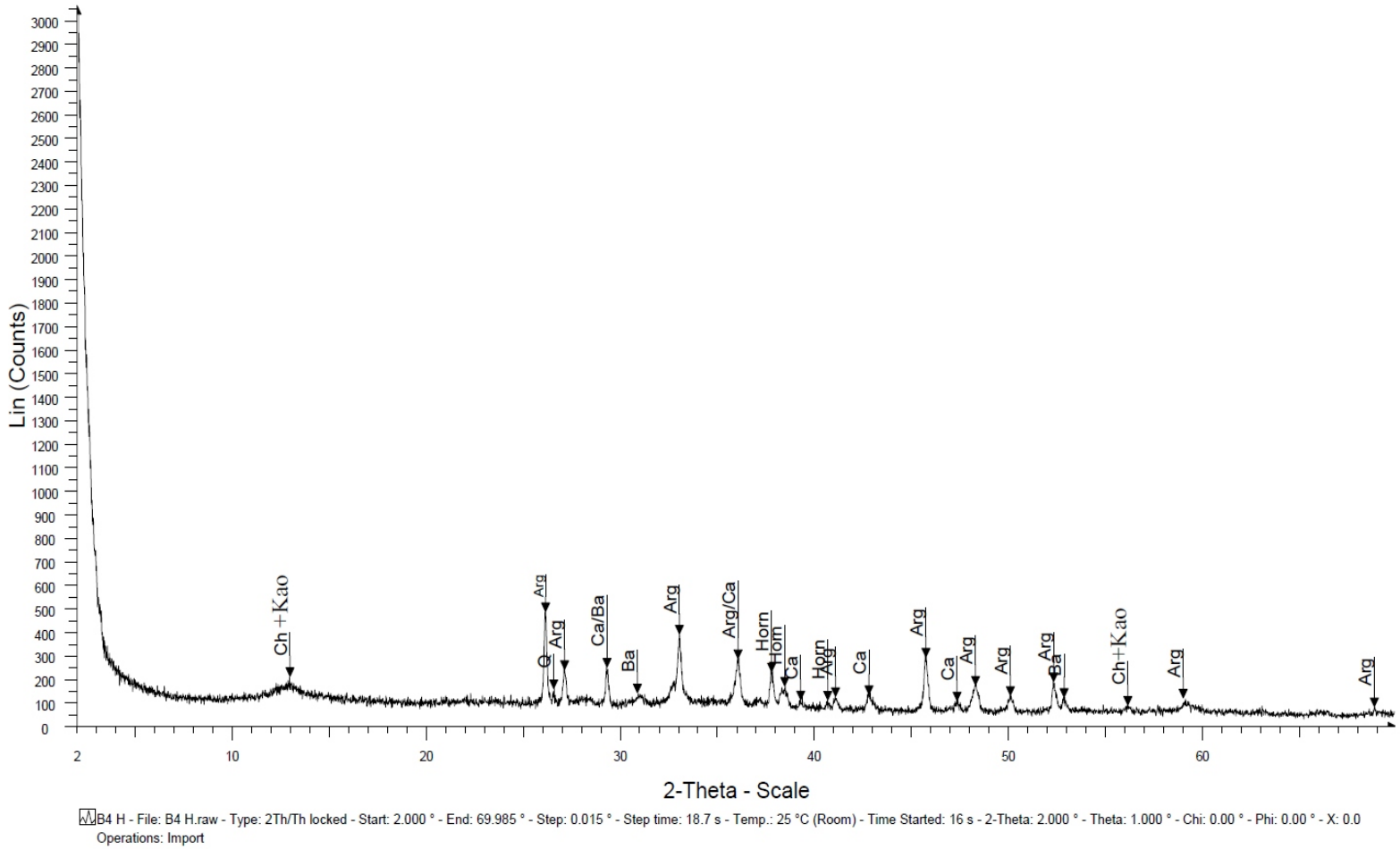

Figure 25. X-ray diffractogram of heavy fraction (inorganic matter) of sample B/4

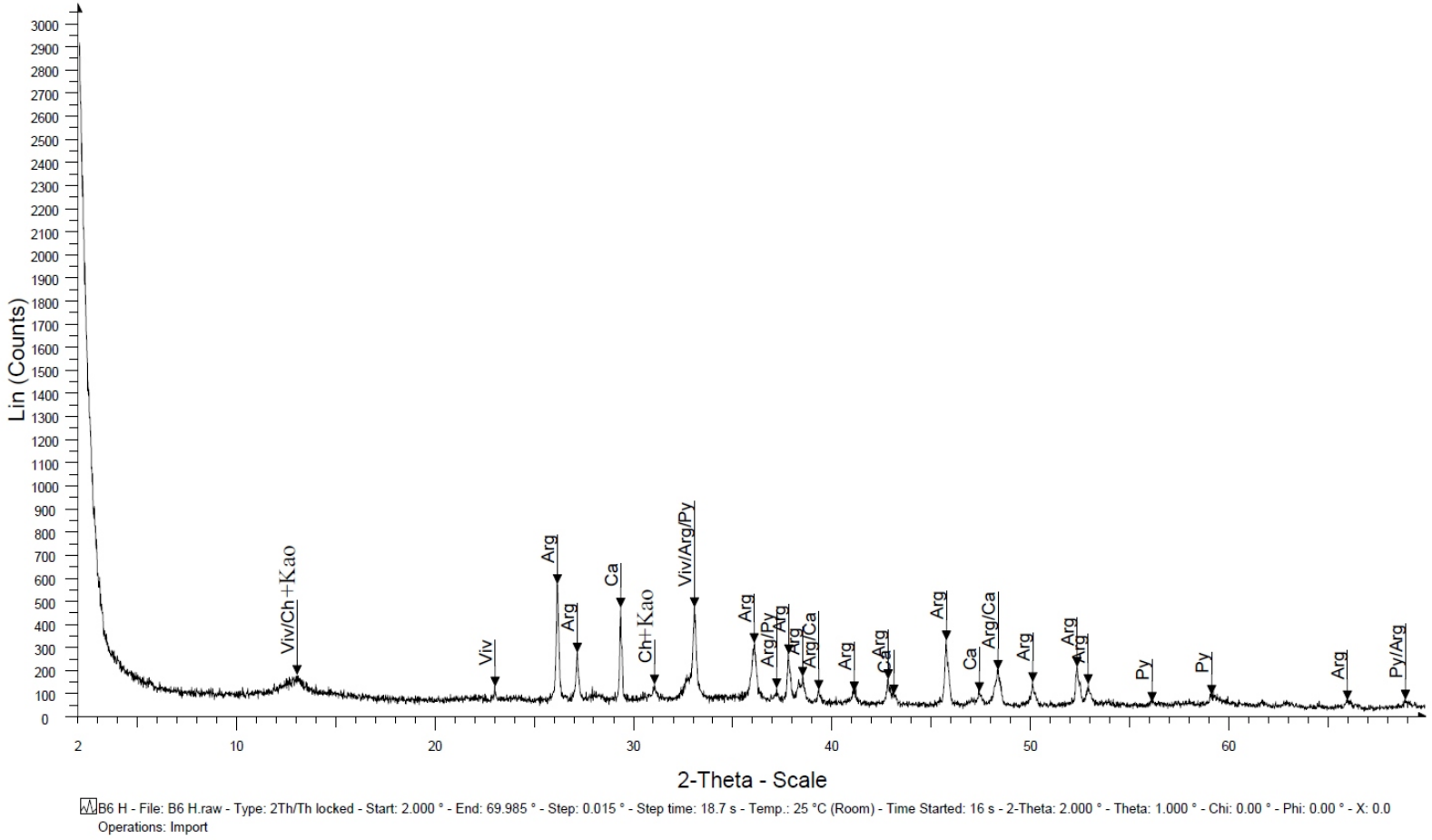

Figure 26. X-ray diffractogram of heavy fraction (inorganic matter) of sample B/6

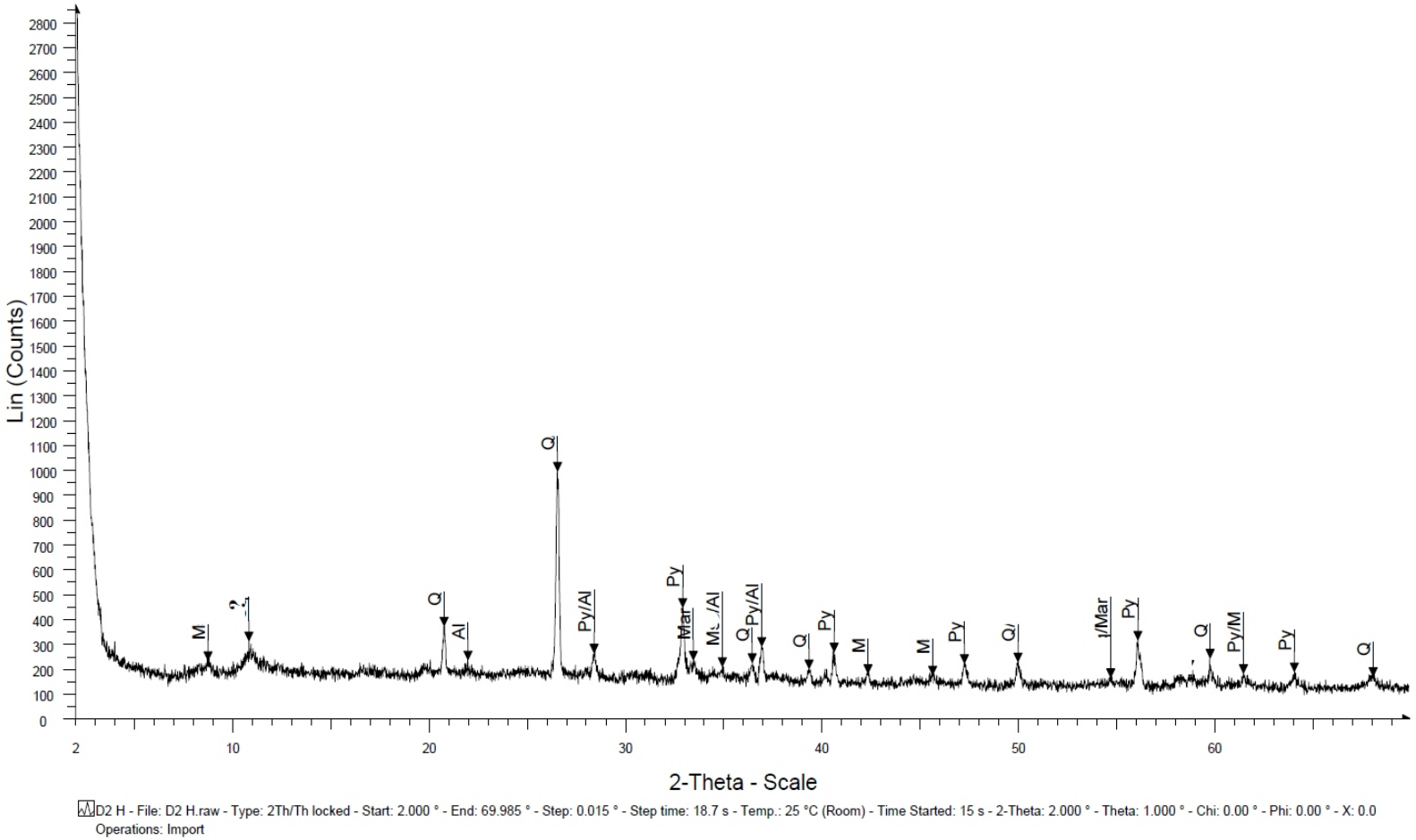

Figure 27. X-ray diffractogram of heavy fraction (inorganic matter) of sample D/2

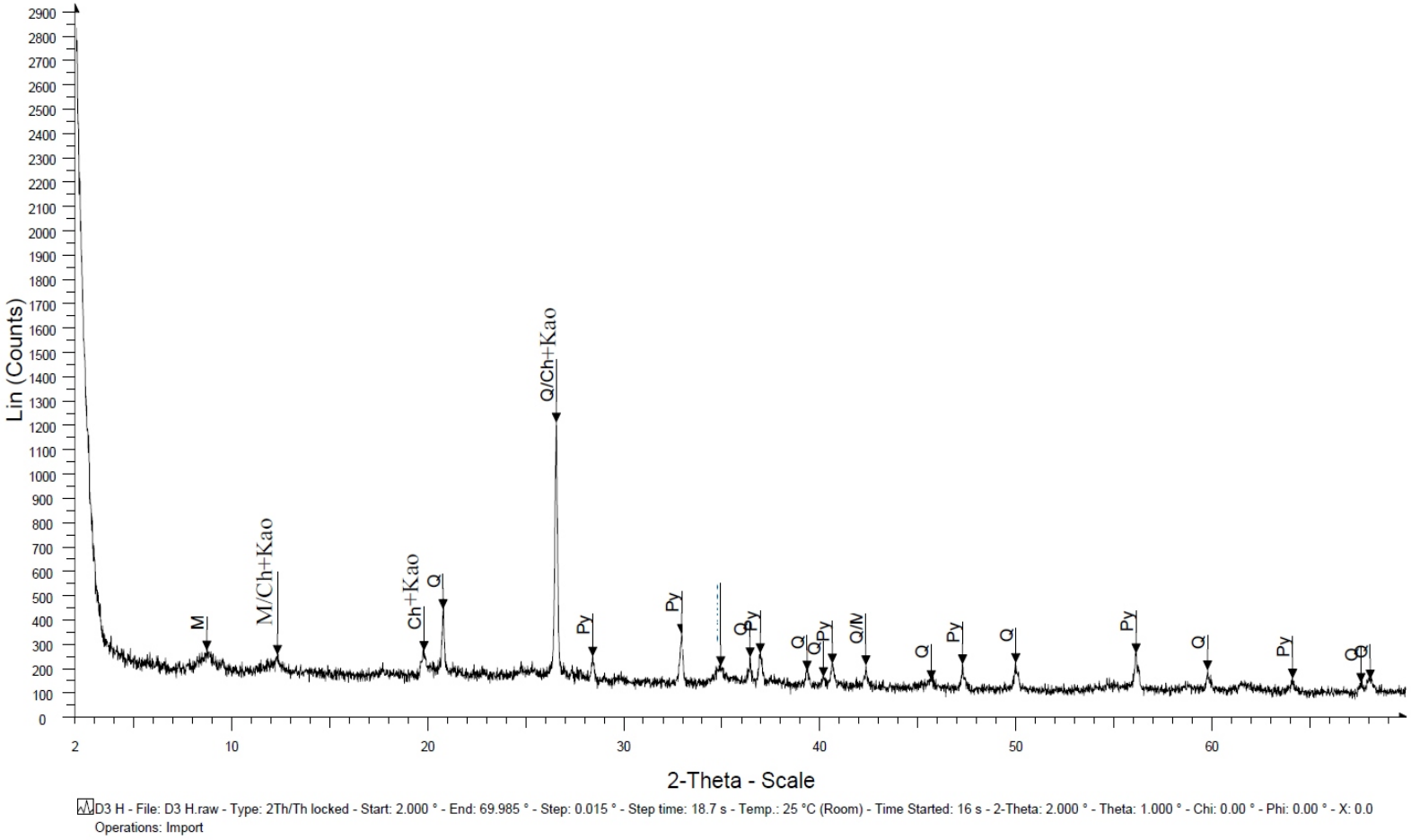

Figure 28. X-ray diffractogram of heavy fraction (inorganic matter) of sample D/3

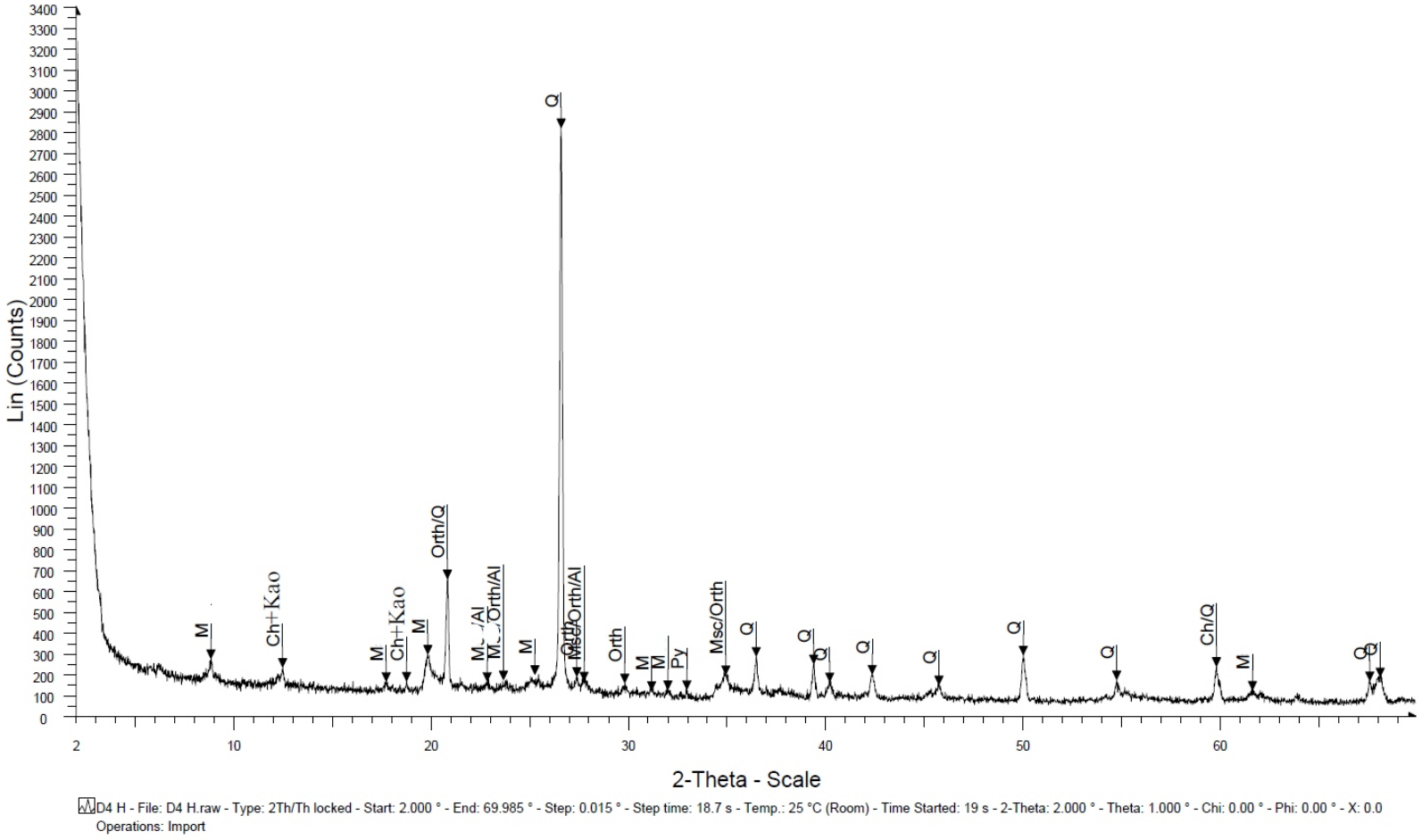

Figure 29. X-ray diffractogram of heavy fraction (inorganic matter) of sample D/4

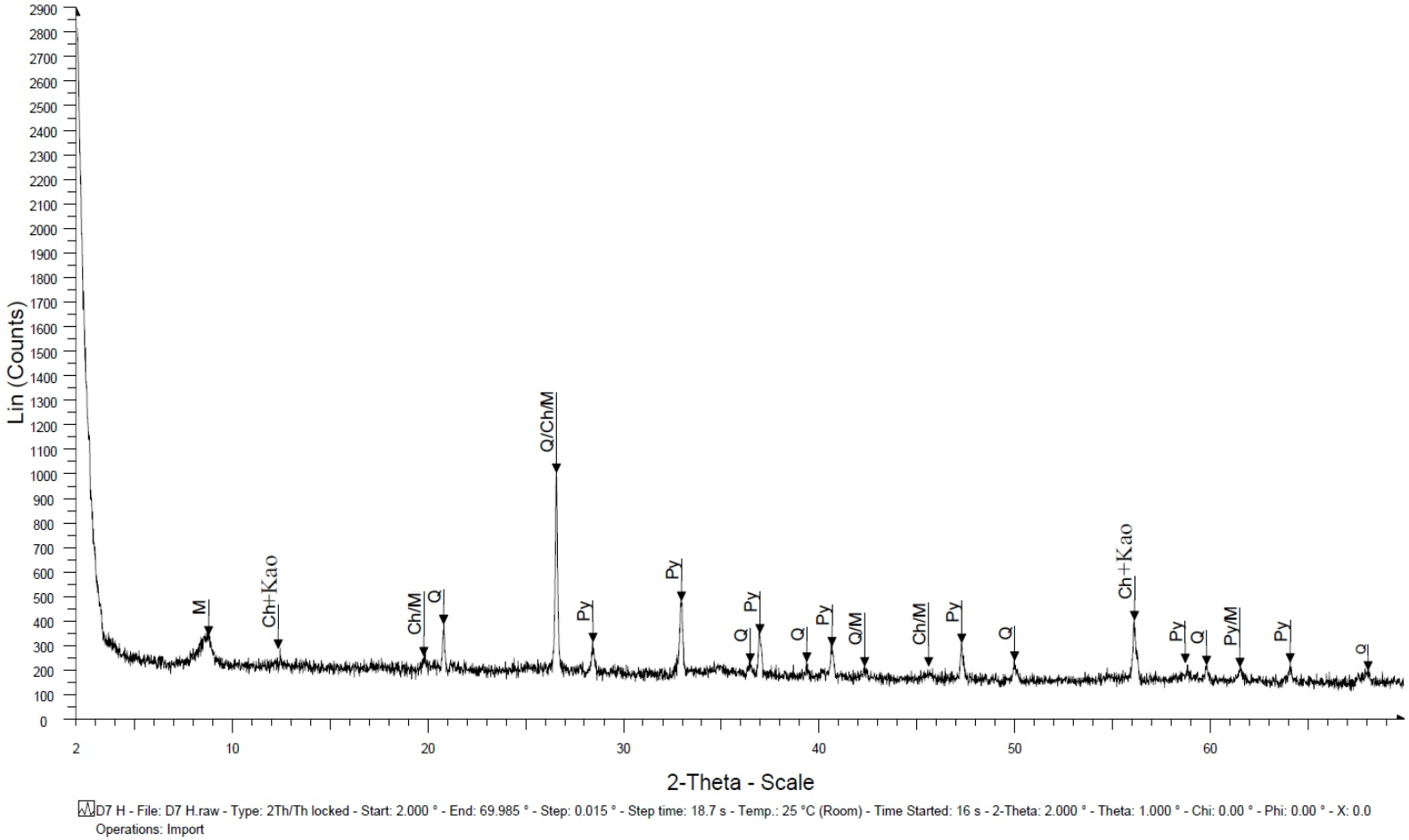

Figure 30. X-ray diffractogram of heavy fraction (inorganic matter) of sample D/7

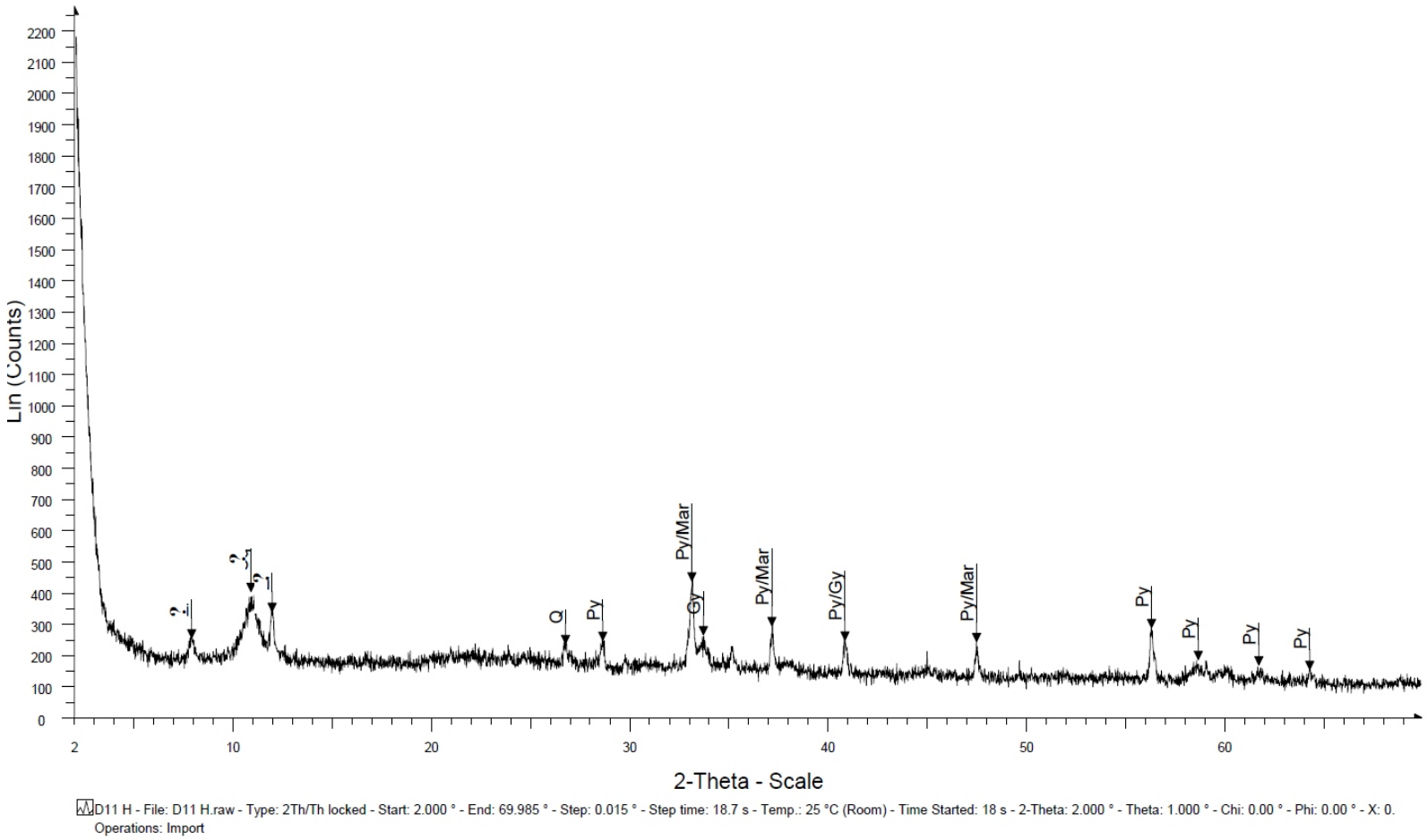

Figure 31. X-ray diffractogram of heavy fraction (inorganic matter) of sample D/11

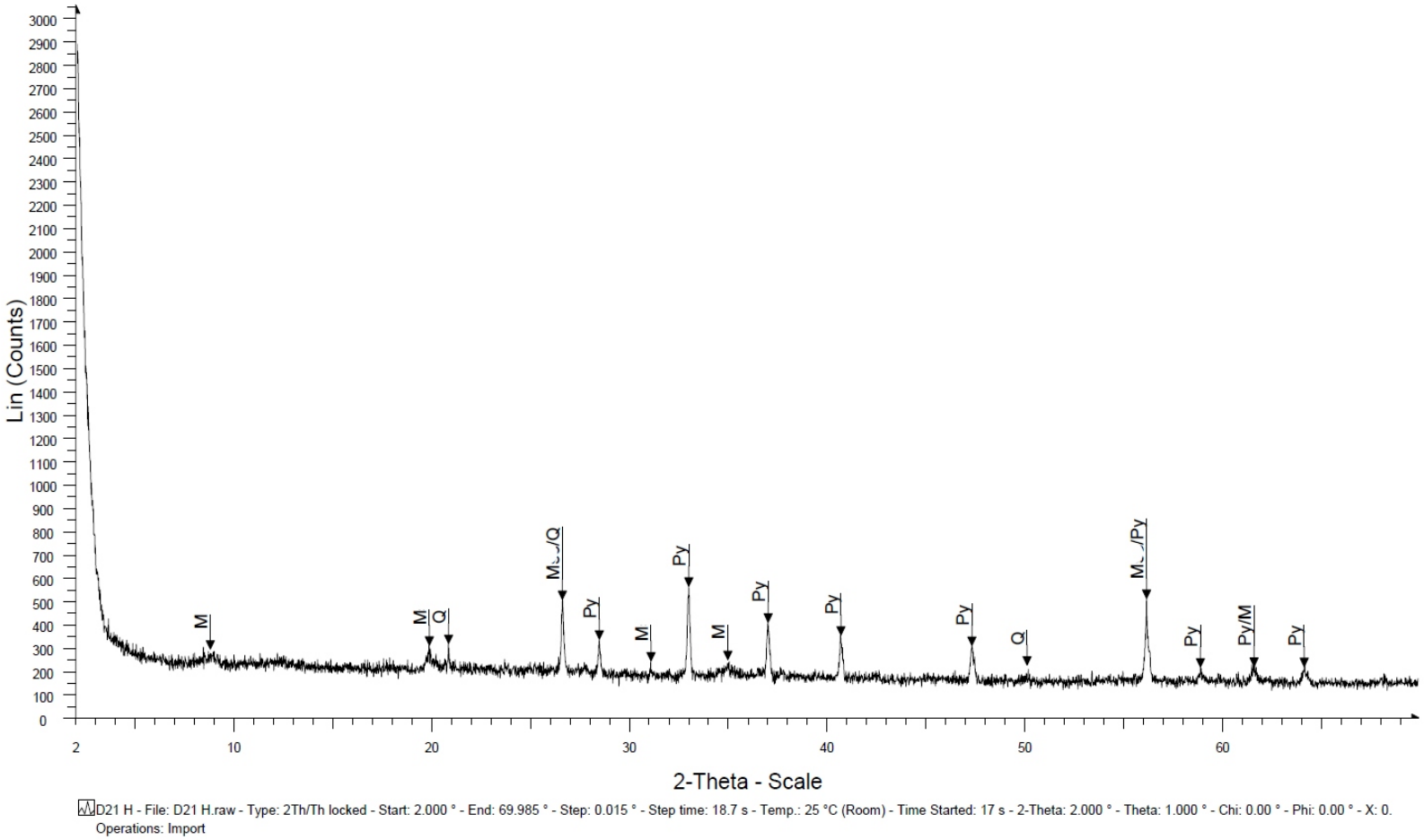

Figure 32. X-ray diffractogram of heavy fraction (inorganic matter) of sample D/21

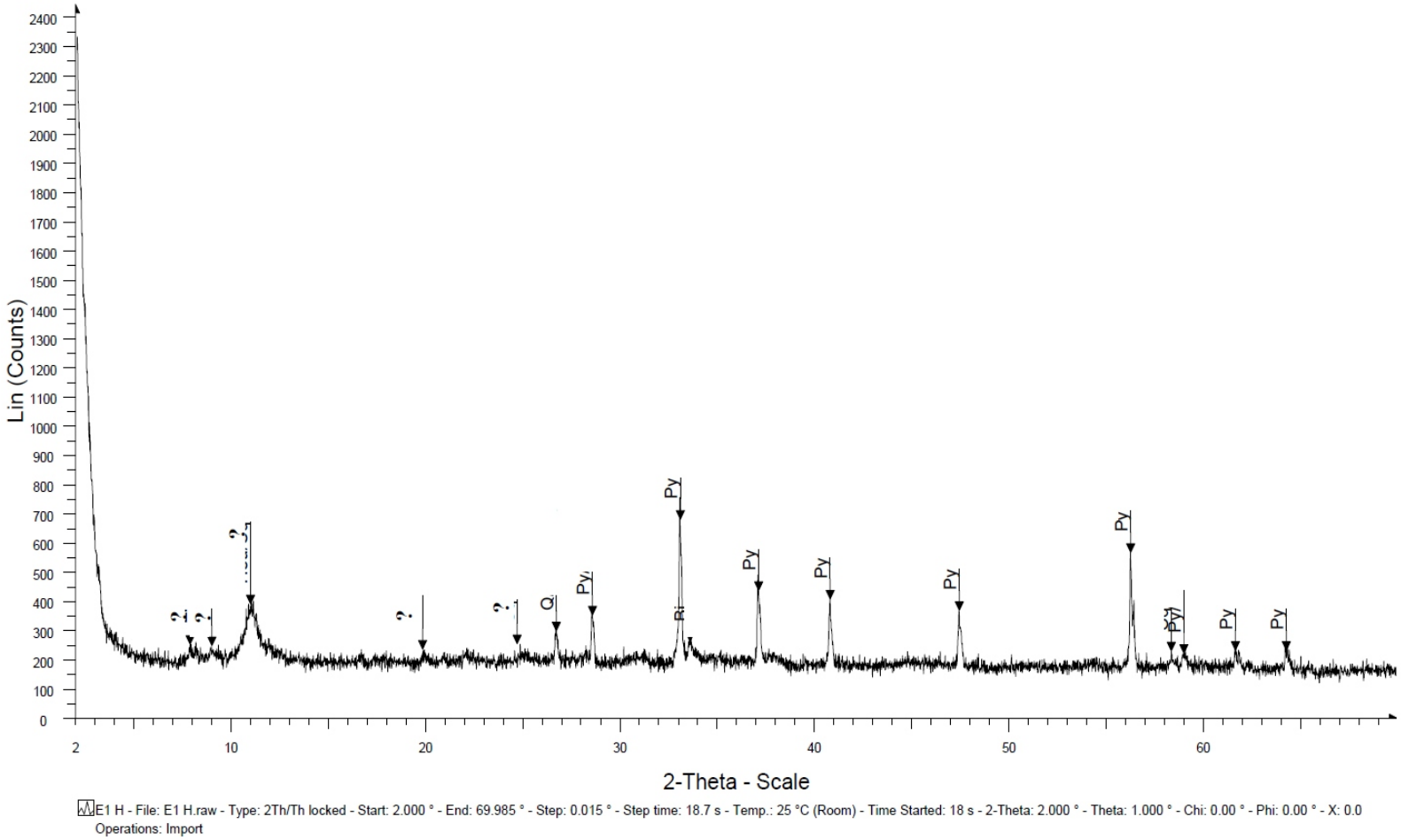

Figure 33. X-ray diffractogram of heavy fraction (inorganic matter) of sample E/1

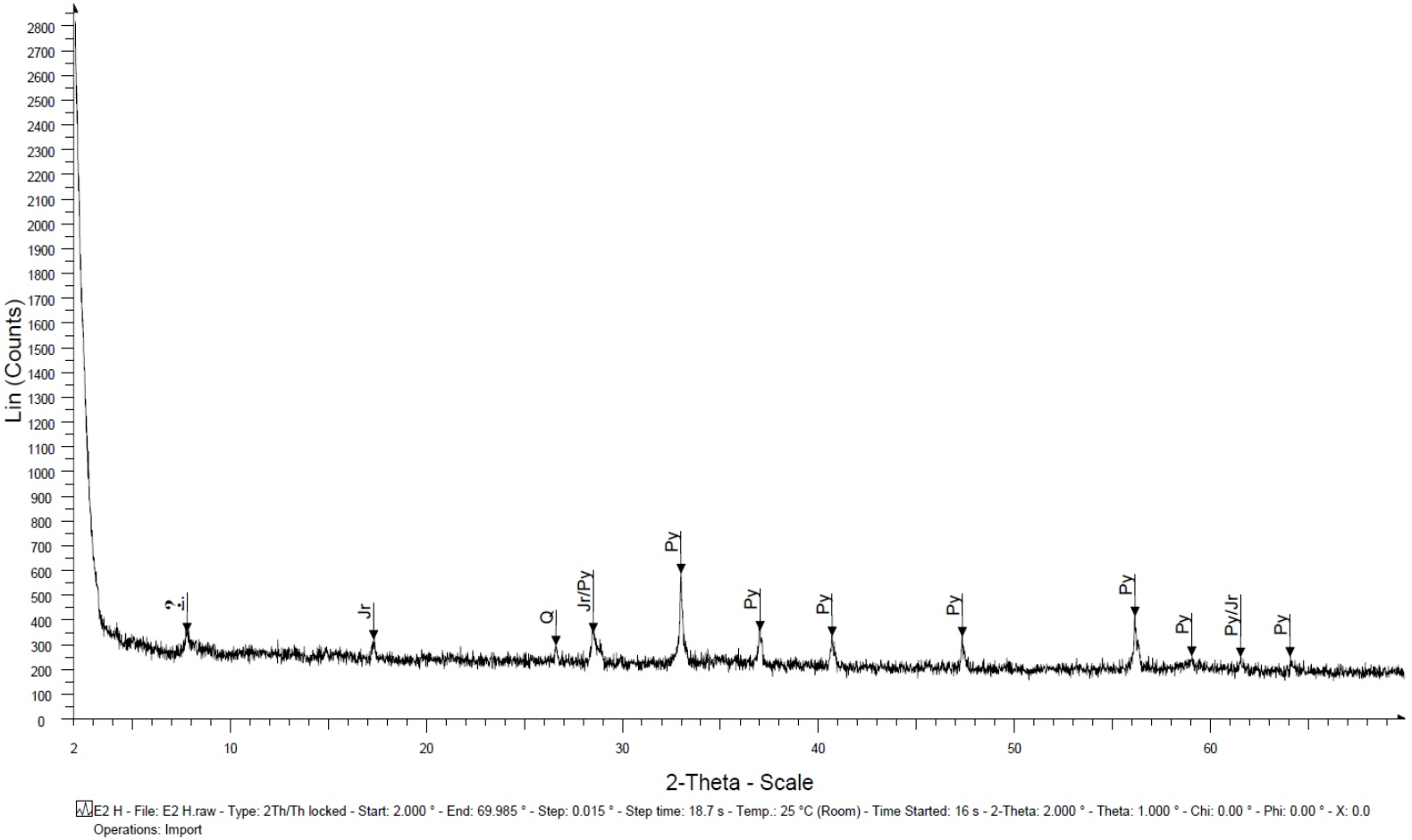

Figure 34. X-ray diffractogram of heavy fraction (inorganic matter) of sample E/2

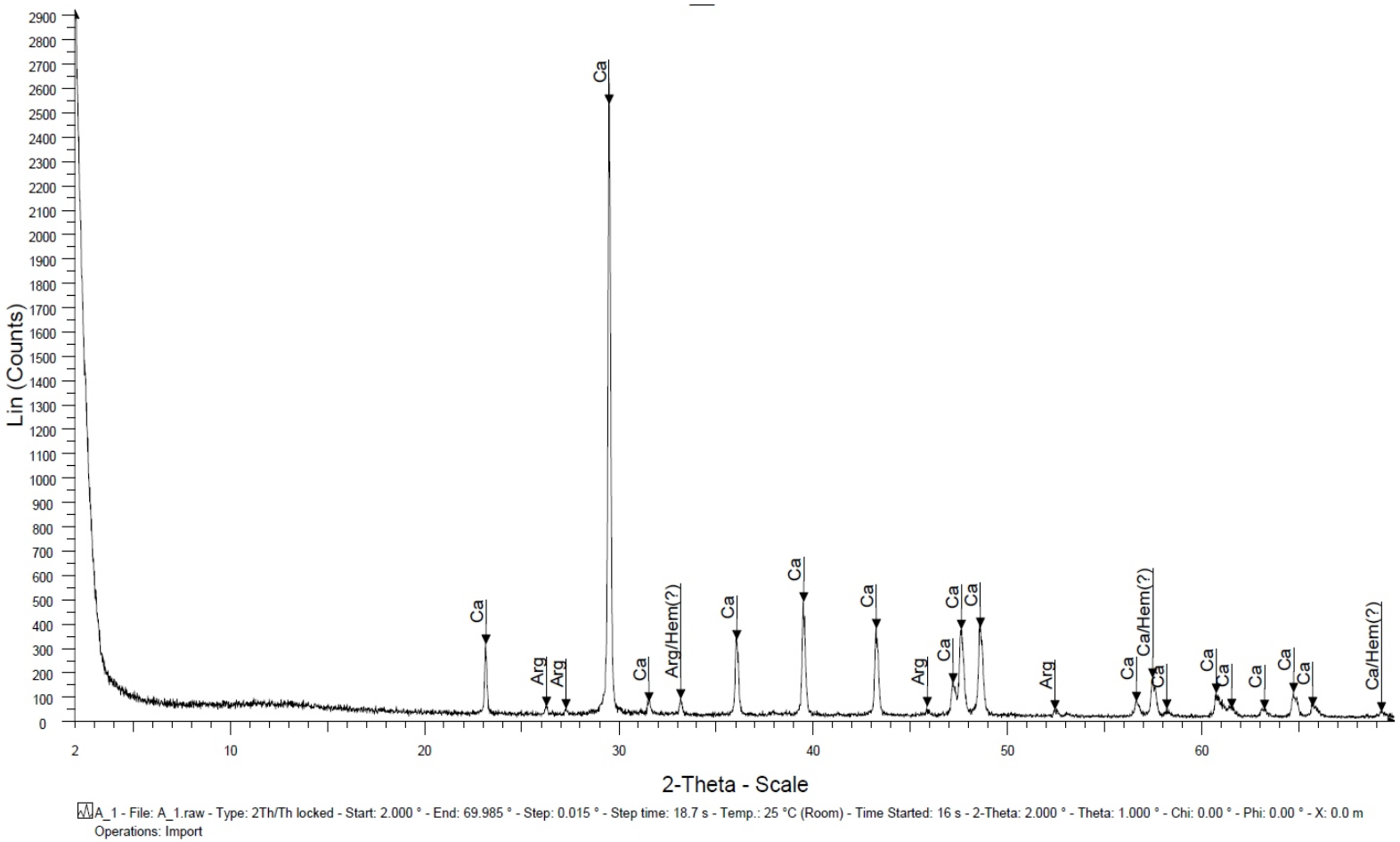

Figure 35. X-ray diffractogram of sample A/1

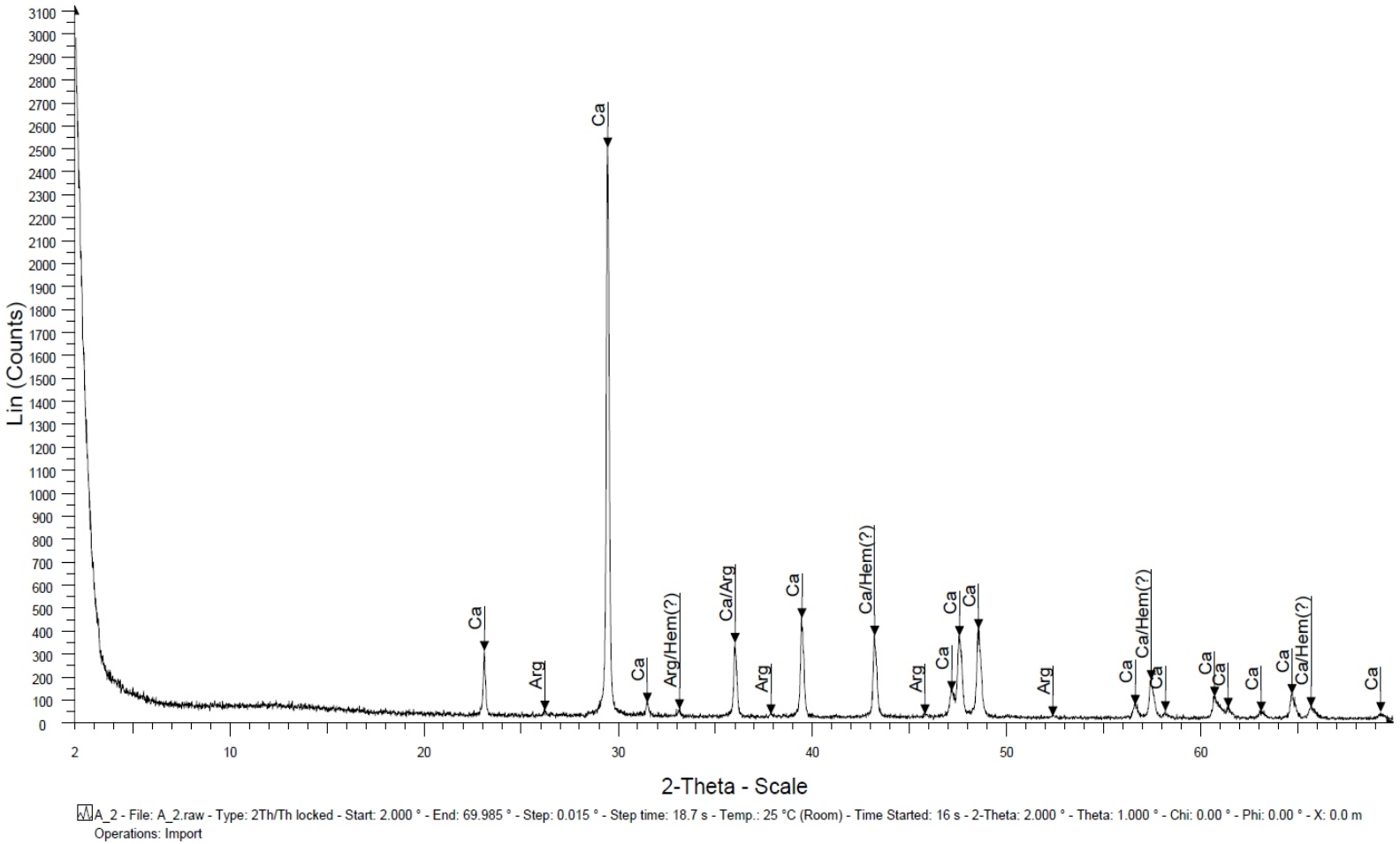

Figure 36. X-ray diffractogram of sample A/2

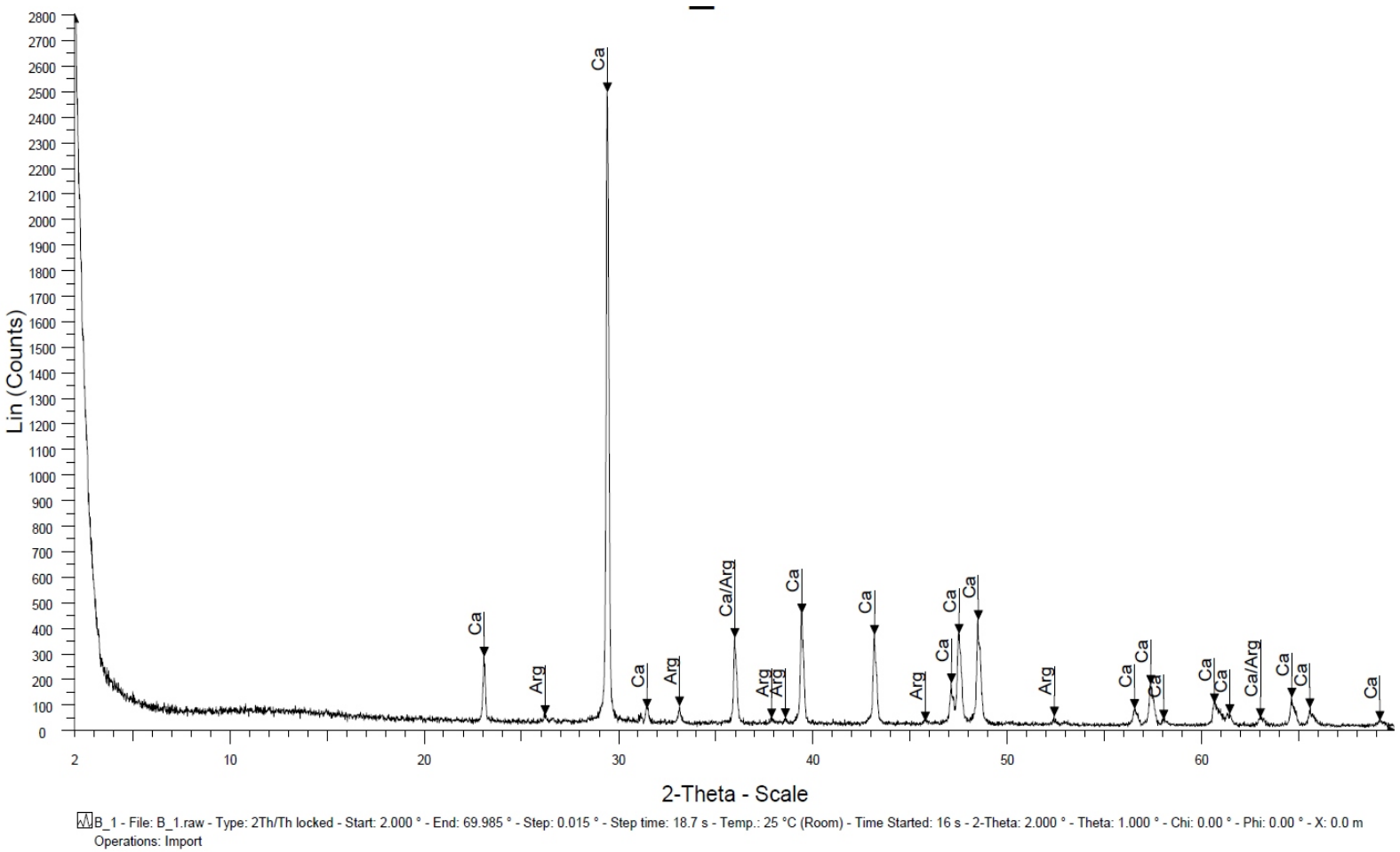

Figure 37. X-ray diffractogram of sample B/1

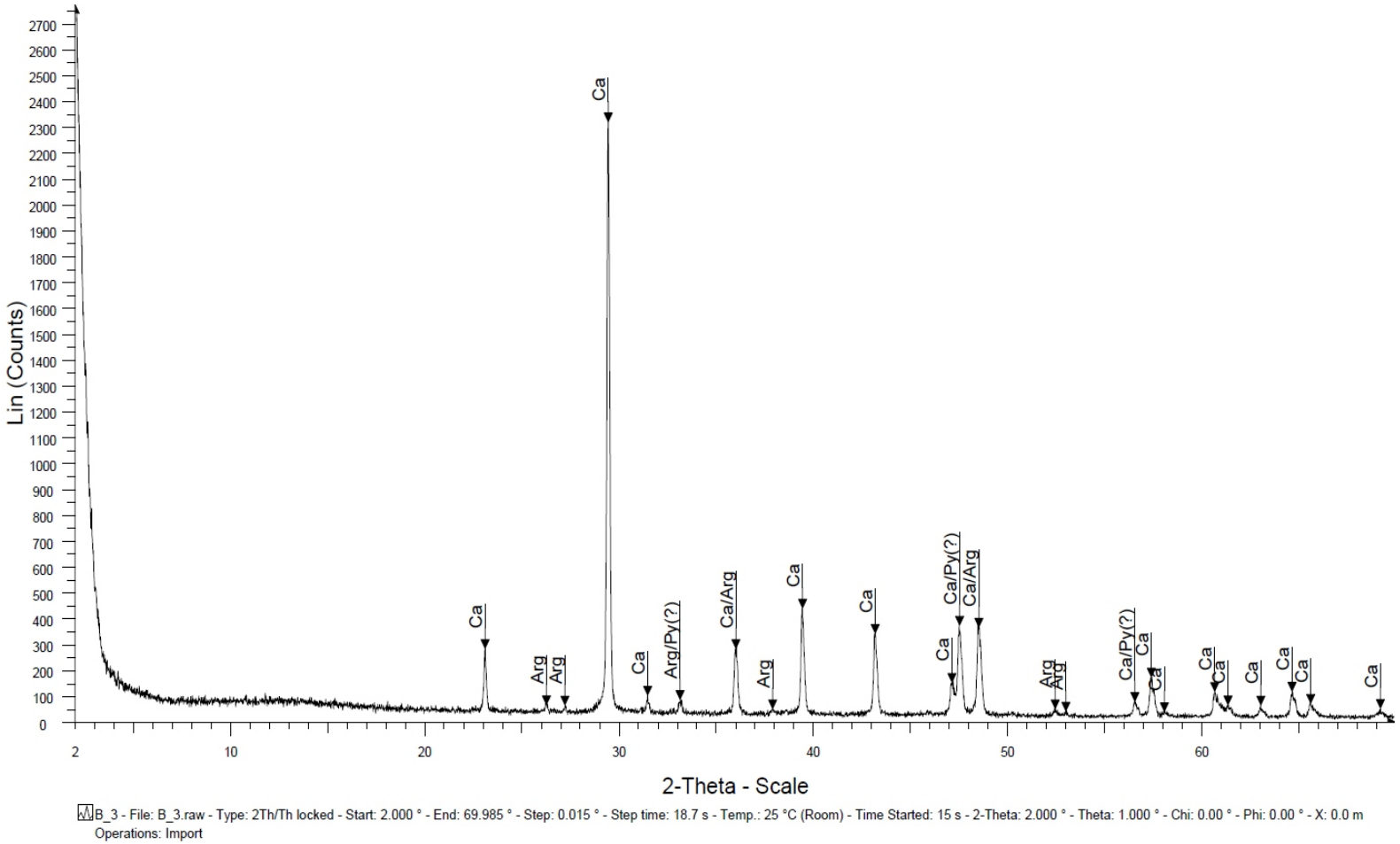

Figure 38. X-ray diffractogram of sample B/3

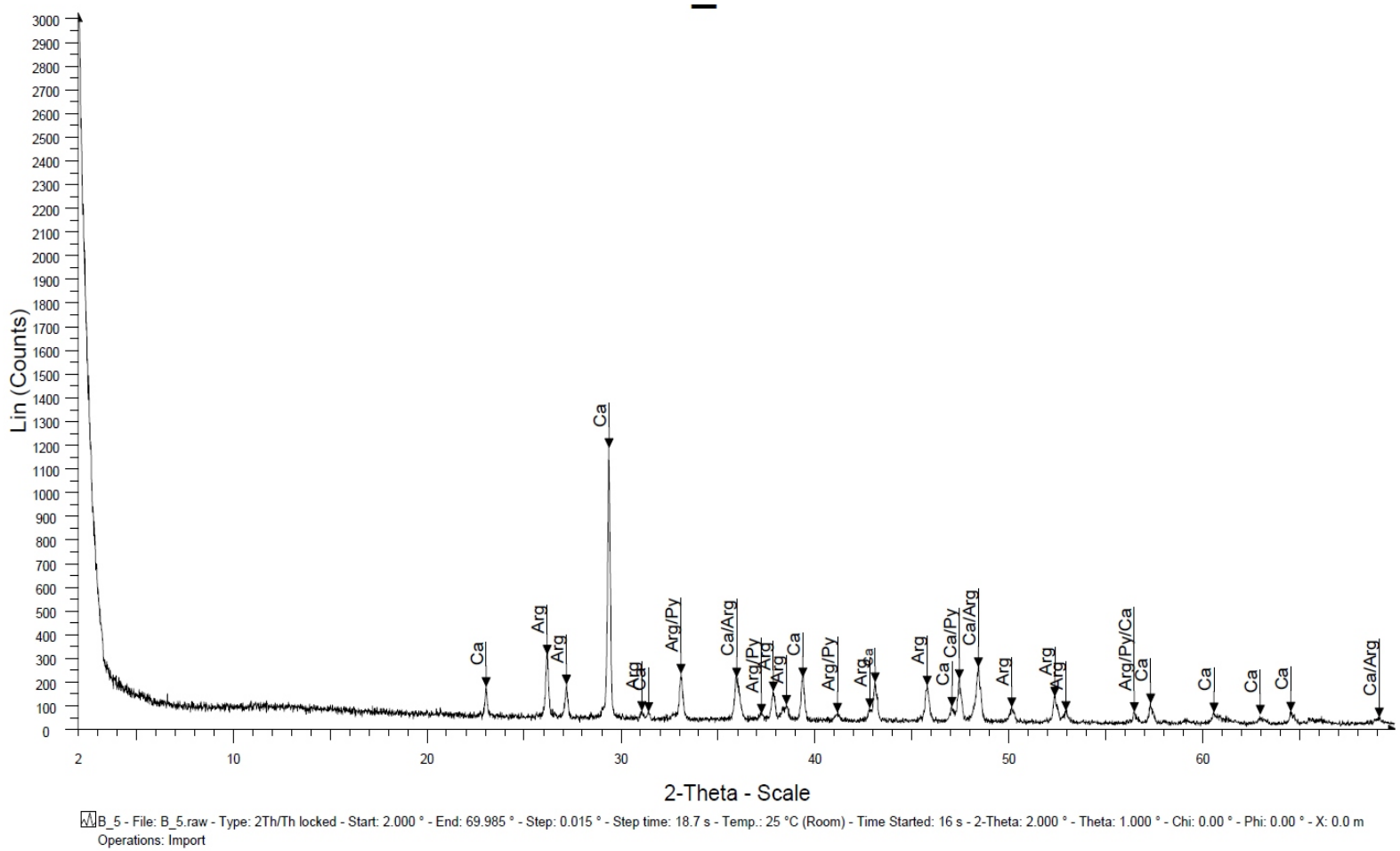

Figure 39. X-ray diffractogram of sample B/5

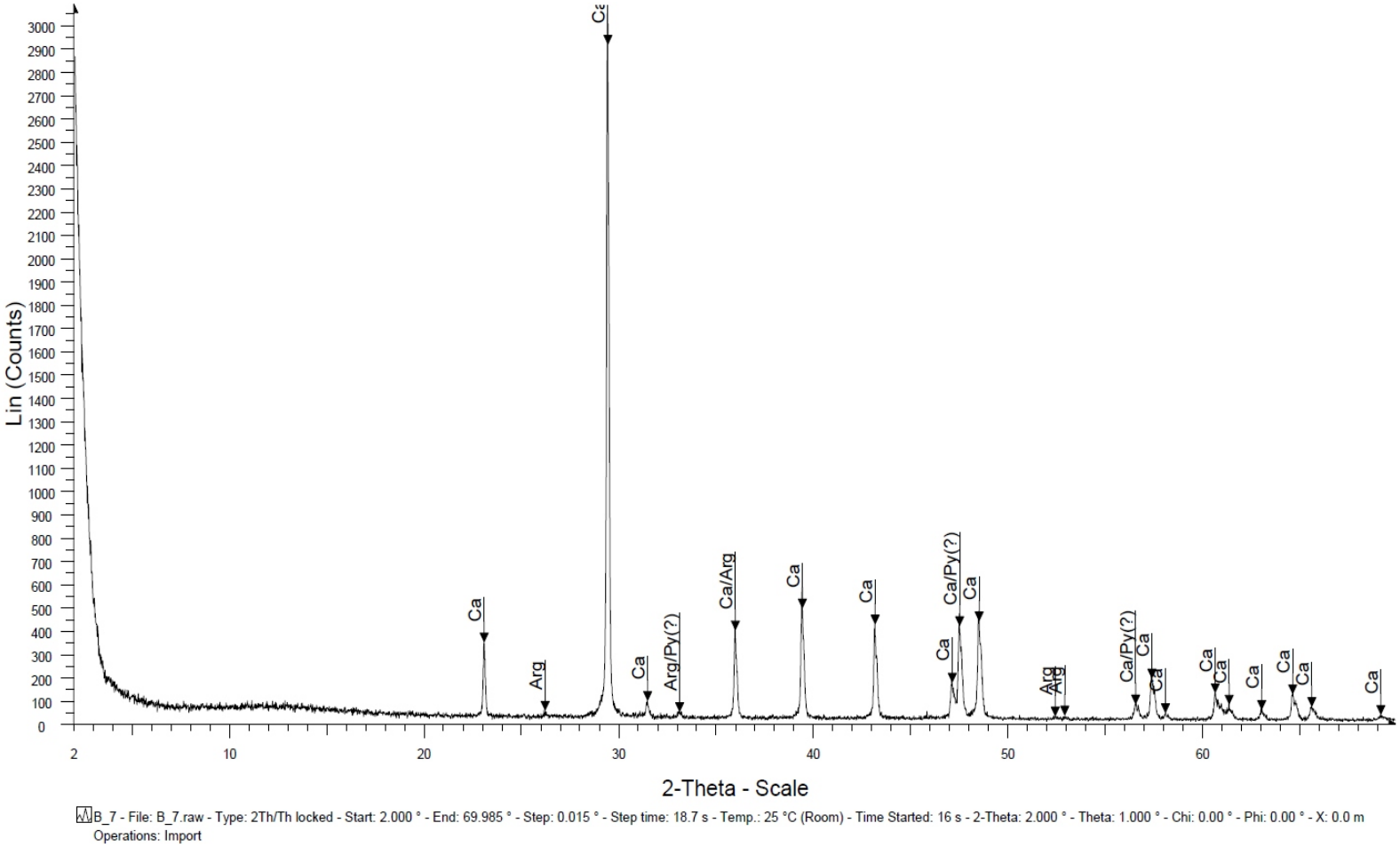

Figure 40. X-ray diffractogram of sample B/7

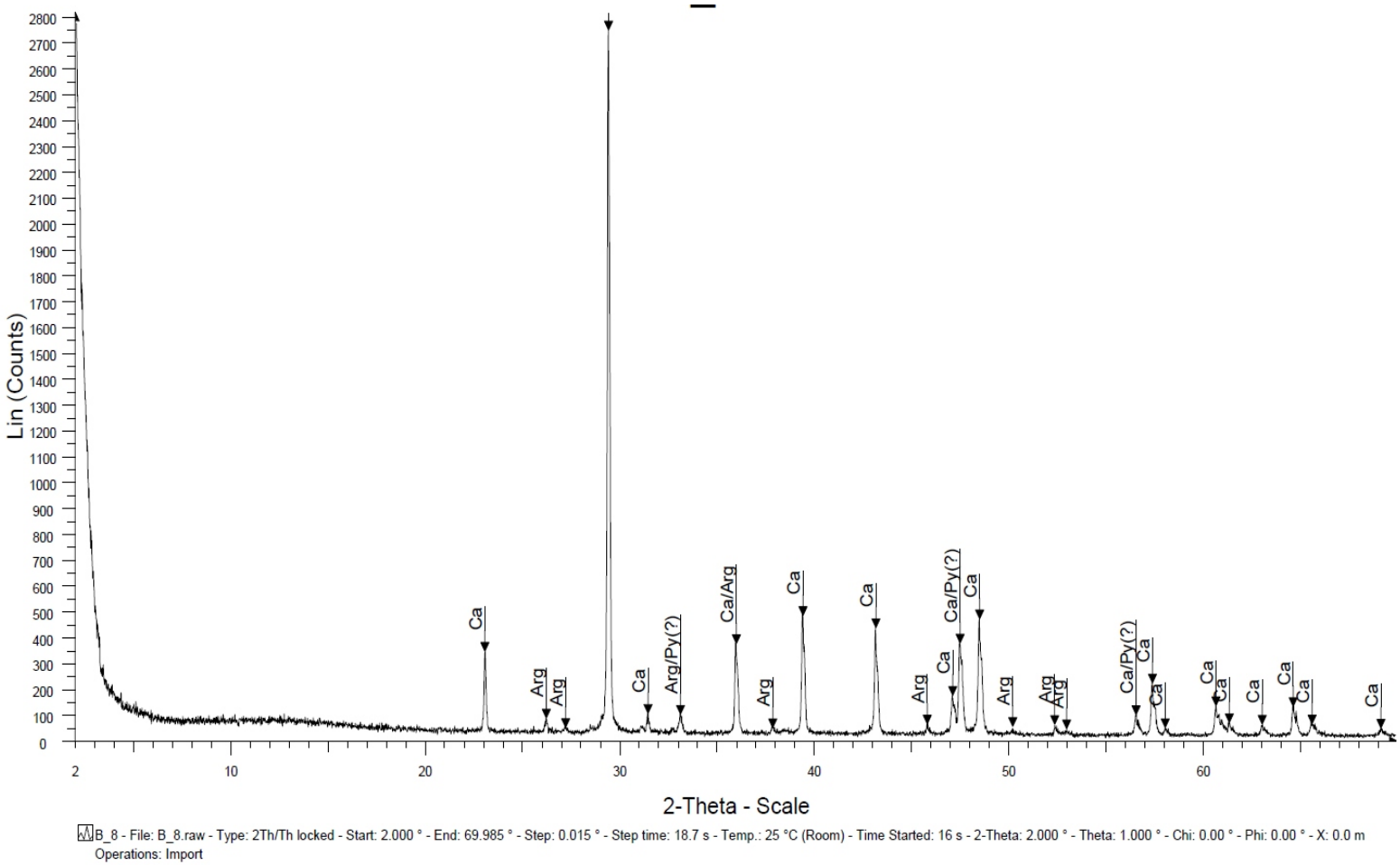

Figure 41. X-ray diffractogram of sample B/8

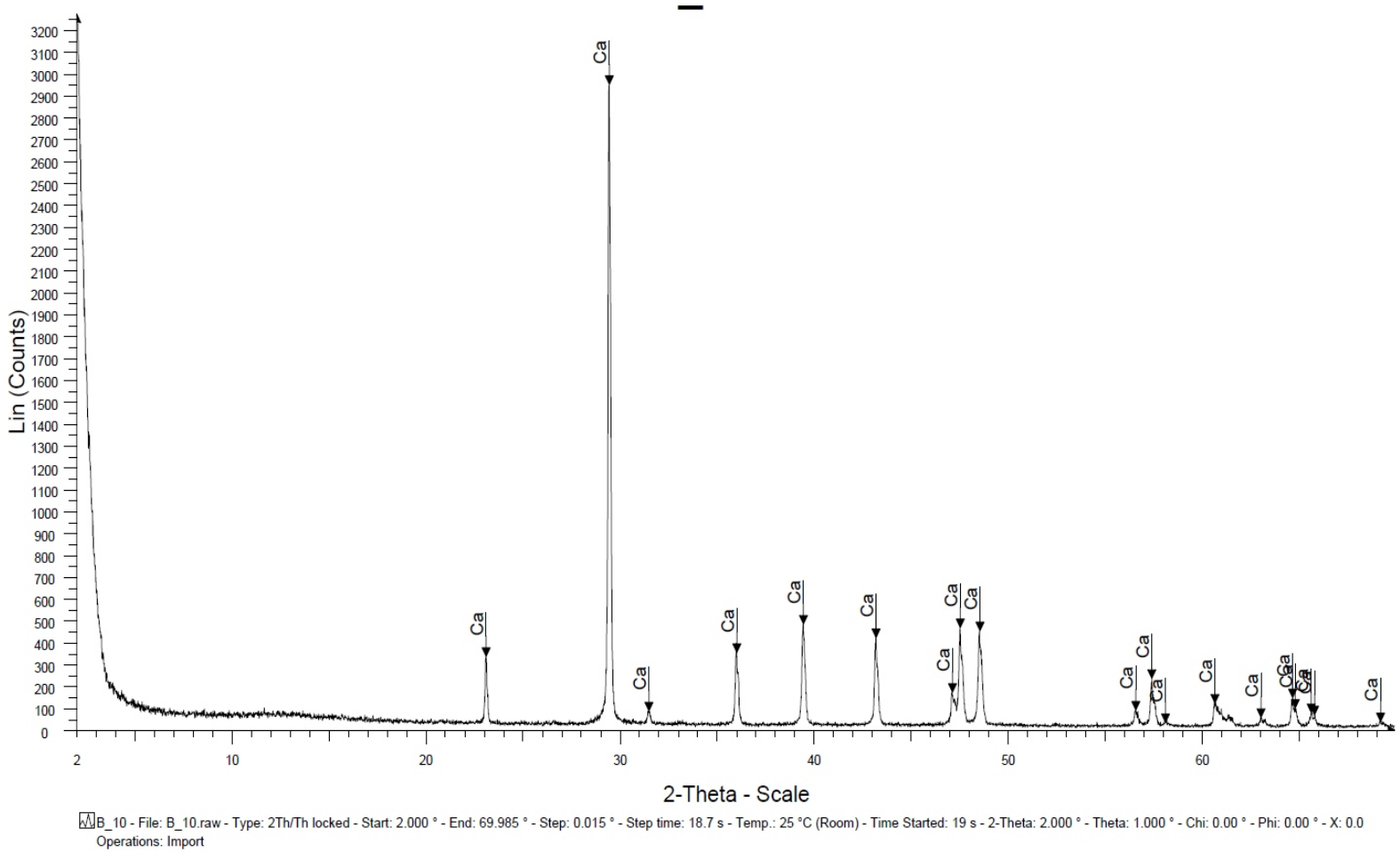

Figure 42. X-ray diffractogram of sample B/10

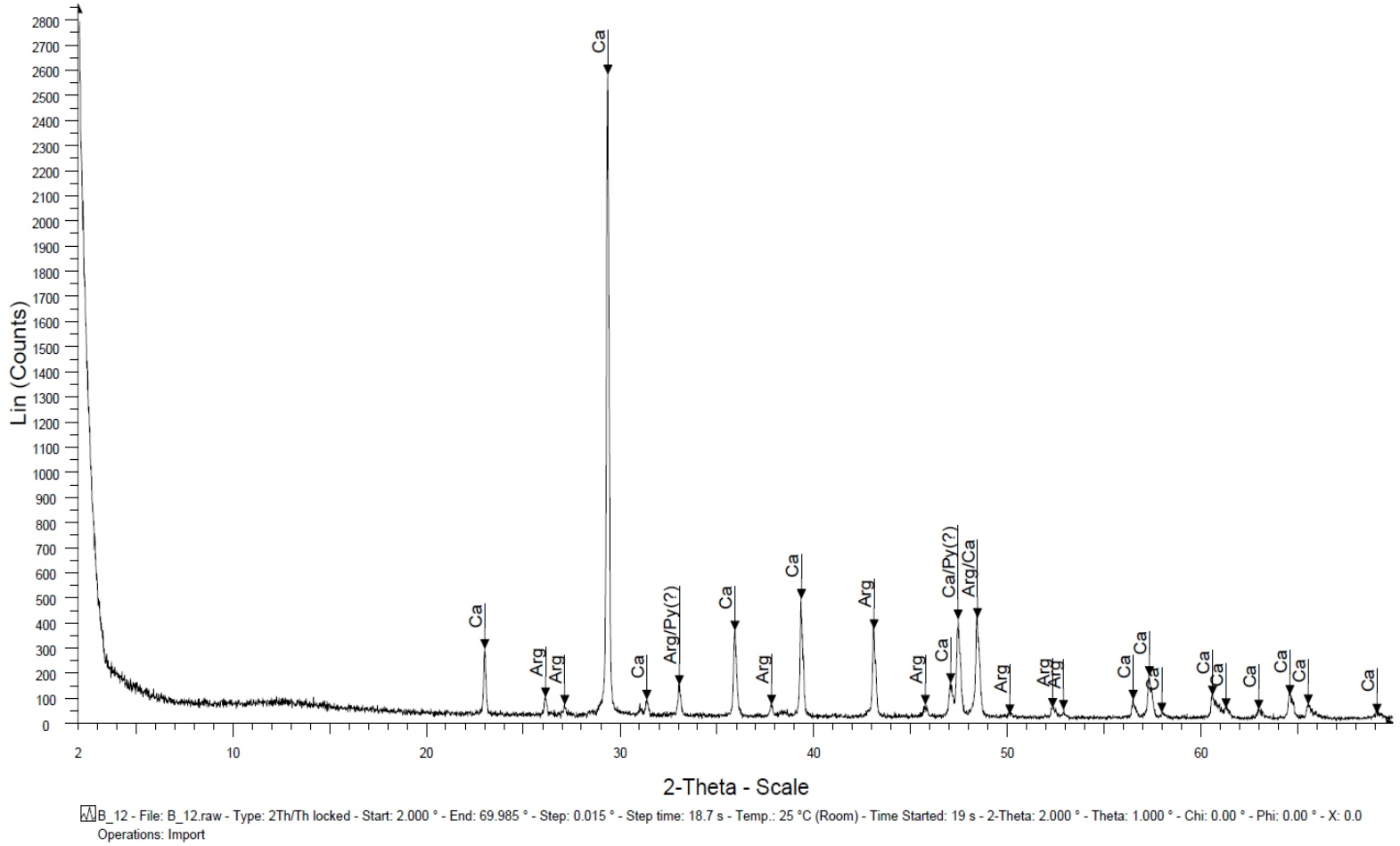

Figure 43. X-ray diffractogram of sample B/12

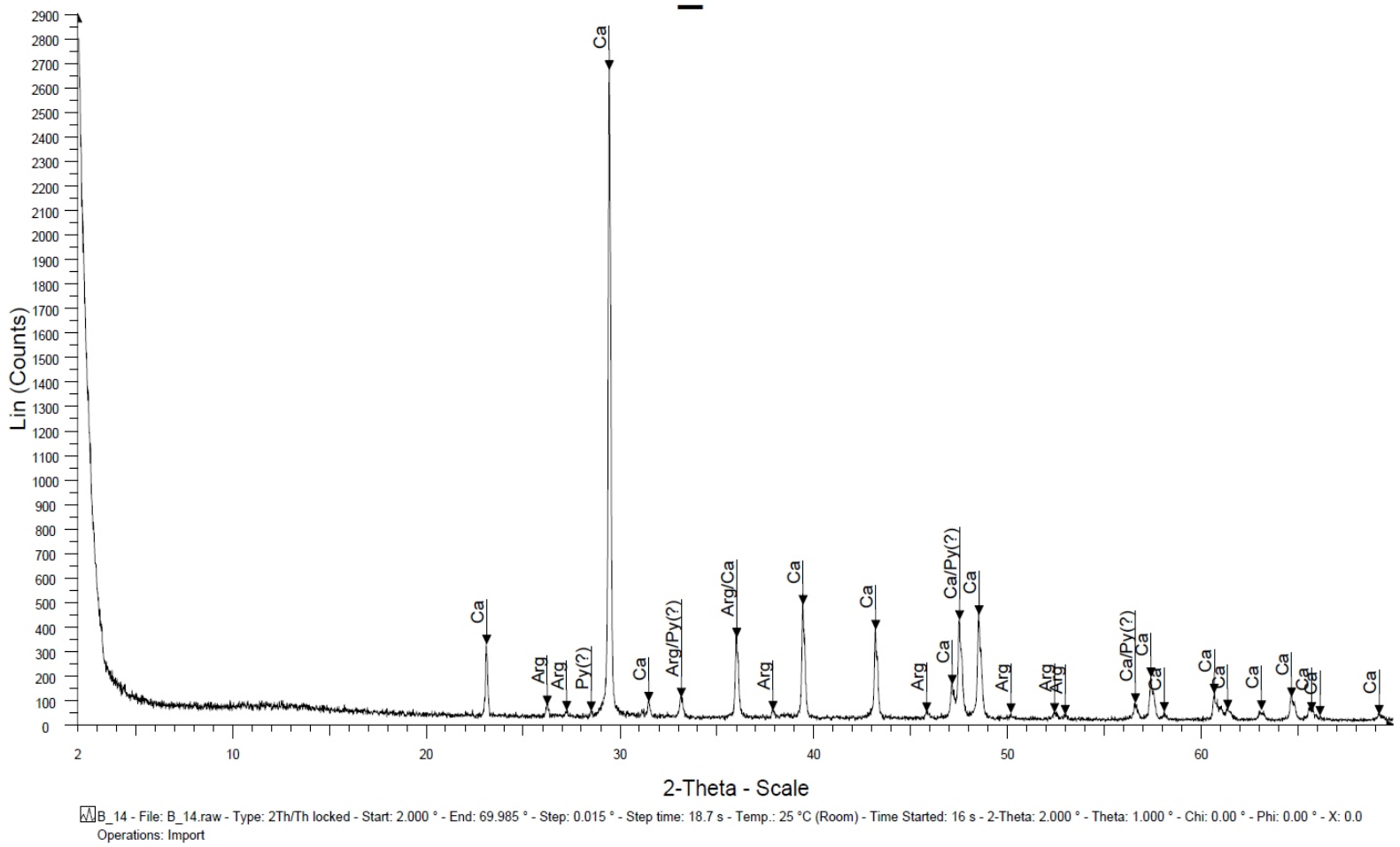

Figure 44. X-ray diffractogram of sample B/14

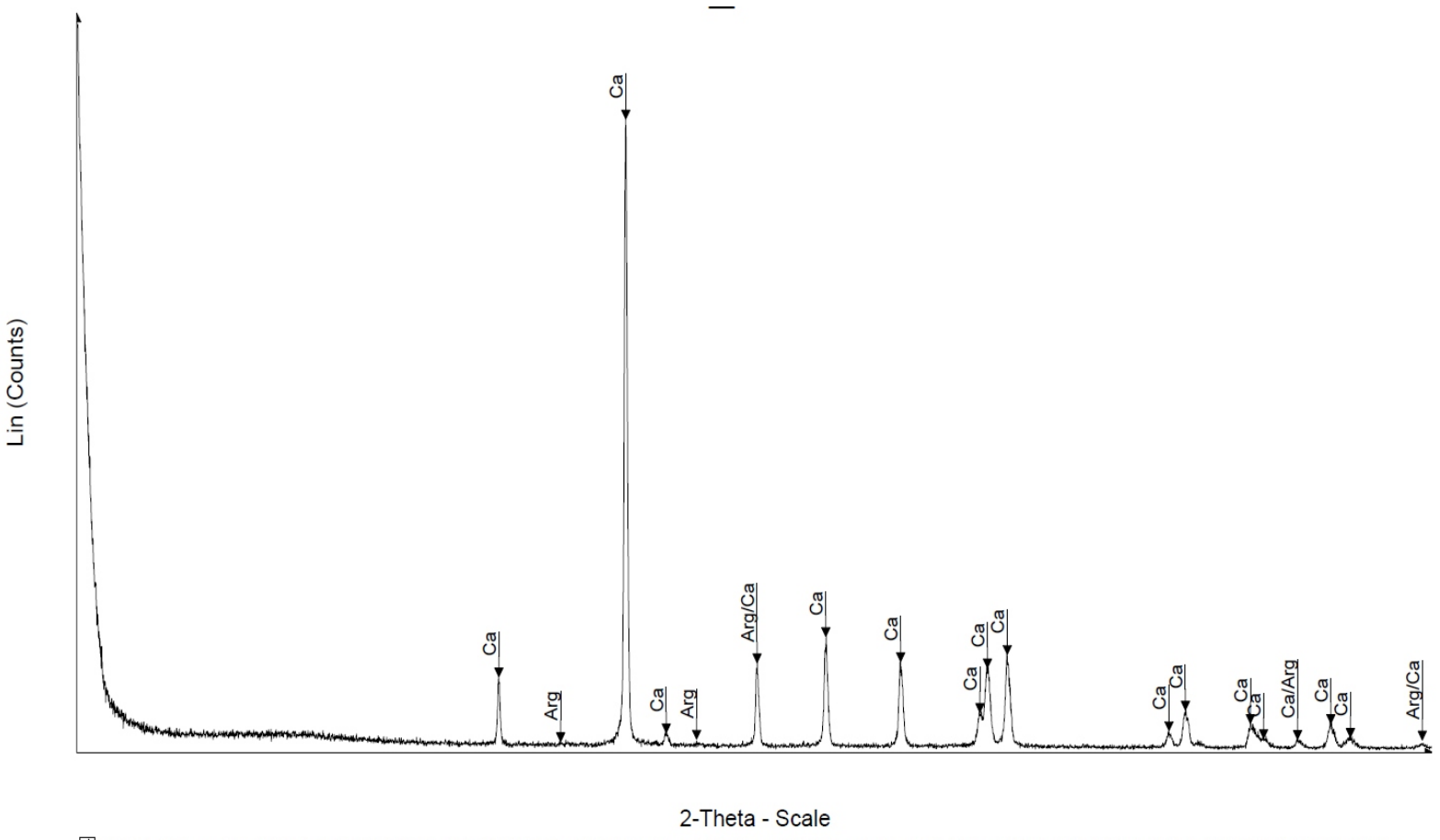

Figure 45. X-ray diffractogram of sample C/1

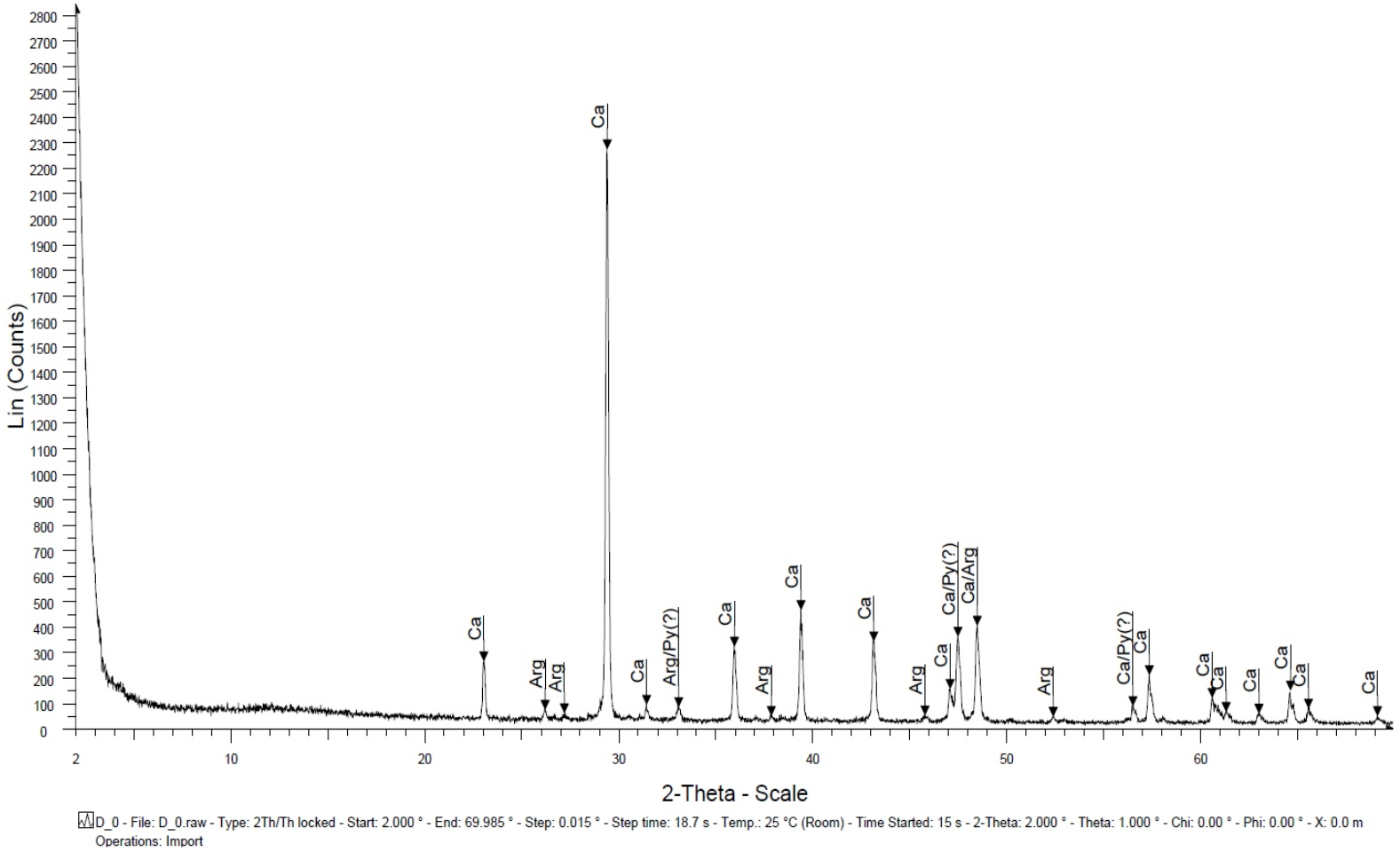

Figure 46. X-ray diffractogram of sample D/0

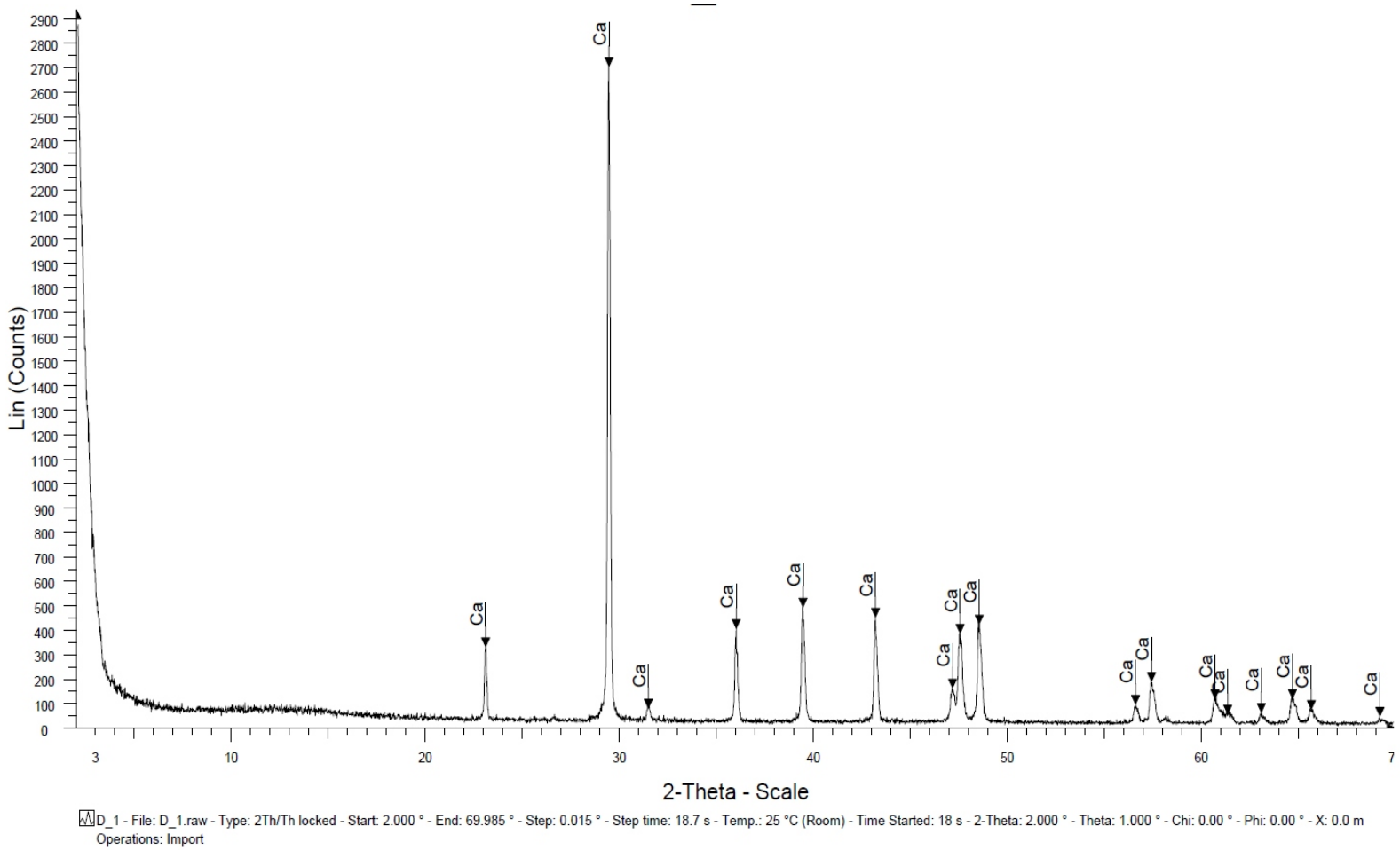

Figure 47. X-ray diffractogram of sample D/1

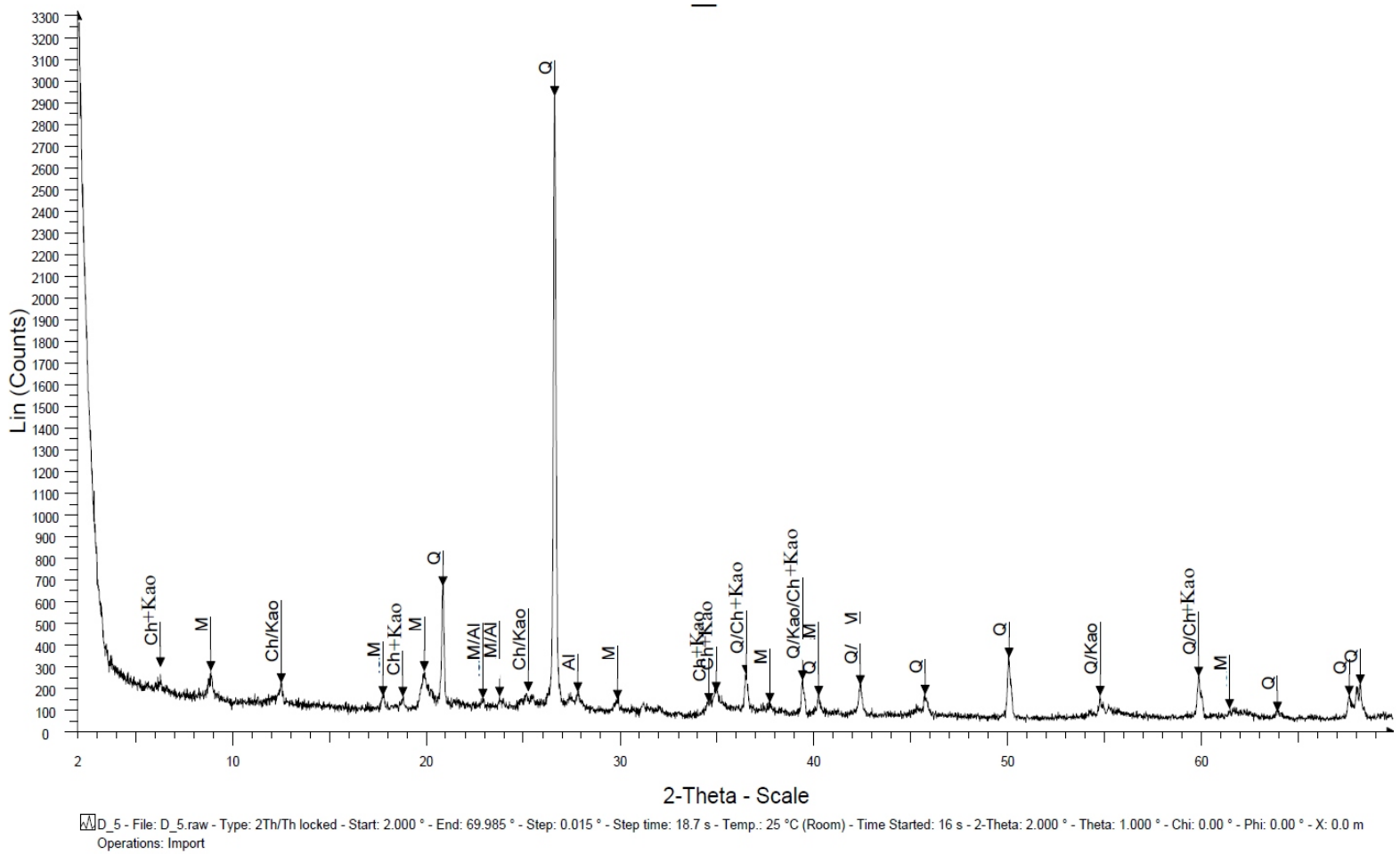

Figure 48. X-ray diffractogram of sample D/5

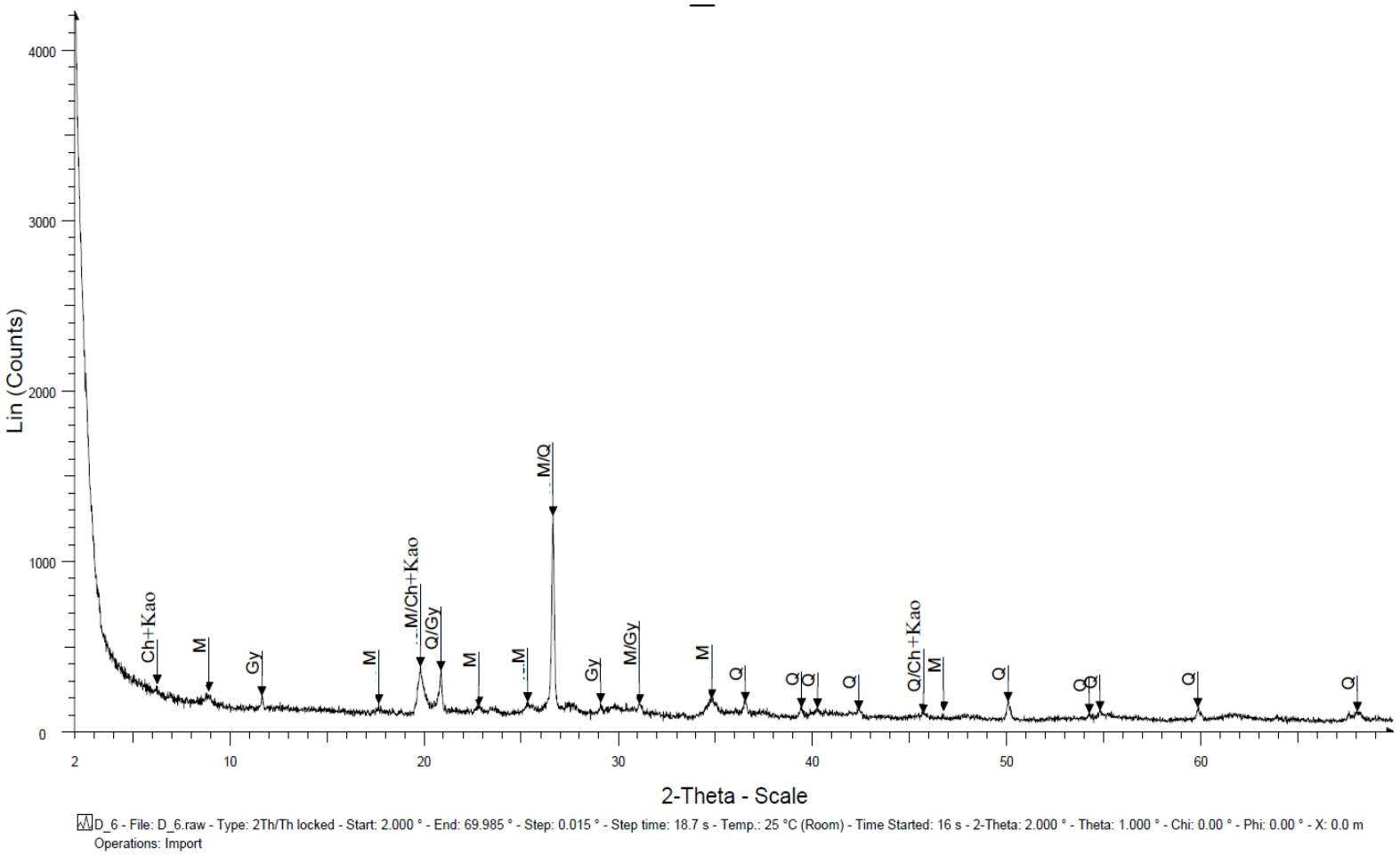

Figure 49. X-ray diffractogram of sample D/6

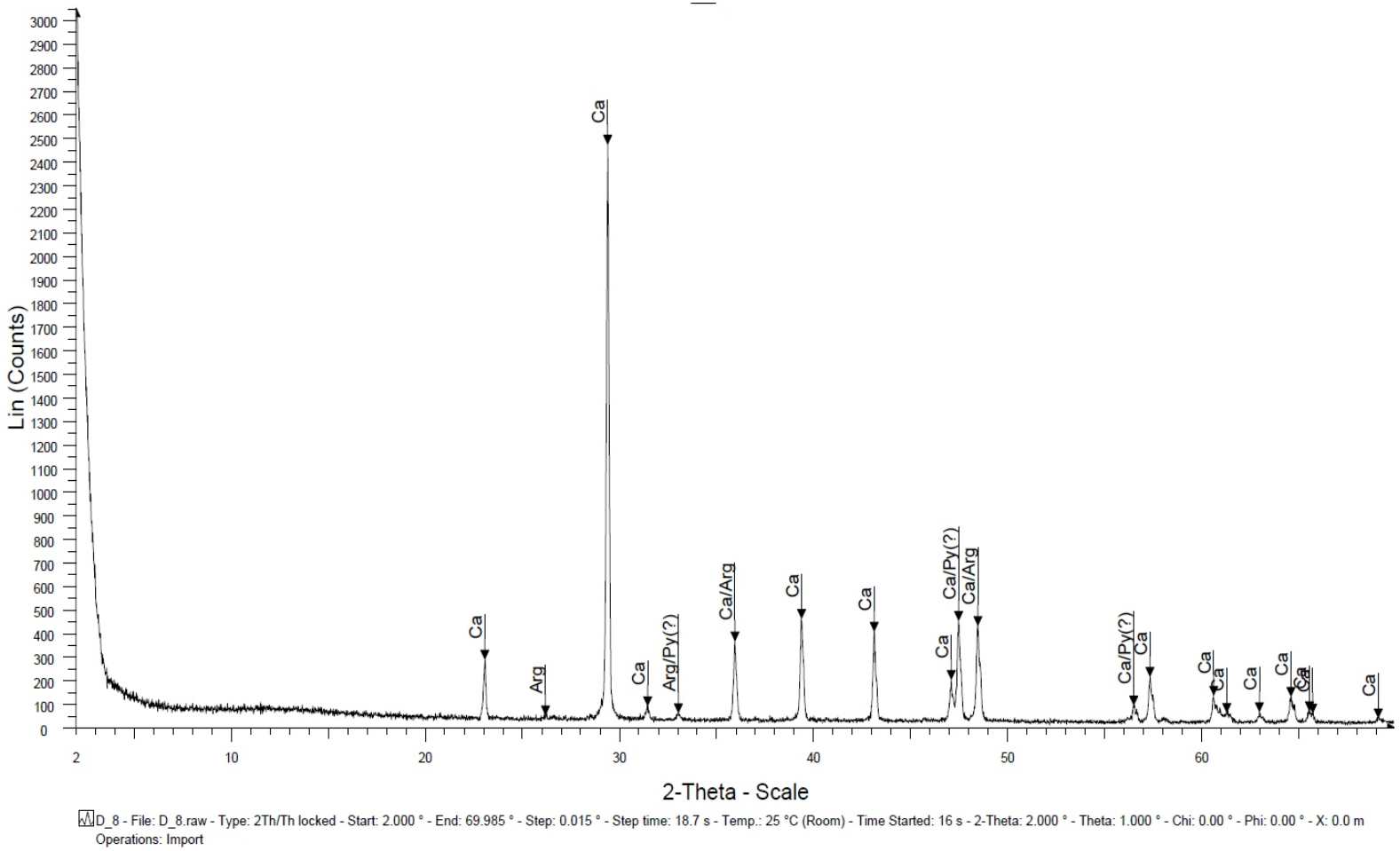

Figure 50. X-ray diffractogram of sample D/8

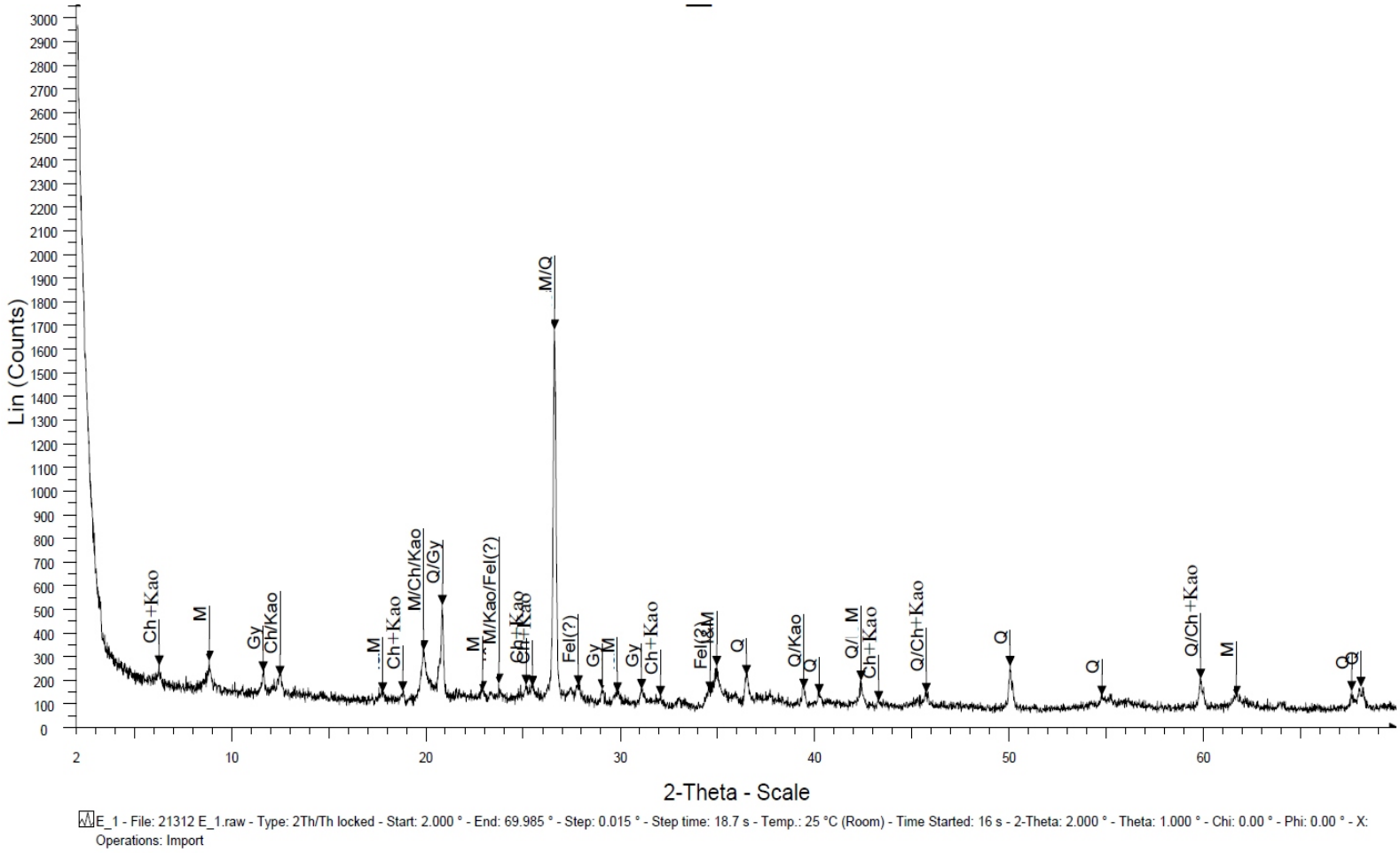

Figure 51. X-ray diffractogram of sample D/10

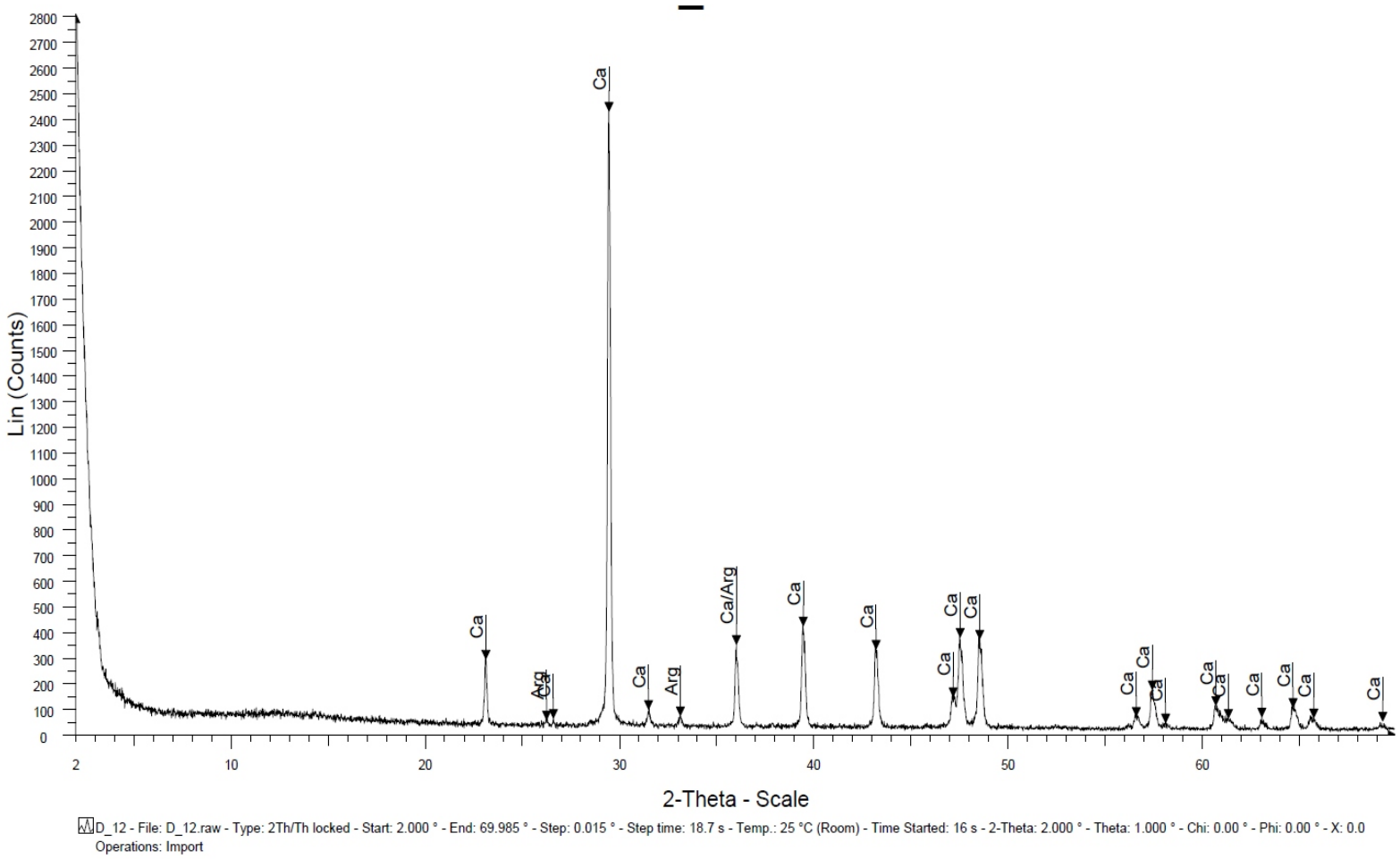

Figure 52. X-ray diffractogram of sample D/12

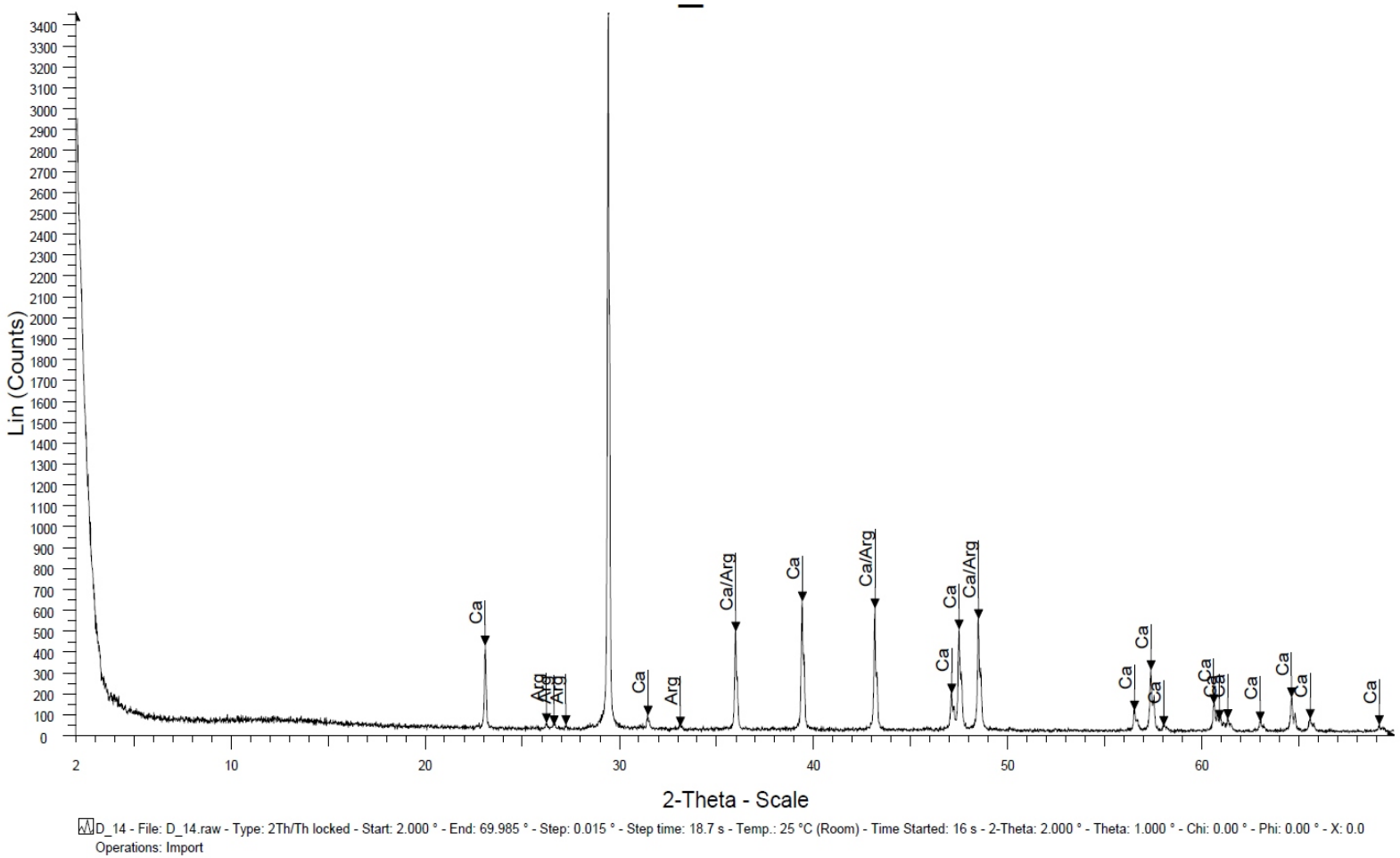

Figure 53. X-ray diffractogram of sample D/14

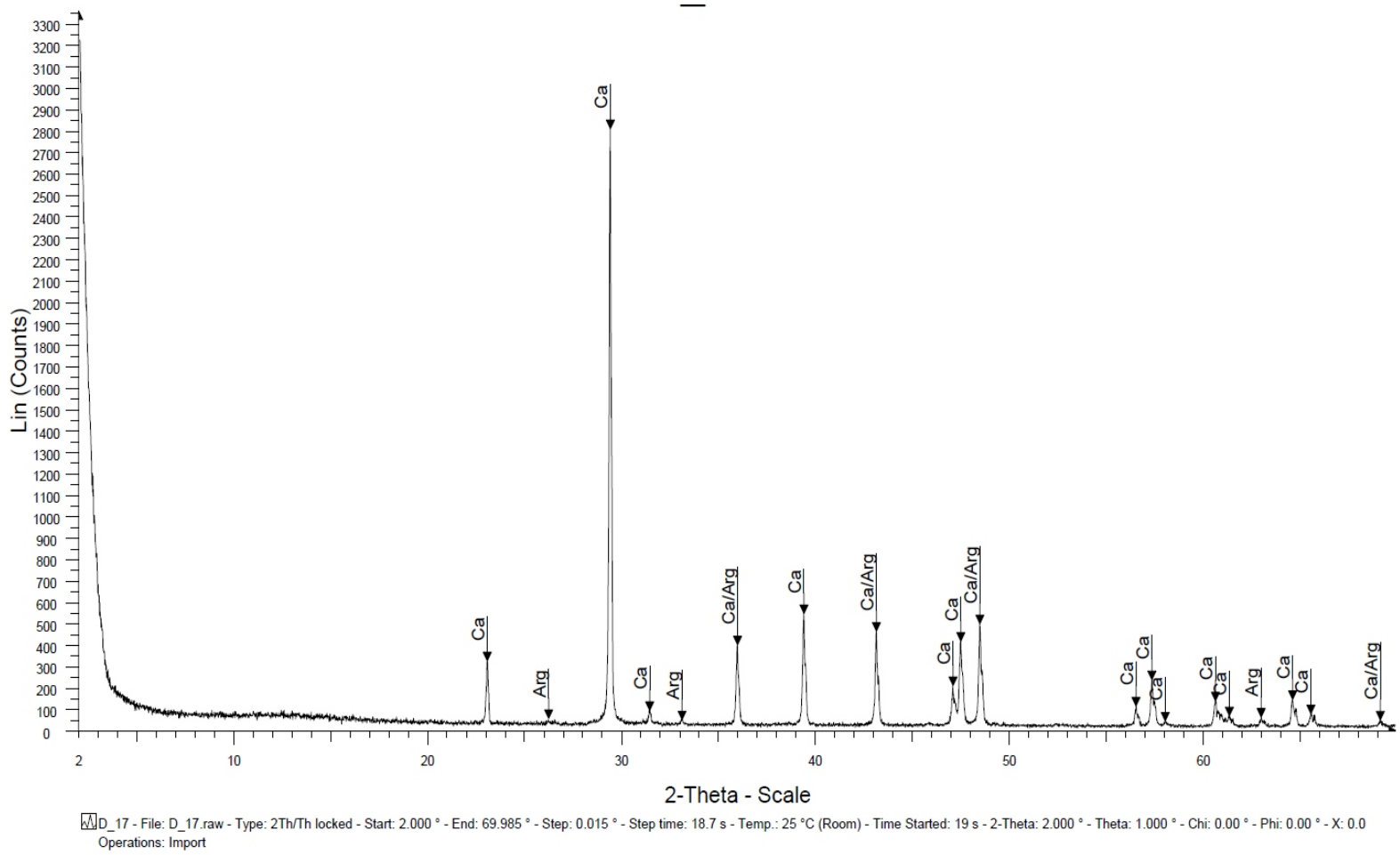

Figure 54. X-ray diffractogram of sample D/17

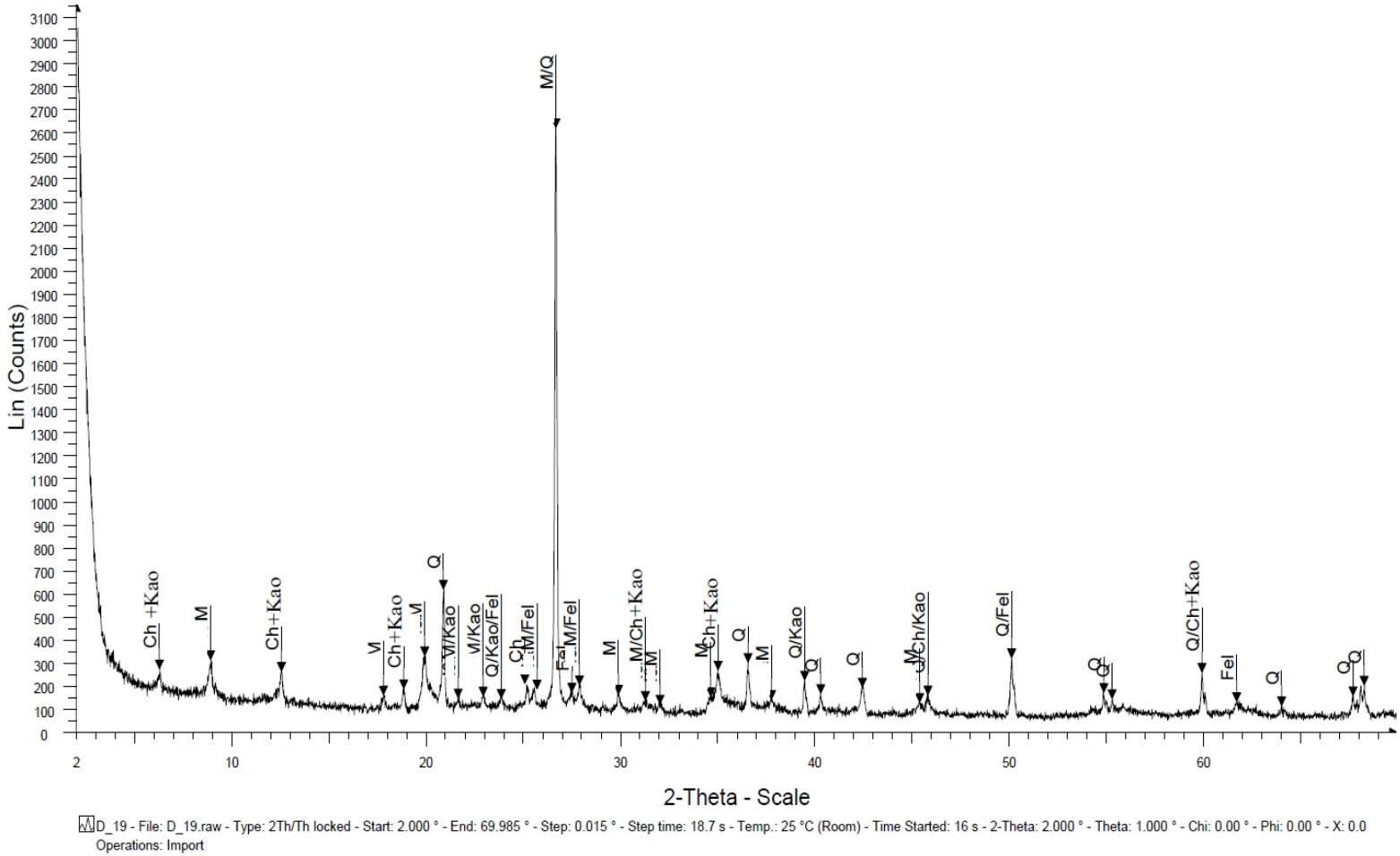

Figure 55. X-ray diffractogram of sample D/19

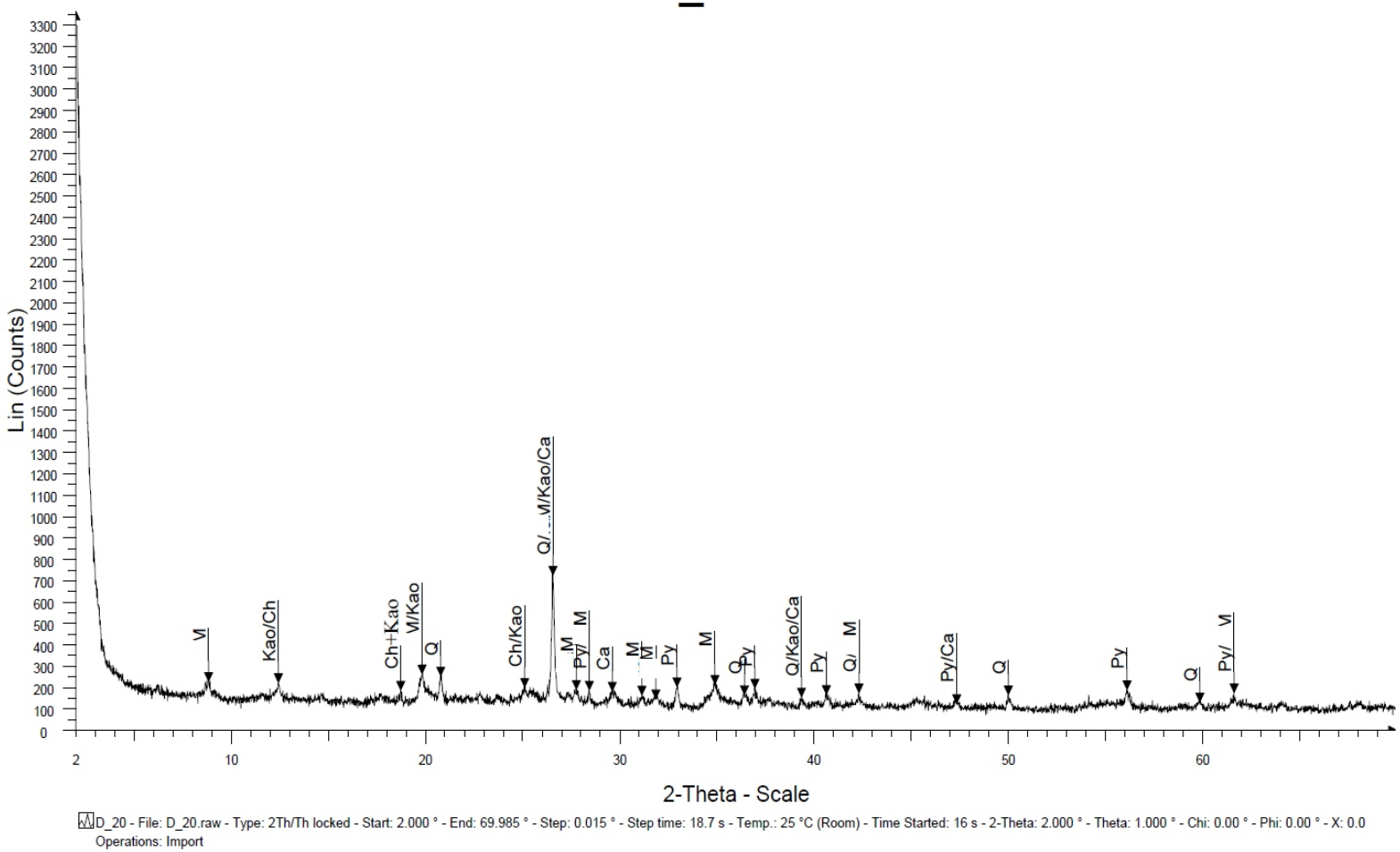

Figure 56. X-ray diffractogram of sample D/20

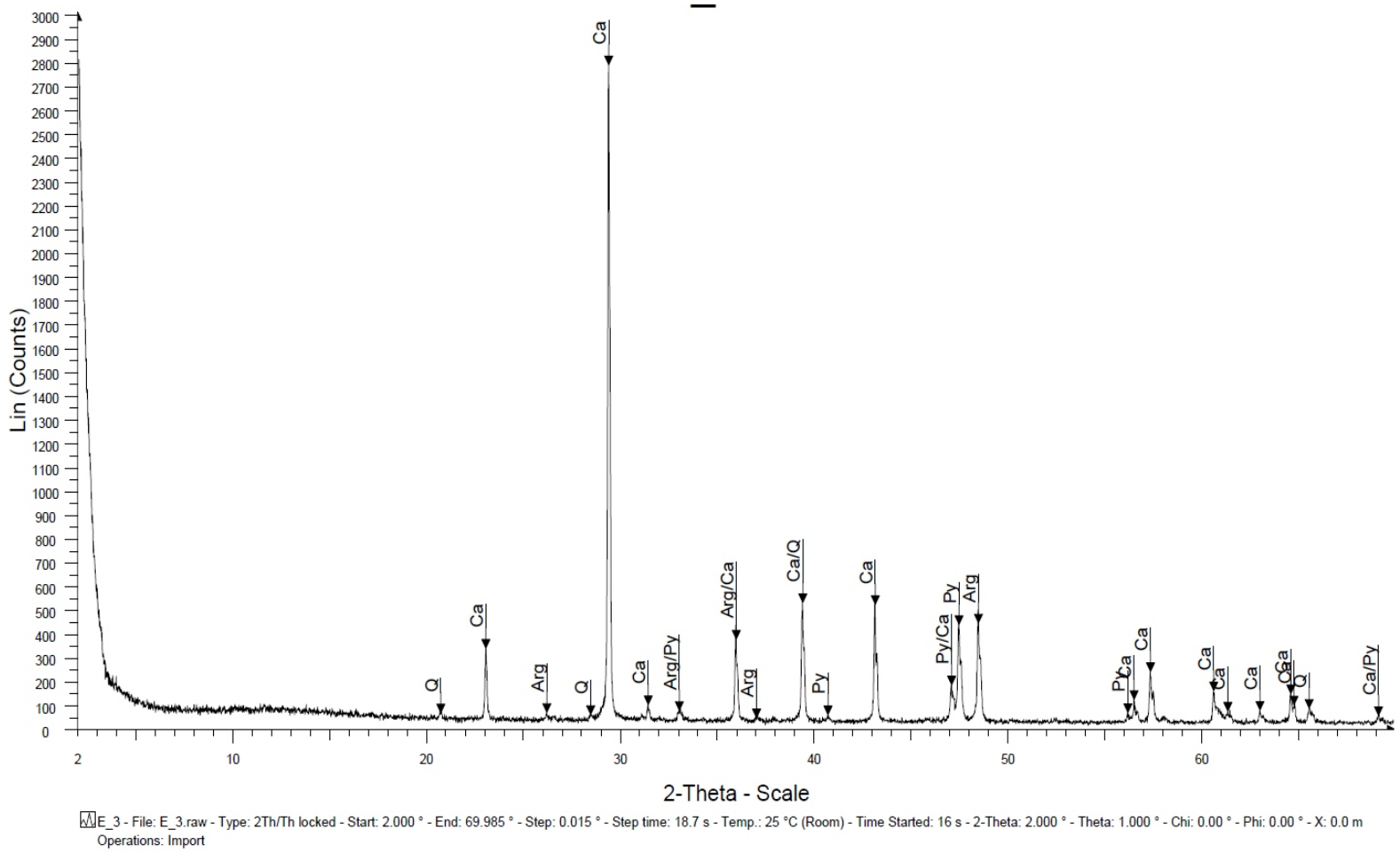

Figure 57. X-ray diffractogram of sample E/3

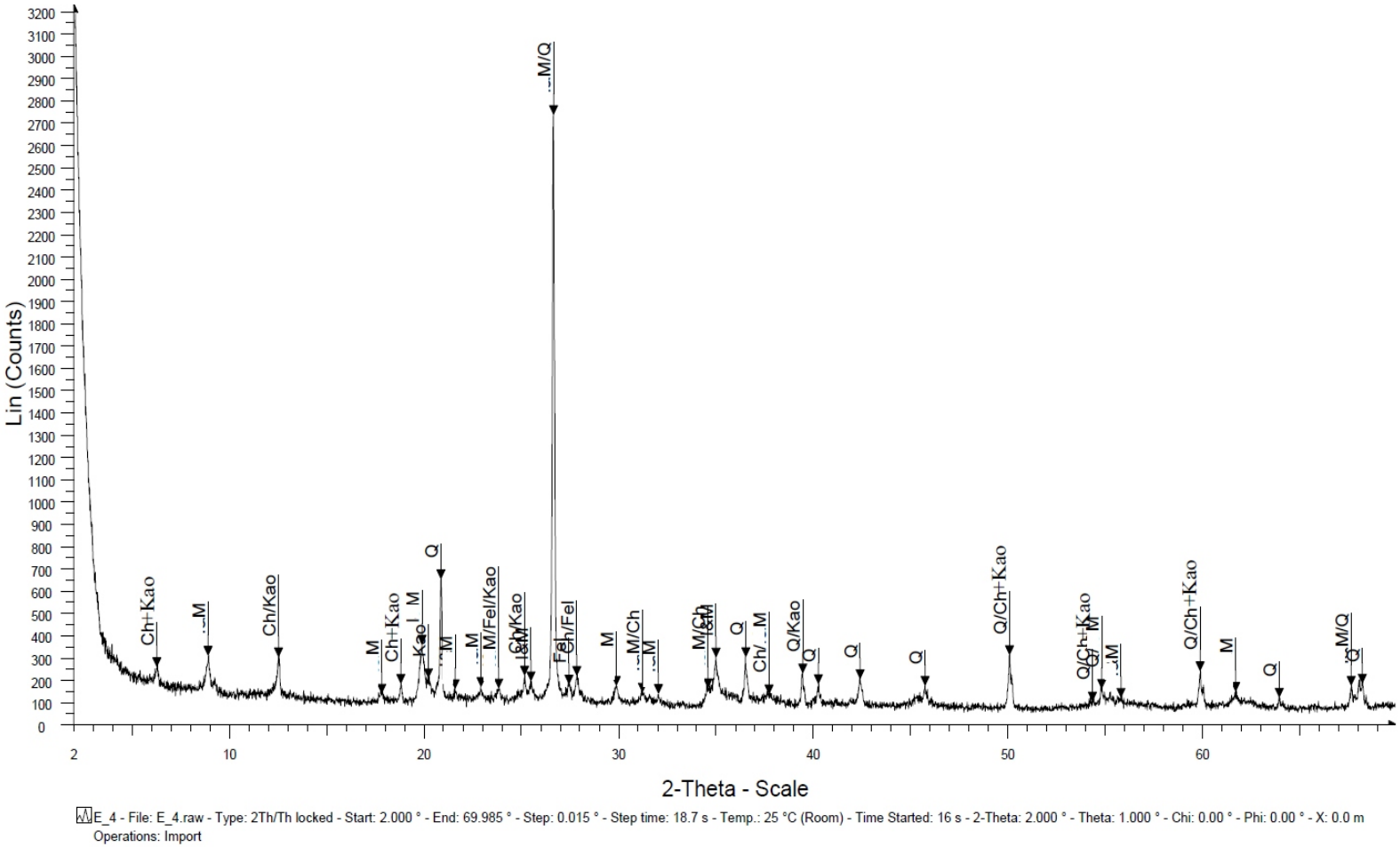

Figure 58. X-ray diffractogram of sample E/4

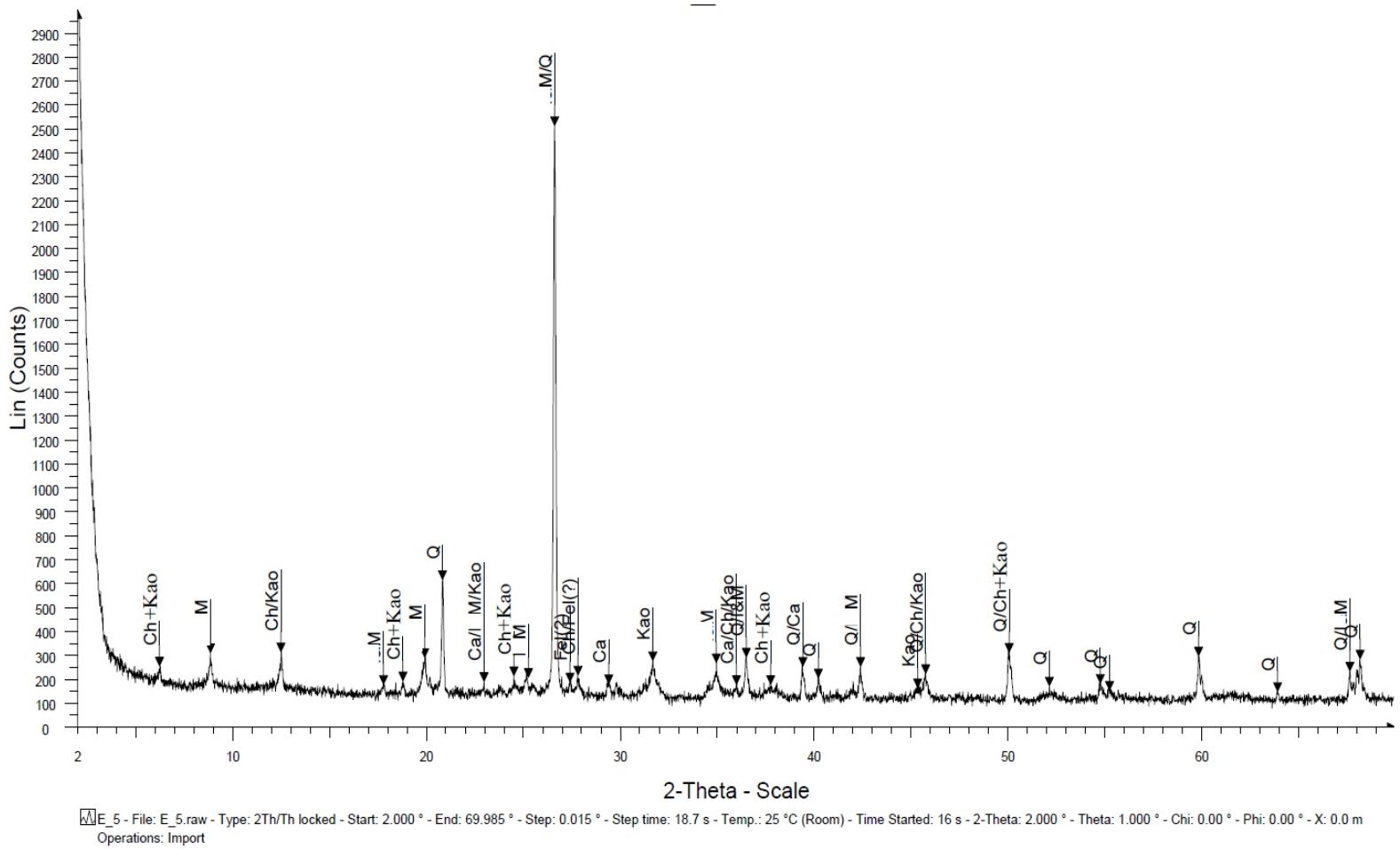

Figure 59. X-ray diffractogram of sample E/5